Author:
Kennedy, Clare L

Title:
An investigation into the genomic actions of glucocorticoid binding receptors in the rat brain following acute stress and circadian influences

An investigation into the genomic actions of glucocorticoid binding receptors in the rat brain following acute stress and circadian influences

Clare Linda Kennedy

A thesis submitted to the University of Bristol in accordance with the requirements of the degree of Doctor of Philosophy in the Faculty of Health Sciences,

Bristol Medical School

September 2019

Word Count: 63, 581

Abstract

Glucocorticoid (GC) hormones secreted upon activation of the HPA axis following stress or circadian input are vital regulators of many important physiological processes. In the brain, genomically acting mineralocorticoid receptors (MRs) and glucocorticoid receptor (GRs), orchestrate the cellular and molecular effects of GCs. Upon receptor occupancy, MRs and GRs translocate to the nucleus where they bind the DNA to transactivate or transrepress GC-target gene expression. Here, we conducted hippocampal ChIP- and RNA-seq to investigate the genome-wide binding of MRs and GRs and the transcriptomic response following elevations in corticosterone, the primary GC in the rat, in response to an acute stressor (Forced swimming – FS) or the circadian rise of GC secretion. ChIP-seq revealed a strikingly distinct profile of MR- and/or GR-binding to over 1,000 loci, while RNA-seq identified transcriptional responses in over 1,000 genes. Cross-correlation of both datasets was carried out for the first time, while extensive pathway analysis highlighted many promising novel targets for further exploration. Of these targets, we further investigated the Krüppel-like factors (KLFs) in a separate cohort of rats while validating findings of ChIP- and RNA-seq. We extended our examination to other brain regions such as the amygdala, PFC and neocortex which showed substantial MR DNA-binding in these regions despite previous reports describing a localised expression of this receptor primarily in the hippocampus. Subsequently, we investigated whether the increases in binding were in fact the underlying events responsible for the observed transcriptional responses by blocking the actions of genomically acting MRs and GRs, using receptor antagonists, inhibitors of corticosterone synthesis and surgical adrenalectomy. This thesis has provided novel insights into the genomic actions of MRs and GRs under physiological conditions of relevance for GC secretion, while providing the groundwork for future experiments aiming to elucidate further the genomic mechanisms underlying GC hormone action in the brain.

Acknowledgements

First and foremost, I would like to thank my supervisor, Professor Hans Reul, for the opportunity to carry out my PhD in his research group, and for his guidance, support and input throughout these 4 years. I am incredibly grateful to the Wellcome Trust and BBSRC; who have provided the funding to support my work. I would like to thank our collaborators at the Wellcome Centre for Human Genetics, Oxford; especially Silvia.

I would like to thank all past and present members of the Reul group. Karen; I could never thank you enough for being my unofficial second supervisor, counsellor and general life saver. Thank you for offering me so much support and guidance and being a fantastic colleague and friend. Emily; these past few years would not have been half as enjoyable without you there to make me laugh. Thank you for always listening to me vent and for proofreading my thesis with your eagle eye. I am going to miss dancing around the lab to Radio1 together and being the victim of your sarcasm! I would also like to thank my lovely colleagues at the Dorothy Hodgkin Building. Dagmara and Paul; without you both, we would all be lost! Astrid, thank you for your kindness and encouragement. Ben, Matt and George, our Friday pub trips, and general excursions have kept me sane; we make a truly fantastic clique. Mom and Dad, thank supporting me throughout this PhD and in my next academic adventure (Bioemphemetics is a far better spelling). Fred, my winning ticket, thank you for everything.

Author's Declaration

I declare that the work in this thesis was carried out in accordance with the requirements of the University's Regulations and Code of Practice for Research Degree Programmes and that it has not been submitted for any other academic award. Except where indicated by specific reference in the text, the work is the candidate's own work. Work done in collaboration with, or with the assistance of, others, is indicated as such. Any views expressed in the dissertation are those of the author.

SIGNED:……..DATE:…….

Abbreviations

3C	Chromatin conformation capture
6-FAM	6-Carboxyfluorescein
A	Adenine
Aβ	Amyloid-beta
ACTH	Adrenocorticotropic hormone
ACTHR	ACTH receptor
ADX	Adrenalectomy
AEBSF	4-(2-Aminoethyl) benzenesulfonyl fluoride hydrochloride
AF-1	Activation function-1
AF-2	Activation function-2
AmPFC	Anterior mPFC
AP1	Activation protein 1
ASM	Airway smooth muscle
ATOH1	Atonal BHLH Transcription Factor
AVP	Arginine vasopressin
Bace1	Beta-Secretase 1
BAFs	BRM/BRG1 associated factors
BBB	Blood-brain barrier
Bdnf	Brain-derived neurotrophic factor
BLA	Basolateral nucleus of the amygdala
BLAM	Baseline a.m.
BLPM	Baseline p.m.
Bmal1	Brain and Muscle ARNT-Like 1
BOLD	Blood oxygenation level dependent
Bps	Base pairs
BRM	Brahma
BRG1	Brahma-related gene 1

BTEB	Basic transcription element-binding protein
C	Cytosine
CA	Cornu ammonis
cAMP	Cyclic adenosine mono phosphate
CBG	Corticosteroid-binding globulin
CBP	CREB binding protein
CCK	Cholecystokinin
CE	Circadian exclusive
CeA	Central nucleus of the amygdala
CFL1	Cofilin 1
ChIP	Chromatin immunoprecipitation
ChIP-seq	ChIP-sequencing
CLOCK	Clock circadian regulator
CNS	Central nervous system
CON	Constitutive
CORT	Corticosterone
CREB	cAMP response element binding protein
CRH	Corticotropin-releasing hormone
CRX	Con-Rod Homeobox
CRY	Cryptochrome circadian regulator
CRY2	Cryptochrome circadian regulator 2
CSF	Cerebrospinal fluid
CYP	Cytochrome P450 family
CyPA	Cyclophilin A
DAVID	Database for Annotation, Visualization and Integrated Discovery
DBD	DNA-binding domain
DEX	Dexamethasone
DG	Dentate gyrus

Disc1	Disrupted-in-schizophrenia 1
DHEA	Dehydroepiandrosterone
DHEAS	Dehydroepiandrosterone sulphate ester
DOC	11-deoxycorticosterone
Dlx2	Distal-Less Homeobox 2
DNA	Deoxyribonucleic acid
dNTP	deoxyribonucleotide triphosphate
DST	Dexamethasone suppression test
EC	Endothelial cell
EDTA	Ethylenediaminetetraacetic acid
EGR	Early growth response
EMAS	Electrophoretic mobility shift assay
Erbb4	Erb-B2 Receptor Tyrosine Kinase 4
ERK	Extracellular regulated kinase
ERK1/2	Extracellular regulated kinase ½
ESR	Estrogen Receptor
EWSR1-FLI1	EWS RNA Binding Protein 1-Fli-1 Proto-Oncogene, ETS transcription factor
exRNA	exonic RNA
FAIRE	Formaldehyde assisted isolation of regulatory elements
FDR	False discovery rate
Fkbp4	FK506 binding protein 52
Fkbp5	FK506 binding protein 51
fMRI	Functional magnetic resonance imaging
Fos	Fos Proto-Oncogene AP-1 Transcription Factor Subunit
FOX	Forkhead box
FOXO3A	Forkhead box O3A
FS	Forced swimming
G	Guanine

GC	Glucocorticoid
GABA	Gamma aminobutyric acid
$GABA_A$	Gamma aminobutyric acid subunit A
GAD	Glutamic acid decarboxylase
GAD65	Glutamic acid decarboxylase 65
GAD67	Glutamic acid decarboxylase 67
Gapdh	Glyceraldehyde 3-phosphate dehydrogenase
GFAP	Glial fibrillary acidic protein
GO	Gene Ontology
GR	Glucocorticoid receptor
GRox	Glucocorticoid receptor over-expressing
GRE	Glucocorticoid response element
GRIA2	Glutamate ionotropic receptor AMPA type subunit 2
GRIN1	Glutamate ionotropic receptor NMDA type subunit 1
GRIN2B	Glutamate ionotropic receptor NMDA type subunit 2B
H	Histone
HAT	Histone acetyltransferase
HBMEC	Human brain microvascular endothelial cells
HDAC	Histone deacetylase
hGR	human GR
hnRNA	Heteronuclear RNA
Homer3	Homer Scaffold Protein 3
HR	Hinge region
HSD3B	Hydroxy-delta-5-steroid-dehydrogenase, 3-beta
Hsp	Heat shock protein
HPA	Hypothalamic-pituitary-adrenal
Hprt1	Hypoxanthine phosphoribosyltransferase 1
inRNA	intronic RNA

i.p.	Intraperitoneal
IPA	Ingenuity pathway analysis
K	Lysine
Kbs	Kilobases
KEGG	Kyoto Encyclopaedia of Genes and Genomes
KLF	Krüppel-like factor
KO	Knock out
L	Leucine
LBD	Ligand-binding domain
LTD	Long-term depression
LTP	Long-term potentiation
MAPK	Mitogen-activated protein kinase
mBMECs	Mouse brain microvascular endothelial cells
MC2R	Melanocortin type-2 receptor
MD	Maternal deprivation
MET	Metyrapone
MMTV-LTR	Mouse mammary tumour virus-long terminal repeat
mPFC	Medial PFC
MR	Mineralocorticoid receptor
mRNA	Messenger RNA
MSK1	Mitogen- and stress- activated kinase 1
mtRNA	Mitochondrially transcribed mRNA
MWM	Morris water maze
N-terminal	Amino-terminal
N2a	Neuro2a
NaBut	Sodium butyrate
NCoR	Nuclear receptor co-repressors
Neurod1	Neuronal differentiation 1

Nf-Kb	Nuclear factor kappa B
nfH_20	Nuclease-free water
NGS	Next generation sequencing
NKX	NKX Homeobox
Nkx2.1	NK2 Homeobox 1
NL1	Nuclear localisation-1
NL2	Nuclear localisation-2
NMDA	*N*-methyl-*D*-aspartate
NMDAR	NMDA Receptor
NR	Nuclear Receptor
NSC	Neural stem cell
NSCC	Normalised Strand Cross-correlation
NPY	Neuropeptide Y
Nr3c1	Nuclear Receptor Subfamily 3 Group C Member 1
Nr3c2	Nuclear Receptor Subfamily 3 Group C Member 2
NTD	Amino-terminal domain
NTS	Nucleus of the solitary tract
P/CAF	p300/CBP-associated factor
PANTHER	Protein Analysis Through Evolutionary Relationships
PAX	Paired Box
PEG	poly-ethylene glycol
Per1	Period 1
Per2	Period 2
PFC	Prefrontal cortex
PKA	Protein kinase A
PND	Post-natal day
PNS	Prenatal stress
POMC	Pro-opiomelanocortin

PTSD	Post-traumatic stress disorder
PVN	Paraventricular nucleus
RELA	RELA Proto-Oncogene, NF-KB Subunit
RFX	Regulatory Factor X
RGC	Retinal ganglion cell
RIA	Radioimmunoassay
RNA	Ribonucleic acid
RNA-seq	RNA-sequencing
Rpl10a	Ribosomal protein L10a
RSC	Relative Strand Cross-correlation
RU	RU486
S	Serine
SCO	Subcommissural organ
SCN	Suprachiasmatic nucleus
SE	Stress exclusive
Sgk1	Serum and glucocorticoid-regulated kinase 1
Shank1	SH3 And Multiple Ankyrin Repeat Domains 1
SMN1	Survival motor neuron 1
SMRT	Silencing mediator of retinoic acid and thyroid hormone receptor
SP	Specificity Protein
SP1	Specificity protein 1
SPIRO	Spironolactone
SRCs	Steroid receptor coactivators
SR&CR	Stress and circadian responsive
SST	Somatostatin
StAR	Steroidogenic acute regulatory protein
STAT	Signal Transducer and Activator of Transcription
SUMO-1	Small ubiquitin-related modifier-1

SWI/SNF	Switch/sucrose non-fermentable
T	Threonine
TAMRA	Tetramethylrhodamine
TE	Tris-EDTA
TF	Transcription factor
TSS	Transcriptional start site
TSLP	Thymic Stromal Lymphopoietin
UTR	Untranslated region
X	Amino acid
Ywhaz	Tyrosine 3-monooxygenase/tryptophan 5-monooxygenase activation protein zeta
Zbtb3	Zinc finger and BTB containing 3
ZNF	Zinc Finger

Table of contents

List of figures

List of Tables

Publications

KENNEDY, C. L. M., CARTER, S. D., MIFSUD, K. R. & REUL, J. 2019. Unexpected effects of metyrapone on corticosteroid receptor interaction with the genome and subsequent gene transcription in the hippocampus of male rats. J Neuroendocrinol, e12820.

Chapter 1 Introduction

1.1 Glucocorticoid hormones: importance for life

1.1.1 The role of glucocorticoid hormones in homeostasis, adaptation and survival

Glucocorticoids (GCs) are a class of steroid hormones synthesised and secreted by the adrenal glands which are part of the hypothalamic-pituitary-adrenal (HPA) axis; a major mammalian neuroendocrine system responsible for the regulation of numerous physiological processes. GCs regulate the sleep-wake cycle, body temperature, renal plasma flow and cardiovascular activity in order to maintain homeostasis in response to environmental changes (De Kloet and Derijk, 2004). Adaptation and survival are also dependent on GC hormone action in the brain, where GCs promote resilience to external stressors. Memory consolidation and behavioural changes mediated by GC hormones facilitate appropriate adaptation to stress, thus preventing physical and psychological disease (Reul et al., 2015). These vital GC hormone actions are orchestrated via receptors found within GC target tissues, of which two have been characterised. The mineralocorticoid receptor (MR) and glucocorticoid receptor (GR) can be found at the cellular membrane or in the cytoplasm, where they mediate rapid non-genomic or slower genomic effects, respectively (Groeneweg et al., 2012). For the purpose of this thesis, GC hormone activity in the brain via genomically acting MRs and GRs will be discussed. Once activated by GCs, MRs and GRs elicit genome-wide effects, exerting transcriptional effects in thousands of GC-target genes involved in circadian variation as well as the brain's response to stress.

1.1.2 The circadian rhythm and the stress response

The secretion of GC hormones by the HPA axis is under circadian control and can also be stimulated by exposure to stress. The central circadian pacemaker, the suprachiasmatic nucleus (SCN) of the anterior hypothalamus, is the main driver of circadian input to the HPA axis and mediates a rhythmic pattern of GC secretion corresponding to the animal's activity phase (Dunlap, 1999). Consequently, circulating levels of GCs are maintained low during the inactive phase and rise during the active phase of the animal (Dickmeis, 2009). The circadian rhythm is shaped by an ultradian rhythm of hourly pulses of GCs (Spiga et al., 2014). Input of stress signals to the HPA axis, via the brain stem and limbic system, elicits what is referred to as the "stress response". The role of the stress response is to allow an animal to respond and adapt to stressors by initiating appropriate physiological and behavioural changes. In

the event that a similar stressor is reencountered in the future, the animal is better equipped to respond (Mifsud and Reul, 2018). Following an acute stressor, plasma levels of circulating GCs are increased up to 100-fold (Mifsud et al., 2016) and the stress response is eventually "switched off", as GCs restore the HPA axis to baseline activity via negative feedback.

Following HPA axis activation by circadian input or by stress (Figure 1.1), paraventricular neurons of the hypothalamus secrete corticotropin-releasing hormone (CRH) and arginine vasopressin (AVP) in the Median Eminence. After transport through the hypothalamic-pituitary portal system, these neuropeptides act upon the anterior pituitary, to induce the synthesis and secretion of adrenocorticotropic hormone (ACTH) (Vale et al., 1981). ACTH stimulates the zona fasciculata of the adrenal cortex, resulting in the synthesis of cortisol or corticosterone (CORT); the primary GC hormones found in man and in rat, respectively, by a process known as steroidogenesis. Within a subset of adrenocortical steroidogenic cells, ACTH binds its endogenous receptor; the melanocortin type-2 receptor (MC2R) (Chhajlani and Wikberg, 1992). Via a rapid non-genomic pathway, ACTH stimulates steroidogenesis via protein kinase A (PKA) activation. PKA phosphorylates and activates hormone sensitive lipase (HSL) and steroidogenic acute regulatory protein (StAR). HSL increases levels of the steroid precursor, cholesterol, while StAR promotes the transport of cholesterol into the mitochondria (Walker et al., 2015). Via a slower, genomic mechanism, ACTH also induces the expression of steroidogenic genes (Chung et al., 2011). Once transported to the mitochondria, cholesterol is converted to cortisol or CORT via a series of enzymatic reactions (Figure 1.2). GCs are secreted into the blood stream where they are transported to target tissues and can bind GC-binding receptors. GC hormones exert negative feedback on HPA axis activity via GR action at the anterior pituitary, hypothalamus and hippocampus, thus terminating the stress response.

The degree to which tissues are exposed to GC hormones is tightly regulated by a transport protein, corticosteroid-binding globulin (CBG). Less than 6% of circulating GCs are unbound or "free" in plasma, with 80-90% of circulating GCs bound by CBG and the remainder bound by plasma albumin (Lewis et al., 2005). CBG maintains a steady state concentration of GCs (Henley et al., 2016), and following a (stress-induced) rise in plasma GC levels, CBG is released from the liver, limiting the proportion of free hormone available to penetrate tissues (Qian et al., 2011). Only the "free" unbound form of GC hormone can penetrate tissues and orchestrate molecular effects via MRs and GRs (Reul et al., 2015).

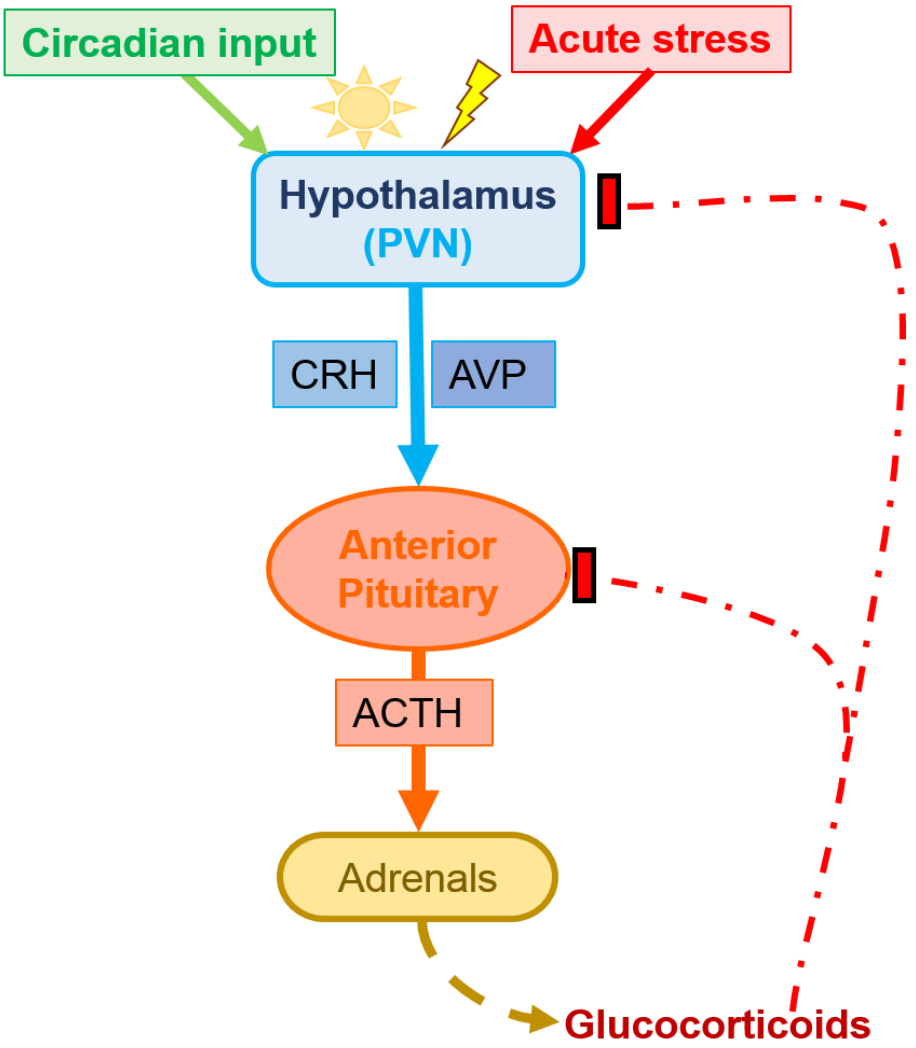

Figure 1.1 A schematic diagram of the hypothalamic-pituitary-adrenal (HPA) axis activated following stress or circadian input

Activation of the HPA axis following acute stress or circadian input resulting in the synthesis and secretion of GC hormones from the adrenal gland. GC hormones exert negative feedback via the anterior pituitary and hypothalamus, terminating the stress response. Paraventricular nucleus (PVN), corticotropin-releasing hormone (CRH), adrenocorticotropic hormone (ACTH).

1.1.3 Animal models to elucidate GC hormone action

Animal models are commonly used to elucidate the effects of GC hormone action on the brain following exposure to an acute stressor. Many behavioural models are dependent on GC hormone action in the hippocampus to induce learning and memory formation, including the forced swim test (Veldhuis et al., 1985), Morris water maze (Sandi et al., 1997) and contextual fear conditioning (Cordero and Sandi, 1998). Restraint stress is a psychogenic stressor which triggers GC receptor action in the hippocampus (Wang et al., 2012), however does not result in an adaptive learning response, and is often used to investigate the negative effects of acute or chronic stressors on the brain (Furay et al., 2008).

The forced swim (FS) test is a widely used behavioural paradigm in which the effects of an acutely stressful situation can be examined on the formation of long-term memories associated with that situation. During the FS test, rats are placed in a water filled beaker from which there is no escape. Upon being placed in the water, rats will initially swim and climb against the wall of the beaker in an attempt to escape from the beaker, however after some time the rat begins to spend less time struggling and more time in an immobile position. After 15 min, the rat is removed from the water and returned to their home cage (Porsolt et al., 1977). Rats exhibit significantly elevated levels of circulating plasma CORT following exposure to the FS test, however levels return to baseline within 3 hrs after the onset of FS (Mifsud and Reul, 2016). Upon re-exposure to the FS test, rats display increased immobility behaviour, which is an adaptive phenomenon reflecting learning and memory formation in response to the stressor (De Pablo et al., 1989). This enhanced immobility behaviour is seen in rats tested up to 4 weeks after the initial FS test (Gutierrez-Mecinas et al., 2011), indicating that the rat has formed a long-term memory of the previous experience, remembering that escape is not possible and adapting its behaviour to conserve energy by assuming an immobile position, as this is the best strategy for survival. Furthermore, the rat may remember that it had been taken from the water eventually at the time of the first test (Reul, 2014). Behavioural immobility in the re-test is critically dependent on GC action via GRs during the hours after the initial test and is prevented in the absence of GC hormones or upon blockade of GR activity (Jefferys et al., 1983, Veldhuis et al., 1985, Bilang-Bleuel et al., 2005, Gutierrez-Mecinas et al., 2011).

1.1.4 Pharmacological and surgical manipulation of the HPA axis

Pharmacological agents which manipulate the HPA-axis are widely used in research to elucidate GC hormone action and the genomic activity of MRs and GRs. Commonly used methods of targeting the stress response include the administration of synthetic GCs, inhibitors of GC synthesis, or antagonists of GC receptors. Some of the effects of GC hormones can be mimicked using the synthetic GC, dexamethasone (DEX). The drug is capable of selectively binding and activating GRs with high affinity *in vivo* (Reul et al., 1987) and is widely used in cell lines and animal models to investigate GC hormone action (Strahle et al., 1987, Roozendaal et al., 1999). Inhibiting GC hormone action can be achieved by targeting the steroidogenic pathway (Figure 1.2) thus preventing hormone synthesis. Metyrapone (MET) is commonly used in research (Liu et al., 1999, Roozendaal et al., 1996) and as therapeutics for the treatment of Cushing's syndrome. MET can reduce GC hormone synthesis by blocking the enzyme 11-β-hydroxylase (CYP11B2), thereby preventing the conversion of deoxycorticosterone to CORT (Strashimirov and Bohus, 1966) in the adrenal gland. The genomic effects of MRs and GRs can be blocked by the antagonists Spironolactone (SPIRO) (Yau et al., 1999) and RU486 (RU) (Baulieu, 1991), respectively.

Adrenalectomy (ADX), a surgical intervention involving the removal of the adrenal glands, is widely used in stress research (Borrell et al., 1983, Jefferys et al., 1983, Veldhuis et al., 1985) as a method of removing the endogenous source of CORT to examine GC hormone activity (Reul et al., 1987). Although ADX may be considered as a more reliable approach over pharmacological intervention due to a lack of pharmacokinetic influences, there are disadvantages as the procedure itself will induce a surgical stress response involving HPA axis activation (Ioannidis et al., 2018). Furthermore, ADX has been shown to induce behavioural changes, such as increased anxiety levels (File et al., 1979) and elicit various side effects in the brain similar to those induced by stress; including oxidative damage and changes in neurotransmitter levels (Hu et al., 1997, Helmreich et al., 1996). In addition, long-term ADX has been shown to cause degeneration of the hippocampal dentate gyrus (DG) (Sloviter et al., 1989).

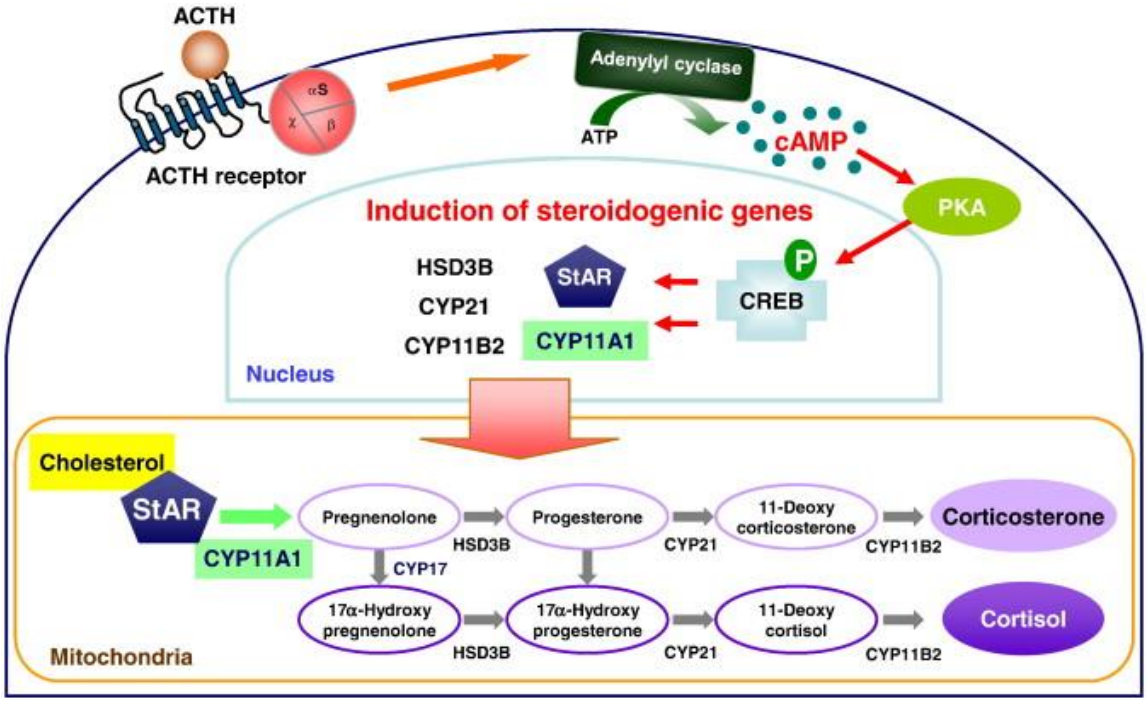

Figure 1.2 Adrenal steroidogenesis and its hormonal regulation

ACTH acts upon ACTH receptors within adrenocortical steroidogenic cells triggering the activation of the ACTHR/cAMP/PKA/CREB signalling cascade, inducing the expression of steroidogenic genes. StAR transports cholesterol and CYP11A1 to the nucleus, where a number of enzymatic reactions result in the synthesis of corticosterone or cortisol. The steroidogenic pathways for cortisol and corticosterone are identical, apart from an initial step occurring only during cortisol synthesis, where pregnenolone is converted to 17α-hydroxypregnenolone. Adrenocorticotropic hormone (ACTH), ACTH receptor (ACTHR), cyclic adenosine mono phosphate (cAMP), protein kinase A (PKA), cAMP response element binding protein (CREB), steroidogenic acute regulatory protein (StAR), cytochrome P450 family 11 subfamily A member 1 (CYP11A1), hydroxy-delta-5-steroid-dehydrogenase, 3-beta (HSD3B), steroid 21-hydroxylase (CYP21), cytochrome P450 family 11 subfamily B member 2 (CYP11B2), cytochrome P450 family 17 member 1 (CYP17). Taken from (Chung et al., 2011).

1.1.5 Dysregulated GC hormone signalling: circadian- and stress-related disorders

Robust HPA axis activity is critical for the maintenance of health and well-being and dysregulations in the acute stress response, chronic stress exposure or impaired circadian rhythms can have detrimental effects on physical and mental health. Evidence suggests that the HPA axis may be involved in the aetiology of many disorders such as Alzheimer's disease and schizophrenia. Exposure to chronic stress has been linked to cognitive impairments and the development of stress-related neuropsychiatric disorders such as anxiety, depression and post-traumatic stress disorder (PTSD) (Finsterwald and Alberini, 2014).

Circadian-related disorders arise due to irregular HPA axis activity, leading to abnormal GC hormone levels. Cushing's syndrome is characterised by an excess of GC hormones and is often accompanied by an impaired circadian rhythm and circadian-related symptoms such as sleep disruptions. Corticotropin-producing tumours which overstimulate the adrenal cortex or abnormal adrenocortical tissue which produces an excess of GCs are often the underlying cause of hypercortisolism in Cushing's syndrome (Chung et al., 2011). Neuropsychiatric disorders are frequently observed in patients with Cushing's syndrome, such as cognitive impairment, anxiety and major depression (Pivonello et al., 2015). Symptoms such as irritability, depressed mood, anxiety and social withdrawal were reported by patients with Cushing's syndrome and a significant correlation has been observed between depressed mood and plasma ACTH levels (Starkman et al., 1981). The cognitive impairments and affective symptoms experienced by patients may be caused by brain atrophy observed in the disease. Decreased volume of the hippocampus (Starkman et al., 1992), cerebral cortex (Bourdeau et al., 2002) and right amygdala (Santos et al., 2017) have all been reported in patients with Cushing's syndrome. Furthermore, a correlation was found between reduced amygdalar volumes, depression and anxiety in patients with active Cushing's syndrome (Santos et al., 2017). Impairments in cognitive function has also been shown to correlate with reduced hippocampal volume and hypercortisolism (Starkman et al., 1992). Although brain atrophy in all three brain regions was shown to be reversed following the correction of hypercortisolism (Bourdeau et al., 2002, Santos et al., 2017, Starkman et al., 1999), the affective and cognitive symptoms may persist after correction of the disease. Anxiety scores reported by patients remained significantly higher following remission (Santos et al., 2017) and no improvement

in cognitive performance was observed in a group of Cushing's syndrome patients six months after hypercortisolism was corrected by surgery (Forget et al., 2002).

Exposure to stress during the prenatal period or during early life has been shown to result in HPA axis changes which may predispose individuals to the development of stress-related neuropsychiatric disorders. During important periods of foetal brain development, exposure of the mother to prenatal stress may lead to aberrant stress responses in the offspring (Lemaire et al., 2000). Furthermore, exposure of young rat pups to stressors during the early post-natal stages of development in which a stress hyporesponsive period is observed may induce profound negative effects on the developing pups (Sapolsky and Meaney, 1986). Adult rats exposed to prenatal stress (PNS) exhibited an enhanced plasma CORT response following exposure to restraint stress, accompanied by increased anxiety-like behaviours in the open-field and elevated plus maze tests (Vallee et al., 1997). PNS exposure was also shown to impair spatial learning in the MWM and decrease in neurogenesis within the DG in response to MWM training (Lemaire et al., 2000). Rats exposed to postnatal maternal deprivation (MD) stress and foot shock during the stress hyporesponsive period exhibited significantly increased plasma levels of ACTH and significantly decreased CRH levels in the anterior pituitary compared with non-deprived controls (Ladd et al., 1996). Decreased hippocampal expression of the neurotrophin *Brain-derived neurotrophic factor (Bdnf)* and NMDA receptor subunits *NR-2A* and *NR-2B* was reported in MD exposed adult rats (Roceri et al., 2002). Exposure of young rats to social isolation for 2 months, beginning at postnatal day 16, led to reduced plasma CORT levels under basal conditions and following restraint stress. Socially isolated rats also exhibited blunted activation of pituitary ACTH-containing cells following exposure to restraint stress and smaller pituitary corticotrophs compared with control animals (Sanchez et al., 1998).

Chronic stress involves the exposure to high levels of GC hormones for prolonged periods of time and has been reported to cause changes to the HPA axis and in the brain. Rats exposed to a 2-week chronic stress protocol showed increased levels of plasma CORT, which may reflect a stress hyper-responsive state. Irregularities in the distribution of CRH among many brain regions was also observed, including the hippocampus and hypothalamus. Increased CRH concentration was shown in the anterior hypothalamic nucleus while CRH was decreased in the ventral hippocampus and medial prefrontal cortex (mPFC) (Chappell et al., 1986). Schizophrenia has been linked to chronic stress, as decreased

expression of *Bdnf* is observed in the hippocampus and prefrontal cortex (PFC) of patients with schizophrenia and in the hippocampus of rats exposed to chronic restraint stress for 3 weeks (Seo et al., 2018). In a post-mortem human study, abnormal GR messenger RNA (mRNA) and protein isoform expression was reported in the PFC of patients that had suffered from schizophrenia and bipolar disorder. Levels of GR mRNA were decreased in the PFC of schizophrenia patients relative to matched controls, while no differences in MR mRNA was detected. Furthermore, increased protein levels of the truncated GRα isoform, GRα-D1 was seen in schizophrenia and bipolar patients, while the full-length isoform of GRα was increased in bipolar patients relative to with schizophrenia patients (Sinclair et al., 2011). Alzheimer's disease has also been linked to chronic stress. Increased CRH mRNA in the PVN and increased neuronal CRH mRNA has been observed in Alzheimer's patients (Raadsheer et al., 1995). Furthermore, exposure to chronic variable stress for 2 weeks resulted in mild cognitive impairments in young mice and severe cognitive impairments in aged mice, as well as increased hippocampal, amygdalar and prefrontal cortex expression of a gene involved in the beta-amyloid pathology of Alzheimer's disease, *Beta-Secretase 1 (Bace1)* (Cordner and Tamashiro, 2016*)*.

Many animal and human studies have established a role of the HPA axis in depression and PTSD. The dexamethasone suppression test (DST), a test initially developed as a diagnostic for Cushing's syndrome, demonstrated a high prevalence of HPA axis abnormalities in depressed patients (Carroll, 1982). CORT has been shown to significantly reduce mRNA levels of *Bdnf* in the rat PFC and hippocampus, an effect which is reversed by antidepressant treatment (Dwivedi et al., 2006). FS has been shown to result in decreased mRNA levels of *Bdnf* within the rat hippocampal DG, CA1, CA3 and CA4 subregions. Antidepressant treatment or exercise attenuated the FS-induced decrease in *Bdnf* mRNA while a combination of both antidepressant treatment and exercise significantly enhanced mRNA levels of *Bdnf* in all 4 hippocampal subregions (Russo-Neustadt et al., 2001). Rats treated with the tricyclic antidepressant drug, imipramine, for 8 weeks exhibited significantly increased mRNA levels of MR in the hippocampus and decreased mRNA levels of CRH in the PVN, pro-opiomelanocortin (POMC) in the anterior pituitary and GR in the pituitary. Decreased plasma pituitary ACTH secretion was also observed alongside increased weight of the adrenal glands (Brady et al., 1991). Patients suffering from PTSD and major depression were shown to have significantly increased 24h secretion of urinary cortisol, compared with normal volunteers (Maes et al., 1998), while plasma cortisol levels of depressed patients was been shown to be consistently elevated over a 30 hour period compared with

healthy controls (Wong et al., 2000). Females with depression or depression alongside dementia were reported to exhibit higher CRH levels in the cerebrospinal fluid (CSF) compared with neurological controls (Banki et al., 1992). Patients with depression also exhibited large increases in the number of CRH neurons and CRH mRNA in the PVN (Raadsheer et al., 1995).

The use of genetically altered animals has also provided evidence for a role of GC receptors in depression. Exposure to chronic mild stress in a transgenic mouse overexpressing GR (GRox) in the forebrain resulted in increased anxiety-like behaviour in the open field test. Greater behavioural sensitivity to cocaine (20 mg/kg) was seen in GRox mice, demonstrated by increases locomotor activity in the OF compared with WT animals. Increased behavioural immobility was also reported in the FS test in GRox mice compared with WT mice, which was reduced with antidepressant treatment (Wei et al., 2004). Interpretation of this finding, however, is difficult, given the incorrect interpretation of the FS test as a measure of depression rather than adaptation and learning driven by GC hormones (Molendijk and de Kloet, 2015). Zebra fish homozygous for a mutant GR with disrupted transcriptional activity exhibited higher levels of CORT under non-stressed conditions. Moreover, exposure to stress failed to induce a significant surge in CORT as would be expected. Dysregulated HPA-axis activity was accompanied by reduced exploratory behaviour and reduced habituation to an anxiogenic environment. Additional changes, such as freezing behaviour and tank wall avoidance, strongly suggested the presence of an anxiety-like phenotype. Upon treatment with the antidepressant, fluoxetine, behavioural changes were reversed, suggesting a role for GR in affective disorders (Ziv et al., 2013).

1.2 Genomic actions of GC hormones

1.2.1 Glucocorticoid-binding receptors: orchestrators of GC hormone genomic action

In the rat brain, CORT acts upon regions expressing MRs and GRs to exert a multitude of effects on behaviour, emotion, cognition, and learning and memory. The MR and the GR were originally identified in the brain by radioligand binding assays (Reul and de Kloet, 1985) and initially referred to as “Type I” and “Type II” receptors, respectively. Despite the ability of MRs and GRs in the hippocampus to bind CORT, marked differences in their properties have been identified. One of the most pivotal initial studies investigating the properties of MR and GR highlighted striking differences in the microdistribution of

both receptors throughout the brain (Reul and de Kloet, 1985). Radioligand binding assays performed on micro-dissected brain tissue of rats revealed a discrete localisation of MR expression to the hippocampus, lateral septum and central amygdala, and a widespread distribution of GRs to regions such as the lateral septum, neocortex, cortical amygdala, paraventricular nucleus and locus coeruleus. A strong co-localisation of both receptors was observed in the hippocampus. Findings of this study also demonstrated that MRs display a very high affinity for CORT (Kd ~ 0.5nM) and are occupied by GCs to a large extent under all physiological conditions, while GRs have a much lower affinity for CORT (Kd ~ 5.0nM) (Reul et al., 1987) and become occupied when CORT levels are significantly elevated such as during the circadian rise or following acute stress (de Kloet, 2013).

The discrete hippocampal localisation of MR and GR mRNA in the rat hippocampus was further examined in later studies using *in situ* hybridization, revealing a widespread distribution of MR among all hippocampal subfields, in particular the cornu ammonis (CA) subfield, CA3. In contrast, the highest concentration of GR mRNA was found in the CA1 and CA2 subfields (Herman et al., 1989, Van Eekelen et al., 1988). Furthermore, radioligand binding studies revealed marked differences in their affinity for and occupancy by ligand (Reul and de Kloet, 1985, Reul et al., 1987). The distribution of MR and GR proteins have also been investigated. In the developing mouse brain, MR protein levels were investigated at different timepoints until adulthood, revealing exclusive expression of the MR within the nuclei of neuronal cell types and a complete lack of glial expression. At adulthood, MR expression was observed in the granule and pyramidal cell layers of the hippocampus, with the strongest expression levels observed in the CA2 (Kretz et al., 2001). In the rat brain, investigation of mRNA and protein levels of GR revealed a high presence of GR mRNA in the cytoplasm, while GR protein was predominantly observed the cell nucleus. The amygdala and hippocampus were among the brain regions where the highest densities of GR mRNA and protein were observed, with a differential pattern of GR protein and mRNA seen in the hippocampus. In the CA1-4, high levels of mRNA were observed, however protein GR was seen highest in the CA1 and CA2. The granule cell layer of the DG exhibited the highest level of GR mRNA and protein (Morimoto et al., 1996).

The MR is encoded by the *Nuclear Receptor Subfamily 3 Group C Member 2* (*Nr3c2)* gene located on chromosome 19, while the GR is encoded by the *Nuclear Receptor Subfamily 3 Group C Member 1* (*Nr3c1)* gene located on chromosome 18 of the rat genome. From these two genes, multiple splice

variants and translational isoforms of the corresponding receptor proteins have been identified, arising from both alternative promoter usage and splicing (Meijer et al., 2019). Alternative splicing of exons within *Nr3c1* has been shown to produce splice variants such as GRα and GRβ (Hollenberg et al., 1985), GR-A and GR-P (Moalli et al., 1993) and GR-γ (Rivers et al., 1999). Translational isoforms of these GR splice variants also arise due to alternative translation initiation, with the GRα mRNA transcript resulting in 8 GRα subtypes (Oakley et al., 2018). Multiple splice variants of the MR have been identified with differential expression occurring across the rat hippocampus (Zennaro et al., 1995). Alternative splicing usage within the 5' untranslated region (UTR) gives rise to three MR variants, however these do not lead to alternative MR protein isoforms. A splice variant within a coding region does give rise to alternative MR protein isoform (Bloem et al., 1995), while a splice variant with a 10 bp deletion in the C-terminal domain producing a truncated MR protein has also been identified in the rat (Zhou et al., 2000). Alternative promoter usage giving rise to variation in the 5-UTR region of the MR and GR may be important for tissue specific receptor expression (Turner et al., 2006).

Both receptors exhibit a structure characteristic of the steroid receptor superfamily (Figure 1.3.a), comprising of a DNA-binding domain (DBD), a hinge region (HR), a ligand-binding domain (LBD) and an amino terminal domain (NTD). A high degree of similarity between the DBD and LBD of both receptors was observed upon cloning of the MR (Arriza et al., 1987), while the NTD varies considerably between both receptors (Meijer et al., 2019). Many structural features of MRs and GRs facilitate their genomic activity. The DBD contains two zinc finger motifs which recognise target DNA sequences, allowing MRs and GRs to activate or repress the transcription of GC-target genes (Oakley and Cidlowski, 2013). Nuclear localisation signals, NL1 and NL2, found within the junction of the DBD/hinge region and the LBD, respectively (Oakley and Cidlowski, 2013), facilitate nuclear translocation of the receptors. Two activation domains, activation function-1 (AF-1) and activation function-2 (AF-2) located within the NTD and LBD, respectively, regulate the transcriptional activity of MRs and GRs via interactions with coactivator proteins (Kumar and Thompson, 2012).

In their inactive form, both receptors form a heteromeric complex with heat-shock proteins (hsps), immunophilins and other cochaperone proteins (Figure 1.3.b). The 90-kDa heat-shock protein Hsp90 binds, as a homodimer, the LBD and DBD of unligated MRs and GRs (Baulieu, 1991). Hsp90-receptor binding is stabilised by p23, a small cochaperone protein (Morishima et al., 2003), and the steroid-

receptor associated immunophilin, FK506 binding protein 51 (FKBP5) (Sanchez, 1990). FKBP5 also acts as a negative regulator of GR function, by reducing the affinity of the GR for GCs and the nuclear translocation of the receptor (Jaaskelainen et al., 2011). Following ligand binding and activation, MRs and GRs undergo a structural rearrangement which exposes the nuclear localisation signals, NL1 and NL2 (Oakley and Cidlowski, 2013). FKBP5 is exchanged for FK506 binding protein 52 (FKBP4), which interacts, via a peptidylprolyl isomerase domain (Galigniana et al., 2002), to cytoplasmic dynein; a molecular motor which transports MRs and GRs, along microtubular tracks to the nucleus (Harrell et al., 2004). The receptor-cochaperone complex passes through the nuclear pore and dissociation of the receptors from the cochaperone complex occurs in the nucleoplasm (Galigniana et al., 2010).

1.2.2 Genomic activity of MRs and GRs

Following nuclear translocation and dissociation from co-chaperone proteins, activated MRs and GRs form various dimeric complexes and exert transactivation or transrepression on GC target genes via interactions with DNA. Ambiguities surrounding the location of dimer formation and dimer composition have been circulating for decades. Initial studies reported nuclear translocation and DNA-binding to precede dimerization (Luisi et al., 1991), however the formation of dimers in the cytoplasm has been reported *in vivo* (Savory et al., 2001). MRs and GRs have been described as monomers (Wrange et al., 1986), homodimers (Wrange et al., 1989), heterodimers (Trapp et al., 1994, Mifsud and Reul, 2016) and tetramers (Presman et al., 2016). MR and GR dimers bind to consensus sequences within the DNA known as glucocorticoid response elements (GREs), thus regulating the expression of target genes.

The high degree of similarity within the DBDs of the MR and GR allows both receptors to interact with the same responsive elements. Positive GREs ((+)GREs) mediate target gene transactivation, while negative GREs ((-)GREs) mediate target gene transrepression. Both sequences have been approximated as “g/aGnACAnnnTGTnCt/c” (Strahle et al., 1987) and “CTCC(n)$_{0\text{-}2}$GGAGA” (Hudson et al., 2013), respectively. The 3 nucleotide spacer located between the two 6-bp half sites facilitate receptor dimerization at (+)GREs (Luisi et al., 1991), however the variable 0-2 nucleotide spacer in (-)GRE sequences indicates that dimerization may not be necessary for gene transrepression (Hudson et al., 2013). MRs and GRs have been found to bind to many variations of these motifs (So et al., 2007). 5 positions of the (+)GRE sequence have been shown to be invariant, and specific contact has been demonstrated between the GR and 4 bases of the 15bp motif (Luisi et al., 1991).

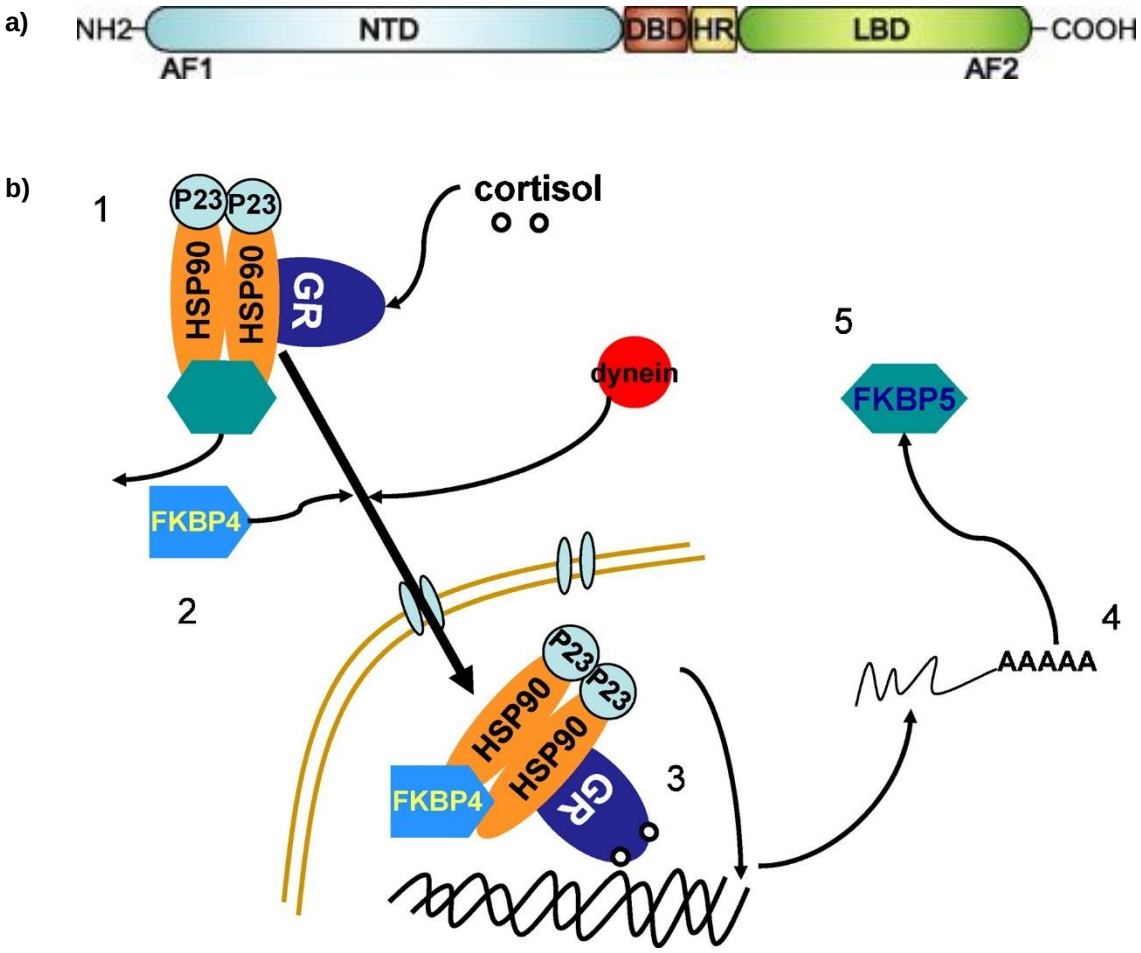

Figure 1.3 Steroid receptor superfamily structure and a schematic representation of the heteromeric GR complex before and after ligand binding

(a) The MR and GR are modulator proteins containing a poorly conserved N-terminal transactivation domain (NTD), a hinge region (HR), a highly conserved DNA-binding domain (DBD) and a ligand-binding domain (LBD). The activation domains, activation function-1 (AP-1) and activation function-2 (AP-2) lie within the NTD and LBD, respectively. Taken from (Ratman et al., 2013). (b) (1) The unligated GR remains sequestered in the cytoplasm by heat-shock proteins (Hsp90), the small cochaperone protein p23 and the steroid receptor associated immunophilin, FKBP5. In this conformation, GR has a low affinity for cortisol. (2) Once the GR becomes occupied by cortisol, FKBP5 is exchanged for FKBP4 which binds dynein, (3) allowing the translocation of the GR-complex into the nucleus. GR can bind to GREs within the DNA and exert transcriptional effects. (4) The GR increases FKBP5 transcription and translation, (5) thus conferring higher GR resistance, completing an ultra-short negative feedback loop on GR sensitivity. Taken from (Binder, 2009).

An in-depth analysis of MR binding motifs is currently lacking, however genome-wide sequencing has revealed many additional motifs to which GRs may bind and exert transcriptional effects on target genes. Motifs such as activation protein 1 (AP1), zinc finger and BTB containing 3 (Zbtb3), specificity protein 1 (SP1) (Polman et al., 2012, Polman et al., 2013) and neuronal differentiation 1 (NeuroD1) (Pooley et al., 2017) have been predicted within sites of the genome bound by GRs. Once bound to GREs or other responsive elements, MRs and GRs undergo additional conformational changes leading to the recruitment of coregulators and chromatin-remodelling complexes that modulate gene transcription rates by affecting the activity of RNA-polymerase (Oakley and Cidlowski, 2013).

1.2.3 Chromatin architecture as a mediator of MR and GR genomic and non-genomic activity

The ability of MRs and GRs to modulate transcription is dependent on a number of factors, one of which involves the accessibility of GRE sequences for binding. Within the cell, genetic material is condensed into a complex collectively known as chromatin. 147 base pairs (bps) of DNA coil around an octameric assembly of histone proteins to form an individual nucleosome unit, which is joined to adjacent nucleosomes by variable lengths of linker DNA (Swygert and Peterson, 2014). Chromatin architecture is a major determining factor in the accessibility of DNA sequences for TF binding, and densely packed chromatin can repress transcription by impeding protein-DNA interactions (King et al., 2012). An association between regions of accessible chromatin and GR binding has been demonstrated *in vitro*. A study employing genome-wide DNase I profiling alongside ChIP-seq demonstrated that the majority of GR binding, in mouse mammary adenocarcinoma cells following DEX treatment, occurred within areas of the genome which were pre-accessible prior to GC exposure or accessible following GC exposure (John et al., 2011). A high correlation between GR binding and chromatin accessibility in A1-2 cells treated with DEX was also demonstrated by formaldehyde assisted isolation of regulatory elements (FAIRE), a technique which isolates nucleosome-depleted DNA from chromatin (Burd et al., 2012).

The N-terminal tails of the core histone proteins, H2A, H2B, H3 and H4, which form the histone octamer core are often targets of covalent post-translational modifications (Wang et al., 2015) as they form flexible bonds with the DNA and adjacent nucleosomes which are easily adapted to allow dynamic changes in the accessibility of the underlying genome (Cheung et al., 2000). A subset of amino acid residues within the N-terminal tails can be covalently modified by the addition of acetyl, methyl and

phosphate groups, including lysine (K), serine (S) and threonine (T) residues (Taverna et al., 2007). Post translational modifications of histone H3 have been associated with transcriptional activation (Taniura et al., 2007), and following exposure to stress may facilitate the transcriptional activity of MRs and GRs. Exposure to an acute FS stressor has been shown to result in phosphorylation of serine10 (S10) and acetylation of lysine14 of histone 3 [H3S10p-K14ac] exclusively within mature neurons of the rat hippocampal DG. Antagonism of the GR was also shown to prevent the formation of this histone modification and of the acquired immobility response upon re-exposure to FS, which is representative of learning and memory formation in response to an acute stressor (Bilang-Bleuel et al., 2002).

Further studies demonstrated that the induction of the immediately early gene, *Fos Proto-Oncogene AP-1 Transcription Factor Subunit* (*Fos)*, was closely linked to the formation of this histone modification within DG granule neurons (Chandramohan et al., 2007). The formation of the H3S10p-K14ac histone modification has also been shown to involve a novel non-genomic mechanism of GR action between activated GRs, the *N*-methyl-*D*-aspartate (NMDA)-receptor and downstream histone modifying enzymes (Figure 1.4). Following FS, the NMDA receptor (NMDAR) initiates an intracellular signalling cascade known as the mitogen-activated protein kinase (MAPK) extracellular regulated kinase (ERK) (MAPK/ERK) cascade. Activation of this pathway leads to the downstream phosphorylation of mitogen- and stress- activated kinase 1 (MSK1) by extracellular regulated kinase 1/2 (ERK1/2). GR may act as a critical scaffold in this pathway for pERK1/2, enabling phosphorylation of MSK1 and of ELK-1, which induce the H3S10p-K14ac histone mark to de-condense chromatin structure, exposing target genes for transcription. Antagonism of the NMDAR, blockade of ERK1/2 or double knock out of MSK1/2 (MSK1/2 KO) attenuated the formation of the H3S10p-K14ac histone modification, and also prevented the adaptive learning (immobility behaviour) induced by FS. MSK1/2 KO also lead to a reduction in the number of DG *Fos*-positive neurons, further supporting that the immediate early gene is a transcriptional target of this pathway (Chandramohan et al., 2008). The acquired immobility behaviour demonstrated by rats in the 24 hr FS retest was shown to be maintained for at least 4 weeks (Gutierrez-Mecinas et al., 2011). The number of early growth response protein (Egr-1) positive DG neurons was also shown to increase significantly following FS, an effect which was attenuated by antagonism of the GR (Gutierrez-Mecinas et al., 2011).

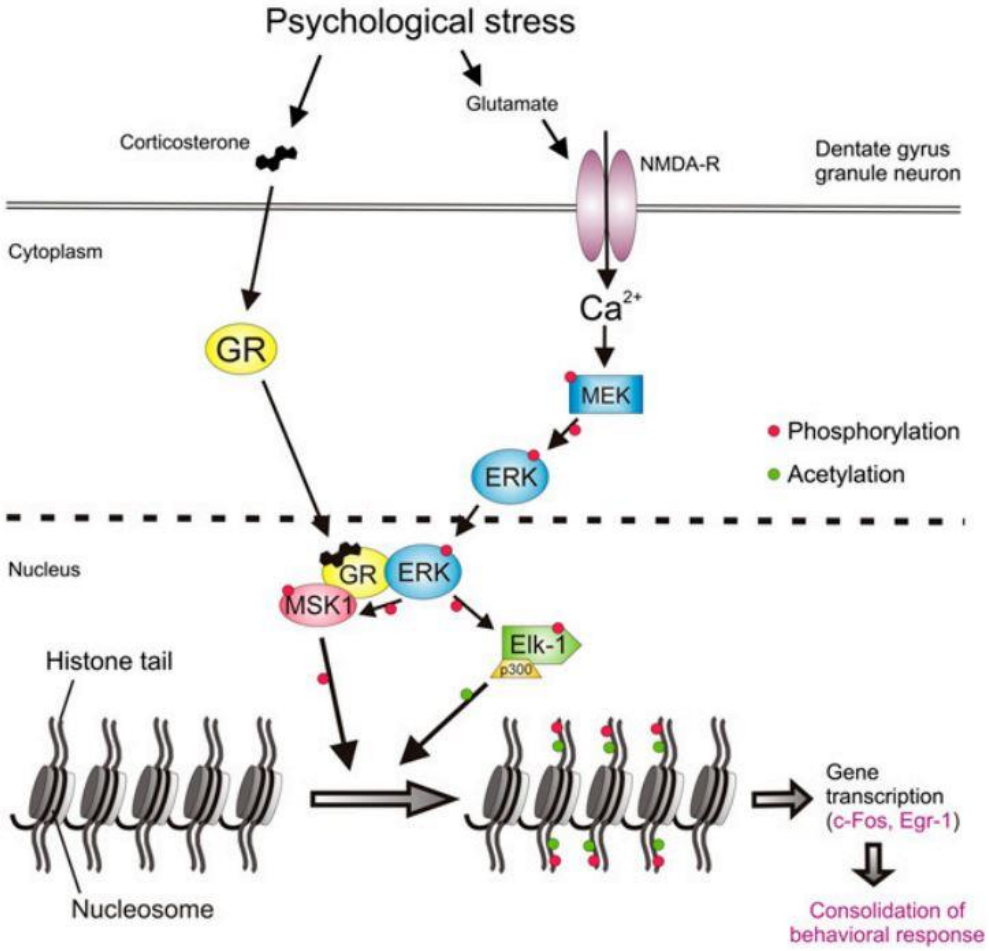

Figure 1.4 Schematic representation of the intracellular signalling cascade leading to the phosphorylation and acetylation of histone H3 within dentate gyrus granule neurons following exposure to psychological stress

Activation of the NMDA receptor initiates the MAPK/ERK signalling cascade and downstream phosphorylation of MSK1 and ERK 1/2. Ligand bound GRs may enhance the phosphorylation of MSK1 by pERK1/2. The red circles indicate a phosphorylated state or phosphorylation process, whereas the green circles indicate an acetylated state or acetylation process. *N*-methyl-*D*-aspartate (NMDA), Taken from (Gutierrez-Mecinas et al., 2011).

1.2.4 Coregulators as mediators of MR and GR genomic activity

Coregulators comprise a large and diverse group of proteins recruited by MRs and GRs that exert transcriptional effects without binding DNA. Coregulators can be subdivided into two classes based on their transcriptional activity, with coactivators inducing transactivation and corepressors inducing transrepression of GC target genes. The induction of gene expression by coactivators can occur via many mechanisms including chromatin remodelling, histone modification, transcription initiation, elongation of RNA chains and RNA splicing (Yang and Young, 2009) while corepressors can interfere with transactivation by inducing histone deacetylase (HDAC) activity, making inhibitory contacts with transcriptional machinery or interfering with the assembly of the transcriptional preinitiation complex (Goodson et al., 2005). MRs and GRs recruit numerous coregulators via their AF-1 and AF-2 domains within the NTD and LBD, respectively. Binding of coregulators within the AF-2 domain is a ligand dependent process often occurring via a conserved nuclear receptor box containing one or more LXXLL motifs (L = leucine, X = amino acid) (Heery et al., 1997), while coregulator recruitment via the AF-1 domain is a ligand independent process not involving the LXXLL motif (Yang and Young, 2009). Due to the high sequence similarity between the LBD of MRs and GRs, the receptors share many AF-2 interacting coregulators (Zalachoras et al., 2013), however many MR- and GR-specific coregulators have also been identified.

An ATP-dependent chromatin remodelling complex known as the switch/sucrose non-fermentable (SWI/SNF) complex was identified in yeast as one of the first GR coactivators (Yoshinaga et al., 1992). This complex utilises energy derived from ATP hydrolysis to separate the bonds between histones and DNA in order to reposition nucleosomes (King et al., 2012). The ATPase activity of SWI/SNF is mediated by one of the two highly homologous catalytic subunits, Brahma (BRM) or Brahma-related gene 1 (BRG1) (Johnson et al., 2008). Several BRM/BRG1 associated factors (BAFS) associate with the catalytic subunit to make up the SWI/SNF complex (King et al., 2012). The transcriptional activity of SWI/SNF has been demonstrated in mouse mammary adenocarcinoma cell lines expressing the steroid responsive mouse mammary tumour virus-long terminal repeat (MMTV-LTR), which contains a high number of GR binding sites. Cells transfected with GR alongside either BRG1 or BRM, were treated with the synthetic GC DEX, resulting in a 33- and 77-fold induction of MMTV transcription, respectively (Johnson et al., 2008). The steroid receptor coactivators (SRCs) have been identified as

coactivators of both MRs and GRs, with SRC-1 to be the first discovered (Onate et al., 1995) of the three distinct subtypes SRC-1, 2 and 3. Expression of SRC-3 has been shown in the hippocampus (Nishihara et al., 2003), while the SRC-1 splice variant, SRC1-a has been found in the hypothalamus and anterior pituitary (Meijer et al., 2000). SRC-1a has been shown to enhance GR-activated MMTV promoter activity in HeLa and A204 cells (Sheppard et al., 1998). This study also demonstrated coregulator activity of CREB binding protein (CBP) and p300, two closely related histone acetyltransferases which also act as coregulators of MRs and GRs. P300 was also shown to enhance GR-activated MMTV promoter activity, while CBP supressed the activity of the GC-responsive MMTV promoter in a dose-dependent manner (Kino et al., 1999). SRCs interact with MRs and GRs via the LXXLL motif within the AF-2 domain or via the AF-1 domain and can stimulate transcription by exerting direct histone acetyltransferase activity or recruiting CBP/p300 (Meijer et al., 2005). MRs have been shown to form a complex with SRC-1 in human embryonic kidney cells, as treatment with aldosterone demonstrated the assembly of MR, SRC-1 and a small ubiquitin-related modifier-1 (SUMO-1) conjugating enzyme, Ubc9, at a promoter of the MR target gene, *Epithelial sodium channel* (Yokota et al., 2007).

Nuclear receptor co-repressors (NCoR) and Silencing mediator of retinoic acid and thyroid hormone receptor (SMRT) have both been identified as corepressors of the MR and GR and shown to exert HDAC activity. GR repression of Thymic Stromal Lymphopoietin (TSLP) cytokine gene expression was shown to be mediated by GR binding within negative GREs and the formation of a NCoR/SMRT transrepression complex, alongside the HDAC activity of HDAC2 and HDAC3 (Surjit et al., 2011). GR repressed the transcription of *Nr3c1* mRNA in A549 cells, by forming a *cis*-acting repression complex with NCoR1 and HDAC3 at the transcriptional start site of *Nr3c1*. Within exon 6, GR and NCoR1 binding was also detected, and chromosome conformation capture (3C) revealed a chromatin loop formation between exon 6 and the promoter-proximal region of *Nr3c1,* allowing the repression complex to assemble and inhibit the initiation of *Nr3c1* transcription (Ramamoorthy and Cidlowski, 2013). MRs and GRs can regulate the transcription of target genes by physically interacting with other transcription factors (TFs) (Oakley and Cidlowski, 2013). GR monomers have been shown to bind and repress proinflammatory transcription factors such as AP-1 (Pearce and Yamamoto, 1993) and nuclear factor kappa B (Nf-kB) (Ronacher et al., 2009) while MR has been shown to transactivate AP-1 (Dougherty et al., 2016) and interact with the TF SP1 (Meinel et al., 2013).

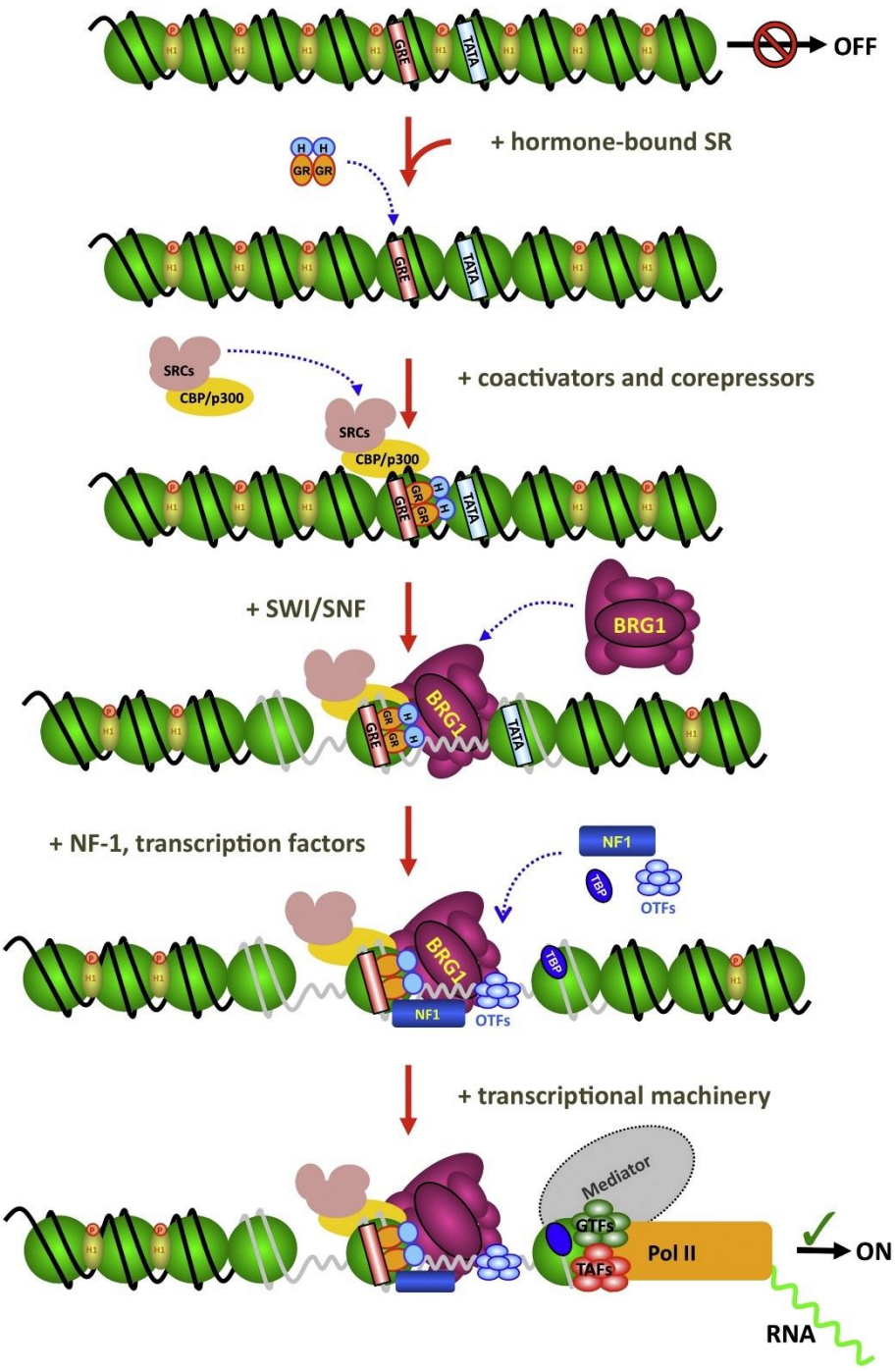

Figure 1.5 The recruitment of GR coactivators and corepressors mediating gene transcription Ligand-bound GR enters the nucleus and binds glucocorticoid response elements (GREs) within chromatin. Co-regulators such as SRC-1 and CBP/p300 are recruited. The BRG1 complex SWI/SNF is recruited to the promoter through an interaction with GR and nucleosomes are repositioned. This allows transcription factors such as NF1 and the octamer transcription factors (OTFs) as well as the TATA-binding protein (TBP). Finally, mediator proteins are recruited and the preinitiation complex forms leading to transcription by RNA Pol II. Taken from (King et al., 2012).

1.2.5 Elucidation of genome-wide MR and GR activity by next generation sequencing

Next generation sequencing (NGS) is emerging as a useful technology to elucidate the genomic actions of MRs and GRs. It is rapidly replacing microarray technology, which is limited to detecting predefined sequences, is associated with high background noise, cross hybridization problems, and is limited to measuring the relative abundance of transcripts (t'Hoen et al., 2008). Regions of the genome to which MRs and GRs bind are identified by sequencing DNA obtained by chromatin immunoprecipitation (ChIP), a technique where DNA-binding proteins are crosslinked to DNA with formaldehyde, the DNA is sheared into fragments, and specific antibodies extract DNA fragments bound by the target DNA-binding protein (Park, 2009). Alongside ChIP-seq, RNA-sequencing (RNA-seq) can be used to analyse the entire transcriptome to determine expression levels of genes which may be under MR and GR regulation. The combined use of ChIP-seq and RNA-seq to determine which genes are targeted by GC action appears promising, however integration of data arising from both technologies remains a significant challenge (Angelini and Costa, 2014).

Sequencing technology has rapidly advanced since the emergence of Sanger dideoxynucleotide sequencing (Sanger et al., 1977) which was limited to sequencing at the single gene level. Many advances have led to the introduction of massively parallel sequencing with higher throughput and improved accuracy, launching the next generation in sequencing technologies. The concept underlying NGS involves a DNA polymerase catalysing the incorporation of fluorescently labelled deoxyribonucleotide triphosphates (dNTPs) into a DNA template strand during sequential cycles of DNA synthesis. During each cycle, at the point of incorporation, the nucleotides are identified by fluorophore excitation. This process is extended across millions of fragments in a massively parallel fashion. Many NGS platforms have been developed based on this concept, however the majority of the world's sequencing data has been generated by the Illumina sequencing platform (Illumina, 2017) which has four basic steps (Figure 1.6).

Following the alignment, bioinformatic analysis of ChIP-seq and RNA-seq data is performed. For analysis of ChIP-seq data, "peaks" or regions of the genome significantly bound by the target transcription factor are annotated to the nearest gene. Differential binding analysis of ChIP-seq data can determine whether the binding of a given transcription factor is significantly upregulated or downregulated between experimental conditions. For analysis of RNA-seq data, read fragments are

mapped, counted and normalised to determine expression levels. Differential expression analysis (Hitzemann et al., 2014) is widely used on RNA-seq data to determine whether the expression of a given gene is significantly upregulated or downregulated between experimental conditions.

A number of studies have been carried out using ChIP-seq and RNA-seq to elucidate the genomic actions of MRs and GRs under various experimental conditions. ChIP-seq and RNA-seq of human A549 lung epithelial carcinoma cells treated with DEX revealed over 4,000 significant GR peaks and differential expression of over 200 genes in response to DEX treatment. GR peaks were primarily found in regions upstream of the transcriptional start site (TSS), while the majority of GR peaks located within genes were found in introns. 62% of GR peaks were found to contain a GRE, while the predominant motif among peaks lacking a GRE was identified as an AP-1 binding site. The majority of genes identified by RNA-seq were upregulated (59%) compared to downregulated (41%), and the upregulation was slightly but significantly stronger than the downregulation. ChIP-seq and RNA-seq datasets were cross-examined, which revealed that 47% of significantly upregulated genes contained a GR peak within 10 kilobases (kbs). GR peaks were located much further from significantly downregulated genes (Reddy et al., 2009).

Later studies identified fewer peaks, with over 1000 significant GR binding sites in neuronal PC12 cells by ChIP-seq (Polman et al., 2012), with more than 50% containing a GRE. These GR peaks were annotated to genes playing a role in neuronal processes such as neuronal projection morphogenesis, neuron projection regeneration and synaptic transmission. The majority of GR peaks were located upstream or downstream of a gene, while GR peaks located within genes were primarily observed within intronic regions. RNA-qPCR on a subset of genes revealed significantly upregulated RNA levels of 6 genes annotated to GR peaks, and significantly downregulated RNA of one gene annotated to a GR peak. GR peaks associated with upregulated RNA were found to contain GREs, while no GREs were found within GR peaks annotated to the downregulated gene.

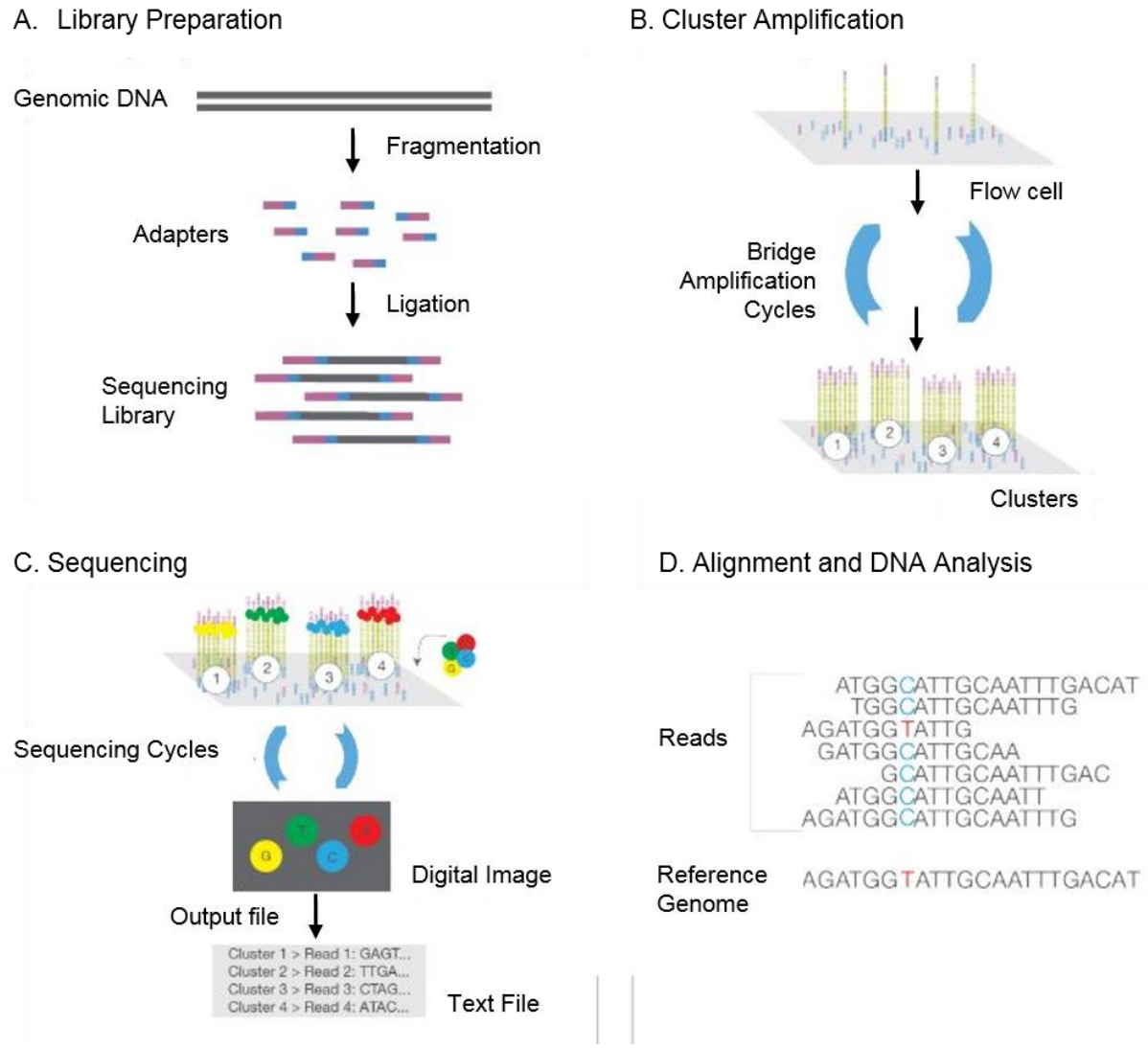

Figure 1.6 A schematic representation of the Illumina next generation sequencing platform

(A) The DNA library is prepared by random fragmentation of the DNA or cDNA sample and the addition of adaptors to the 3' and 5' end of the DNA or cDNA fragments. (B) The library is loaded into a flow cell containing surface bound oligos complimentary to adaptors added during library preparation and each fragment is amplified into distinct, clonal clusters. (C) Sequencing reagents and fluorescently labelled nucleotides are added to the flow cell, and the first sequencing primer is extended to produce the first read. With each cycle, fluorescently tagged nucleotides compete for addition to the growing chain however only one is incorporated, based on the sequence of the template. After the addition of each nucleotide, the clusters are excited by a light source and a characteristic fluorescent signal is emitted. Hundreds of millions of clusters are sequenced in this massively parallel process, with the read depth ranging from 20 to 400 million reads. (D) Once sequencing has been completed, the sequence read pairs are aligned to a reference genome. Adapted from (Illumina, 2017).

ChIP-seq of hippocampal tissue of ADX rats supplemented with low or high doses of CORT revealed over 2400 significant GR peaks (Polman et al., 2013). These GR peaks were annotated to genes playing a role in neurite projection, neuron differentiation and cell survival. Over 99% of these GR peaks contained a GRE and the majority were located upstream or downstream of a gene, while GR peaks located within genes were primarily observed within intronic regions. ChIP-qPCR was carried out on a subset of genes and revealed a differential binding pattern of the MR, particularly with higher CORT concentrations. As a follow on from this work (Polman et al., 2013), MR ChIP-seq was conducted on hippocampal tissue of ADX rats exposed to both low (300µg/kg) and high (3000µg) doses of CORT. The MR peaks were compared with previously identified GR peaks present in ADX rats supplemented with high doses of CORT, to identify distinct and overlapping regions of the genome to which MRs and GRs bind. Over 1,400 GR-exclusive binding sites were identified, while fewer MR-exclusive (n=918) and MR-GR overlapping (n=475) were found. All peaks were found to contain a GRE, while the Atoh1 motif was reported as the most prominent motif in MR-exclusive binding sites. Biological processes associated with specific and overlapping peaks were subsequently identified by pathway analysis, with genes annotated to MR-exclusive peaks linked to cell projection and adhesion, genes annotated to overlapping peaks associated with synaptic plasticity and GR-exclusive peaks linked to synaptic vesicles (van Weert et al., 2017). A recent ChIP-seq study carried out on stressed and non-stressed ADX rats supplemented with CORT identified over 7000 GR enrichment sites in the hippocampus (Pooley et al., 2017). These GR peaks were annotated to genes involved in neuron development and differentiation, synaptogenesis and neuron projection development. Surprisingly, GR binding was not shown to be significantly different between stress and non-stressed rats. The majority of GR peaks were detected in intergenic regions or within introns. 49% of GR peaks contained a GRE while 61.2% of all GR peaks contained a motif resembling a GRE half-site.

These studies, however, pose many limitations. The lack of biological replicates (n = 1) in these studies increases the possibility that the high number of binding peaks reported may not be reproducible. PC12 cells have been extensively used to study neuronal function in relation to GCs and display properties similar to those of sympathetic neurons such as neurite development, and electrical activity (Polman et al., 2012). Human A549 lung epithelial carcinoma cells are also widely used in GC hormone research (Reddy et al., 2009), however cell lines simply cannot replicate the properties of cells in an intact animal. Studies conducted on ADX rats supplemented with CORT do not represent physiological conditions,

due to the depletion of endogenous CORT and potential effects of ADX on the neurodegeneration of hippocampal DG cells (Sloviter et al., 1989). Furthermore, MR ChIP-seq is limited to a single study (van Weert et al., 2017), and no study has currently investigated the genome-wide binding of both MRs and GRs under physiological conditions to determine how they interact with stress and one another under stress or circadian conditions.

1.2.6 The Krüppel-like factors: MR and GR target genes

Many members of the Krüppel-like factor (KLF) family of transcription factors have been identified as transcriptional targets following elevations in CORT (Datson et al., 2011, Mychasiuk et al., 2016, Reddy et al., 2009), therefore may play a role in orchestrating GC-related effects during the acute stress response or following circadian input. The KLFs have been named based on their sequence homology with the DNA-binding domain of Krüppel protein; an embryonic pattern regulator found in *Drosophila melanogaster* (Yin et al., 2015). All KLF family members contain a characteristic zinc finger domain also shared by the Specificity Protein (SP) family of transcription factors (Wimmer et al., 1993). Although KLFs are often grouped with the SP family, little homology is observed between the KLFs and SPs outside of the characteristic zinc finger domain (Suske et al., 2005). 17 members of the KLF family have been characterised to date in humans and are named chronologically; KLF1-17 (Turner and Crossley, 1999), with 11 of these 17 homologs found in rat (Kaczynski et al., 2003). Many physiological processes regulated by GCs are also regulated by the KLFs, such as metabolism, immunity and cardiovascular function (McConnell and Yang, 2010). KLFs have been widely implicated in proliferation, differentiation and development of many cell types (McConnell and Yang, 2010), and in the brain where KLFs are abundantly expressed where they have been shown to influence processes such as neural development and response to injury (Yin et al., 2015).

KLF family members exhibit a characteristic structure (Figure 1.7.a). Like MRs and GRs, KLFs share a highly conserved DNA-binding domain which facilitates their transcriptional effects. Within the DBD, three Cys_2/His_2 zinc fingers allow KLFs to bind CACCC elements and GC-rich regions of DNA and regulate transcription (Pearson et al., 2008). Each zinc finger recognizes three base pairs in the DNA sequence, interacting with nine base pairs in total (McConnell and Yang, 2010). Similar to MRs and GRs, KLFs also contain nuclear localisation sequences, which are found within or in close proximity to zinc finger motifs of the DNA-binding domain. The NTD of KLF proteins varies significantly between

subtypes and contains domains that mediate transcriptional activation or repression. KLFs also recruit co-regulatory proteins such as co-activators, co-repressors and chromatin remodelling factors to domains within the N-terminal to exert transcriptional effects (Kaczynski et al., 2003).

The genes encoding the KLFs are randomly dispersed throughout the genome, which may explain the diversity of function observed among the KLF proteins (Kaczynski et al., 2003). KLF1, 2 and 4, however are more closely related to one another than to other members of the protein family (Dang et al., 2000) and the amino acid sequences of KLF6 and KLF7 show a high degree of homology and almost identical NTDs (Laub et al., 2001). Based on the diversity of function observed among the KLF proteins, they have been divided into three distinct subgroups according to their transcriptional effects (Figure 1.7.b). KLF3, 8 and 12 are classified as “Group 1” KLFs and repress transcription via interactions with C-terminal binding protein (CtBP) at a CtBP-binding site located in the N-terminal region. Group 2 KLFs include KLF 1, 2, 4, 5, 6 and 7 and predominantly activate transcription. Group 3 KLFs such as KLF9, 10, 11, 13, 14 and 16 interact with Sin3A, a common transcriptional co-repressor, via a Sin3A binding site within the N-terminal region to repress transcription. KLF15 and 17 have not been grouped as they contain no defined protein interaction motifs. Histone acetyltransferases (HATs) which interact with MRs and GRs, such as CBP, p300 and p300/CBP-associated factor (P/CAF) also interact with KLFs to facilitate transcriptional repression or activation depending on the KLF subtype. (McConnell and Yang, 2010).

A number of KLFs are found in various cell types throughout the nervous system, such as neurons, astrocytes, microglia, oligodendrocytes and cerebral vascular cells and many neurobiological processes have been shown to be mediated by KLFs (Yin et al., 2015). A role of KLF4 in neurite and axon outgrowth has been suggested, and KLF4 was shown to suppress neurite and axon outgrowth of optic nerve retinal ganglion cells (RCGs) and increase the regeneration potential of damaged RGCs (Moore et al., 2009). Neurogenesis and neuronal migration may also involve KLF4, as constitutive expression of KLF4 prevented the migration and development of neural progenitors in the cerebral cortex (Qin and Zhang, 2012). Studies investigating the expression pattern of KLF7 during embryogenesis and development strongly suggest a role of this gene in neurogenesis (Laub et al., 2001). KLF7 is also believed to play a role in differentiation, with delayed neuronal differentiation of embryonic stem cells observed upon silencing of the gene (Caiazzo et al., 2010). A relationship between

KLF9 expression and neural development has also been shown, with forced expression of the gene resulting in increases in cells reflective of neuronal differentiation and maturation (Bonett et al., 2009).

Many of these effects may be mediated by GC action on KLF gene expression, as many studies have identified the KLFs as GC target genes. In the PFC, exposure to chronic stress led to upregulated mRNA expression of *Klf4* in male rats (Mychasiuk et al., 2016). Expression of the *Klf4* protein was significantly increased in the hippocampus and cortex of male rats exposed to psychological stress, while increased *Klf4* mRNA and protein levels were elevated in HT-22 cells following CORT treatment. Antagonism of the GR, by treatment with RU486, abolished increases in *Klf4* protein levels (Li et al., 2017). Cardiac expression of *Klf13* mRNA and protein was significantly reduced in mice following GR KO. Moreover, increased GR binding at a GRE within intron-1 of *Klf13* following exposure of HL-1 cardiac muscle cells to the synthetic GR agonist, DEX (Cruz-Topete et al., 2016). DEX was shown to significantly increase the expression of *Klf4*, *Klf5, Klf6* and *Klf9* and decrease the expression of *Klf10* in human A549 lung epithelial cells. Furthermore, GR binding sites harbouring GREs have also been found in close proximity to *Klf5* and *Klf9*, indicating that GR transactivation at this site may be inducing the expression of these genes (Reddy et al., 2009). In particular, *Klf9* has been shown to respond to changes in GC levels. *In silico* GRE prediction identified a GRE within *Klf9* and *Klf9* mRNA levels have been found to be upregulated by CORT in the dentate gyrus of the rat hippocampus (Datson et al., 2011).

These findings are supported by the observation of high levels of GR binding in close proximity to *Klf9* within rat hippocampal tissues (Polman et al., 2013). Exposure to acute restraint stress and CORT treatment was shown to increase hippocampal *Klf9* mRNA levels in mice, while no significant changes were detected following exposure to chronic restraint stress (Besnard et al., 2018). Increased *Klf9* mRNA expression was observed in DEX treated mouse liver, an effect which was attenuated following antagonism of GR by treatment with RU486 (Cui et al., 2019). A role for signalling between GCs, KLF15 and branched chain amino acid signalling in spinal muscle atrophy was shown in *survival motor neuron 1 (SMN1)* KO mice. The *SMN1* gene encodes the survival motor neuron (SMN) protein which maintains motor neuron function. Skeletal muscle mRNA expression of *Klf15, GRα* and *GRβ* were dysregulated in *SMN1*-KO mice, while treatment with the GR agonist prednisolone significantly enhanced *Klf15* mRNA levels (Walter et al., 2018). Although GC hormones have been shown to induce *Klf* expression,

the effects of stress and the circadian drive on *Klf* expression have not been fully investigated. Presently it is also unclear whether genomically acting GC receptors, in particular the MR, are responsible for GC regulation of *Klf* expression.

1.3 Glucocorticoid hormone action throughout the brain via MRs and GRs

GC hormones elicit a broad range of physiological responses following acute stress or circadian input by acting on the brain. CORT freely passes the rat blood-brain barrier (BBB); a structure which functions to regulate the movement of compounds from the plasma circulation to the brain. Once GC hormones have dissociated from CBG and are freely available to penetrate tissues, they exert a diverse range of effects on a number of brain regions which play a role in memory, anxiety and decision making in response to arousing or stressful situations.

1.3.1 Glucocorticoids and the hippocampus

The initial discovery of GC hormones in the rodent brain identified the hippocampus, a structure shown to play a significant role in learning and memory (Scoville and Milner, 1957), as a GC hormone target (McEwen et al., 1968). The hippocampal structure consist of the DG, CA fields which are subdivided into four regions; CA1-4, and the subiculum (Wible, 2013). The DG of the hippocampus is of particular interest, as it is one of the few brain regions in which the process of “neurogenesis”, involving the generation of new-born neurons typically occurring during development, persists throughout adulthood (Kaplan and Hinds, 1977). Primarily within the subgranular zone of the DG, granule cells are born and migrate into the granule cell layer, where they form synaptic connections and differentiate into glial cells or neurons (Cameron et al., 1993). The sensitivity of the hippocampus to stress is not surprising given the high degree of MR and GR co localisation in this brain region. The highest concentrations of MRs are typically found within the DG, dorsal subiculum, CA1 and CA2 subfields while the highest levels of GRs are found in the lateral septum, DG and CA3 (Herman et al., 1989, Reul and de Kloet, 1985, Van Eekelen et al., 1988).

GC hormone action, via hippocampal MRs and GRs, has been shown to regulate hippocampal gene expression, development, neurogenesis, morphology and hippocampal-dependent learning and memory. Furthermore, hippocampal-dependent learning has been shown to enhance neurogenesis within the DG (Gould et al., 1999), an effect which may be mediated by GC hormone action.

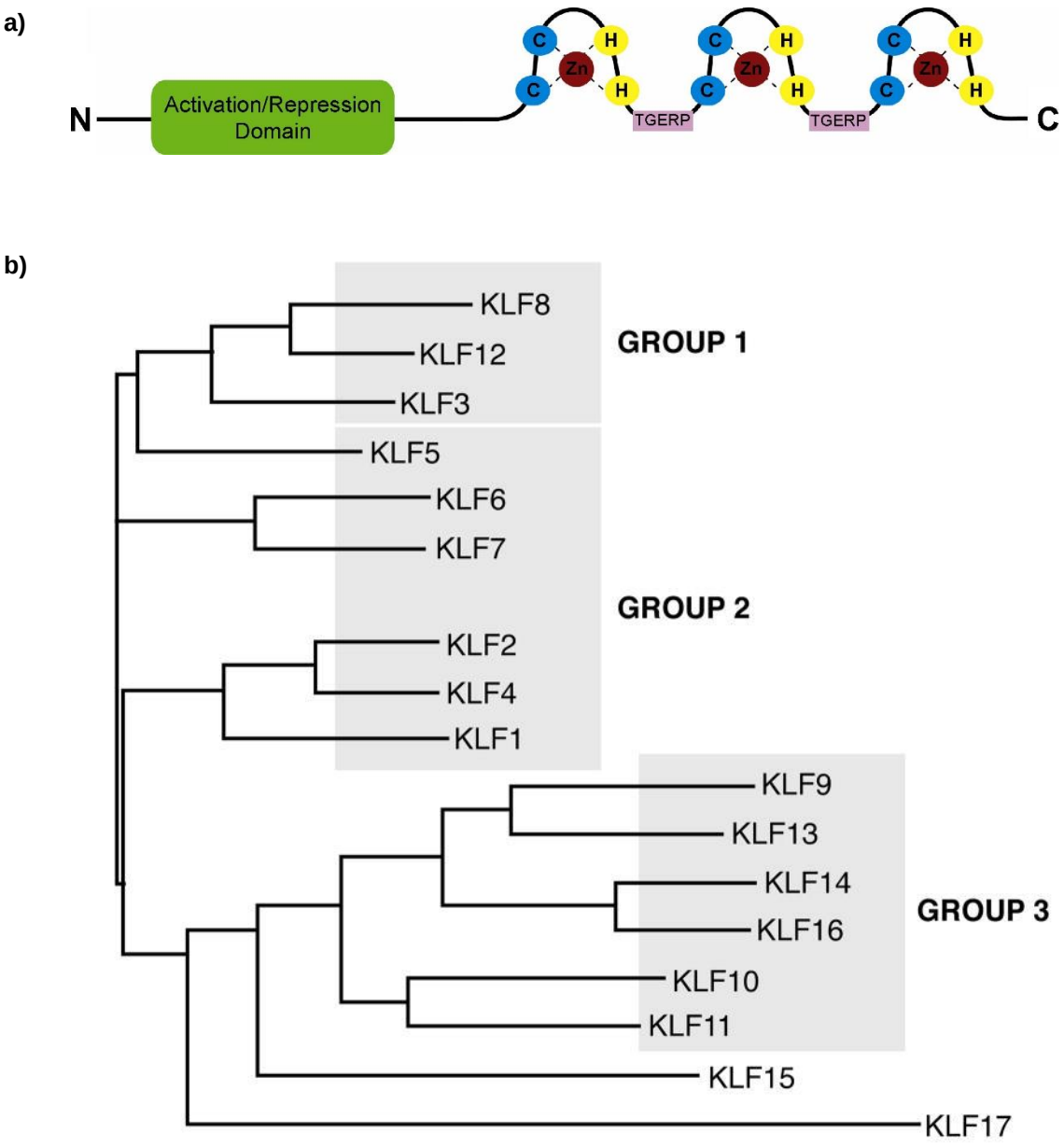

Figure 1.7 Schematic representation of the KLF transcription factor structure (a) and the grouping of KLF family members according to phylogeny and functional similarities (b)

(A) Members of the KLF family exhibit a characteristic structure consisting of an N-terminal Activation/Repression domain, three C-terminal Zinc fingers, each chelating a single zinc ion. Each Zinc finger is linked by a TGERP-like motif which facilitates DNA binding. Taken from (Pearson et al., 2008). (B) KLFs are subdivided into three groups based on their structural characteristics and functional effects. Group 1 and 3 KLFs repress transcription while group 2 KLFs activate transcription. Taken from (McConnell and Yang, 2010).

GC hormones exert a wide range of genomic affects within the hippocampus via MRs and GRs, with genome-wide changes in the transcription of many genes observed following exposure to stress. Exposure of rats to an acute FS stressor was shown to significantly upregulate the binding of MRs and GRs at responsive elements within 3 well-established GC-inducible genes; *FK506 binding protein 51* (*Fkbp5), Period 1 (Per1)* and *Serum and glucocorticoid-regulated kinase 1 (Sgk1).* Increased levels of hippocampal heteronuclear RNA (hnRNA) and mRNA levels of *Fkbp5, Per1* and *Sgk1* were also observed at various timepoints following exposure to FS, indicating that the binding of MRs and GRs may underlie these transcriptional responses (Mifsud and Reul, 2016). In a microarray study on RNA isolated from human hippocampal progenitor cell lines treated with high and low doses of GCs, a number of GC responsive genes were identified. These genes were predicted to be associated with signalling pathways such as Hedgehog signalling, a pathway involved in neuronal differentiation, and Forkhead box (FOX) O3A (FOXO3A) signalling which has been implicated in neurogenesis, depression and GC action (Anacker et al., 2013). The effect of chronic stress exposure on gene expression within the hippocampal DG was examined in rats using microarray, revealing 90 genes to be significantly differentially expressed. These genes were predicted to play a role in long-term potentiation (LTP) and long-term depression (LTD) (Datson et al., 2012). RNA-seq identified changes in gene expression within the hippocampus of rats exposed to a novel environment stressor daily for 2 weeks, with 15 genes differentially expressed in male rats and 16 genes differentially expressed in female rats. Interestingly, the mRNA expression of the hsp90 gene, *Heat shock protein 90-alpha,* was downregulated. These genes were predicted, by pathway analysis software, to regulate LTP (Mychasiuk et al., 2016).

GC hormones play an important role in regulating neurogenesis within the DG, which, unlike other brain structures, generates the majority of its cells postnatally (Cameron et al., 1993). The period during which cell birth and cell death is maximal in the DG coincides with the early postnatal stress hyporesponsive period, which is characterised by naturally low GC levels (Gould et al., 1991a). GCs have been shown to regulate the rate and pattern in which granule cells are generated postnatally, with GC administration during the first postnatal week shown to inhibit neurogenesis (Bohn, 1980). Furthermore, increased GC levels during the first postnatal week was shown to decrease the density of pyknotic cells in the granule cell layer (Gould et al., 1991b). The effects of GC hormones on adult neurogenesis have been shown to vary depending on the duration and degree of exposure to GC hormones. Enhanced generation of glial cells and neurons within the DG has been reported following the removal of GC hormones by ADX

(Gould et al., 1992). Exposure to physiological levels of GC hormones imposed by the circadian rhythm, however, was reported to have no effect on neurogenesis, while decreased cell proliferation was observed following exposure to persistently high GC levels (Ambrogini et al., 2002). Antagonism of the GR was shown to rapidly reverse the impairments in neurogenesis seen in adult rats following chronic GC exposure (Mayer et al., 2006). The MR and GR may have differential roles in regard to neurogenesis, with MR-dependent increases in proliferation and differentiation of NPCs into astrocytes and GR-dependent decreases in proliferation and differentiation reported following exposure of hippocampal progenitor cells to low and high GC levels, respectively (Anacker et al., 2013). GCs may also play a role in the maintenance of hippocampal structure. A steroidogenic disorder characterised by GC deficiency has been shown to lead to changes in hippocampal structure. The hippocampi of female congenital adrenal hyperplasia (CAH) patients were shown, by functional magnetic resonance imaging (fMRI), to exhibit lower fractional anisotropy; a measure of axonal structure integrity in the brain influenced by fibre density, myelination and axonal calibre (Webb et al., 2018). MRI showed a significant negative correlation between the hippocampal volume and the ratio of serum GC to dehydroepiandrosterone (DHEA) and its sulphate ester (DHEAS); hormones thought to antagonise the effects of GCs in the central nervous system (CNS). Moreover, in subjects with major depressive disorder, a significant positive correlation was observed between DHEAS levels and hippocampal volume (Jin et al., 2016).

An “inverted-U” relationship has been described between GCs and learning and memory, in which low to moderate GC levels facilitate, while high GC levels impair learning and memory. LTP, an electrophysiological process involving a long-lasting enhancement of synaptic efficacy following high frequency stimulation of afferent fibers, is a widely used model of hippocampal memory formation and also exhibits an inverted-U relationship with GC levels (Diamond et al., 1992, Yau et al., 1995). This inverted-U relationship has led to studies reporting conflicting results regarding the effects of GC in tasks involving hippocampal-dependent learning and memory. Many studies have reported enhanced hippocampal-dependent learning and memory formation following acute exposure to moderate levels of GCs. Enhanced learning and memory formation following acutely stressful challenges which engage the hippocampus, such as FS, has been shown to depend on the presence of GC hormones (Jefferys and Funder, 1987, Mitchell and Meaney, 1991, Veldhuis et al., 1985, Jefferys et al., 1983). Reduced levels of GR mRNA in the hippocampal DG has been shown to impair learning and memory in the FS

test (Korte et al., 1996), while hippocampal MRs have been shown to significantly increase following FS training (Gesing et al., 2001). Blockade of MR action, however, does not affect FS behaviour. Following FS, GRs have also been shown to interact with the NMDAR-activated MAPK-ERK pathway, allowing consolidation of long-lasting behavioural responses (Gutierrez-Mecinas et al., 2011). GC hormones have also been shown to play an important role in tasks involving hippocampal-dependent spatial learning and memory formation, including the Morris water maze (MWM) paradigm (Oitzl et al., 1998). A positive correlation was found between antidepressant induced elevations in MR mRNA expression and MWM performance (Yau et al., 1995) while antagonism of MRs has been shown to impair spatial learning in the MWM (Yau et al., 1999). Furthermore, ADX experiments have shown that GCs are essential for enhancing the acquisition of associative memories following a stressful experience. ADX prevented hippocampal-dependent acquisition of trace conditioning and hippocampal-independent delay conditioning (Beylin and Shors, 2003). Despite the role of GC hormones in hippocampal dependent memory has been widely reported, findings vary between studies. Following administration of exogenous cortisol, no increase in cerebral blood flow to the hippocampus was detected by fMRI during autobiographical memory retrieval; a type of long-term memory involving episodic memory and autobiographical knowledge (Fleischer et al., 2019).

In contrast, negative effects on hippocampal-dependent learning and memory formation have been reported by studies examining chronic exposure to high GC levels. Exposure of rats to a potent stressor was shown to impair hippocampal LTP and had a negative impact on working memory (Diamond and Rose, 1994), while continuous blockade of the GR was shown to enhance hippocampal-dependent spatial learning in the MWM (Oitzl et al., 1998). Furthermore, rats exposed to single-prolonged stress exhibited decreased levels of hippocampal MRs and GRs, a reduced MR/GR ratio in the hippocampus and changes in the distribution of GR among hippocampal subregions (Zhe et al., 2008). The negative effects of GC hormones on learning and memory may be influenced by age, as exposure to high social stress was shown to induce significant spatial learning impairments in the MWM in middle aged rats, while young rats did not display any behavioural deficits following short-term exposure to moderate GC levels (Bodnoff et al., 1995). Long-term exposure to high GC hormone levels, however, was reported to induce cognitive deficits in young rats (Dachir et al., 1993), indicating that chronic stress may have a negative impact on the hippocampus irrespective of age.

1.3.2 Glucocorticoids and the amygdala

The amygdala, a key limbic brain region essential for adaptation to stress, is an important target of GC hormone action (Kolber et al., 2008), with high levels of GR expression and to a lesser extent, MR expression observed within the central and cortical amygdala (Reul and de Kloet, 1985). Furthermore, the amygdala also contains CRH nerve terminals (Uryu et al., 1992), cell bodies (Cummings et al., 1983) and receptors (De Souza et al., 1985) and stimulation of the amygdala has been shown to promote the release of GC hormones, which may enhance the HPA response to behavioural stressors (Shepard et al., 2003). To date, no published studies have examined changes in MR and GR binding to GREs within the amygdala following exposure to stress, however GC hormone action has been shown to regulate gene expression within the amygdala. The nuclear translocation and DNA-binding of GRs in the amygdala has been investigated in ADX rats following treatment with low, intermediary and high doses of CORT. Intermediate and high doses of CORT significantly increased the nuclear translocation of the GR within the amygdala, while DNA binding was significantly increased by a high dose of CORT (Spiga and Lightman, 2009). Many studies have reported changes in gene expression in the amygdala following exposure to stress. Exposure of rats to a single restraint stress was shown to result in the differential mRNA expression of over 600 genes and the differential protein expression of over 200 proteins within the basolateral nucleus of the amygdala (BLA), including proteins known to regulate intracellular stress responses (Sillivan et al., 2019). Daily chronic restraint stress for 2 weeks resulted in the differential expression of 125 genes in the amygdala which were predicted to be associated with Huntington's disease (Andrus et al., 2012). The mRNA expression levels of GABAergic marker genes *glutamic acid decarboxylase (GAD) 65* and *GAD67, neuropeptide Y (NPY), somatostatin (SST)* and *cholecystokinin (CCK)* were increased in the BLA of water exposed stress rats compared with rats undergoing MWM training. Stress has been shown to modulate GABAergic signalling within the BLA, while *NPY, SST* and *CCK* encode neuropeptides expressed within hippocampal subregions involved hippocampal-dependent spatial learning (Hadad-Ophir et al., 2014). In a mouse model of PTSD, induced by chronic foot shock fear conditioning, over 1000 genes were differentially expressed in the amygdala, including genes predicted to be related to nervous system development, neurogenesis and neural precursor cell proliferation (Tanaka et al., 2019).

Following a stressful or emotionally arousing experience, GC hormones act on the amygdala to promote memory consolidation (Roozendaal et al., 2009) by interacting with the amygdalar noradrenergic system (Roozendaal et al., 1999). The memory enhancing effects of GC hormones are believed to occur as a result of the amygdala modulating memory storage processes in other brain regions (McGaugh et al., 1996). Training known to involve the amygdala induces the expression of transcriptionally regulated genes implicated in synaptic plasticity in brain areas including the hippocampus, striatum and cortex. (McGaugh, 2004). Furthermore, the amygdala may modulate hippocampal function in response to stress (Kim et al., 2001) and has been shown to interact with the hippocampus via direct and indirect projections (McGaugh, 2004). The amygdala has been shown to play an important role in the regulation of hippocampal LTP, as studies have reported lesions of the BLA to attenuate LTP within the DG (Ikegaya et al., 1994). In addition to blocking stress effects on hippocampal LTP, amygdalar lesions were also found to block stress effects on hippocampal-dependent memory formation (Kim et al., 2001). Acute stress has been shown result in changes in the functional connectivity within the amygdala. fMRI of stress responsive humans revealed enhanced resting state functional connectivity within the amygdala during stress exposure, in addition to increased connectivity between the amygdala and the hippocampus during the stress recovery period (Quaedflieg et al., 2015).

Many studies have examined the role of GC hormone action within the BLA which plays a role in the acquisition and consolidation of fear memory and the central nucleus of the amygdala (CeA), which plays a role in the expression of autonomic and behavioural correlates of conditioned fear (Kolber et al., 2008). Administration of a GR agonist to the BLA was shown to enhance memory retention following an inhibitory avoidance task, while treatment with a GR antagonist impaired memory within the MWM (Roozendaal and McGaugh, 1997). This GC-induced enhancement of memory-consolidation via the BLA may also involve GR action within noradrenergic cell groups of the nucleus of the solitary tract (NTS) of the brain stem, via noradrenergic projections from the NTS to the amygdala (McGaugh, 2004). Administration of a GR agonist to the NTS enhanced retention performance in inhibitory avoidance training, an effect which was blocked by, antagonism of β-adrenergic activity within the BLA (Roozendaal et al., 1999). Fewer studies have examined GC hormone action on the CeA, however conditioned fear (Thompson et al., 2004) and GC treatment (Shepard et al., 2000) have been shown to increase CRH within the CeA. The CeA may be a site of memory acquisition and consolidation possibly

attributed to GRs, as GR deletion in the CeA of mice has been shown to prevent the development of fear conditioning behaviour (Kolber et al., 2008). Stereotaxic delivery of GCs to the amygdala was shown to enhance GC production in response to a behavioural stressor, without altering plasma GC concentrations in non-stressed rats (Shepard et al., 2003). Activation of both the BLA and CeA has been demonstrated by fMRI of mice following exposure to learned aversive stimuli. Mice were conditioned to associate a conditioned stimulus (flashing light) with foot shock, leading to enhanced activation of the amygdala compared with mice receiving unpaired foot shock and flashing light exposure (Harris et al., 2015).

1.3.3 Glucocorticoid and neocortical regions

GC hormones also act upon neocortical regions via MRs and GRs, such as the PFC and neocortex, key brain regions involved in regulating cognition and emotion (Yuen et al., 2009). The PFC plays a role in processing of emotional stimuli (Cerqueira et al., 2007) and translating stressful emotional information into action (McKlveen et al., 2013) and many studies have demonstrated the region to be strongly influenced by stress. The neocortex is critical for cortical memory consolidation (Wiltgen et al., 2004) and in contrast to the hippocampus, amygdala and PFC, the effects of GCs on the neocortex have not been as extensively studied.

The PFC comprises several functionally distinct areas, however the mPFC appears to be particularly involved in memory retrieval and consolidation (Preston and Eichenbaum, 2013) and MRs and GRs are expressed in this region (Diorio et al., 1993). Changes in gene expression within the PFC have been observed following exposure to stress, however the binding of MRs and GRs to GREs within the PFC has not been extensively examined. One study has, however, investigated the changes in nuclear translocation and GRE binding of GRs in the PFC of the rat following stress and circadian influences. During the circadian rise and following exposure to acute restraint stress, western blot demonstrated increased nuclear GR within the PFC, while a gel shift assay demonstrated increased GR binding to a ^{32}P-labelled GRE sequence within the PFC (Kitchener et al., 2004). Nuclear translocation and DNA-binding of the GR in the PFC of ADX rats was also shown to increase following rises in GC levels. Intermediate and high doses of CORT significantly increased the nuclear translocation of the GR within the PFC, while DNA binding was significantly increased by a high dose of CORT (Spiga and Lightman, 2009). Stress has also been shown to alter gene expression within the PFC, however the relationship

between GC receptor binding and changes in gene expression has not been evaluated. RNA-seq identified changes in gene expression within the mPFC in rats exposed to a novel environment stressor daily for 2 weeks, with 8 genes differentially expressed in male rats and 17 genes differentially expressed in female rats. These genes were predicted, by pathway analysis software, to upregulate processes such as LTP and participate in corticotrophin releasing hormone signalling (Mychasiuk et al., 2016). Exposure to chronic mild stress was also shown to alter the expression of genes involved in the circadian clock, which are collectively termed clock genes, with increased mRNA levels of *Brain and Muscle ARNT-Like 1 (Bmal1)* and decreased mRNA levels of *Cryptochrome 2 (Cry2)* and *Period 2 (Per2)* shown in the PFC of rats exposed to a chronic stress regime for 7 weeks (Calabrese et al., 2016). Acute stress has also been shown to mediate the expression of genes involved in synaptic plasticity and dendritic spine architecture within the PFC. Rats exposed to acute foot shock for 7 days exhibited increased mPFC mRNA levels of *SH3 And Multiple Ankyrin Repeat Domains 1 (Shank1)*, a member of the Shank family of scaffolding proteins found at the post-synaptic density of glutamatergic synapses. 14 days of exposure to foot shock decreased PFC mRNA levels of the scaffolding protein *Homer Scaffold Protein 3 (Homer3)* and *Cofilin 1 (CFL1)* (Nava et al., 2017).

Alongside the hippocampus and hypothalamus, the PFC plays a role in the negative feedback of the HPA axis (Mizoguchi et al., 2004), and lesions of the cingulate gyrus region of the mPFC have been shown to increase plasma levels of ACTH and GCs following restraint stress (Diorio et al., 1993). Studies have demonstrated GC action in the PFC to exert both positive and negative influences on memory formation, depending on the type of exposure. Exposure to acute stress enhanced performance on a behavioural task involving PFC-mediated working memory (Yuen et al., 2009) while chronic stress impaired working memory, via a mechanism involving dopaminergic neurotransmission in the PFC (Mizoguchi et al., 2004). Some level of GC hormones are required for enhancement of memory within the PFC, however, as complete removal of GCs by ADX was been shown to impair working memory (Mizoguchi et al., 2004). The effects of GC hormone action on memory consolidation via the PFC may be mediated by interactions between the PFC and the hippocampus. The mPFC is connected to the hippocampus via axonal projections originating in the hippocampal subiculum and ventral CA1 subfields terminating in the pyramidal cells and interneurons of the mPFC (Jay and Witter, 1991) and synaptic activity within the hippocampal-mPFC circuitry has been shown to regulate learning and memory processes (Wall and Messier, 2001). High frequency stimulation of the hippocampus can

induce LTP within the PFC via glutamatergic projections from the CA1 to the prelimbic area of the PFC. Exposure to an acute inescapable stress was shown to completely inhibit hippocampal-PFC LTP within the prelimbic PFC, an effect which was abolished by antidepressant pre-treatment (Rocher et al., 2004). Within the PFC, acute stress was shown to impair spatial memory in the radial arm water maze, a hippocampal-dependent memory task and reduce levels of neural cell adhesion molecule; a cell-surface glycoprotein implicated to play a critical role in memory formation and the induction of hippocampal LTP (Sandi et al., 2005).

Acute and chronic stress have been shown to induce changes in the morphology of neurons within the mPFC. Daily exposure to a mild stressor for 1 week was sufficient to significantly alter the dendritic morphology of layer II-III pyramidal neurons in the mPFC (Brown et al., 2005). Furthermore, exposure to daily restraint stress for 3 weeks produced a decrease in branch number and length of the apical dendrites of layer II-II pyramidal neurons in the mPFC (Cook and Wellman, 2004). Significant apical dendritic retraction and spine loss was reported in callosal neurons of the infralimbic and prelimbic PFC following exposure of rats to daily restraint stress for 3 weeks (Luczynski et al., 2015). Exposure to changes in cortisol has been shown to result in changes in activity within the anterior mPFC (amPFC). Following administration of hydrocortisone, a significant increase in the blood oxygenation level dependent (BOLD) response was seen by fMRI within the amPFC during AM retrieval (Fleischer et al., 2019).

In contrast with the PFC, very little information is available regarding GC hormone action within the neocortex, however evidence suggests MRs and GRs may influence gene expression in this brain region following exposure to stress. Microarray analysis of neocortical tissue from mice exposed to acute immobilisation stress and treated with a gamma aminobutyric acid (GABA) subunit A ($GABA_A$) inhibitor revealed differential RNA expression of 7 genes, including upregulated expression of *Fos* (Kurumaji et al., 2008), a marker of neuronal activation commonly upregulated following exposure to stress (Chandramohan et al., 2008). Exposure of rats to immobilisation stress significantly reduced mRNA levels of the highly expressed brain neurotrophin, *Bdnf*, in the rat neocortex. BDNF regulates processes such as cell survival and differentiation and decreased expression associated with age-related memory deficits (Park et al., 2009). Stress may also influence neurogenesis of the neocortex during development. Prenatally stressed mice exhibited delayed migration of GABAergic progenitors

within the neocortex, a reduced number of GABAergic progenitors within the neocortex and decreased expression of transcription factors which regulate interneuron migration, such as *Distal-Less Homeobox 2 (dlx2), NK2 Homeobox 1 (nkx2.1)* and their downstream target *Erb-B2 Receptor Tyrosine Kinase 4 (erbb4)*.

1.4 Rationale, hypotheses, aims and objectives

1.4.1 Rationale

Previous work in the Reul laboratory has shown significantly upregulated binding of MRs and GRs to GREs within well-known GC-target genes during the circadian rise in GC levels or following exposure to an acute stressor (Mifsud and Reul, 2016). Strong evidence was also provided which supports heterodimerisation formation between MRs and GRs at these GREs. Furthermore, hnRNA and mRNA levels of these genes are also shown to increase significantly under these conditions, indicating the binding of MRs and GRs may be exerting transcriptional activation of the corresponding genes. Although the regulation of gene expression by MRs and GRs has been examined within the hippocampus, a comprehensive *in vivo* investigation into the genome-wide binding of both MRs and GRs in the brain and associated transcriptional responses remains to be undertaken.

GC hormones have been associated with a wide range of processes in the brain, including learning and memory, neurogenesis, neuronal morphology and the pathophysiology of neuropsychiatric disorders. Some studies have established a link between the genomic actions of MRs and GRs with these processes in the brain and have identified GC target genes which may be involved; however, these studies have been limited to investigating a handful of genes at a time and provide little insight into what is happening at the network level. Pathway analysis of the genome wide targets of MRs and GRs and the transcriptomic wide responses following acute stress or circadian input may provide insight into how networks of GC hormone target genes influence processes such as learning and memory or the development of stress related neuropsychiatric disorders such as depression and PTSD.

Following elevations in GC hormone levels during the acute stress response or by circadian input, MR and GR binding to GREs has been associated with changes in RNA expression of nearby genes. It is unclear, however, whether the genomic actions of MRs and GRs are critical for the RNA responses

observed in these genes. The effects of suppressing GC hormone action or antagonising GR hormone receptors on RNA expression has hardly been examined.

GC hormones have been shown to act upon many brain regions, such as the amygdala, PFC and neocortex, however very few studies have investigated the genomic actions of MRs and GRs in these tissues. It is presently unknown whether MRs and GRs regulate gene expression in these brain regions, following exposure to acute stress or under circadian conditions, as seen in the hippocampus. The KLFs have been identified as GC-target genes and are shown to play important roles in processes such as differentiation and development, however their regulation by MRs and GRs has not been studied extensively.

1.4.2 Hypotheses

Based on the rationale, the hypothesis of this work was that following elevations in levels of circulating CORT, MR and GR binding to GREs within the genome will increase significantly. This will be accompanied by changes in RNA levels of the corresponding gene. The MR and GR binding pattern will differ depending on whether CORT was induced by stress or circadian input and will lead to activation or suppression of specific groups of genes with differential functions linked with the stress response or the circadian rhythm.

Based on the overarching hypothesis, the additional **sub-hypotheses** were formulated:

1. A subset of regions will show overlapping MR and GR binding supporting heterodimerisation formation, while certain regions of the genome will be exclusively bound by the MR or the GR.
2. Pathway analysis will predict a link between MR and GR bound genes and numerous physiological processes in the brain and will reveal distinct signalling pathways, diseases and functions associated with either receptor.
3. Inhibiting the synthesis and secretion of CORT in the rat, pharmacologically with metyrapone and surgically by ADX, will prevent the binding of MRs and GRs to GREs and subsequent changes in RNA expression.
4. Antagonising MRs and GRs, with Spironolactone or RU486, will prevent interactions between GC receptors and the transcriptional initiation machinery, subsequently attenuating changes in RNA expression.

5. MRs and GRs bind to responsive elements within KLF genes under circadian conditions and following exposure to acute stress, within the hippocampus, amygdala, PFC and neocortex. RNA expression of genes exhibiting significant MR or GR binding will increase significantly.

1.4.3 Aim and objectives

The overall aim of this thesis was to investigate the genome-wide changes in MR and GR binding and the associated transcriptional responses the rat hippocampus under circadian conditions and following exposure to acute stress. Furthermore, the binding of MRs and GRs to overlapping or distinct regions of the genome was to be examined, to determine whether the receptors act largely in parallel or whether they regulate specific subsets of genes alone.

The main objectives of this PhD study were as follows;

1. To identify genomic regions which are significantly bound by MRs and GRs following acute stress and under circadian rise conditions, and to determine whether this binding is upregulated or downregulated in comparison to the circadian trough.
2. To establish an extensive time course of transcriptome-wide RNA expression following acute stress, cross-correlating MR and GR binding at GREs with changes in RNA expression.
3. To predict downstream pathways, diseases and functions affected by the genes becoming bound by MRs and GRs or exhibiting differential RNA expression following acute stress or the circadian rise.
4. To observe the effects of the removal of endogenous CORT, prevention of CORT synthesis and the pharmacological antagonism of the MR and GR on the binding of MRs and GRs at GREs and the RNA expression of GC target genes.
5. To investigate the genomic action of MRs and GRs in the hippocampus, amygdala, prefrontal cortex and neocortex following acute stress and circadian influences.

Chapter 2 Materials and Methods

2.1 Animals

For all animal experiments, adult male Wistar rats (150-200g on arrival) were purchased from Envigo (formerly known as Harlan (Oxon, UK)) and group-housed (2-3 per cage). Rats were housed under standard lighting (lights on 05:00– 19:00 h, approximately 80-100 Lux) and environmentally controlled conditions (temperature 21 ± 1 °C; relative humidity 40–60%) with food and water available *ad libitum*. Rats were randomly assigned to cages and these were labelled randomly to avoid subjective bias. All rats were handled daily for at least 5 days prior to experimentation to reduce non-specific handling stress on the day of the experiment. All animal work was approved by the University of Bristol Ethical Committee and the Home Office of the United Kingdom (Animal Scientific Procedures Act, 1986, UK) and under the Project Licences held by Johannes Reul (Ref: P396EB569), protocol 1: "Molecular and cellular changes in stressful behavioural models" and protocol 2: "Elucidation of the mediators involved in the molecular and cellular changes in stressful behavioural models", severity category; moderate.

2.2 Stress procedures

Stress procedures were carried out with the assistance of Miss Emily Price. Baseline rats were killed straight from their home-cages between either 7-9am (circadian trough, 'baseline AM' (BLAM)) or 5-7pm (circadian peak, 'baseline PM' (BLPM)). Alternatively, rats were forced to swim for 15 min in 25°C (±1) water in individual glass beakers (height 35 cm, diameter 21.7 cm), towel dried, returned to their home cage and killed at various timepoints after the start of forced swimming (FS). Rats were decapitated following quick isoflurane anaesthesia (<10sec).

2.3 Drug treatment

All drugs and chemicals were purchased from Sigma (Dorset, UK) unless stated otherwise. To block MR- and GR-mediated effects, rats were voluntarily dosed with the MR antagonist spironolactone or the GR antagonist RU486 (Mifepristone). All rats underwent a 5-day acclimatisation period in which a 1ml syringe containing a mixture of 50% condensed milk and 50% tap water was suspended through

the home cage bars. Once the rat approached, the experimenter pushed down gently on the syringe, allowing the rats to drink the mixture voluntarily. The advantage of this method is that the rat does not need be touched or restrained which would cause stress for the animal. On the day of the experiment, 1ml syringes containing vehicle (50% condensed milk, 50% tap water) or the drug suspended in the vehicle were suspended through home cage bars. The rats consumed the contents voluntarily within 5 minutes. Rats receiving drug suspension either received RU486 alone (30mg/kg), or a combination of RU486 (30mg/kg) and Spironolactone (50mg/kg).

Metyrapone experiments were conducted by Dr Sylvia Carter with the assistance of Dr Karen Mifsud. In an alternative approach to block CORT-mediated effects, rats were intraperitoneally (i.p.) injected either once or twice at 90-minute intervals with the 11-β-hydroxylase inhibitor metyrapone (75 or 100 mg/kg). As a control condition, the same amount of vehicle (40% poly-ethylene glycol 300 (PEG), 60% 0.9%-saline; 1ml/kg i.p.) was injected at corresponding intervals. A full schedule for metyrapone dosing, FS and killing can be seen in Table 2.1, Table 2.2 and Table 2.3.

2.4 Surgical procedures

Surgical procedures were performed by Dr Karen Mifsud. To remove the endogenous source of CORT, a cohort of rats underwent adrenalectomy (ADX) or sham surgery. All ADX procedures were performed according to the latest guidelines, under aseptic conditions and with appropriate analgesia to relieve peri-operative pain (monitored using the rat grimace scale and other subtle pain-related behavioural features). All adrenalectomies were done bilaterally through two dorsolateral midflank skin and muscular incisions. Sham surgeries were identical to ADX except that the adrenals were not removed. Muscle incisions were sutured, and skin incisions were clipped with Michel suture clips. All rats were anesthetised with isoflurane gas during surgery. All rats that underwent ADX were allocated 5 days of post-surgical recovery, during which time 0.9% saline containing CORT (Sigma, UK) supplementation (15 mg/l) was provided in their drinking water to maintain isotonic salt levels and homeostasis of the HPA-axis. One-week post-surgery, CORT supplementation was discontinued 1 day before experimentation.

2.5 Tissue dissection and storage

Tissue dissection was performed by Professor Hans Reul. Following decapitation and removal of the brain, the hippocampus, amygdala, neocortex and prefrontal cortex were dissected on an ice-cold steel box. All tissues were snap-frozen in liquid N_2 and stored at -80 °C. Trunk blood was also collected at the point of decapitation and stored on ice in tubes containing EDTA and aprotinin for determination of plasma CORT concentration. Blood samples were centrifuged at 1500 × g for 30 min to separate plasma, which was collected into fresh tubes and stored at -80°C until analysis.

2.6 Radioimmunoassay

The plasma CORT concentration in samples of rat plasma was determined using the commercial Corticosterone ^{125}I Double Antibody radioimmunoassay (RIA) kit for rats and mice (MP Biomedicals, New York). The RIA was carried out as per the manufacturer's instructions. Plasma samples were diluted using steroid diluent according to the dilution table (Table 2.4). Each sample was run in triplicate and standards provided in the kit were used. 50 µl of ^{125}I-labelled corticosterone and 50 µl of anti-corticosterone were added to 25 µl of each sample and vortexed to mix. The mixture was incubated in a lead-lined box for precisely 2 hrs. Once incubation time had elapsed, 125 µl precipitant solution was added to each sample and samples were centrifuged at 2500 x g for 15 min at 4 ºC (Eppendorf centrifuge, 5417R, Eppendorf, Stevenage, UK). The supernatant was aspirated to leave a precipitate. The samples were analysed using a WIZARD automatic gamma counter (2470 model, PerkinElmer, London, UK). The detection limits were 0.25 ng/ml. Inter and intra-assay variations are given individually in the results chapters. Inter-assay variation was calculated based on the average % coefficient of variation for the high standards across 5 assays. Intra-assay variation was calculated based on the average coefficient of variation within the assay for each triplicate sample.

<table>
<tr><td>Experiment</td><td></td><td colspan="14">Time (min)</td></tr>
<tr><td>Chapter 7.4.2</td><td>Time of 1st injection</td><td>0</td><td>5</td><td>10</td><td>15</td><td>20</td><td>25</td><td>30</td><td>35 - 85</td><td>90</td><td>95</td><td>100</td><td>105</td><td>110</td><td>115</td><td>120</td></tr>
<tr><td>No injection</td><td>N/A</td><td colspan="3">FS</td><td colspan="3">Home cage</td><td>Kill</td><td></td><td colspan="3"></td><td colspan="3"></td><td></td></tr>
<tr><td>Vehicle</td><td>~8:15 - 10:45 am</td><td colspan="8">Injection (i.p.)</td><td colspan="3">FS</td><td colspan="3">Home cage</td><td>Kill</td></tr>
<tr><td>Met (75 mg/kg)</td><td>~8:30 - 11:15 am</td><td colspan="8">Injection (i.p.)</td><td colspan="3">FS</td><td colspan="3">Home cage</td><td>Kill</td></tr>
<tr><td>Met (100 mg/kg)</td><td>~9:00 - 10:30 am</td><td colspan="8">Injection (i.p.)</td><td colspan="3">FS</td><td colspan="3">Home cage</td><td>Kill</td></tr>
</table>

Table 2.1 The schedule of metyrapone dosing experiments described in Chapter 7.4.3

Rats were intraperitoneally (i.p.) injected once with metyrapone (75 or 100 mg/kg) or vehicle (40% PEG, 60% 0.9%-saline; 1ml/kg i.p). 90 minutes later, rats underwent FS (15 min in 25°C (±1) water), returned to their home cage and killed 30 minutes after the onset of FS.

Experiment		Time (min)						
Chapter 7.4.2	Time of 1st injection	0 - 50	90 - 115		120	125 - 175	180 - 205	210
Vehicle BLAM	~8:45 - 11:15 am	Injection (i.p.)	Home cage		**Kill**			
Vehicle FS30	~8:00 - 11:30 am	Injection (i.p.)	**FS**	Home cage	**Kill**			
Met (100 mg/kg) BLAM	~8:55 – 9:05 am	Injection (i.p.)	Home cage		**Kill**			
Met (100 mg/kg) FS30	~8:30 - 11:00 am	Injection (i.p.)	**FS**	Home cage	**Kill**			
Met (2*100 mg/kg) BLAM	~9:15 - 9:30 am	Injection (i.p.)	Injection (i.p.)				Home cage	**Kill**
Met (2*100 mg/kg) FS30	~8:15 - 10:00 am	Injection (i.p.)	Injection (i.p.)				**FS** Home cage	**Kill**

Table 2.2 The schedule of metyrapone dosing experiments described in Chapter 7.4.2

Rats were intraperitoneally (i.p.) injected either once or twice at 90-minute intervals with metyrapone (100 mg/kg) or vehicle (40% PEG, 60% 0.9%-saline; 1ml/kg i.p). 90 minutes later, rats underwent FS (15 min in 25°C (±1) water), returned to their home cage and killed 30 minutes after the onset of FS.

Experiment	Time (min)					
Chapter 7.4.3	Time of 1st injection	0 - 50	90 - 175	180 - 235		240
Vehicle BLAM	~7:00 - 9:00 am	Injection (i.p.)	Injection (i.p.)	Home cage		**Kill**
Vehicle FS30	~8:00 -10:00 am	Injection (i.p.)	Injection (i.p.)	**FS**	Home cage	**Kill**
Met (2*100 mg/kg) BLAM	~7:00 - 9:00 am	Injection (i.p.)	Injection (i.p.)	Home cage		**Kill**
Met (2*100 mg/kg) FS30	~8:00 -10:00 am	Injection (i.p.)	Injection (i.p.)	**FS**	Home cage	**Kill**

Table 2.3 The schedule of metyrapone dosing experiments described in Chapter 7.4.3

Rats were intraperitoneally (i.p.) injected twice at 90-minute intervals with metyrapone (100 mg/kg) or vehicle (40% PEG, 60% 0.9%-saline; 1ml/kg i.p). 90 minutes later, rats underwent FS (15 min in 25°C (±1) water), returned to their home cage and killed 60 minutes after the onset of FS.

Sample	Dilution
BLAM	1:75
FS30	1:300
FS60	1:200
FS120	1:200
FS180	1:100
FS360	1:200
BLPM	1:200

Table 2.4 The dilution of plasma samples with steroid diluent for Corticosterone I^{125} Double Antibody RIA

Plasma samples were diluted using steroid diluent according to the dilution table and the RIA was carried out as per the manufacturer's instructions.

2.7 Chromatin immunoprecipitation

2.7.1 Buffers for ChIP

Formaldehyde solution with protease, phosphatase and histone deacetylase inhibitors

1X PBS (phosphate buffered saline, Sigma-Aldrich)

1% w/v formaldehyde solution (Sigma-Aldrich)

0.1 mM PMSF (phenylmethanesulfonylfluoride, Sigma-Aldrich)

5 mM NaBut (Sodium butyrate, Merck Millipore, Nottingham, UK)

1 tablet PhosSTOP phosphatase inhibitor cocktail (Roche, West Sussex, UK)/10ml

PBS with inhibitors

1X PBS (Sigma-Aldrich)

5 mM NaBut (Merck Millipore)

1 mM Na_3VO_4 (Sodium orthovanadate, Sigma-Aldrich)

0.1 mM PMSF (Sigma-Aldrich)

1 tablet PhosSTOP phosphatase inhibitor cocktail (Roche, West Sussex, UK)/10ml

Lysis buffer

50 mM Tris-HCL pH 8.0 (Trizma hydrochloride, Sigma-Aldrich)

150 mM NaCl (Sodium chloride, Sigma Aldrich)

5 mM EDTA (Ethylenediaminetetraacetic acid, Sigma-Aldrich)

0.5% w/v Igepal (Sigma-Aldrich)

0.5% w/v Sodium deoxycholate (Sigma-Aldrich)

1% SDS (Sodium dodecyl sulphate, Sigma-Aldrich)

5 mM NaBut (Merck Millipore)

2mM AEBSF (4-(2-Aminoethyl) benzenesulfonyl fluoride hydrochloride, Sigma-Aldrich)

1 mM Na_3VO_4 (Sigma-Aldrich)

1X dilution of protease inhibitor solution from Complete Ultra EDTA-free protease inhibitor tablets (Roche); 1 tablet per 1ml nfH_20

1 tablet PhosSTOP phosphatase inhibitor cocktail (Roche, West Sussex, UK)/10ml

Dilution buffer with inhibitors

50 mM Tris-HCL pH 7.4 (Sigma-Aldrich)

150 mM NaCl (Sigma-Aldrich)

5 mM EDTA pH 7.5 (Sigma-Aldrich)

1% Triton (Sigma-Aldrich)

0.1% w/v Sodium deoxycholate (Sigma-Aldrich)

5 mM NaBut (Merck Millipore)

1 mM AEBSF (Sigma-Aldrich)

1X dilution of protease inhibitor solution from Complete Ultra EDTA-free protease inhibitor tablets (Roche)

1 tablet PhosSTOP phosphatase inhibitor cocktail (Roche, West Sussex, UK)/10ml

Dilution buffer without inhibitors

50 mM Tris-HCL pH 7.4 (Sigma-Aldrich)

150 mM NaCl (Sigma-Aldrich)

5 mM EDTA pH 7.5 (Sigma-Aldrich)

1% Triton (Sigma-Aldrich)

0.1% w/v Sodium deoxycholate (Sigma-Aldrich)

5 mM NaBut (Merck Millipore)

RIPA wash buffer with inhibitors

10 mM Tris pH 7.5 (Sigma-Aldrich)

1 mM EDTA pH 7.5 (Sigma-Aldrich)

0.1% SDS (Sigma-Aldrich)

0.5 mM EGTA (ethylene glycol tetra-acetic acid, Sigma-Aldrich)

1% Triton (Sigma-Aldrich)

140 mM NaCl (Sigma-Aldrich)

Elution buffer I

10 mM Tris pH 7.5 (Sigma-Aldrich)

50 mM NaCl pH 7.5 (Sigma-Aldrich)

1.5% SDS (Sigma-Aldrich)

Elution buffer II

10 mM Tris pH 7.5 (Sigma-Aldrich)

50 mM NaCl pH 7.5 (Sigma-Aldrich)

0.5% SDS (Sigma-Aldrich)

2.7.2 Chromatin extraction

Hippocampal tissue from 2 rats, amygdala tissue from 2 rats, prefrontal cortex tissue from 1 rat or neocortex tissue from 1 rat was cross-linked in formaldehyde solution with protease, phosphatase and histone deacetylase inhibitors, transferred to DNase/RNase free tubes and rotated at RT for 10 min. Cross-linking was terminated by the addition of 1.25 M glycine to a final concentration of 200 mM, and the solution was rotated for 5 min at RT and subsequently centrifuged (5 min, 6,000 × g, 4 ºC). The resultant pellet was washed three times, with a centrifuge step between each wash (5 min, 7500 rpm,

4 ºC), with ice cold PBS with inhibitors. The pellet was resuspended in 1 ml ice-cold Lysis buffer and rotated at 4 ºC for 15 min.

2.7.3 Chromatin fragmentation

Chromatin was fragmented by sonication using a Bioruptor (UCD-300 or Picoruptor; Diagenode, Liege, Belgium) at 4 °C. Hippocampal chromatin sonicated by the UCD-300 were aliquoted into 200µl aliquots and each aliquot was sonicated on high power for three sets of 10 cycles (30s on and 60s off). Samples were vortexed between each cycle. Chromatin from the hippocampus, amygdala and prefrontal cortex sonicated by the Picoruptor was aliquoted into 300µl aliquots and each aliquot was sonicated on high power for one set of 3 cycles (30s on and 30s off). Chromatin from the neocortex sonicated by the Picoruptor were aliquoted into 300µl aliquots and each aliquot was sonicated on high power for one set of 4 cycles (30s on and 30s off). Following sonication, samples were centrifuged (20,817 × g 10 min, 4 ºC) and the supernatant containing sheared chromatin was collected. Aliquots of 200 µl were taken from each sample for chromatin-immunoprecipitation (ChIP) and two aliquots of 20 µl was taken from each sample and diluted in 280 µl of 1X Tris-EDTA (TE) (Sigma-Aldrich); one to be used as Input DNA and the other to be used to check the size of the sheared chromatin fragments. To check the size of the sheared chromatin fragments, samples were reversed by adding 5 M NaCl to the samples (to a final concentration of 200 mM) and incubating at 65 ºC overnight. The following day, ribonuclease A from bovine pancreas (Sigma-Aldrich) was added to each sample, to a final concentration of 60 µg/ml and incubated for 1 hr at 37 ºC. Subsequently, proteinase K from Tritirachium album (Sigma-Aldrich) was added to a final concentration of 250 µg/ml and incubated for 3h at 37 ºC. A QIAquick PCR purification kit (Qiagen) was used, as per the manufacturer's instructions, to purify the DNA. Purified samples were run on a 1.5% agarose gel (w/v dissolved in TAE buffer), alongside a 100 base pair DNA ladder (NEB). Samples and DNA ladder were made up to a final volume of 24 µl by the addition of 10% loading buffer (20% Ficoll (Sigma-Aldrich), 0.1 M EDTA (Sigma-Aldrich), 1% SDS (Sigma-Aldrich), 1.5% Xylene Cyanol (Sigma-Aldrich)), 10% Midori green (Midori green Advance DNA stain (Nippon Genetics, Europe, Dueren, Germany)) and run at 50 V for 3.5 hrs.

2.7.4 Chromatin immuno-precipitation (ChIP)

Each 200 µl aliquot of chromatin was mixed with 1,800 µl of ice-cold dilution buffer, 10 µl of antibody (Table 2.5) was added and the solution was rotated overnight at 4ºC. For each sample, an aliquot of 150 µl of Protein-A coated Dynabeads (Thermo Fisher) magnetic beads was washed with 0.5% BSA in 1X PBS using a Magna GrIP™ magnetic rack (Merck Millipore) and rotated overnight at 4ºC. The following day, the magnetic beads were washed once in ice-cold dilution buffer without inhibitors. Dilution buffer was removed from the magnetic beads and the antibody/chromatin mixture was added. The resultant mixture was rotated for 3 hours at 4ºC. Using the magnetic rack, the "unbound" fraction was separated and discarded. The beads were washed three times with ice-cold RIPA buffer with inhibitors and twice with ice cold 1X TE (Sigma-Aldrich). 200 µl of elution buffer I was added to the beads at room temperature and the mixture was vortexed for 15 min to elute the antibody-bound fraction. The sample was placed on a magnetic rack and the solution was collected and placed in a fresh tube. A second elution step was carried out at room temperature by adding 100 µl of elution buffer II to the beads and vortexing the mixture for 15 min. The sample was placed on a magnetic rack and the solution was collected and pooled with the collected solution from elution buffer I. The protein-DNA crosslinks were reversed by adding 5 M NaCl to the bound samples and input samples (to a final concentration of 200 mM) and incubating at 65 ºC overnight. The following day, ribonuclease A from bovine pancreas (Sigma-Aldrich) was added to each sample, to a final concentration of 60 µg/ml and incubated for 1 hr at 37 ºC. Subsequently, proteinase K from *Tritirachium album* (Sigma-Aldrich) was added to a final concentration of 250 µg/ml and incubated for 3h at 37 ºC. A QIAquick PCR purification kit (Qiagen) was used, as per the manufacturer's instructions, to purify the DNA. Total dsDNA content of each sample was determined with a High-Sensitivity Qubit DNA Assay Kit (Life Technologies) as per the manufacturer's instructions and quantified using a Qubit 2.0 Fluorometer.

	MR ChIP	GR ChIP
Chapter 3	MR H-300, sc11412x, Santa Cruz	GR H-300, sc8992x, Santa Cruz
Chapter 5	MR ab64457, Abcam	GR 24050-1-AP, Proteintech
Chapter 6	MR ab64457, Abcam	GR 24050-1-AP, Proteintech
Chapter 7	MR H-300, sc11412x, Santa Cruz	GR H-300, sc8992x, Santa Cruz

Table 2.5 Antibodies used for chromatin-immunoprecipitation

Antibodies used for ChIP experiments and the source they were purchased from are listed for each chapter.

2.7.5 Primers and probes for ChIP-qPCR

Primers and dual-labeled probe with 6-Carboxyfluorescein (6-FAM) as the fluorescent dye and tetramethylrhodamine (TAMRA) as the quencher were designed using Primer Express software (version 3.0.1; Life Technologies). Primers were designed to cover glucocorticoid responsive elements (GREs) identified by ChIP-seq. All primers and probes were ordered from Sigma (Dorset, UK). Primer and probe sets used for ChIP-qPCR are shown in Table 2.6.

Standard curves were performed for each primer pair, and the qPCR efficiency was calculated using the equation E = ((10 − 1/slope) − 1) × 100 (where E is qPCR efficiency, and the slope is the gradient of the standard curve). Only primer pairs with efficiencies greater that 80% were used.

2.7.6 Real-Time Polymerase chain reaction for DNA

All bounds and inputs were diluted to a standardised concentration with nuclease-free water (nfH_20; Promega) and 2 µl was added to 18 µl mastermix in a 96-well plate. Mastermix was prepared containing 900 nM forward and reverse primers, 250 nM probe, and 1× TaqMan Fast Mastermix (Life Technologies) and made up to volume with nfH_20 (Promega). Samples were run in duplicate. Plates were covered with an adhesive clear seal (Life Technologies) and spun down in a plate mini centrifuge prior to qPCR. qPCR was performed using a StepOne Plus Machine (Life Technologies). Taq enzymes were activated at 95 °C for 20 s, and then, 40 cycles of 95 °C (1 s) to 60 °C (20 s) were performed to amplify samples.

A standard curve, created from 2-fold serial dilutions of rat brain genomic DNA (Biochain, CA, USA), was included in each qPCR run. Data are expressed as quantity of bound DNA divided by the respective quantity of input DNA (i.e., B/I), which is a measure of the enrichment of steroid receptor bound to specific genomic sequences.

Gene symbol	Ensemble gene ID	Region	Forward primer sequence	Reverse primer sequence	Probe sequence
Klf2	ENSRNOG00000014205	GRE	TCGGGTGAGCACAGTAGTGACT	TCAGGCCCCGGGAAAC	CAGACTCCCCATGCATCGGTCCA
Klf9	ENSRNOG00000014215	GRE	TGCGGTGCGGACTATGTTTAG	ATCCTCGAAGATCAGGAAAACCT	TCATCGCGACACCCTCTACTCTGCAG
Klf15	ENSRNOG00000017808	GRE1	TCAGGGAGGACTCTTATTTTGAAGA	CCCCCATTCGCCACCCCC	CATTGGGTCAGCGTGCAA
		GRE2	ACTGGGCCCTGAGTTCCTAAA	TTGCCCAAGCCCTTACCCTACCCC	AGCAGTCCCCAGGGTTGAG

Table 2.6 DNA primers and probe sequences used for ChIP-qPCR

The Ensemble gene ID for each gene is shown, as well as the region where the primers and probes have been designed to span, and the primers and probe sequences. Primers were designed to the latest version of the rat gene, Rnor_6.0 and all had efficiencies of 90% or higher.

2.8 ChIP sequencing

Sequencing, quality control and basic bioinformatic analysis was performed by collaborators at the Wellcome Centre for Human Genetics, University of Oxford.

2.8.1 ChIP seq library construction and sequencing

DNA was quantified using Qubit (Invitrogen) and the size profile analysed on the 2200 or 4200 TapeStation (Agilent, dsDNA HS Assay). Input material was normalised to 5 ng prior to library preparation. Automated library preparation was performed using the Apollo prep system (Wafergen, PrepX ILMN 32i, 96 sample kit) and standard Illumina multiplexing adapters following manufacturer's protocol up to pre-PCR amplification. Libraries were PCR amplified (18 cycles) on a Tetrad (Bio-Rad) using the NEBNext® High-Fidelity 2X PCR Master Mix (NEB) and in-house (Wellcome Centre for Human Genetics, University of Oxford) single indexing primers (Lamble et al., 2013). Individual libraries were normalised using Qubit, and the size profile was analysed on the 2200 or 4200 TapeStation. Following normalisation, individual libraries were pooled accordingly. The pooled library was diluted to ~10 nM for storage. The 10-nM library was denatured and further diluted prior to loading on the sequencer. Samples were pooled and multiplexed libraries were sequenced on 5 lanes of an Illumina HiSeq4000 System to generate 75 basepair (bp) paired end reads. All samples were assessed for a number of QC metrics, including Q30 and acceptable Passing Filter (%PF).

2.8.2 Genome mapping and bioinformatic analysis of ChIP-seq data

At least 25 million read pairs reads were produced per sample using Illumina's bcl2fastq2 and trimmed to remove any multiplex PCR or index primers using Skewer (Jiang et al., 2014), with settings:

-f sanger -x AGATCGGAAGAGCACACGTCTGAACTCCAGTCACNNNNNNNNATCTCGTATGCCGTCTTCTGCTTG -y AGATCGGAAGAGCGTCGTGTAGGGAAAGAGTGTAGATCTCGGTGGTCGCCGTATCATT -mpe -l 25 -r 0.1

Adapter-trimmed reads were aligned using Burrows-Wheeler Aligner (BWA-MEM) (Li and Durbin, 2009) to the Rattus norvegicus (rn_06) genome build (Ensembl) using default parameters. Reads with

mapping quality < 20, not properly paired, or with insert size > 1000 bp were filtered out using Bamtools (Barnett et al., 2011). BAM files from individual sequencing lanes were merged and duplicate reads were removed with PICARD (http://broadinstitute.github.io/picard). The degree of enrichment for the proteins of interest was evaluated through the Normalised Strand Cross-correlation (NSCC) and the Relative Strand Cross-correlation (RSC) coefficients, which were calculated for each ChIP sample; in all cases, NSCC and RSC values were > 1.05 and > 0.8, respectively, in agreement with the ENCODE guidelines (Landt et al., 2012). To identify significantly enriched regions, the peak caller Model based Analysis of ChIP-seq (MACS2) (Zhang et al., 2008) was used with parameters -f BAMPE -g 2.5e9 for GR and MR narrow peaks. Peaks with a false discovery rate (FDR) lower than 5% were reported and annotated to their nearest genes (Ensembl release 81) using the Bedtools suite (Quinlan, 2014).

The difference in binding levels between conditions - measured by differences in read densities - was performed using the R Bioconductor package DiffBind (version 2.4.8) (Ross-Innes et al., 2012) (Stark and Brown, 2011). The significantly differentially bound sites between sample groups resulting from this analysis were used as input to carry out known and de novo motif search using FIMO (MEME suite, version 4.11.2) (Bailey et al., 2015) and the position weight matrices for vertebrates from the JASPAR CORE database (Sandelin et al., 2004). All bioinformatic analyses were executed using in-house scripts written in the Python and R programming languages.

2.9 RNA analysis

2.9.1 RNA extraction

Brain tissue was homogenised (600 rpm) in ice-cold TRI Reagent (Sigma) using a polymix homogeniser (polymix PX-SR 90D, Kinematica Ag, Littau-Luzern, Switzerland). The homogenate was transferred to a DNase/RNase-free tube and placed on ice. All samples were centrifuged at 12,000 × g for 10 min at 4 ºC to remove insoluble material. The supernatant was transferred to a fresh tube and allowed to stand for 5 min at room temperature. 100 µl of 1-bromo-3-chloropropane (Sigma-Aldrich) was added to each sample and shaken vigorously for 15 seconds before allowing to stand for 15 min at room temperature. The resulting mixture was centrifuged at 12,000 × g for 10 min at 4 ºC to separate the mixture into three phases; a lower red organic phase (containing protein), an interphase (containing DNA), and a colourless upper aqueous phase (containing RNA). The upper aqueous phase was carefully transferred

to a fresh tube and 500 µl 2-propanol (Sigma-Aldrich) was added. Samples were mixed, allowed to stand for 10 min then centrifuged at 12,000 × g for 10 min at 4 ºC. The RNA precipitate formed a pellet at the bottom of the tube. The supernatant was removed, and the RNA pellet was washed by adding 1 ml of 75% ethanol (Sigma-Aldrich) and centrifuging at 12,000 × g for 5 min at 4 ºC. The pellet was washed with ethanol once more. The ethanol was then removed, and the pellet left to air dry for 20-30 min before adding 50 µl 1X TE (Sigma-Aldrich). The sample was then heated at 60 ºC for 10 minutes to facilitate dissolution.

2.9.2 Reverse Transcription

The RNA was quantified using a NanoPhotometer P300 (Implen, Germany). Total RNA (3µg) was reverse transcribed into cDNA using the QuantiTect Reverse Transcription Kit (Qiagen, Manchester, UK) as per the manufacturer's instructions. 4 µl of 7 x gDNA wipeout buffer was added to 3 µg of each RNA sample in 24 µl nfH_20. Samples were placed in a BioRad T1000 Thermal Cycler (Bio-Rad, Hercules, CA, USA), incubated at 45 ºC for 2 min and then held at 4 ºC. An RNA reverse-transcription reaction mix was made up using 2 µl Quantiscript reverse transcriptase, 8 µl Quantiscript RT buffer 5x, 2 µl RT primer mix per reaction. 12 µl of the mix was added to each sample, and samples were incubated at 42 ºC for 15 min then 95 ºC for 5 min and finally held at 4 ºC. The resultant cDNA was diluted fourfold in nfH_20 and stored at -20 ºC.

2.9.3 Primers and probes for RNA-qPCR

Primers and dual-labeled probe with 6-Carboxyfluorescein (6-FAM) as the fluorescent dye and tetramethylrhodamine (TAMRA) as the quencher were designed using Primer Express software (version 3.0.1; Life Technologies). All primers and probes were ordered from Sigma (Dorset, UK). Primer and probe sets used for RNA-qPCR are shown in Table 2.7 for hnRNA and Table 2.8 for mRNA.

Standard curves, created from 2-fold serial dilutions of rat brain cDNA (BioChain, CA, USA), were performed for each primer pair, and the qPCR efficiency was calculated using the equation E = ((10 − 1/slope) − 1) × 100 (where E is qPCR efficiency, and the slope is the gradient of the standard curve). Only primer pairs with efficiencies greater that 90% were used.

Gene symbol	Accession number	Forward primer sequence	Reverse primer sequence	Probe sequence	Efficiency (%)
CyPA	NM_017101.1	AGCATACAGGTCCTGGCATCTT	CTTTCAACTGATCCATTCATTTTTTC	CATGGCAAATGCTGGACCAAACACAAA	90%
Hprt1	NM_012583.2	TGTGCTTGCAGACCAAATACTCTTA	CGTGGATCAAGACGAGACATTG	CCACTGAGTCACCTCCCCAATGCC	90%
Klf2	NM_001007684.1	ACCAACTGCGGCAAGACCTA	CTGAACTCGCTCCCATCCAT	CGCCTGGCCTCACTCCCCG	94%
Klf4	NM_053713.1	GCGGGAAGGGAGAAGACACT	CCCCATCTGCAGAAATCTAAAGG	CGTCCAGCAGGTGCCCCGA	90%
Klf9	NM_057211.1	TGTTATGTCCTGGTTTCCTTCTCTT	CGAGCGCGAGAACTTTTTAAG	TCCCCTGCACGTGGCCAGACT	91%
Klf15	NM_053536.1	TGGCACTGGCTTTGAAGTCA	AACTCATCTGAGCGTGAAAACCT	CCCACGATGGCCTGGCTGACC	94%
Ywhaz	NM_013011.3	GGGCACATGTGTCCGATACTG	CACCCTAGGGACAGCTTACAACA	CGCGATTGGATCCCCCGGAAT	90%

Table 2.7 hnRNA primers and probe sequences for RNA-qPCR

The Accession number of each gene, the primers and probe sequences and the efficiency of each primer/probe set is shown. Primers were designed to the latest version of the rat gene, Rnor_6.0.

Gene symbol	Accession number	Forward primer sequence	Reverse primer sequence	Probe sequence	Efficiency (%)
Gapdh	NM_017008.4	AAGAGAGAGGCCCTCAGTTGCT	ATTGTGAGGGAGATGCTCAGTGT	AGTCCCCATCCCAACTCAGCCCC	90%
Hprt1	NM_012583.2	CCTCCTCAGACCGCTTTTCC	CATAACCTGGTTCATCATCACTAATCA	CATGTCGACCCTCAGTCCCAGCG	95%
Klf2	NM_001007684.1	TGAGAAGCCTTATCATTGCAACTG	CCGTGTGCTTGCGGTAGTG	CGCGCGCTCTGACGAGCTTACC	93%
Klf4	NM_053713.1	GGCCCAGCTACCCTCCTTT	GGATCCCGGTGGCATGA	TGCCAGACCAGATGCAGTCGCAA	98%
Klf9	NM_057211.1	CCATTACAGAGTGCATACAGGTGAA	CGAGCGCGAGAACTTTTTAAG	CCTTCCCCTGCACGTGGCCA	100%
Klf15	NM_053536.1	GCTGCGGCTGGAGGTTTT	TTCACACCCGAGTGAGATCGT	CGCTCAGATGAGTTGTCACGGCACC	101%
Rpl10a	NM_031065.1	GAAGAACTACGACCCTCAGAAGGA	AGGACGCACACGGAGAACTT	AAACGCTTCTCGGGCACCGTCA	94%
Ywhaz	NM_013011.3	TGCTGCTGGTGATGACAAGAA	CATCTCCTTTTTGCTGATTTCAAA	TGGACCAGTCACAGCAAGCATACCAAGAA	99%

Table 2.8 mRNA primers and probe sequences for RNA-qPCR

The Accession number of each gene, the primers and probe sequences and the efficiency of each primer/probe set is shown. Primers were designed to the latest version of the rat gene, Rnor_6.0.

2.9.4 Real-time polymerase chain reaction for cDNA

2 µl cDNA was added to 18 µl mastermix in a 96-well plate. Mastermix was prepared containing 900 nM forward and reverse primers, 250 nM probe, and 1× TaqMan Fast Mastermix (Life Technologies) and made up to volume with nfH_20 (Promega). Plates were covered with an adhesive clear seal (Life Technologies) and spun down in a mini centrifuge prior to qPCR. Samples were run in duplicate and expression of RNA was calculated based on the Pfaffl method of relative quantification (Pfaffl, 2001) standardised to the expression of housekeeping genes (Table 2.9). qPCR was performed using a StepOne Plus Machine (Life Technologies). Taq enzymes were activated at 95 °C for 20 s, and then, 40 cycles of 95 °C (1 s) to 60 °C (20 s) were performed to amplify samples.

2.9.5 Selection of reference genes

One or more of the reference genes hypoxanthine phosphoribosyltransferase 1 *(Hprt1)* and tyrosine 3-monooxygenase/tryptophan 5-monooxygenase activation protein, zeta *(Ywhaz),* Glyceraldehyde 3-phosphate dehydrogenase *(Gapdh), Ribosomal protein L10a (Rpl10a),* Cyclophilin A *(CyPA)* were used to standardise RNA expression within the hippocampus (Figure 2.1), amygdala (Figure 2.2), prefrontal cortex (Figure 2.3) and neocortex (Figure 2.4). The data were expressed as fold change over baseline. Table 2.6 indicates which reference genes were used to normalise hnRNA and mRNA within each tissue.

	Brain Region	Reference genes
Chapter 5	Hippocampus	*Hprt1* and *Ywhaz*
	Amygdala	*Hprt1* and *Gapdh*
	Prefrontal cortex	*Hprt1* and *Ywhaz*
	Neocortex	*Rpl10a* and *CyPA*
Chapter 6	Hippocampus – RU/SPIRO	*Hprt1* and *Gapdh*
	Hippocampus – ADX	*Hprt1* and *Ywhaz*
Chapter 7	Hippocampus – MET	*Hprt1* and *Ywhaz*
	Hippocampus – ADX	*Hprt1* and *Ywhaz*

Table 2.9 Reference genes selected to normalise RNA levels within each brain region

For each RNA extraction, the corresponding reference gene used to normalise RNA levels are shown.

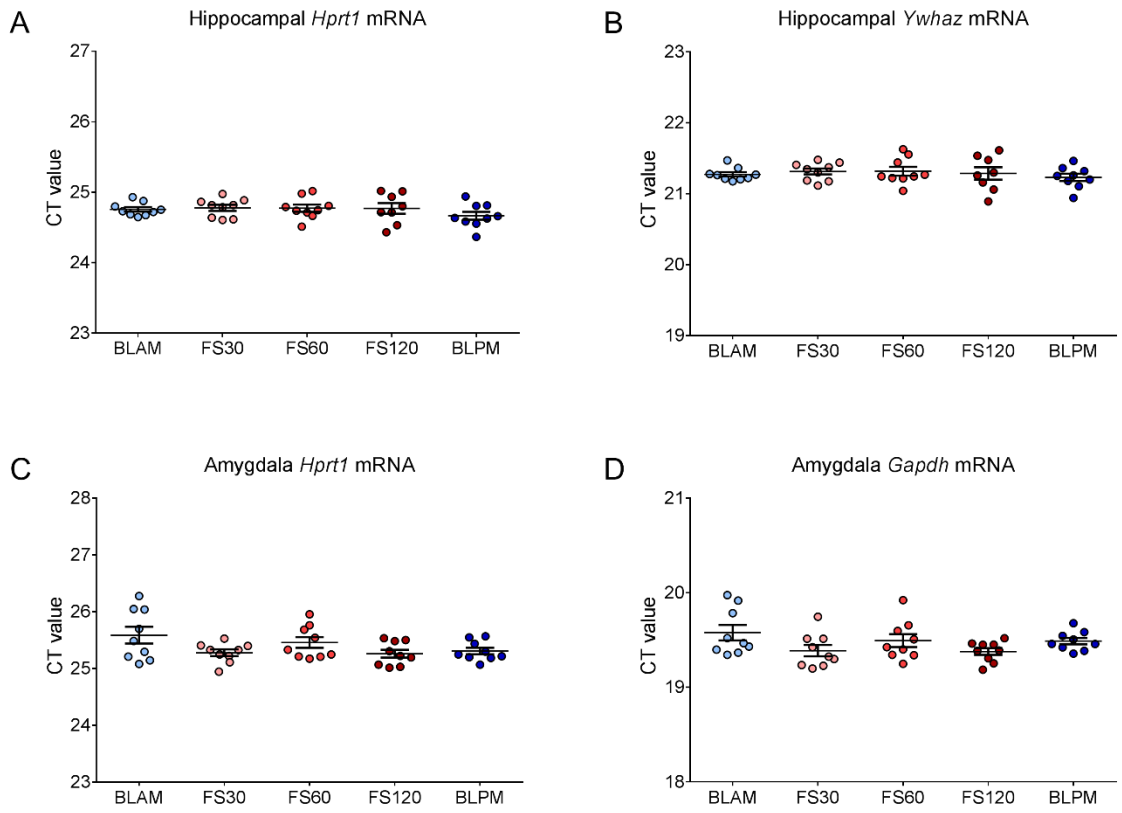

Figure 2.1 Hippocampal and Amygdala RNA CT values of reference genes *Hprt1, Ywhaz* and *Gapdh*

CT values from hippocampal (A-B) and amygdala (C-D) RNA samples for housekeeping genes *Hprt1, Ywhaz* and *Gapdh.* Rats were killed directly from their home cage under early baseline conditions ((~7:00 am), BLAM), 30 min (FS30), 60 min (FS60) or 120 min (FS120) following forced swimming or under late baseline conditions ((~5:00 pm), BLPM). RNA was extracted from the hippocampus and amygdala and reverse transcribed to cDNA. qPCR was carried out using dual-labelled primers and probes designed to amplify the reference genes shown. CT values of reference genes were used to normalise the expression of genes of interest using the Pfaffl method. Statistical analysis; One-way ANOVA (A) $F_{(4, 39)} = 0.8285$, $p = 0.5152$, (B) $F_{(4, 39)} = 0.3995$, $p = 0.8106$, (C) $F_{(4, 40)} = 2.285$, $p = 0.0769$, (D) $F_{(4, 40)} = 1.981$, $p = 0.1160$.

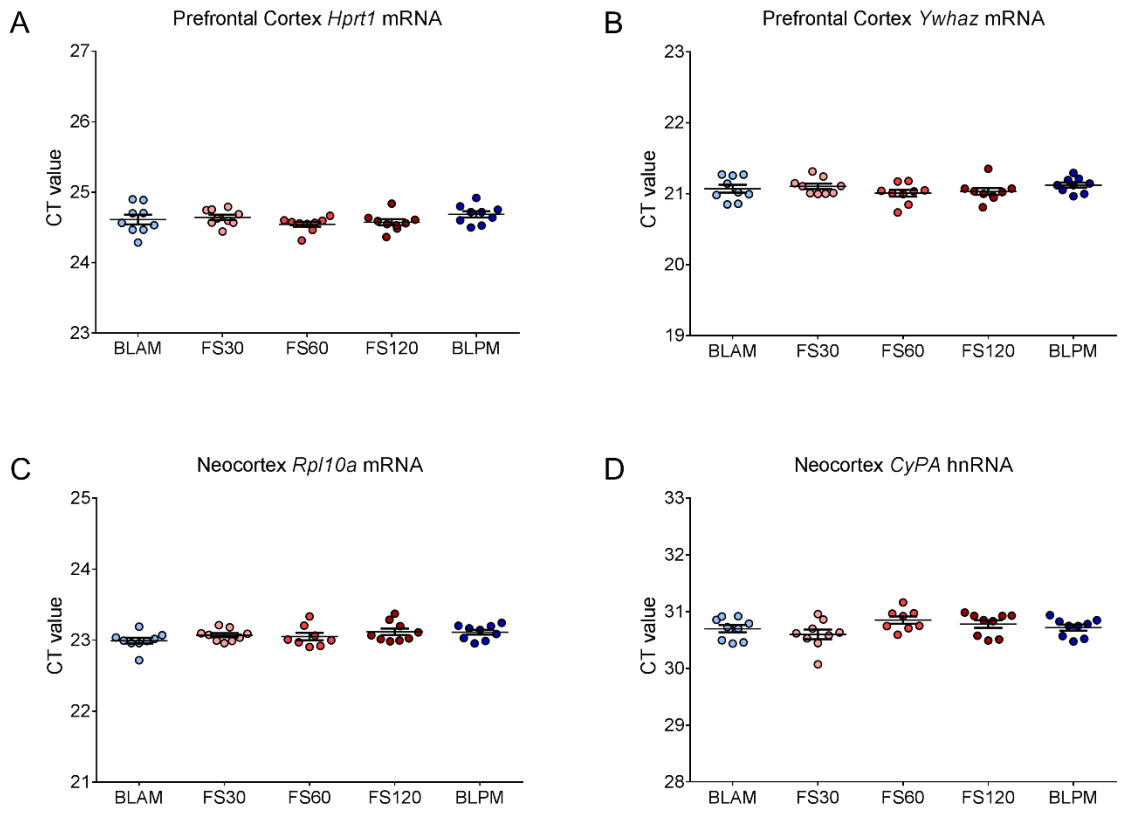

Figure 2.2 PFC and Neocortex RNA CT values of reference genes *Hprt1*, *Ywhaz, Rpl10a* and *CyPA*

CT values from PFC and neocortex RNA samples for housekeeping genes *Hprt1, Ywhaz, Rpl10a* and *CyPA.* Rats were killed directly from their home cage under early baseline conditions ((~7:00 am), BLAM), 30 min (FS30), 60 min (FS60) or 120 min (FS120) following forced swimming or under late baseline conditions ((~5:00 pm), BLPM). RNA was extracted from the PFC and neocortex and reverse transcribed to cDNA. qPCR was carried out using dual-labelled primers and probes designed to amplify the reference genes shown. CT values of reference genes were used to normalise the expression of genes of interest using the Pfaffl method. Statistical analysis; One-way ANOVA (A) $F_{(4, 40)} = 1.442$, $p = 0.2382$, (B) $F_{(4, 40)} = 1.128$, $p = 0.3571$, (C) $F_{(4, 39)} = 1.89$, $p = 0.1316$, (D) $F_{(4, 39)} = 1.574$, $p = 0.2004$.

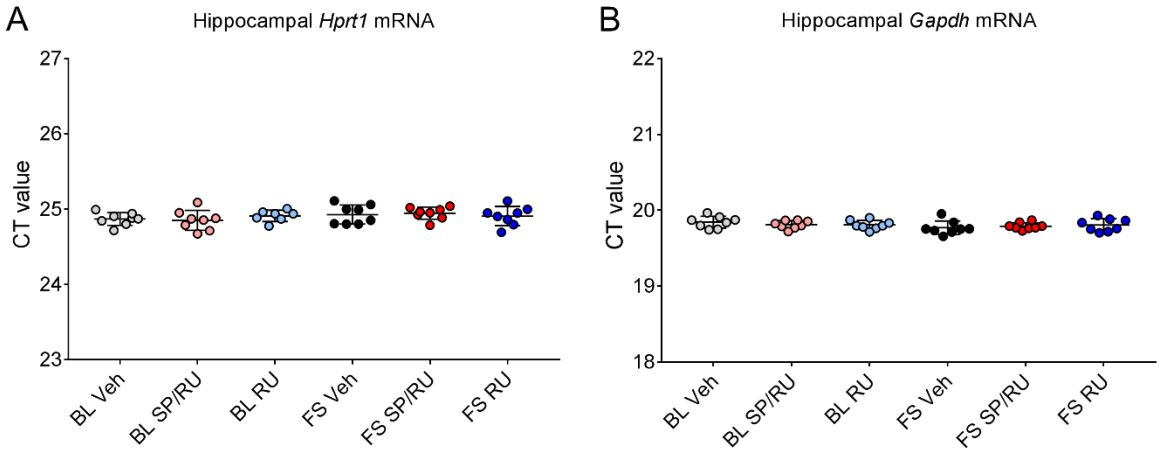

Figure 2.3 Hippocampal RNA CT values of reference genes *Hprt1* and *Gapdh* of rats treated with SP and RU

CT values from hippocampal RNA samples for housekeeping genes *Hprt1* (A) and *Gapdh* (B). Rats were voluntarily dosed with vehicle, a combination of SP (50 mg/kg) and RU (30mg/kg) or RU only (30mg/kg). Baseline rats were killed 120 minutes after voluntary dosing under early baseline conditions (~7:00 am (BL)). Stressed rats were voluntarily dosed 60 minutes before the onset of FS and killed 60 min after the start of FS (15 min, 25 °C water). RNA was extracted from the hippocampus and reverse transcribed to cDNA. qPCR was carried out using dual-labelled primers and probes designed to amplify the reference genes shown. CT values of reference genes were used to normalise the expression of genes of interest using the Pfaffl method. Statistical analysis; One-way ANOVA (A) $F_{(5, 41)} = 0.8563$, $p = 0.5185$, (B) $F_{(5, 42)} = 0.9829$, $p = 0.4395$.

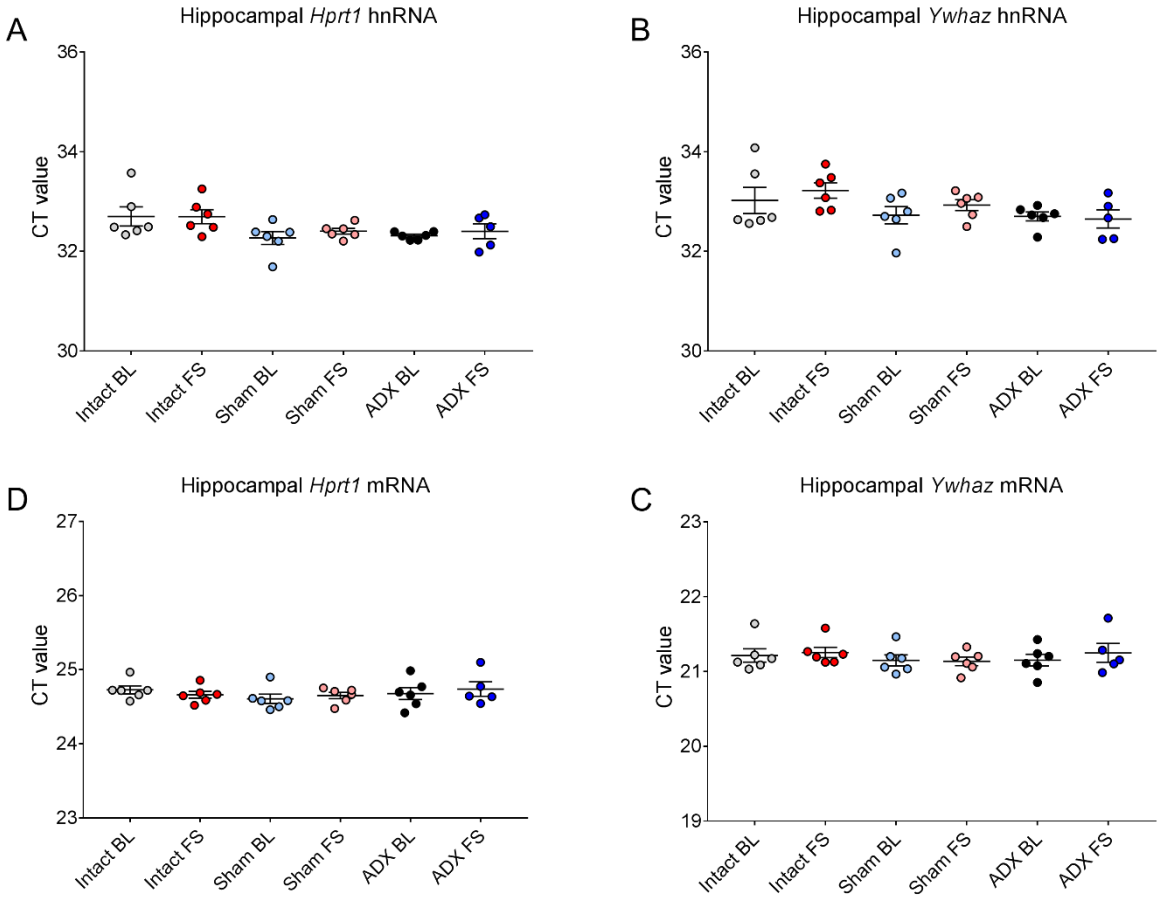

Figure 2.4 Hippocampal RNA CT values of reference genes *Hprt1* and *Ywhaz* of rats undergoing sham or ADX surgery

CT values from hippocampal RNA samples for housekeeping genes *Hprt1* (A and D) and *Ywhaz* (B and C). Rats underwent sham surgery or ADX and 1 week later, alongside an intact group, were killed under early baseline conditions (~7:00 am (BL)) or 60 min after the onset of FS (15 min, 25 °C water). RNA was extracted from the hippocampus and reverse transcribed to cDNA. qPCR was carried out using dual-labelled primers and probes designed to amplify the reference genes shown. CT values of reference genes were used to normalise the expression of genes of interest using the Pfaffl method. Statistical analysis; One-way ANOVA (A) $F_{(5, 29)} = 2.243$, $p = 0.0767$, (B) $F_{(5, 29)} = 1.683$, $p = 0.1702$, (C) $F_{(5, 29)} = 0.5743$, $p = 0.7191$, (D) $F_{(5, 29)} = 0.4114$, $p = 0.8369$.

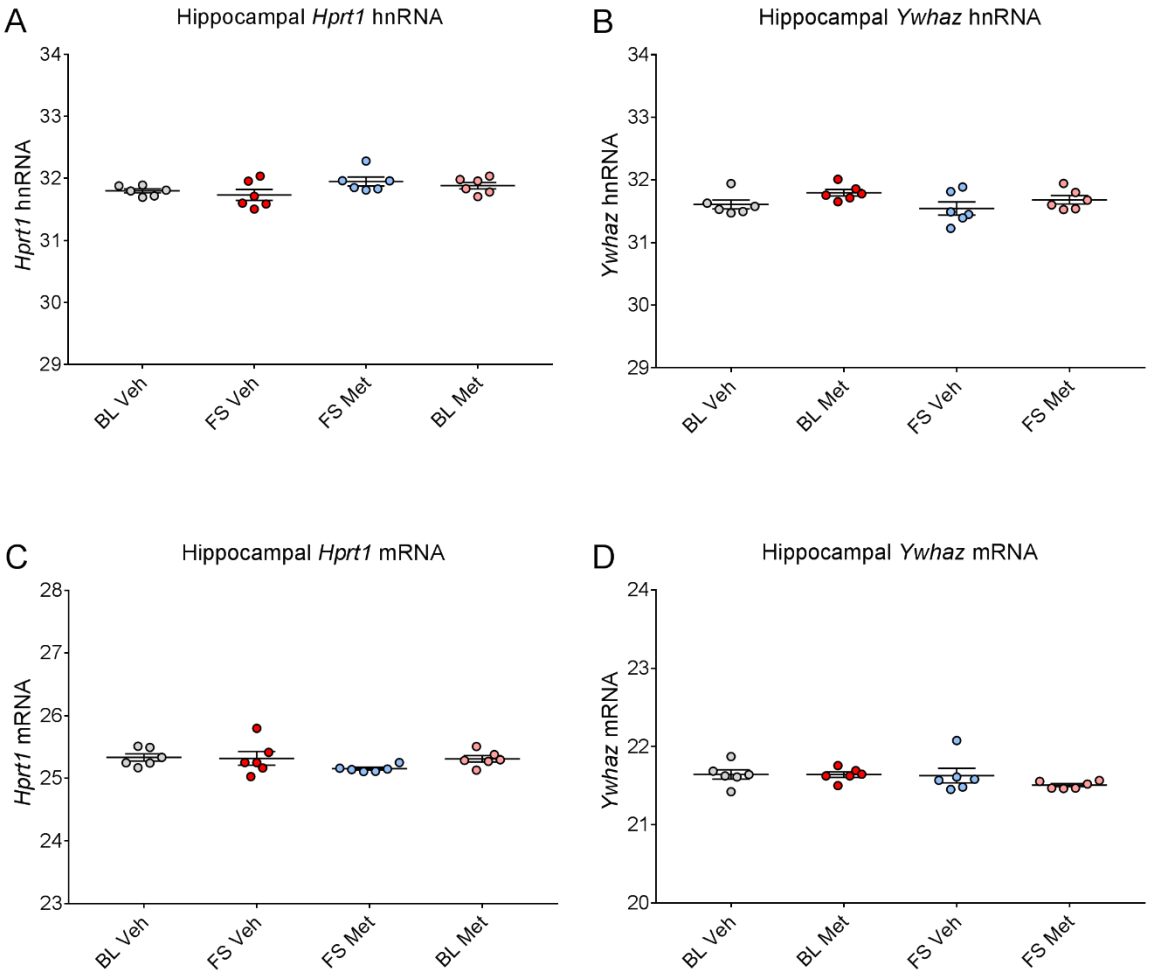

Figure 2.5 Hippocampal RNA CT values of reference genes *Hprt1* and *Ywhaz* of rats injected with vehicle or metyrapone

CT values from hippocampal RNA samples for housekeeping genes *Hprt1* (A and D) and *Ywhaz* (B and C). Rats were injected twice with vehicle or MET (100mg/kg) 90 minutes before the onset of FS, with a 90-minute interval between injections. Rats were killed 60 min after the start of FS (15 min, 25 °C water). RNA was extracted from the hippocampus and reverse transcribed to cDNA. qPCR was carried out using dual-labelled primers and probes designed to amplify the reference genes shown. CT values of reference genes were used to normalise the expression of genes of interest using the Pfaffl method. Statistical analysis; One-way ANOVA (A) $F_{(3, 20)} = 1.544$, $p = 0.2342$, (B) $F_{(3, 20)} = 1.26$, $p = 0.3148$, (C) $F_{(3, 20)} = 2.16$, $p = 0.1245$, (D) $F_{(3, 20)} = 2.033$, $p = 0.1416$.

2.10 RNA sequencing

2.10.1 RNA-seq library construction and sequencing

RNA was quantified using RiboGreen (Invitrogen) on the FLUOstar OPTIMA plate reader (BMG Labtech) and the size profile and integrity analysed on the 2200 or 4200 TapeStation (Agilent, RNA ScreenTape). RIN (RNA integrity number) estimates for all samples were between 7.4 and 8.5. Input material was normalised to 1 μg prior to library preparation. Total RNA was depleted of ribosomal RNA using Ribo-Zero rRNA Removal Kit (Epicentre/Illumina, Human/Mouse/Rat) following manufacturer's instructions. Library preparation was completed using TruSeq Stranded Total RNA kit (Illumina) following manufacturer's instructions. Libraries were amplified (15 cycles) on a Tetrad (Bio-Rad) using in-house unique dual indexing primers (Lamble et al., 2013). Individual libraries were normalised using Qubit, and the size profile was analysed on the 2200 or 4200 TapeStation. Individual libraries were normalised and pooled together accordingly. The pooled library was diluted to ~10 nM for storage. The 10 nM library was denatured and further diluted prior to loading on the sequencer. Paired-end sequencing was performed using a HiSeq4000 75bp platform (Illumina, HiSeq 3000/4000 PE Cluster Kit and 150 cycle SBS Kit), generating a raw read count of >45 million reads per sample.

2.10.2 Genome mapping and bioinformatic analysis of RNA-seq data

Quality control analysis was performed on data generated from individual samples as per ChIP (see above). RNA-Seq read pairs were aligned to Rattus norvegicus reference genome, Rnor_6.0 using a splice-aware aligner, Hisat2 version-2.0.4 (Kim et al., 2015). Gene annotation files were downloaded in GTF format from Ensembl, release 81 (Cunningham et al., 2015). GTF files with intron coordinates were prepared by subtracting annotated exon features from full-length transcripts using subtractBed implemented in Bedtools suite v2.26.0. Read fragments mapping to annotated exon features, or intron features were separately quantified to obtain exon, or intron count tables, respectively. All reads were counted with featureCounts (Liao et al., 2014), part of subread-v1.5.0 (Liao et al., 2013), using the specified parameters ("-M" "-O" "--fraction" "-p"). Values for duplication rates and median 3' bias were estimated using MarkDuplicates.jar, and CollectRnaSeqMetrics.jar implemented in Picard tools v1.92

(https://broadinstitute.github.io/picard/), respectively. Normalised read counts and count based metrics were obtained using in-house R scripts (Team, 2014), R core tools, v 3.1.0.

Differentially expressed genes were identified for each comparison using edgeR v3.20.4 (McCarthy et al., 2012, Robinson et al., 2010), R core tools, v3.4.2. Each comparison was analysed separately using subsets of the exon and intron count tables. First, the count tables were selected to samples of interest and expressed genes, keeping genes with greater than 10 reads in each biological replicate in a group. Then, count table subsets were normalised, and data were fit using generalised linear models as implemented in edgeR. Normalised fitted expression values were tested for differential expression between groups using likelihood ratio tests, and finally corrected for multiple comparisons using Benjamini-Hochberg correction to control the FDR; the probability of type II error (Benjamini and Hochberg, 1995). One biological replicate from the BLAM group, RN067, showed a different gene expression profile as compared to other samples in the experiment. We excluded this potential outlier from all downstream analysis as this sample consistently separated from the data and especially the BLAM group in hierarchical clustering as well as principal component analysis (PCA).

2.11 Pathway Analysis

Ingenuity Pathway Analysis (IPA) software was used to interpret data from ChIP-seq and RNA-seq experiments (QIAGEN Inc.,) (Kramer et al., 2014). A “Core Analysis” was performed on datasets included to predict diseases and functions associated with genes becoming bound by MRs or GRs or exhibiting differential RNA expression after acute stress and during the circadian rise.

2.11.1 ChIP-seq dataset preparation

A ChIP-seq dataset comprising all genes annotated to an MR or GR peak included in DiffBind analysis was uploaded to IPA. For each gene, the fold change in receptor binding, *p*-value and false discovery rate (FDR) was included. In instances where multiple peaks of the same category were annotated to a single gene, the largest fold change value was included in the dataset. A total of 1996 genes were included in the dataset, with IPA mapping 1495 gene IDs and 501 gene IDs left unmapped. 1303 genes with MR binding and 740 genes with GR binding were analysed.

2.11.2 RNA-seq dataset preparation

An RNA-seq dataset comprising all genes with significant (FDR<0.05) differential intronic RNA (inRNA) or exonic RNA (exRNA) expression following acute stress or the circadian rise was uploaded to IPA. For each gene, the fold change in RNA expression, *p*-value and FDR was included. CON genes were not included in the dataset as the number of CON genes exceeded the limit possible to upload to IPA. For genes responding at multiple timepoints during the acute stress time course, the maximal fold change expression value was included in the dataset. Data concerning 2238 genes were uploaded, with IPA mapping 2056 gene IDs and 182 IDs left unmapped.

2.11.3 Core Analysis

A core analysis was performed on each dataset by IPA which identified canonical pathways, upstream regulators, diseases and functions and networks predicted to be associated with genes present in the dataset. The settings for all core analyses were as follows; the reference set of genes was taken from the Ingenuity Knowledge base, interaction networks were considered, all node types and data sources were included, experimentally observed predictions were considered, all species were considered, nervous tissues and neuroblastoma cell lines were considered, and all mutations were considered. An FDR cut off of 1.0 was used to include constitutively bound genes.

Core Analysis identified canonical pathways predicted to be influenced by the genes in the datasets based on the directional changes in receptor binding or gene expression. Upstream regulators of the genes in the reference datasets were also predicted based on published experimental molecular interactions by correlating literature-reported effects with observed gene expression. Core analysis also identified diseases and functions predicted to be influenced by genes in the reference datasets. A directional change was also predicted on cellular processes and biological functions by correlating observed expression with reported experimental gene effects. Networks were predicted involving non-directional gene interactions.

An “overlap *p*-value” was calculated using a Right-Tailed Fisher’s Exact Test and reflects the likelihood that the association or overlap between the set of significant molecules from the datasets and a given pathway/interaction/network is due to random chance. The smaller the *p*-value the less likely that the association is random. The *p*-value does not consider the directional effect of one molecule on another, or the direction of change of molecules in the dataset.

A “z-score” was applied in some analysis types and provided predictions about upstream or downstream processes, considering the directional effect of one molecule on another molecule or on a process, and the direction of change of molecules in the dataset.

An additional analysis was performed where genes were separated based on the category of their respective peak or RNA response i.e. stress and circadian responsive (SR&CR), stress exclusive (SE), circadian exclusive (CE) and constitutive (CON). For the ChIP-seq dataset, there were too few peaks in the SE category for the MR (n=50) and in the SE (n=23), CE (n=6) and CON (28) category for GR, therefore, results of this analysis were difficult to interpret. Based on these observations, pathway analysis findings of ChIP-seq and RNA-seq datasets are presented as a whole in this thesis.

2.12 Statistical Analysis

The statistical and graphical package GraphPad Prism 7 (GraphPad Software, San Diego, CA, USA) was used to generate figures and perform statistical analysis. Results are presented as group means ± SEM; sample sizes are indicated in the figures. Data was tested for normality and homogeneity of variance using Shapiro-Wilk test. Statistical comparisons were conducted on normally distributed data with one- or two-way ANOVA. If significant, a Dunnett’s or Sidak post hoc test was performed for one- or two-way ANOVA respectively. Non-parametric data were tested using Kruskal-Wallis and if significant, a Dunn’s posthoc test was performed. Correlation analysis was performed using Spearman’s or Pearson’s correlation test on parametric or non-parametric data respectfully. $P<0.05$ were considered statistically significant.

Chapter 3 MR and GR genomic activity investigated by hippocampal genome-wide ChIP-sequencing and RNA-sequencing following acute stress and during the circadian rise

3.1 Abstract

GC hormones are of critical importance for physiological regulation across the circadian cycle and behavioural adaptation following stressful experiences. In the rat hippocampus, GCs act via MRs and GRs, which bind to responsive elements within the DNA and regulate the expression of GC target genes. MR and GR binding to GREs within promoter and intronic regions and corresponding transcriptional responses of GC target genes have been observed in the rat hippocampus following elevations in GC levels; however how GCs act to regulate gene transcription within the hippocampus at a genome-wide level is still largely unknown.

This study integrated ChIP- and RNA-seq in order to investigate the genome-wide binding of MRs and GRs and the associated transcriptional responses in the rat hippocampus under physiological conditions with differing GC secretion patterns (circadian variation and acute stress). Genome-wide binding peaks of MRs and GRs were identified primarily within distal intergenic, promoter and intronic regions of the DNA under all physiological conditions. In the majority of loci, acute stress and/or the circadian rise resulted in enhanced MR and/or GR binding, while a subset of loci exhibited constitutive binding of MRs or GRs. Moreover, the transcription factor recognition site composition within MR and GR binding peaks showed marked differences depending whether the site was constitutively or dynamically bound by either receptor. This binding motif analysis revealed that MR and GR bind to GC responsive elements (GREs) but also, most likely via intrinsic transcription factors, to many other motifs. In a subset of genes, MR and GR binding was accompanied by associated gene transcriptional changes. A positive correlation was found between changes in MR binding and the corresponding RNA responses, while changes in GR binding correlated with RNA responses to a lesser extent. These results show that hippocampal MRs and GRs, constitutively and dynamically, regulate hippocampal gene expression following physiologically driven GC secretion.

3.2 Introduction

GC hormones are of critical importance for central nervous system functioning during daily activities and following a stressful challenge. They play a pivotal role in stress resilience and behavioural adaptation (Oitzl and de Kloet, 1992, Roozendaal et al., 1996, Reul et al., 2015, Reul, 2014, McEwen, 2012). Impaired GC secretion and function has been associated with stress-related disorders like major depression, schizophrenia and post-traumatic stress disorder (de Kloet et al., 2005, McEwen, 2012, Reul et al., 2015). The link between GC hormone activity and the manifestation of these disorders remains yet to be elucidated.

GC secretion from the adrenal glands varies over the circadian cycle peaking at the onset of the active phase. Exposure to a stressful event results in a transient surge of GC secretion that is superimposed on the circadian rhythm. In the brain, GCs bind to two types of receptors, the MR and the GR (Reul and de Kloet, 1985), which co-localize in hippocampal neurons (Reul and de Kloet, 1986, van Steensel et al., 1996). Once bound and activated by GCs, MRs and GRs translocate to the cell nucleus where they behave as ligand-dependent transcription factors. MRs and GRs recognise and bind to GREs within the DNA, where they recruit coregulators to initiate or repress the transcription of GC target genes. It is thought that genomic actions in the hippocampus underlie the distinct roles of MR and GR in the control of circadian and stress-related physiology, cognition and behaviour, however, the molecular underpinnings of these receptor-mediated actions are still largely unresolved (Mifsud and Reul, 2018, Oster et al., 2017).

Comprehensive knowledge about genome-wide MR and GR interactions within the hippocampus under physiological conditions is currently lacking. Specifically, many of the genes affected by MR and/or GR across the circadian cycle or following stress are yet to be identified. Recently, chromatin immunoprecipitation (ChIP) analysis has been used to investigate the binding of MR and GR to well-known GC-target genes in the hippocampus (Mifsud and Reul, 2016). Although these experiments have demonstrated MR and GR binding to GREs within these genes and associated transcriptional responses, they do not provide a genome-wide insight into GC receptor interaction with DNA and largely focus on well-established GC target genes rather than novel targets.

The combination of ChIP with NGS technology provides the opportunity to sequence regions of the entire genome bound by MRs and GRs. Although a handful of ChIP-seq studies have been performed to elucidate the genomic actions of MRs and/or GRs in the rat hippocampus, they pose many limitations. So far, ChIP-seq studies have failed to represent physiological conditions of GC secretion, as they have been carried out in cell lines (Polman et al., 2012) or the hippocampus of ADX rats supplemented with CORT (Polman et al., 2013b, Pooley et al., 2017, van Weert et al., 2017). In particular, the existence of selectively MR- or GR-regulated genes within the genome has remained elusive, as parallel MR and GR ChIP-seq is limited to a single study (van Weert et al., 2017). Presently, MR and GR ChIP-seq has not been integrated with RNA-seq to determine the transcriptomic responses following transcription factor binding. Technically, these sequencing studies have been carried out with a low number of biological replicates and annotated to outdated versions of the rat genome. As long as the identity of all MR- and GR-targeted genes is undetermined, comprehensive insight into the function of these corticosteroid receptors in the hippocampus will be lacking.

Therefore, in this chapter, MR and GR binding is examined throughout the entire rat hippocampal genome under early morning baseline (BLAM) and late afternoon baseline (BLPM) conditions, representing the circadian trough and peak, and after exposure to an acute stressor (forced swimming (FS)). Moreover, this data is integrated with genome-wide transcriptional responses occurring in the rat hippocampus under the same conditions. This approach revealed comprehensive insight into the genomic loci bound by MR and/or GR and the transcription factor binding motifs involved. Motif analysis suggests alternative motifs to which MRs and GRs may indirectly bind, in the absence of a classical GRE. Furthermore, a subset of genomic loci constitutively bound my MRs and GRs are characterised, and changes in MR and GR binding are correlated with transcriptional responses in the target gene. Overall, this study offers the most detailed investigation to date into the genomic actions of MRs and GRs in the rat hippocampus under physiological conditions.

3.3 Materials and Methods

3.3.1 Animals

Male Wistar rats (150-175g) were purchased from Envigo (Oxon, UK) and group housed (two to three animals per cage). Animals were kept under standard light (lights on 5:00–19:00; 80–100 Lux) and environmentally controlled conditions (temperature 21 ± 1 °C; relative humidity 40–60%) with food and water available *ad libitum*. Until the day of the experiment all rats were handled (2 min per rat per day; min. 5 days) to reduce any nonspecific stress effects.

3.3.2 Stress Procedures

Rats were killed under early or late baseline conditions or following forced swimming (FS) as described in Chapter 2. Rats undergoing FS were killed at a number of timepoints following FS; timepoints are described in the text and figure legends and in each case refer to the amount of time from the start of FS.

3.3.3 Tissue Collection

Following quick isoflurane anaesthesia (<10sec) and decapitation, the brain was removed, and hippocampus dissected on an ice-cold steel box. Hippocampus tissues were snap-frozen in liquid N_2 and stored at -80 °C.

3.3.4 Radioimmunoassay

Trunk blood was collected at the point of decapitation and stored on ice in tubes containing EDTA and aprotinin for determination of plasma corticosterone concentration. Blood samples were prepared, and Corticosterone ^{125}I Double Antibody radioimmunoassay was carried out as described in Chapter 2.

3.3.5 ChIP-Seq sample preparation

Four independent biological replicates were sequenced per condition (BLAM, FS30, BLPM), each replicate consisting of the dissected hippocampi from two animals. Frozen hippocampus tissues were cross-linked in a buffered 1% formaldehyde solution, sonicated (Bioruptor (UC 300; Diagenode) (high power; 3 x 10 cycles, 30s on, 60s off) and chromatin prepared as previously described in Chapter 2. ChIP was performed by incubation with antibodies (10 µl/ChIP sample) against either MR (MR H-300,

sc11412x, Santa Cruz) or GR (GR H-300, sc8992x, Santa Cruz) with 200 µl chromatin as previously described in Chapter 2. Corresponding input samples were prepared as described in Chapter 2.

3.3.6 ChIP-seq library construction, sequencing, genome mapping and bioinformatic analysis

ChIP-seq library construction, sequencing, genome mapping and bioinformatic analysis was performed as previously described in Chapter 2.

3.3.7 RNA sample preparation

RNA was extracted from 9 independent biological samples per group (BLAM, FS30, FS60, FS120, FS180, FS360 and BLPM) as previously described in Chapter 2. Each biological sample comprised RNA from hippocampi of one rat. Three biological samples were randomly selected from the FS60 and FS120 groups to send for initial sequencing to confirm the possibility of conducting Ribo-Zero RNA-Seq. Following the success of this initial test, a further three randomly chosen samples from these groups (FS60 & FS120), along with 5 randomly selected samples from each of the other condition (BLAM, FS30, FS180, FS360 and BLPM) were subjected to RNA-seq.

3.3.8 RNA-seq library construction and sequencing

RNA-seq library construction, sequencing, genome mapping and bioinformatic analysis of RNA-seq data was performed as previously described in Chapter 2.

3.3.9 Statistical Analysis

The statistical and graphical package GraphPad Prism 7.04 was used to generate figures and perform Spearman rank correlation and other statistical analyses on the ChIP-qPCR and RNA RT-qPCR data (GraphPad Software, San Diego, CA, USA). The independent biological sample sizes (n-values) are indicated in the legends to the figures. Data were analysed with students t-test or one-way ANOVA followed by the *post-hoc* Dunnett's multiple comparison test, as appropriate. *P*-values <0.05 were considered statistically significant.

3.4 Results

3.4.1 Characterization of MR and GR binding peaks throughout the rat hippocampal genome

Genome-wide changes in hippocampal MR and GR binding following acute stress, or in response to the circadian rise in corticosterone levels, were quantified by ChIP-seq. MR and GR ChIP-seq was performed on hippocampal chromatin samples from rats killed under baseline conditions (BLAM, 7am-9am; BLPM, 5.30-7.00 pm, representing the trough and peak of circadian GC secretion in the rat, respectively), or 30 min after the start of an acute 15 min FS challenge, i.e. at the peak of the stress-evoked plasma corticosterone rise (FS30). Changes in plasma corticosterone levels (Figure 3.1) following acute stress and the circadian rise were examined. Compared with BLAM conditions, plasma corticosterone levels increased significantly following acute stress (> 64-fold) or in response to the circadian rise (> 17-fold).

Areas of the genome with significant peaks of MR or GR binding (Figure 3.2) under baseline conditions and following acute stress were identified. Under BLAM conditions, MRs (Figure 3.2.a) bound to >300 sites on average which increased significantly following acute stress (>5-fold) or in response to the circadian rise (>7-fold). GRs (Figure 3.2.b) bound to <100 sites on average under BLAM condition, however this number increased significantly following acute stress (~20-fold) and in response to the circadian rise (>8-fold).

The genomic location of MR and GR binding peaks was analysed (Figure 3.3). The highest levels of binding were seen within distal intergenic regions (A – MR, 40-50% of peaks; B – GR, 50-70% of peaks, depending on the experimental condition). The remaining peaks were predominantly located in the promoter or intronic regions. Acute stress and circadian influences led to increases in the number of both MR (Figure 3.3.a) and GR (Figure 3.3.b) peaks within exonic, intronic and 3'-untranslated regions (3'UTR) and a corresponding relative reduction of peaks at promoter (MR) or intergenic regions (GR), representing a shift in the genomic distribution of peaks due to the experimental condition.

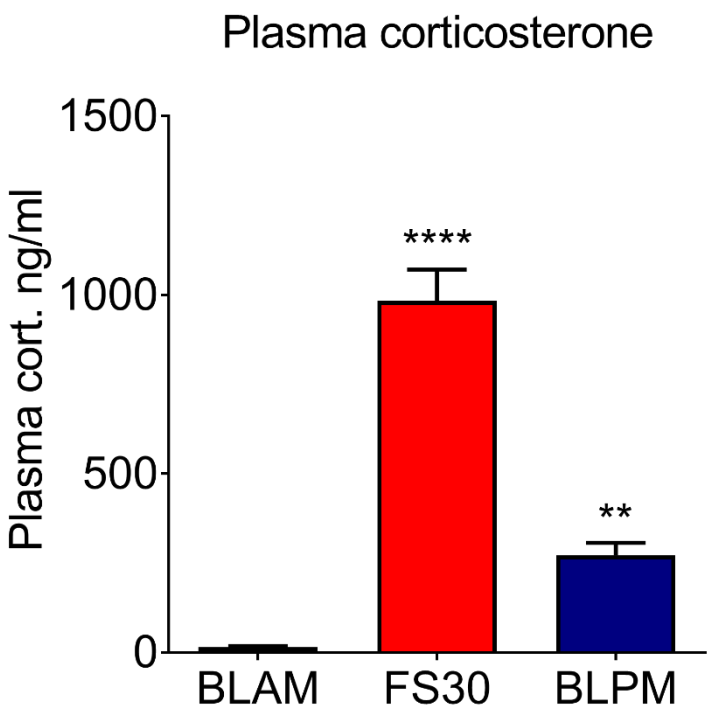

Figure 3.1 Plasma corticosterone levels in rats under early morning baseline conditions, following acute stress or under late afternoon baseline conditions

Rats were killed under early morning baseline conditions (~7:00 hrs (BLAM)), 30 min (FS30) after the start of FS (15 min, 25ºC water) or under late afternoon baseline conditions (~17:00 hrs (BLPM)). Plasma corticosterone levels are expressed as ng/ml (mean ± SEM, n=12 per group). Average concentration at BLAM, 15.20 ng/ml. Statistical analysis: one-way ANOVA, $F_{(2, 33)} = 85.07$, $p<0.0001$, Dunnett's post hoc test, $^{**}P<0.01$, $^{****}P<0.0001$ significantly different from BLAM. Inter-assay coefficient of variation, , intra-assay coefficient of variation, 2.57%.

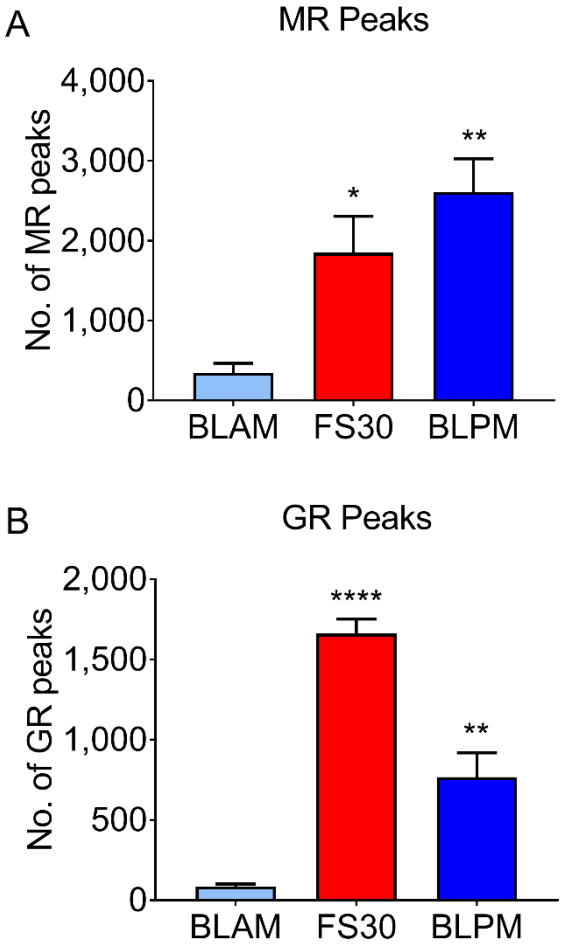

Figure 3.2 Identification of significant MR and GR binding peaks under early morning baseline conditions, following acute stress and under late afternoon baseline conditions

Rats were killed under early morning baseline conditions (~7:00 hrs (BLAM)), 30 min (FS30) after the start of FS (15 min, 25ºC water) or under late baseline conditions (~17:00 hrs (BLPM)). MR and GR binding peaks in the hippocampus were determined by ChIP-seq. Data is presented as number of MR peaks (A) and GR peaks (B) under each biological condition (mean ± SEM, n=4 per group). Statistical analysis: one-way ANOVA, MR: $F_{(2, 9)}$ =10.06, p<0.01, GR: $F_{(2, 9)}$=59.01, p<0.0001, Dunnett's post hoc test, *P<0.05, **P<0.01, ****P<0.0001 significantly different from BLAM.

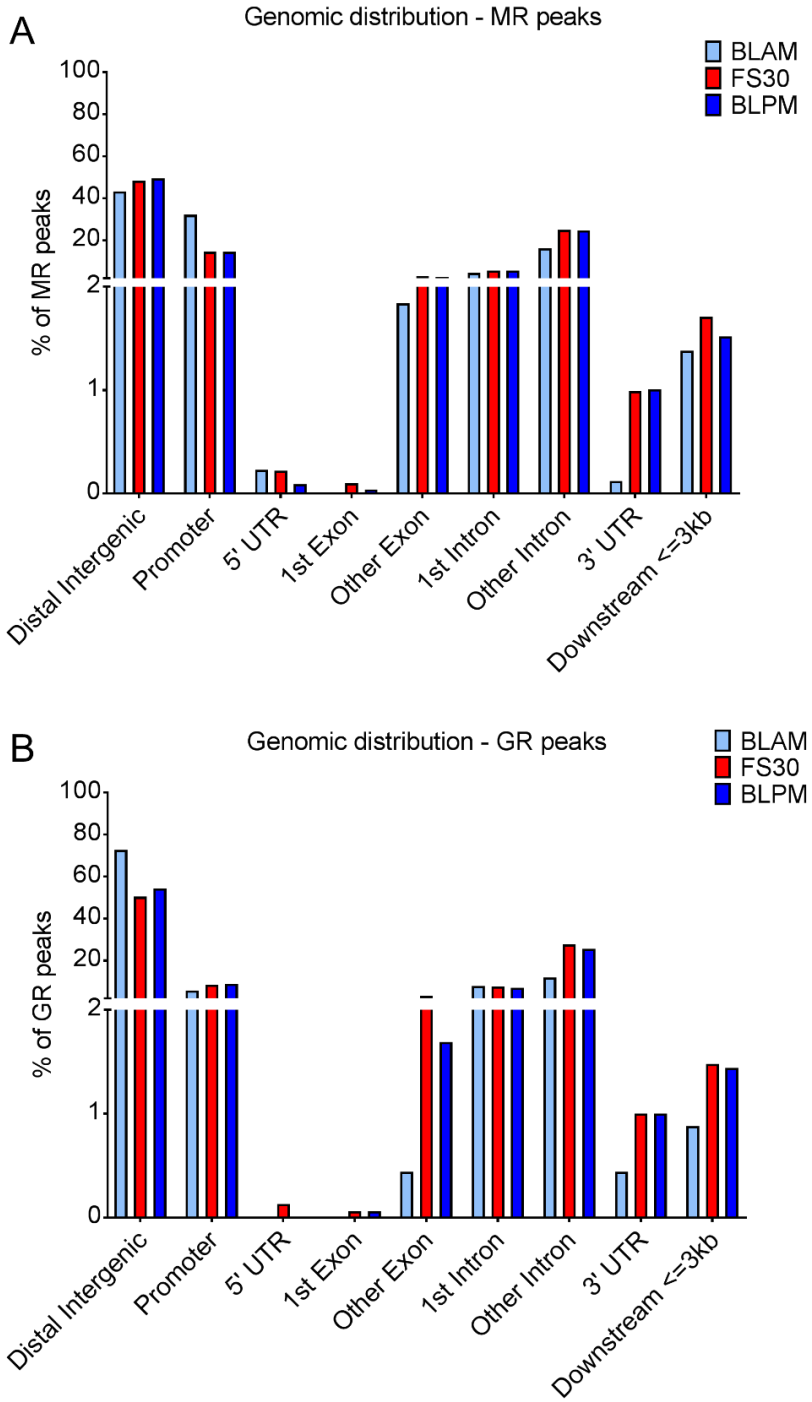

Figure 3.3 Genomic distribution of MR and GR binding peaks under early baseline conditions, following acute stress and under late baseline conditions

Rats were killed under early morning baseline conditions (~7:00 hrs (BLAM)), 30 min (FS30) after the start of FS (15 min, 25ºC water) or under late baseline conditions (~17:00 hrs (BLPM)). Data is presented as % of MR peaks (A) and % of GR peaks (B) under each physiological condition (mean, n = 4 per group). Untranslated region, (UTR). Absence of bars indicate peaks were not detected in the genomic region under the corresponding physiological condition.

3.4.2 Genome-wide MR and GR binding is regulated by acute stress and circadian influences

To determine whether genome-wide binding of MRs and GRs changed following acute stress and during the circadian rise, differential binding analysis was carried out, which identified genomic regions in which MR binding and GR binding was significantly upregulated or downregulated at FS30 or BLPM compared with BLAM. A correlation heat map of the read count data shows a robust clustering of biological replicates within each experimental condition and shows a clear differentiation between samples collected under BLAM, FS30 and BLPM conditions for the MR ChIP (Figure 3.4.a) and GR ChIP (Figure 3.4.b).

A total of 1753 MR peaks (Figure 3.5.a) and 1066 GR peaks (Figure 3.5.b) were selected for differential binding analysis by the computational package, “DiffBind”. The majority of genomic locations identified by DiffBind analysis were stress- and circadian-responsive (SR&CR) i.e. became differentially bound under both physiological conditions (MR: 60%; GR: 92%). In contrast, only a very limited number of binding sites were stress exclusive (SE) i.e. became differentially bound solely in response to acute stress (MR: 3%; GR: 2%). A higher percentage of MR peaks (9%) were circadian exclusive (CE) i.e. showed differential binding selectively in response to the circadian drive, when compared with GR peaks (1%). The percentage of genomic loci which showed constitutive (CON) binding, i.e. the level of binding did not change between conditions, was also substantially higher for MR (28%) than GR (5%).

Almost all differentially bound MR peaks and GR peaks were upregulated following acute stress (MR, Figure 3.6.a; GR, Figure 3.6.b) and the circadian rise (MR, Figure 3.7.a; GR, Figure 3.7.b). The magnitude of change in MR binding (Figure 3.8.a) was also significantly larger following acute stress (2.489 ± 0.034, mean ± SEM, n=4; Log_2FC). compared with the circadian rise (2.24 ± 0.028, mean ± SEM, n=4; Log_2FC). Similarly, for the GR (Figure 3.8.b), acute stress induced a significantly larger change in binding (4.063 ± 0.041, mean ± SEM, n=4; Log_2FC) compared with the circadian rise (3.37 ± 0.037, mean ± SEM, n=4; Log_2FC).

A

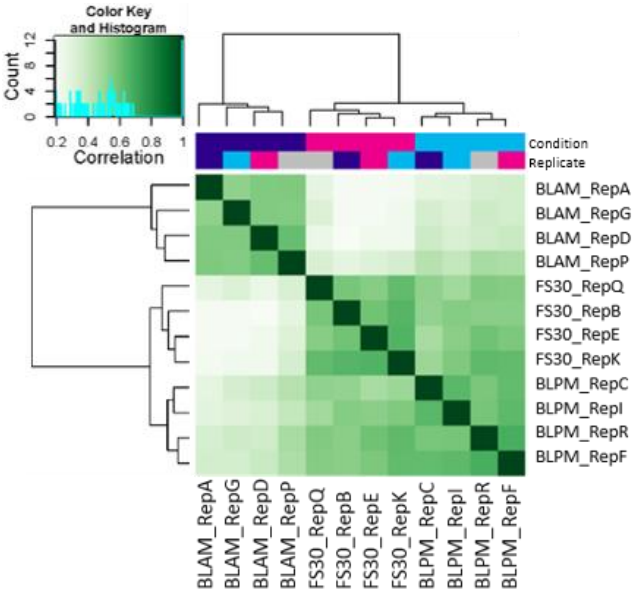

B

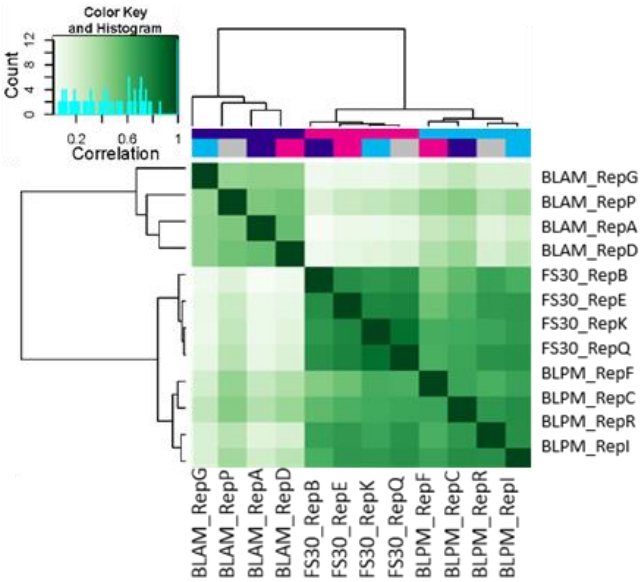

Figure 3.4 Quality control heat maps of MR peaks and GR peaks from each biological replicate undergoing differential binding analysis

Significant (A) MR peaks and (B) GR peaks from each biological replicate underwent differential binding analysis. Quality control reveals clustering of samples under each physiological condition (n=4 per group).

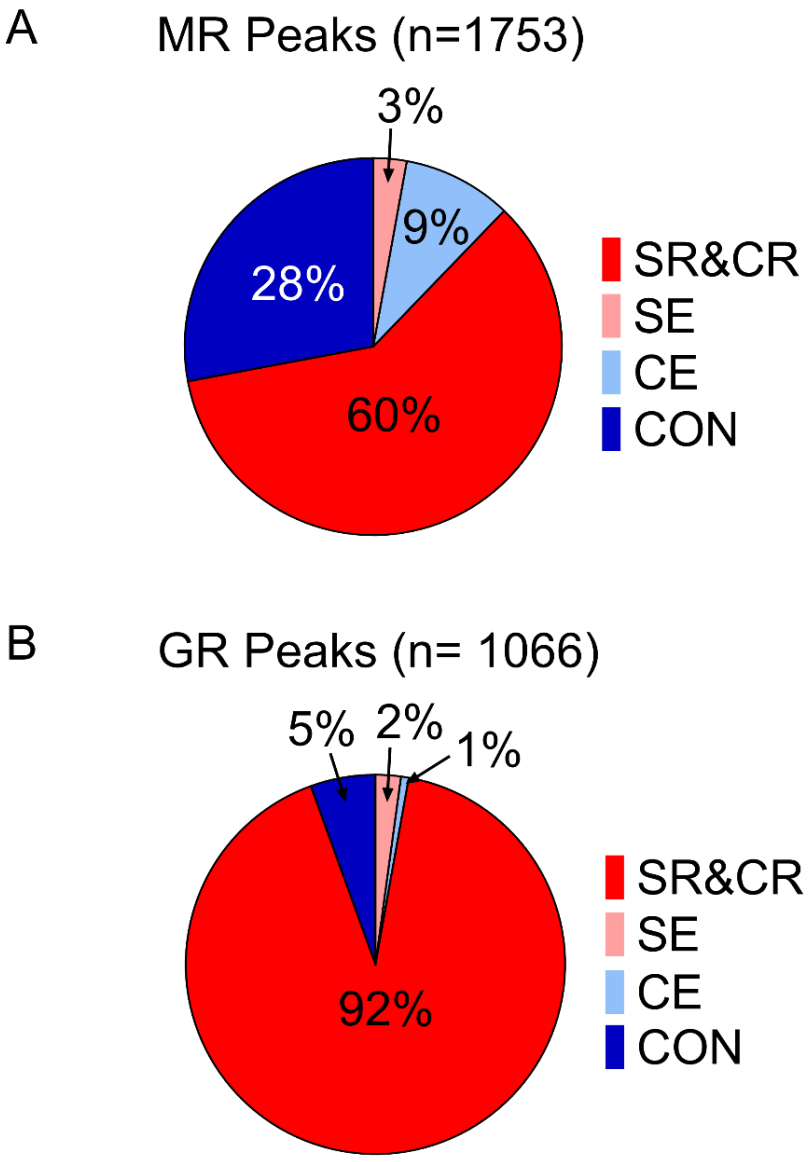

Figure 3.5 Categorisation of MR and GR peaks based on the physiological condition(s) in which binding significantly changed

Pie charts display the proportion of (A) MR peaks and (B) GR peaks becoming differentially bound in response to both stress and the circadian rise (Stress-responsive and circadian-responsive - SR&CR), exclusively following stress (Stress exclusive – SE), exclusively under the circadian rise (Circadian exclusive – CE), or peaks in which the binding of the receptor remains unchanged between conditions (Constitutively bound - CON).

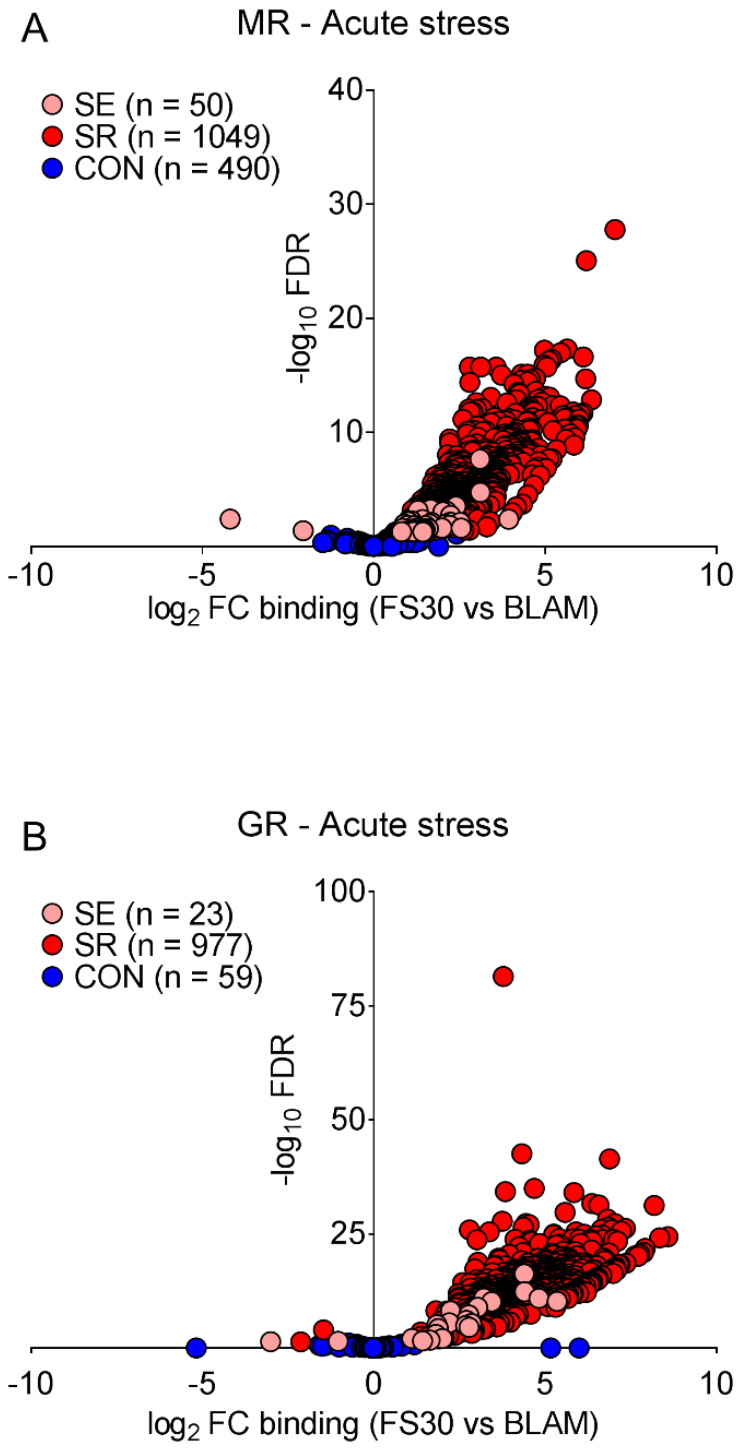

Figure 3.6 Acute stress results in genome-wide changes in the binding of MRs and GRs

DiffBind analysis identified MR and GR peaks which were differentially bound following acute stress. Scatterplots exhibit the fold change in binding (log_2 FC) of the (A) MR and (B) GR versus the significance of the change ($-log_{10}$FDR) following acute stress (FS30 vs BLAM). SE; stress exclusive, SR; stress responsive, CON; constitutive.

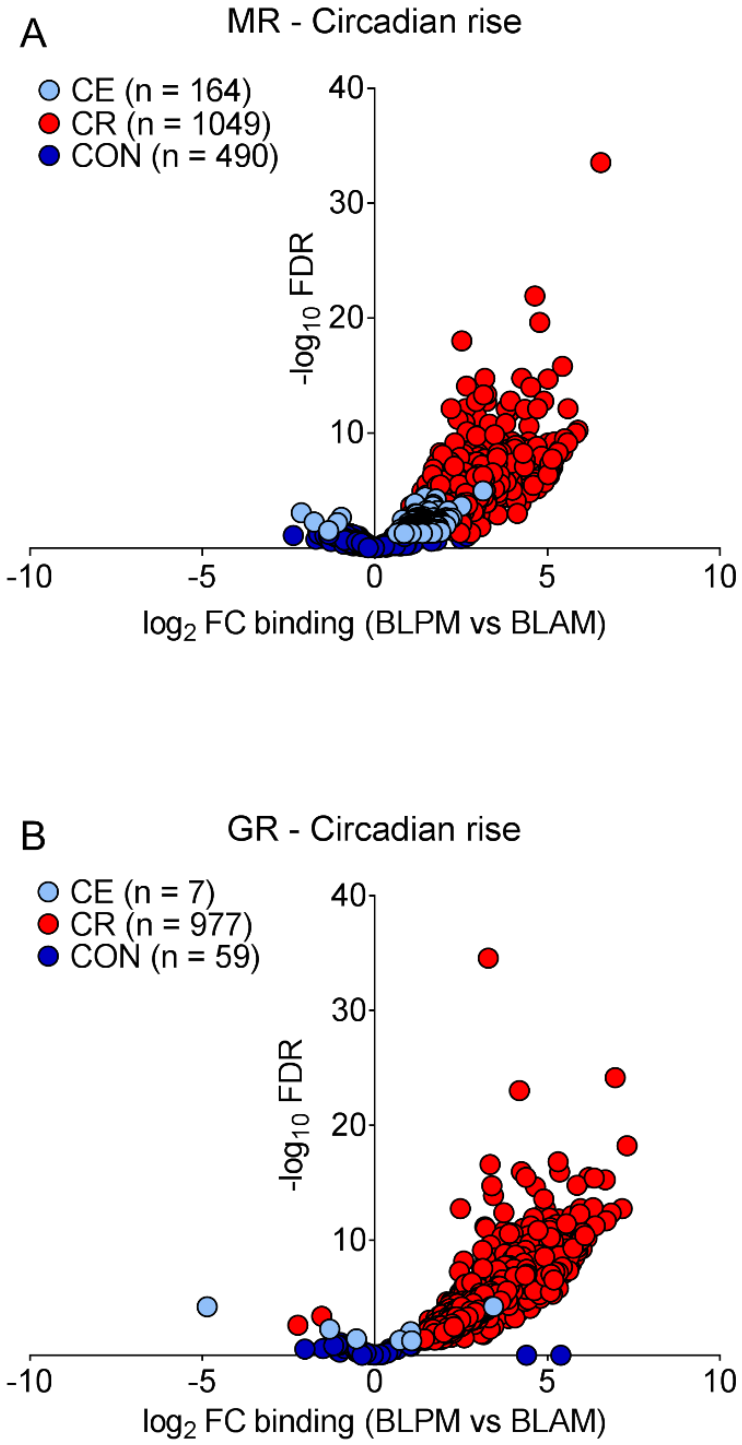

Figure 3.7 The circadian rise results in genome-wide changes in the binding of MRs and GRs

DiffBind analysis identified MR and GR peaks which were differentially bound during the circadian rise. Scatterplots exhibit the fold change in binding (log_2 FC) of the (A) MR and (B) GR versus the significance of the change ($-log_{10}$FDR) following the circadian rise (BLPM vs BLAM). CE; circadian exclusive, CR; circadian responsive, CON; constitutive.

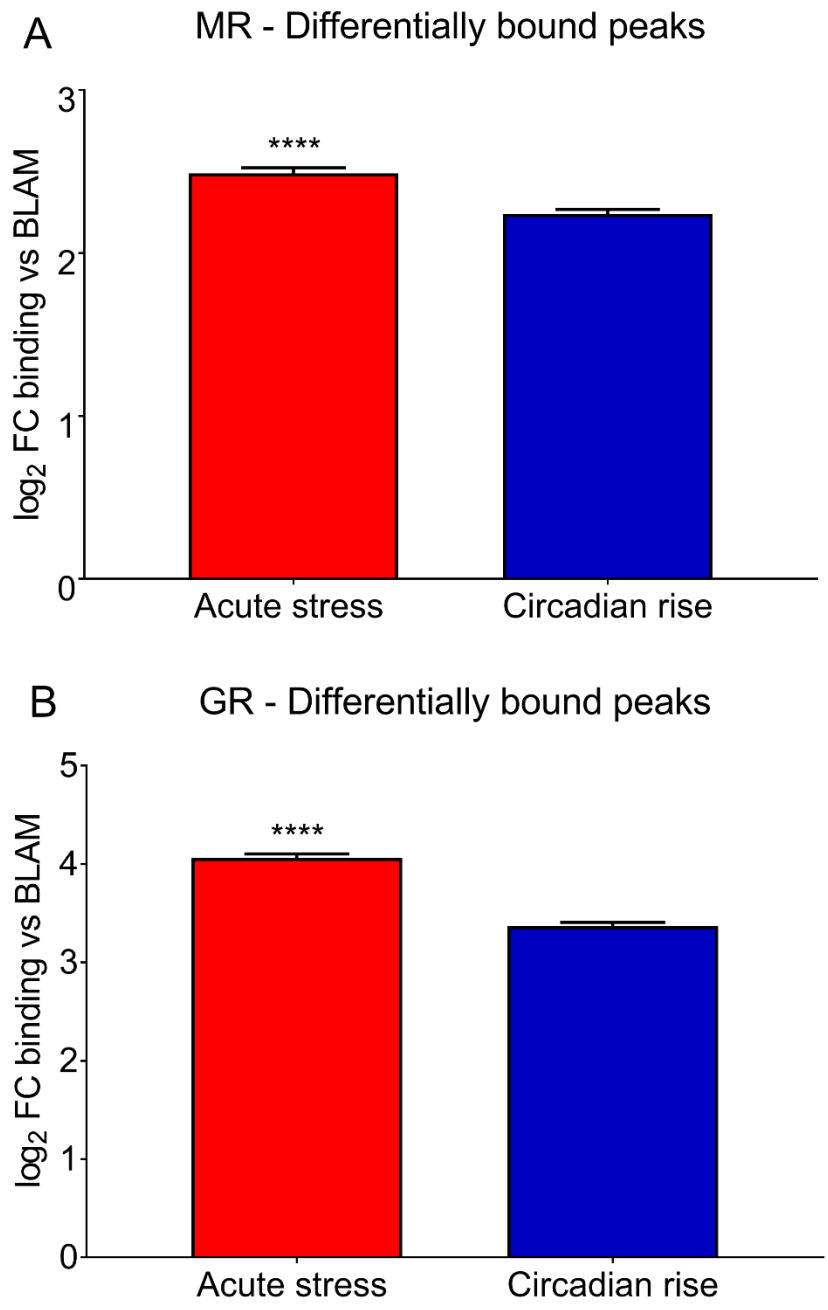

Figure 3.8 Acute stress induces a larger change in MR and GR binding compared with the circadian rise

Following acute stress, the average fold change in binding, as calculated by DiffBind, for the MR (A) and the GR (B) was significantly higher compared with the average fold change in binding during the circadian rise. Binding levels are expressed as $\log_2$ fold change in binding vs levels under BLAM conditions (mean ± SEM, n=4). Statistical analysis: unpaired t-test, (A) t=5.685, p<0.0001, (B) t=12.53, p<0.0001.

3.4.3 MR and GR peaks are associated with distinct transcription factor binding motif patterns, depending on the physiological condition

The top-500 peaks, based on statistical significance (false discovery rate, FDR) from the MR and GR datasets were subject to *de novo* motif analysis, identifying the binding motif with the highest occurrence and statistical significance. The most prevalent motif was matched to a palindromic GRE for both MR (Figure 3.9.a) and GR (Figure 3.9.b) binding datasets. Whilst a GRE was present in 100% of the top-500 GR peaks, only ~67% of the top-500 MR peaks contained a GRE. Find Individual Motif Occurrences (FIMO) software was used to identify motifs present in the 1753 MR and 1066 GR peaks included in the DiffBind analysis. The 5 most prominent motifs within each peakset were identified. Overall, GREs were the most prominent motif found within each peakset, with this response element observed in 77% of all MR peaks (Figure 3.10) and 93% of all GR peaks (Figure 3.11). A similar incidence of Zinc Finger (ZNF), Specificity Protein (SP) and Krüppel-like Factor (KLF) motifs within MR peaks (70-76%) and GR peaks (68-74%) was observed. Early Growth Response (EGR) motifs were found in 64% of MR peaks (Figure 3.10), while 44% of GR peaks (Figure 3.11) contained EWS RNA Binding Protein 1-Fli-1 Proto-Oncogene, ETS transcription factor (EWSR1-FLI1) motifs.

The top-5 most prominent motifs were subsequently identified according to peak category. The GRE was no longer one of the top-5 motifs in CON MR peaks (Figure 3.10) or in CON and CE GR peaks (Figure 3.11). ZNF, SP and EGR motifs remained in the top-5 among all MR peak categories, while KLF motifs were present in the top-5 for CON and SE peaks (Figure 3.10). Regulatory Factor X (RFX), Atonal BHLH Transcription Factor (ATOH1) and EWSR1-FLI1 motifs entered the top-5 for CON, CE and SR&CR MR peaks, respectively (Figure 3.10). For the GR (Figure 3.11), SP motifs remained in the top-5 among CE, SE and SR&CR peaks, while ZNF motifs remained in the top-5 among SE and SR&CR peaks. KLF and EWSR1-FLI1 motifs remained in the top-5 among SR&CR peaks only. A number of motifs entered the top-5 list, including Nuclear Receptor (NR), NKX Homeobox (NKX), Signal Transducer and Activator of Transcription (STAT), Paired Box (PAX), ATOH1 and Estrogen Receptor (ESR) motifs. Caution is required when interpreting the top-5 motifs in the CE GR binding peaks, due to the low number of peaks. Ten motifs were selected based on the top-5 among all peak categories and their incidence among peak categories are presented as stacked bars for the MR (Figure 3.12.a) and GR (Figure 3.12.b). This view clearly displays the higher percentage of MR peaks showing CON and CE binding when compared with percentages of GR peaks presenting this binding.

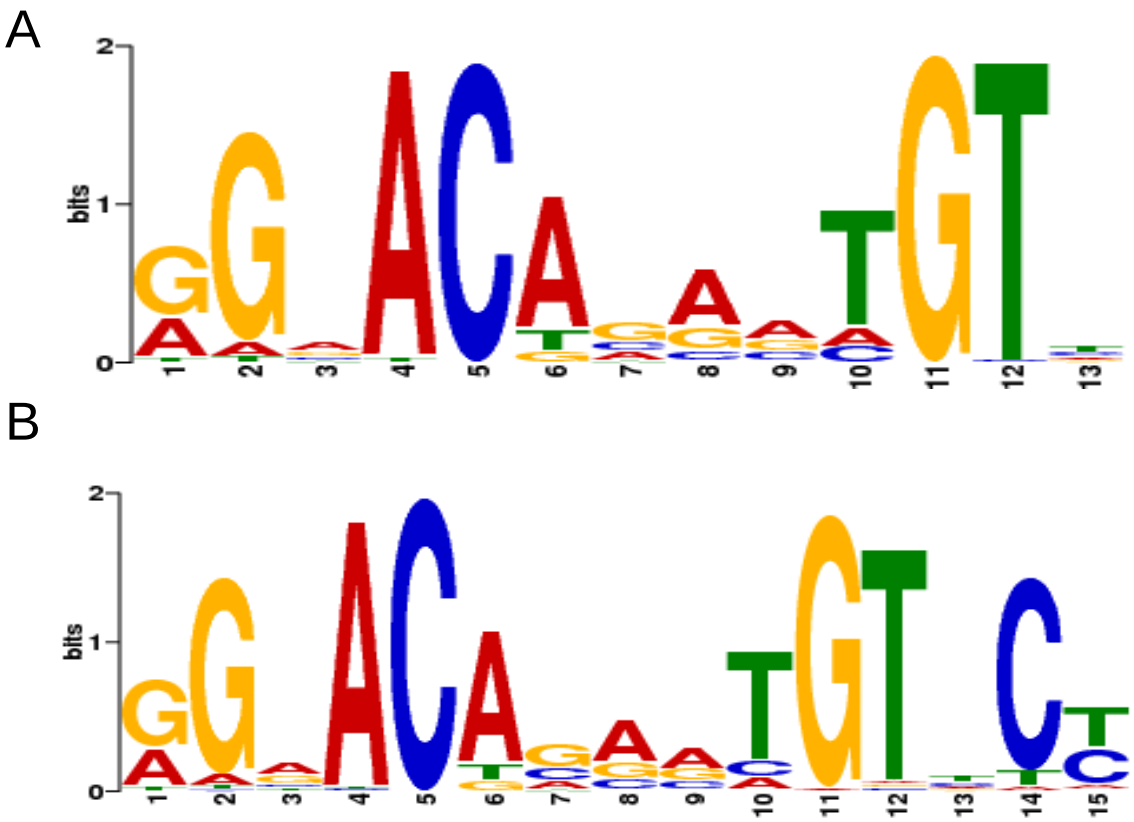

Figure 3.9 MEME analysis of the top 500 MR and GR binding peaks across all biological conditions reveals the motif with the highest occurrence and statistical significance

The top-500 MR and GR binding peaks across all biological conditions underwent MEME analysis to identify the motif with the highest occurrence and statistical significance. (A) MR peaks were associated with a motif matching the palindromic GRE (E = 1.2e-157). The motif was present in 67% of the top 500 MR peaks. (B) GR peaks were associated with a motif matching the palindromic GRE (E = 8.7e-668). The motif was present in 100% of the top GR peaks.

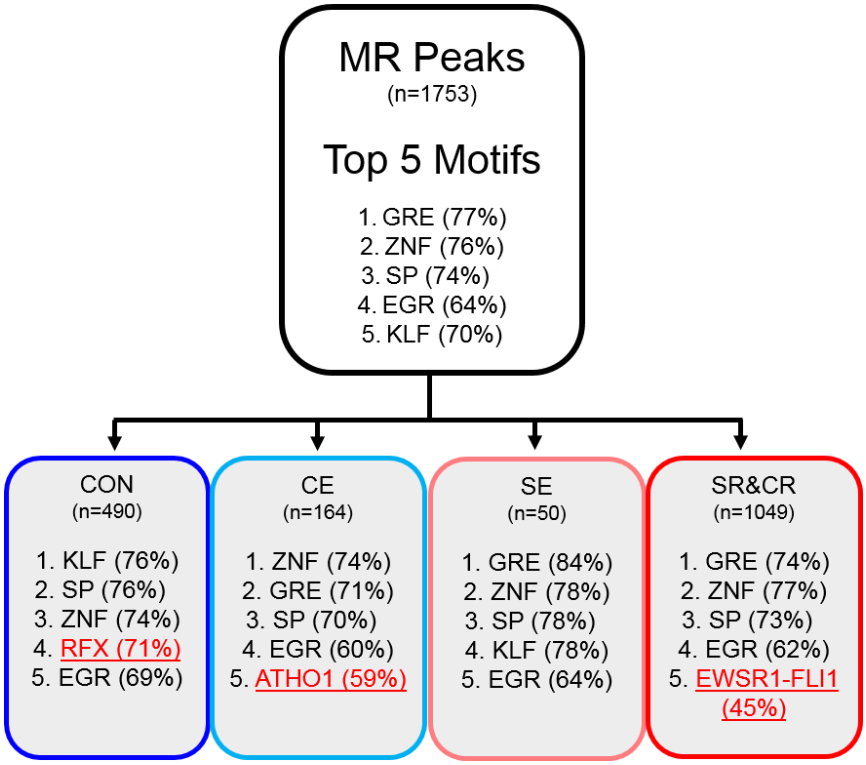

Figure 3.10 FIMO analysis reveals the top 5 transcription factor binding site motifs predicted within all MR peaks and each MR peak subcategory

A flowchart displays the top-5 motifs found within MR peaks. The first level of the flowchart shows the top-5 motifs within all MR peaks. The second level of the flowchart shows the top-5 motifs within CON (constitutive), CE (circadian exclusive), SE (stress exclusive) and SR&CR (stress & circadian responsive) peaks for the MR. Motifs underlined and highlighted in red are only found in the top 5 within that peak category. The percentage of peaks containing the respective motif is indicated between brackets. Glucocorticoid Response Element (GRE), Zinc Finger (ZNF), Specificity Protein (SP), Early Growth Response (EGR), Krüppel-like Factor (KLF), Regulatory Factor X (RFX), Atonal BHLH Transcription Factor 1 (ATOH1), EWS RNA Binding Protein 1-Fli-1 Proto-Oncogene, ETS transcription factor (EWSR1-FLI1).

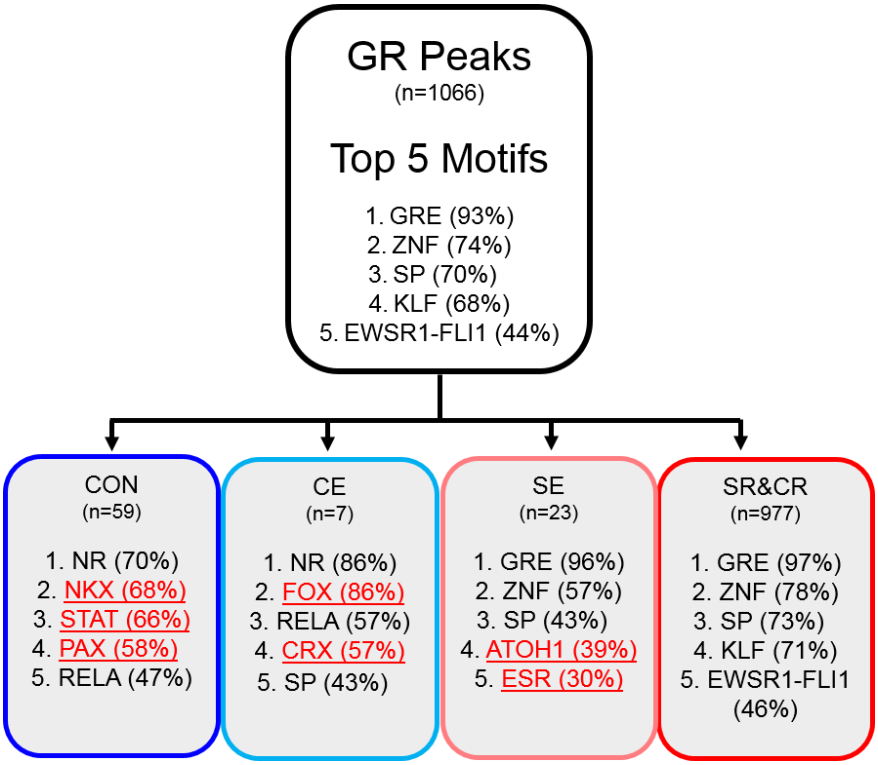

Figure 3.11 FIMO analysis reveals the top 5 transcription factor binding site motifs predicted within all GR peaks and each GR peak subcategory

A flowchart displays the top-5 motifs found within GR peaks. The first level of the flowchart shows the top-5 motifs within all GR peaks. The second level of the flowchart shows the top-5 motifs within CON (constitutive), CE (circadian exclusive), SE (stress exclusive) and SR&CR (stress & circadian responsive) peaks for the GR. Motifs underlined and highlighted in red are only found in the top 5 within that peak category. The percentage of peaks containing the respective motif is indicated between brackets. Glucocorticoid Response Element (GRE), Zinc Finger (ZNF), Specificity Protein (SP), Krüppel-like Factor (KLF), EWS RNA Binding Protein 1-Fli-1 Proto-Oncogene, ETS transcription factor (EWSR1-FLI1), Nuclear Receptor (NR), NKX Homeobox (NKX), Signal Transducer and Activator of Transcription (STAT), Paired Box (PAX), RELA Proto-Oncogene, NF-KB Subunit (RELA), Forkhead Box (FOX), Con-Rod Homeobox (CRX), Atonal BHLH Transcription Factor (ATOH1), Estrogen Receptor (ESR).

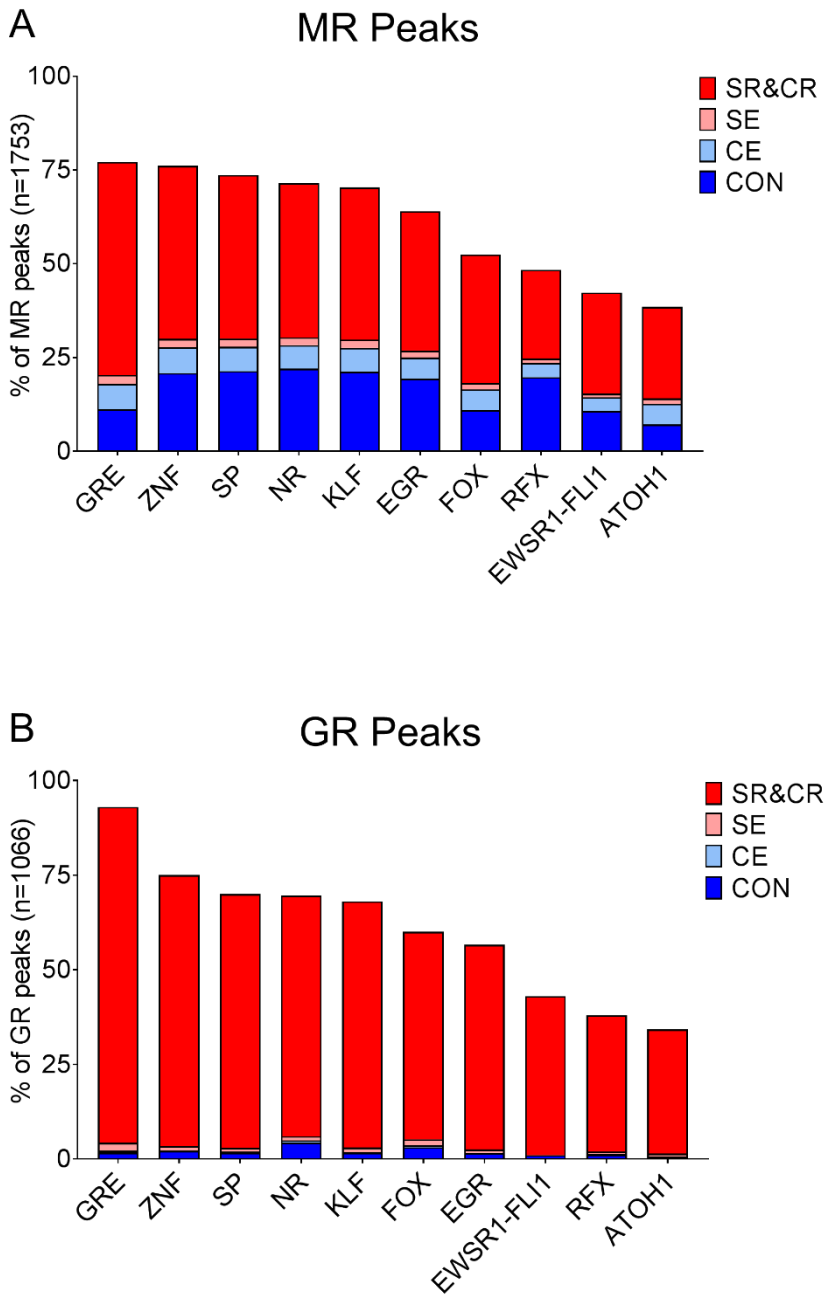

Figure 3.12 Top motifs predicted within MR and GR peak subcategories

10 motifs were selected for further analysis based on identification of the top motifs within each peak category. Stacked bar charts show the percentage of SR&CR (stress and circadian responsive), SE (stress exclusive), CE (circadian exclusive) and CON (constitutive) (A) MR peaks and (B) GR peaks containing a top-10 motif. Glucocorticoid Response Element (GRE), Zinc Finger (ZNF), Specificity Protein (SP), Nuclear Receptor (NR), Krüppel-like Factor (KLF), Forkhead Box (FOX), Early Growth Response (EGR), EWS RNA Binding Protein 1-Fli-1 Proto-Oncogene ETS transcription factor (EWSR1-FLI1) Regulatory Factor X (RFX), Atonal BHLH Transcription Factor (ATOH).

3.4.4 In the absence of a GRE, MR and GR peaks are associated with distinct transcription factor binding motif patterns

MR peaks (n = 401) and GR peaks (n = 74) that did not encompass a GRE motif were analysed to determine alternative motifs to which MRs and GRs may be binding. FIMO analysis identified the SP, ZNF, KLF, EGR and RFX motifs as the predominant motifs within the non-GRE-containing MR peaks (Figure 3.13.a). Strikingly, apart from the RFX motif which is only found within the top-5 of CON MR peaks, these motifs are also amongst the most prominently present motifs if all MR peaks were considered (Figure 3.10) indicating that MRs may interact with such motifs in the presence or absence of a GRE. Within the non-GRE-containing GR peaks, the most frequently observed motifs were NR, STAT, PAX, EGR and Retinoic Acid Receptor Gamma (RARG) (Figure 3.13.a). Interestingly, these motifs were not present among the top-5 motifs after FIMO analysis on all GR peaks (Figure 3.11). They were also absent among the top-5 motifs within GR peaks associated with the SR&CR and SE groups whereas NR, STAT and/or PAX were present within GR peaks of the CE and CON groups.

Stacked bars (Figure 3.13.b) present the relative percentage of MR and GR peaks associated with the different physiological conditions and depending on whether peaks contained a GRE motif or not. The presence of a GRE is strongly associated with MR and GR binding after acute stress or at the circadian rise (SR&CR). Conversely, the majority of MR (n = 407) and GR (n = 74) peaks lacking a consensus GRE are CON.

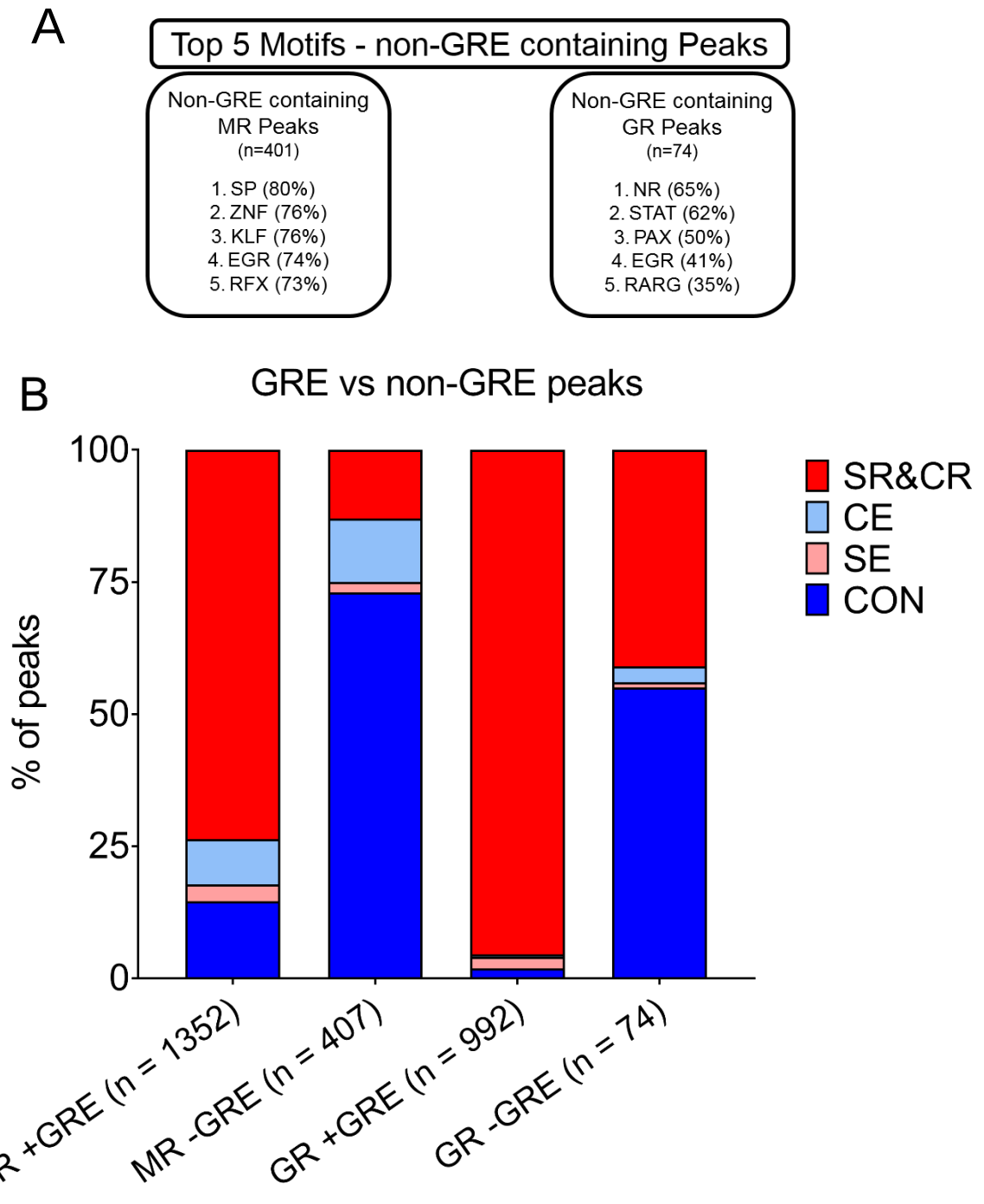

Figure 3.13 FIMO analysis reveals the top 5 transcription factor binding site motifs predicted within MR and GR peaks lacking a GRE

A flowchart shows the top-5 motifs (A) within MR and GR peaks lacking a GRE. A stacked bar chart (B) shows the percentage of SR&CR (stress and circadian responsive), SE (stress exclusive), CE (circadian exclusive) and CON (constitutive) peaks predicted to contain a GRE (+GRE) or not predicted to contain any GREs (-GRE).

3.4.5 Acute stress impacts hippocampal gene transcription more greatly than the circadian drive

Transcriptome-wide changes in hippocampal gene expression following acute stress, or in response to the circadian rise in corticosterone levels, were quantified by RNA-seq. RNA extracted from the hippocampi of rats killed under baseline conditions (BLAM or BLPM) or at various time points after acute FS stress was sequenced following ribosomal RNA (rRNA) depletion (Ribo-Zero RNA-seq). inRNA reads were an approximation of hnRNA, while exRNA reads were representative of mRNA. Changes in plasma CORT levels (Figure 3.14) following acute stress and the circadian rise were examined. Compared with BLAM conditions, plasma CORT increased following acute stress (> 90-fold, FS30; > 10-fold, FS60; >15-fold, FS360) and in response to the circadian rise (> 20-fold).

To investigate the effects of acute stress and the circadian drive on hippocampal gene transcription, differential expression analysis was carried out which compared the expression levels of inRNA and exRNA at each time point after stress or at the circadian rise with expression levels at BLAM (Figure 3.15). This analysis measured the highest number of changes in inRNA expression at FS60 and the highest number of exRNA changes at FS120. Genes were subsequently categorised based on the physiological conditions under which a transcriptional response was elicited (Figure 3.16). To collate the stress-responsive genes in terms of transcriptional responses, the maximal fold change in intronic and exonic reads (regardless of time point and direction) was determined for each gene along with its relative significance value. A higher percentage of genes responded with inRNA changes (13%; Figure 3.16.a) compared with exRNA changes (3%; Figure 3.16.b), however the majority of inRNA (87%) and exRNA (97%) were expressed CON. Of the 13% of genes exhibiting differential inRNA expression, 9% exhibited a SE response, 1% were CE and 3% responded to both (SR&CR). Of the 3% of genes exhibiting differential exRNA expression, 1% were SE, 1% were CE and 1% were SR&CR. The magnitude of differential expression for genes in terms of inRNA (Figure 3.17.a) and exRNA (Figure 3.17.b) is illustrated by volcano plots. SR&CR genes were examined to determine whether the inRNA and exRNA responses were occurring in the same direction. A highly significant positive correlation was observed between the magnitude of the stress-induced versus circadian rise-associated changes in intronic (Figure 3.18.a) and exonic (Figure 3.18.b) RNA expression, strongly indicative of a shared regulatory mechanism for SR&CR genes. Very few genes showed opposing inRNA responses (n = 5) or opposing exRNA responses (n = 4) to acute stress and the circadian drive.

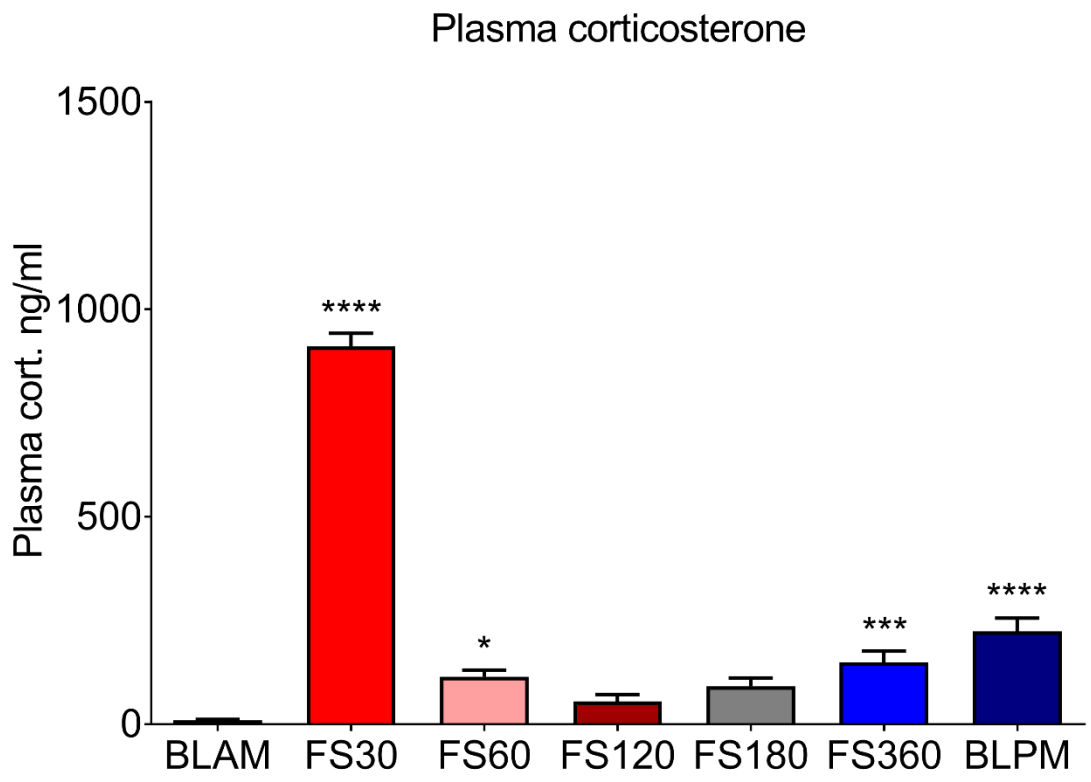

Figure 3.14 Plasma corticosterone levels of rats under early morning baseline conditions, at various timepoints following acute stress or under late afternoon baseline conditions

Rats were killed under early morning baseline conditions (~7:00 hrs (BLAM)), 30 min (FS30), 60 min (FS60), 120 min (FS120), 180 min (FS180), or 360 min (FS360) after the start of FS (15 min, 25 ºC water) or under late afternoon baseline conditions (~17:00 hrs (BLPM)). Plasma corticosterone levels are expressed as ng/ml (mean ± SEM, n=9 per group). Average concentration at BLAM, 9.84 ng/ml. Statistical analysis: one-way ANOVA, $F_{(6,\ 56)}$=185.9, p<0.0001, Dunnett's post-hoc test, *P<0.05, **P<0.01, ***P<0.001, ****P<0.0001 significantly different from BLAM. Inter-assay coefficient of variation, , intra-assay coefficient of variation, 2.43%.

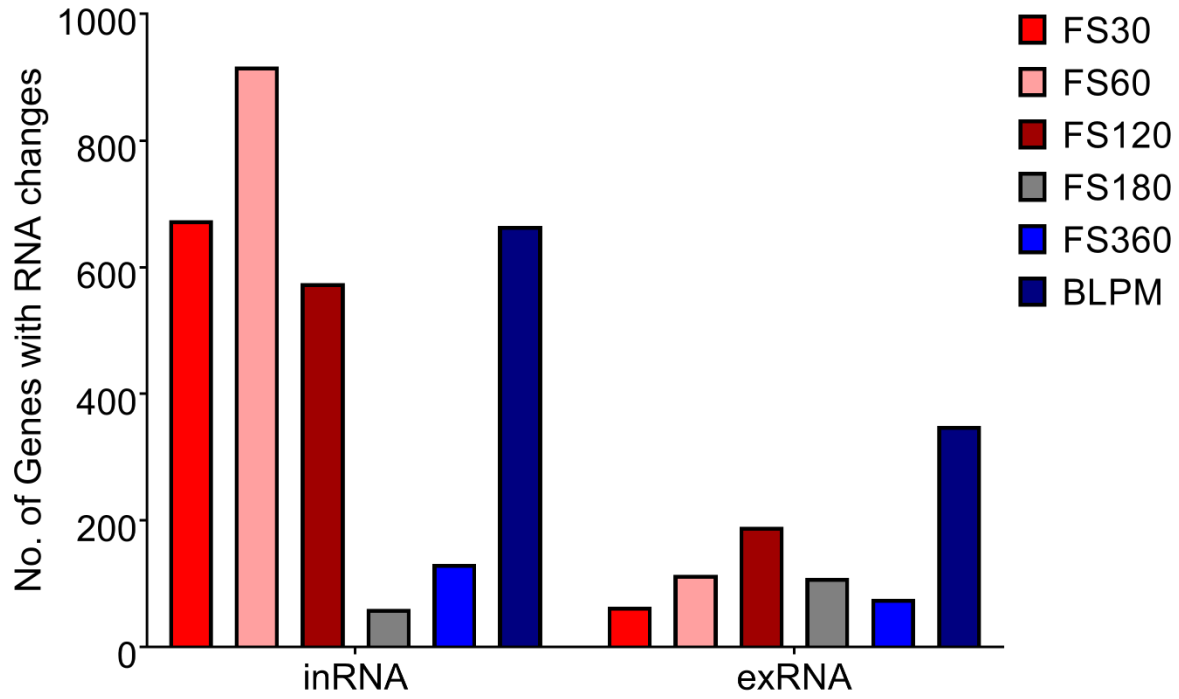

Figure 3.15 RNA-seq reveals genes responding with changes in inRNA and exRNA transcripts following acute stress or during the circadian rise

RNA-seq was carried out on hippocampal tissue from rats under early morning baseline conditions (BLAM), killed at various timepoints (30-360 min) following exposure to FS (15 min, 25 ºC water) or under late afternoon baseline conditions (BLPM). Differential expression analysis identified changes in the inRNA or exRNA expression of genes following FS or at BLPM compared with BLAM conditions. The number of genes exhibiting significant changes in the expression of inRNA and exRNA transcripts are shown for each condition.

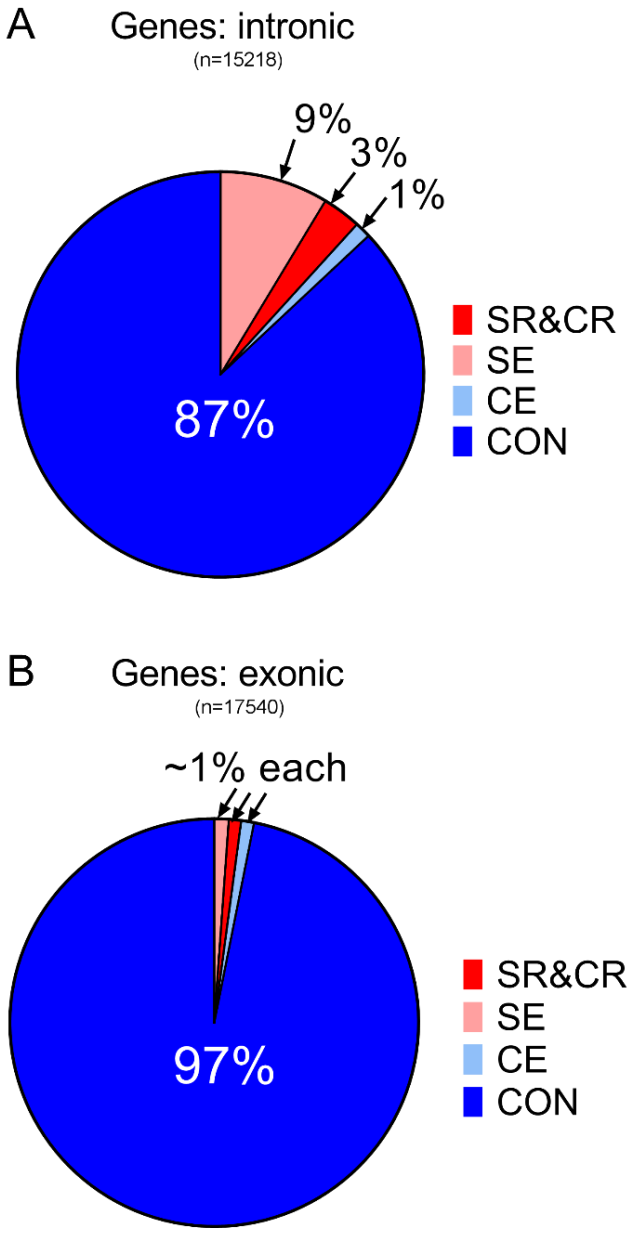

Figure 3.16 Differential expression analysis of inRNA and exRNA following acute stress or during the circadian rise compared with early morning baseline conditions

Differential expression analysis identified genes of which the intronic or exonic expression was upregulated, downregulated or remained stable following acute stress or the circadian rise. Pie charts display the proportion of genes of which the (A) intronic and (B) exonic RNA expression is significantly altered in response to both stress and the circadian rise (Stress-responsive and circadian-responsive - SR&CR), exclusively following stress (Stress exclusive – SE), exclusively under the circadian rise (Circadian exclusive – CE), or genes in which RNA expression remains unchanged between conditions (Constitutively expressed - CON).

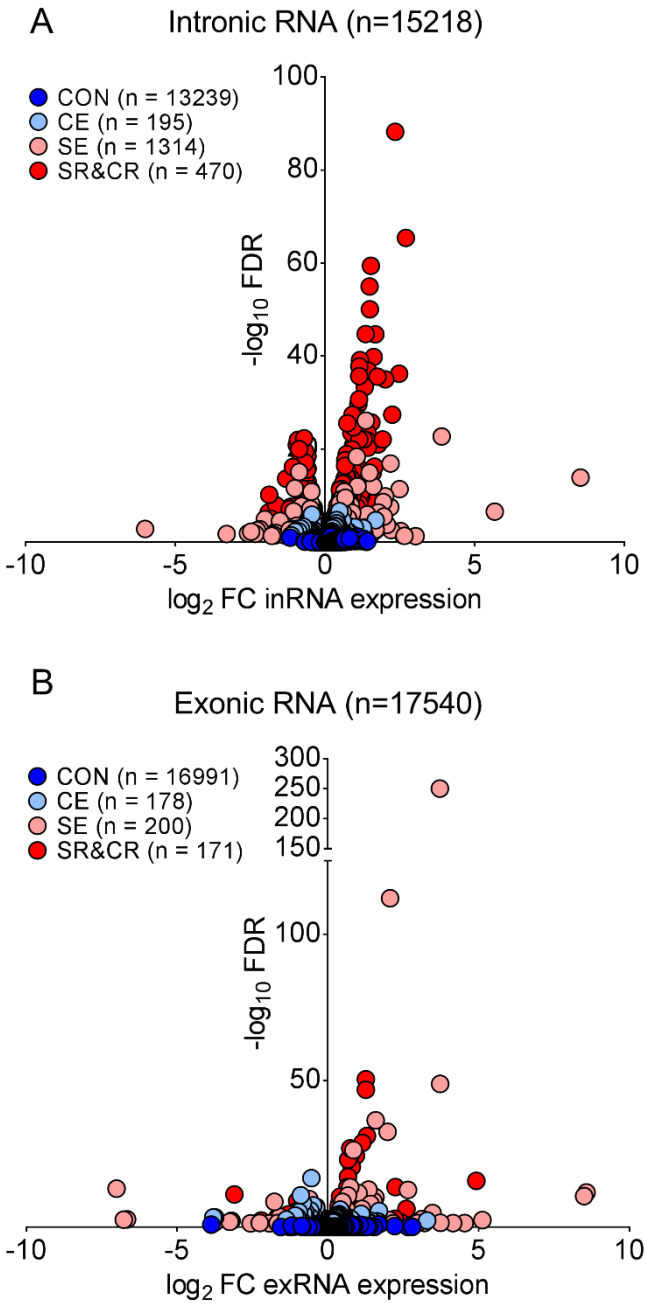

Figure 3.17 Acute stress and the circadian rise result in differential intronic RNA (inRNA) and exonic RNA (exRNA) expression

Differential expression analysis identified genes of which the intronic or exonic expression was upregulated, downregulated or remained stable following acute stress or the circadian rise. Volcano plots show the fold change in (A) intronic RNA and (B) exonic RNA expression (log_2 FC) versus the statistical significance of the change ($-log_{10}$ FDR). Stress and circadian-responsive (SR&CR), Stress exclusive (SE), Circadian exclusive (CE), Constitutively expressed (CON).

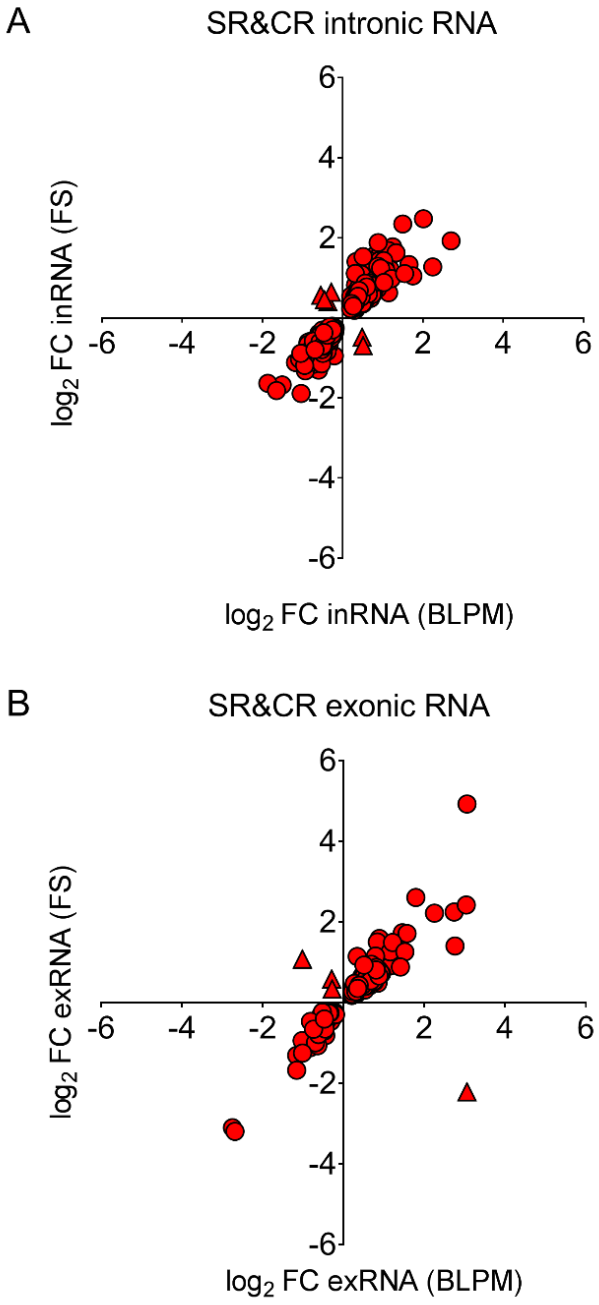

Figure 3.18 Genes exhibiting changes in RNA expression following acute stress and during the circadian rise

Correlation analysis was carried out to determine the relationship between changes in gene expression following stress (FS) or during the circadian rise (BLPM). A Scatterplot displays the magnitude of stress-induced and circadian-induced changes in (A) intronic RNA (n=470) and (B) exonic RNA (n=171) expression for SR&CR genes. Genes in which the change of expression correlated between stress and circadian conditions are depicted in red circles. Genes in which the change of inRNA and exRNA expression did not correlate between stress and circadian conditions are depicted in red triangles. Statistical analysis: Spearman correlation analysis: (A) $r_s(470)=0.9281$, p <0.0001, (B) $r_s(171) = 0.8909$, p<0.0001.

3.4.6 Integration of ChIP-seq and RNA-seq data

The extent to which MR or GR binding was associated with an RNA response of the corresponding genes was subsequently addressed. Peaks were annotated to the gene in closest proximity (Figure 3.19.a); MR peaks, 1505 genes; GR peaks, 932 genes. 662 genes (48%) were distinctly associated with MR binding while 182 genes (13%) were specifically annotated to GR peaks. 536 genes (39%) were associated with both MR and GR binding. The transcription factor binding profile of the distinct and overlapping genes was examined. Almost 50% of “MR only” genes were constitutively bound by the MR, while the majority of “MR/GR” and “GR only” genes exhibited SR&CR binding. Of the 1505 genes annotated to MR peaks and the 932 genes annotated to GR peaks across all conditions, the expression of 1198 (~80%) and 718 (77%) genes, respectively, could be detected based on intronic and/or exonic RNA count data. The differential expression patterns for the top-5 upregulated and downregulated genes with the largest changes in inRNA (Figure 3.20.a) or exRNA (Figure 3.20.b) expression following acute stress or the circadian rise and showing significant MR and/or GR binding are presented as heatmaps. Whilst all of the top-5 upregulated genes based on inRNA expression have SR&CR binding of MR and/or GR, four of the top-5 downregulated genes show CON binding of MR and/or GR and only one gene in the top-5 downregulated genes, Cd180, shows SR&CR binding of GR (Figure 3.20.a). All of the top-5 upregulated and downregulated genes based on exonic expression have SR&CR or SE binding of MR and/or GR (Figure 3.20.b).

Correlation analysis was performed to determine whether changes in MR or GR binding were correlated with the transcriptional RNA responses in the respective gene. A positive correlation was found between the fold change in MR binding and changes in associated inRNA (Figure 3.21.a) and exRNA (Figure 3.21.b). These correlations persisted when the data was split, according to physiological condition i.e. acute stress or circadian rise. When the data was split according to the RNA response i.e. SR&CR, SE or CE, changes in MR binding correlated with changes in inRNA levels within the SR subset and with changes in exRNA levels within the SR and CE subsets. Regarding the GR, a positive correlation was found between the fold change in binding and changes in associated inRNA (Figure 3.22.a) only. When the data was split, according to physiological condition, these correlations did not persist, however when the data was split according to the RNA response, changes in GR binding correlated with changes in inRNA levels within the SE subset. No correlation between changes in GR binding and changes in exRNA (Figure 3.22.b) expression was observed.

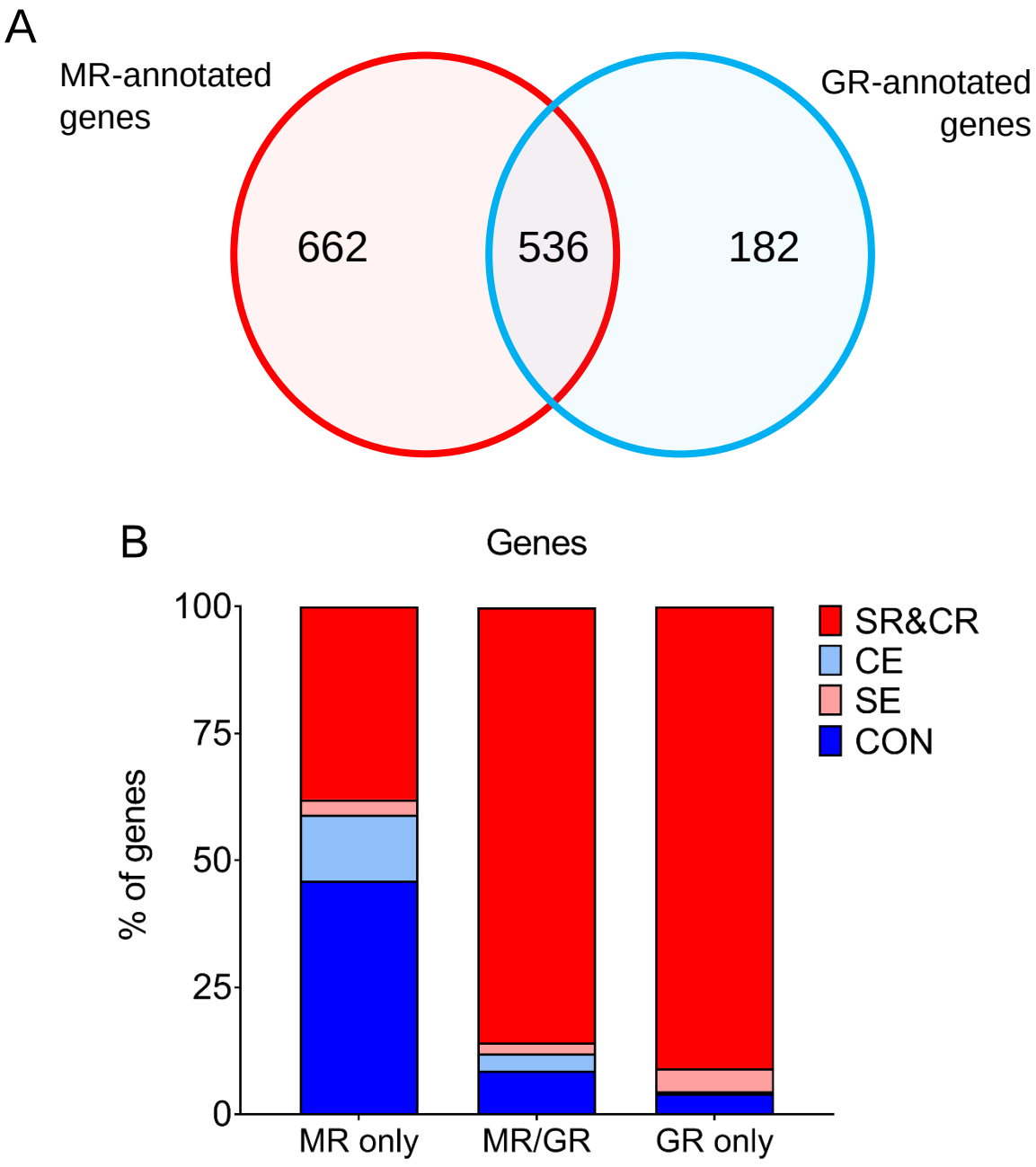

Figure 3.19 Genes annotated to MR peaks only, GR peaks only or both MR and GR peaks

Identification of genes showing MR and/or GR binding following acute stress or the circadian rise. (A) MR and GR peaks were annotated to the gene in closest proximity. These genes were examined to identify genes exclusively bound by MRs or GRs, and genes bound by both MRs and GRs. (B) "MR only", "GR only" and "MR/GR" genes were subsequently examined to determine the category of binding associated with these genes.

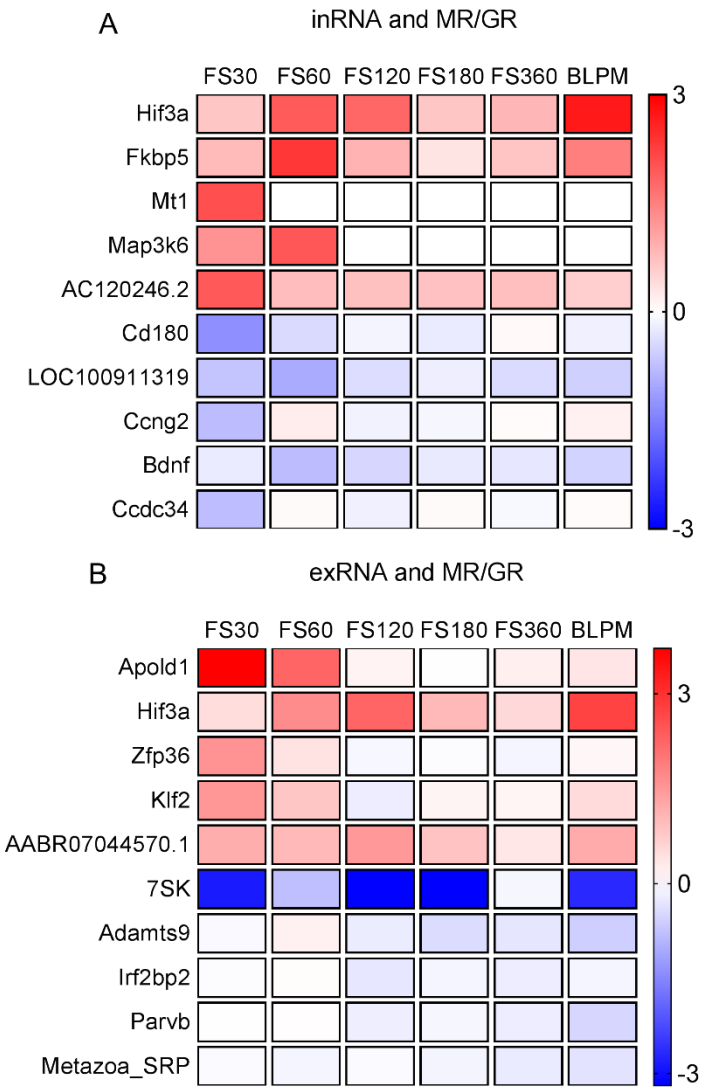

Figure 3.20 Genes exhibiting changes in RNA expression and significant MR or GR binding following acute stress and during the circadian rise

Identification of genes showing MR and/or GR binding and differential RNA expression following acute stress or the circadian rise. MR and GR peaks were annotated to the closest gene, with 1753 MR peaks annotated to 1505 genes and 1066 GR peaks annotated to 932 genes. Heatmaps based on the differential expression (log_2 fold change) of (A) intronic and (B) exonic RNA show the top-5 upregulated and top-5 downregulated genes to which MR or GR is binding.

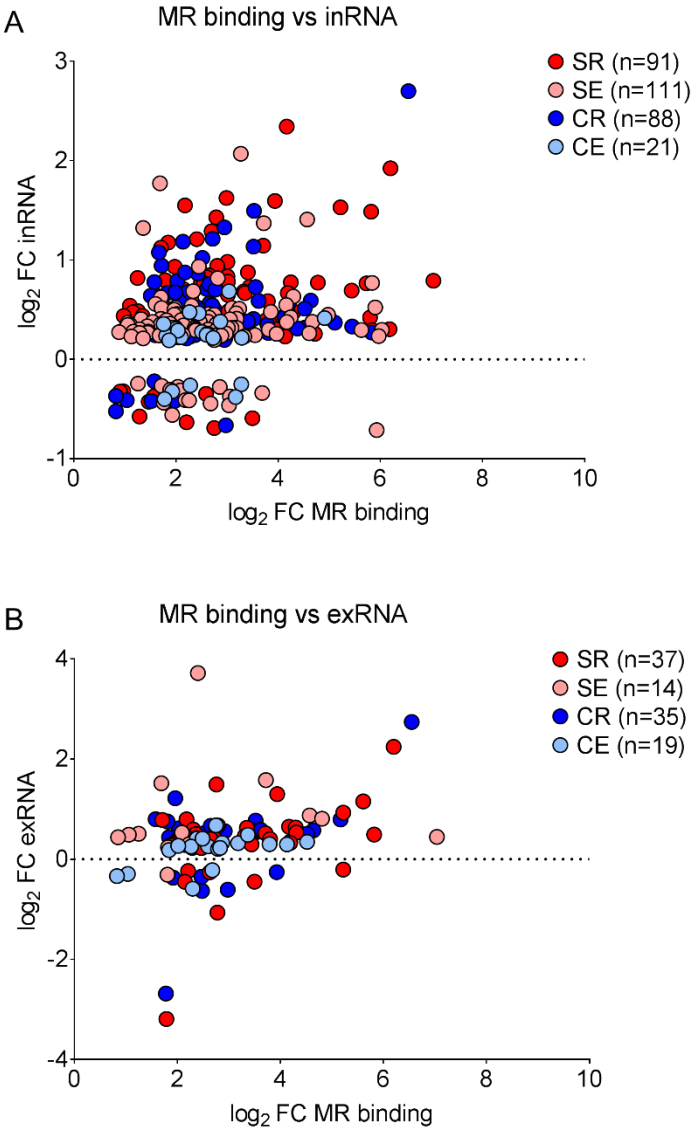

Figure 3.21 Genes exhibiting changes in MR binding and intronic RNA or exonic RNA expression following acute stress and during the circadian rise

Correlation analysis was carried out to determine the relationship between changes in gene expression and changes in MR binding following acute stress or during the circadian rise. A scatterplot displays the magnitude of change in MR binding vs the magnitude of change in (A) intronic RNA (log_2 FC inRNA) expression or (B) exonic RNA (log_2 FC inRNA) expression. Spearman correlation analysis: (A) All data $r_s(311)=0.2061$, $p<0.001$; Acute stress $r_s(202)=0.2014$, $p<0.01$; Circadian rise $r_s(109)=0.2139$, $p<0.05$; Circadian Exclusive $r_s(21)=0.1364$, $p=0.555$; Stress Exclusive $r_s(111)=0.1188$, $p=0.2142$; Circadian Responsive $r_s(88)=0.2026$, $p=0.0583$; Stress Responsive $r_s(91)=0.2082$, $p=0.0477$. (B) All data $r_s(105)=0.2884$, $p=0.0028$; Acute stress $r_s(51)=0.3081$, $p<0.05$; Circadian rise $r_s(54)=0.2854$, $p<0.05$; Circadian Exclusive $r_s(19)=0.5526$, $p=0.0141$; Stress Exclusive $r_s(14)=0.3187$, $p=0.2666$; Circadian Responsive $r_s(35)=0.2048$, $p=0.238$; Stress Responsive $r_s(37)=0.3593$, $p=0.0289$.

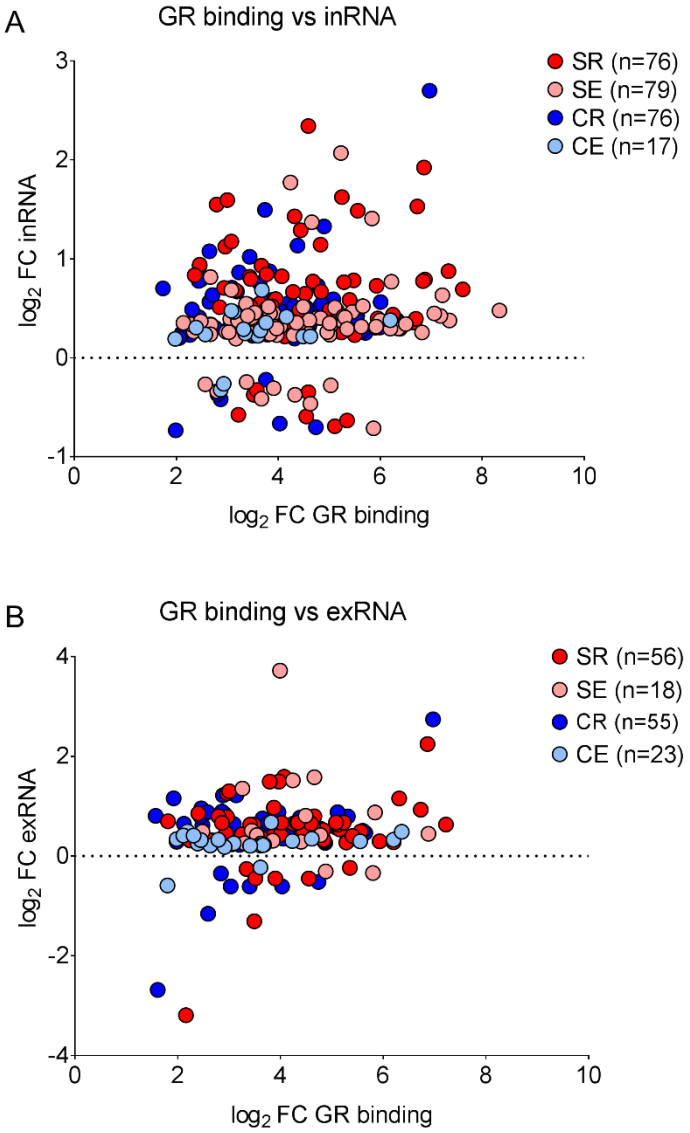

Figure 3.22 Genes exhibiting changes in GR binding and intronic RNA or exonic RNA expression following acute stress and during the circadian rise

Correlation analysis was carried out to determine the relationship between changes in gene expression and changes in GR binding following acute stress or during the circadian rise. A scatterplot displays the magnitude of change in GR binding vs the magnitude of change in (A) intronic RNA (log_2 FC inRNA) expression or (B) exonic RNA (log_2 FC inRNA) expression. Spearman correlation analysis: (A) All data $r_s(248)=0.1314$, $p=0.0387$; Acute stress $r_s(155)=0.1102$, $p=0.1721$; Circadian rise $r_s(93)=0.1436$, $p=0.1696$; Circadian Exclusive $r_s(17)=0.2745$, $p=0.2853$; Stress Exclusive $r_s(79)=0.2288$, $p=0.0426$; Circadian Responsive $r_s(76)=0.09541$, $p=0.4123$; Stress Responsive $r_s(76)=0.005332$, $p=0.9635$. (B) All data $r_s(152)=0.09917$, $p=0.2242$; Acute stress $r_s(74)=0.03677$, $p=0.7558$; Circadian rise $r_s(78)=0.07245$, $p=0.5285$; Circadian Exclusive $r_s(23)=0.09125$, $p=0.6788$; Stress Exclusive $r_s(18)=0.000$, $p>0.999$; Circadian Responsive $r_s(55)=-0.09137$, $p=0.507$; Stress Responsive $r_s(56)=0.01648$, $p=0.904$.

3.5 Discussion

Integrated ChIP- and RNA-seq has revealed the complexity of GC action in the hippocampus under physiological conditions which are of significance for GC secretion, i.e. during the circadian rise and trough and following acute stress. The MR/GR ChIP studies show that binding can be constitutive or responsive to stress and circadian influences and mediated by classical GREs or many alternative TF binding motifs. Cross-correlation of the ChIP- and RNA-seq datasets shows that changes in receptor binding to the genome impacts on gene transcriptional activities. These data significantly expand our knowledge of GC-controlled genes under baseline and stress conditions, how these genes are controlled and what their putative functions are. The purely physiological approach adopted in this study differs substantially from earlier genome-wide MR and GR binding studies that used hippocampal tissues of corticosterone-injected ADX rats (Polman et al., 2013a, van Weert et al., 2017, Pooley et al., 2017). The present results are not affected by any influences of ADX, directly on MR and/or GR binding characteristics and indirectly because of loss of dentate gyrus neurons due to lack of endogenous corticosterone (Sloviter et al., 1993). Furthermore, ADX may influence hippocampal RNA responses, as Gray et al. (2014) found relatively little overlap in hippocampal RNA responses of mice subjected to FS or corticosterone injection (Gray et al., 2014). Also technically, it is difficult to compare this present study with previous studies, as this analysis is based on 4 independent biological samples (cf. n=1 in earlier studies), the ChIP-seq was performed at a much higher depth and these sequencing results were aligned to the latest rat genome version (Rnor_6.0; cf. Rnor_4 (Polman et al., 2013b, van Weert et al., 2017)).

ChIP-seq identified MR and GR binding peaks throughout various genomic regions under all physiological conditions. Although it is generally accepted promoter regions are the primary site of transcription factor binding (Finsterwald and Alberini, 2014), the majority of MR and GR peaks identified in this study were located in distal intergenic regions under all physiological conditions. Little is presently known regarding the functions of intergenic DNA; however accumulating evidence suggests that genome architecture may be regulated by intergenic regions that influence the spacing of neighbouring genes. Interestingly, genes with more complex functions were shown to be flanked by significantly more intergenic DNA compared with genes with simple or housekeeping functions (Nelson et al., 2004). As MRs and GRs have been shown to interact with coregulators and other transcription factors, it is

possible that intergenic regions facilitate the assembly of large regulatory complexes which may be recruited by genes with more complex functions. Under circadian trough conditions, a considerable proportion of MR peaks were detected within promoter regions, while only a modest fraction of GR peaks was observed. Interestingly, following acute stress and the circadian rise, MR binding within promoter regions decreased by almost 50%, while a small increase in the proportion of GR peaks was seen. Under GC-elevated conditions, MR and GR binding increased substantially within intronic regions. Although intronic regions were initially believed to represent non-functional "junk-DNA" (Li et al., 2012), they have been found to contain DNA elements that regulate transcription initiation (Chorev and Carmel, 2012) which may be recognised by MRs and GRs. These observations indicate the presence of a distinct binding pattern of MRs and GRs which may be important in the regulation of GC target genes. It also challenges the previous belief that MR and GR binding predominantly occurs in promoter regions and indicates that more work needs to be done on elucidating the regulatory roles of intergenic and intronic DNA regions.

Upon differential binding analysis, regions of the genome were identified in which the binding of MRs and GRs was upregulated or downregulated following acute stress and/or the circadian rise. A considerable number of loci were also identified which showed no changes in MR or GR binding between these physiological conditions (i.e. constitutive binding). MR peaks (1753) and GR peaks (1066) diverged considerably regarding their distribution across the CON, CE, SE and SR&CR categories. While more than 90% of GR peaks were SR&CR, fewer MR peaks (60%) exhibited this type of binding. This disparity is largely due to the much greater relative (and absolute) number of CON MR peaks (28%) than CON GR peaks (5%). A reason for the high number of CON MR peaks may be due to the high degree of MR occupancy by endogenous corticosterone under all physiological conditions (Reul and de Kloet, 1985, Reul et al., 1987) rendering these receptors in a constantly activated state. Although a recent study has reported relatively low binding of occupied MRs at GREs of stress responsive genes under BLAM conditions (Mifsud and Reul, 2016), it is possible that in the case of CON MR binding, MRs are selectively recruited by transcription factors at distinct genomic loci, which are not responsive to stress or circadian conditions. GRs only become occupied under GC-elevating conditions, such as stress and the circadian rise (Reul and de Kloet, 1985, Reul et al., 1987), therefore the dynamic binding of these receptors to DNA may correspond with their occupancy profile. Similarly,

the fraction of CE MR peaks was much higher, approximately 9-fold, than the fraction of CE GR peaks. It appears that MR-selective circadian factors may play a decisive role in the CE binding and the nature of these factors needs to be delineated in future studies.

Based on MEME analysis of the top-500 MR and GR peaks, the GRE consensus sequence was, with very high statistical significance, the predominant recognition site for MR and GR binding underscoring the high specificity of this ChIP analyses. Further examination of all 1753 MR and 1066 GR peaks revealed alternative motifs to which MRs and GRs may be binding. To a certain degree, these motifs overlap with those reported by previous studies, such as EGR and ATOH1 (van Weert et al., 2017), however FIMO analysis on this data discovered many additional motifs in substantial numbers of peaks including KLF, SP, FOX, STAT and RFX motifs which had not been revealed previously. It is possible that ADX conditions in the study by van Weert and colleagues may restrict the access of MRs and GRs to these motifs. Access to binding motifs is controlled by local epigenetic modifications and changes in chromatin architecture. It has previously been reported that acute FS stress indeed results in distinct epigenetic changes including histone modifications (Gutierrez-Mecinas et al., 2011) and DNA demethylation (Saunderson et al., 2016). Thus, under changing physiological (environmental) conditions, access to the chromatin landscape is likely to alter, shaping accessibly of binding motifs and thereby MR and GR binding patterns.

A number of MR and GR peaks were shown to lack a GRE motif, the majority of which were bound constitutively under all physiological conditions. The most prominent motifs present within loci lacking a GRE differed substantially for the MR and the GR. For the MR, apart from RFX which is only found within the top-5 of CON MR peaks, the motifs associated with non-GRE-containing loci overlapped with the top-5 motifs within all MR peaks, indicating that MR can bind these motifs in the presence or absence of a GRE. GR binding to non-GRE-containing loci was associated with a very different motif profile compared with the top-5 most prominent motifs within all GR peaks. It seems, that in the absence of a GRE, GRs may bind NR, STAT, PAX, EGR and RARG motifs. The high incidence of MR and GR binding to loci that do not contain a GRE element prompts the question whether these receptors bind directly or indirectly to such non-GRE motifs. An indirect action of MR and/or GR at a non-GRE motif would require the local binding of the intrinsic transcription factor to such motifs. Interestingly, RNA

analyses revealed the induction of the respective transcription factor RNAs for members of the EGR and KLF superfamilies of transcription factors following acute stress and/or circadian influences. Constitutive RNA expression of a number of members of the SP, RFX, ZNF and NR, PAX and RARG superfamilies was also observed. Strikingly, we found that a number of genes (i.e. *Klf2, Klf7, Klf9, Klf13, Klf15*) showed increased MR and GR binding after stress or at the circadian rise. Previously, FS was shown to induce EGR1 in distinct hippocampal neurons; a process requiring a convergence of NMDAR-mediated MAPK/ERK and (non-genomic) GR signalling, formation of the dual histone mark H3K14ac-S10p at the gene promoter, as well as DNA demethylation of the promoter and 5'-UTR of the *Egr1* gene (Saunderson et al., 2016, Gutierrez-Mecinas et al., 2011, Chandramohan et al., 2008). Moreover, Chen et al. recently provided evidence that GR and EGR1 interact at the EGR motif within the *Bdnf* gene (Chen et al., 2019). Such interactions have also been reported for GR and STAT3/STAT5b, and GR and KLF2/KLF4/KLF9 at STAT and KLF/GRE binding motifs, respectively, in various cell types (Engblom et al., 2007, Petta et al., 2016, Chinenov et al., 2014, Sevilla et al., 2015). Thus, it may be that corticosteroid receptor action involves direct interaction with GRE motifs and indirect interactions via other transcription factors with their intrinsic binding motifs, whereby GCs can enhance the latter mode of interaction through induction of the respective transcription factor.

The Ribo-Zero RNA sequencing method detected more than 3-times the number of responsive genes when considering intronic versus exonic expression. Thus, this data supports that assessment of intronic expression is a much more sensitive approach to detect changes in gene transcription due to acutely changing physiological conditions. This notion is reflected in the numbers of responsive intronic vs exonic RNAs in the sub-divided data sets CE, SE and SR&CR. There were more than 6-times as many genes with SE differential inRNA expression than there were genes with SE differential exRNA expression. In contrast, the number of genes with CE inRNA and exRNA responses were similar, possibly because the circadian rise targets less acutely changing RNAs. Correlation analysis between ChIP- and RNA-Seq datasets indicated that in particular changes in MR binding were significantly correlated with associated intronic and exonic RNA responses under both stress and circadian conditions. Changes in GR binding were only correlated with inRNA responses when data from both physiological conditions were considered. It was surprising that more significant positive correlations were found for MR binding than for GR binding as, classically, GRs have been found to be more

responsive to stress- and circadian-induced changes than MR (Reul and de Kloet, 1985, De Kloet and Reul, 1987). Furthermore, in early work *in vitro*, GR has been shown to have much stronger transactivation potency than MR (Rupprecht et al., 1993). Presently, the exact reason for the relative deficiency of correlation between GR binding and corresponding RNA responses is unclear. An additional factor affecting the relationship between MR/GR binding and gene transcription is the phenomenon of chromatin looping enabling transcription factor-bound enhancers to interact with gene promoters across substantial distances within the genome and affect transcriptional activities (Rajarajan et al., 2016, Matharu and Ahituv, 2015). Accordingly, MR/GR binding may not necessarily impact on transcription of the nearest gene to which it has been annotated. As a consequence, chromatin looping may have contributed to a certain level of 'fuzziness' in the cross-correlation of MR/GR binding and gene transcriptional responses. The contribution of this phenomenon will need to be clarified by future chromatin conformation capture (3C) analyses. Furthermore, epigenetic factors determining MR/GR binding as well as binding of and interaction with other transcription factors may have influenced MR/GR binding and associated transcriptional responses. The identification of multiple recognition sites other than GREs underline such putative involvement. Future studies involving comprehensive transcription factor (co-)binding and epigenomic analysis in combination with whole-genome 3C (Hi-C) and intron-transcriptomics will shed further light on the relationship between MR/GR binding and gene transcriptional responses.

The data presented in this Chapter shows that the interaction of MRs and GRs with the hippocampus genome *in vivo* is highly complex, involving interactions with GREs and possibly other transcription factors. These interactions can be constitutive and, depending on the environmental circumstances (stress, active phase of circadian cycle), can be enhanced resulting in gene transcriptional changes. The main physiological effector is CORT whose increased secretion after stress and during the circadian rise is key to the activation of GR in particular. In addition, however, there are countless co-regulators, (GC-inducible and constitutively expressed) transcription factors, and epigenetic modulators requiring further examination to fully elucidate MR's and GR's interaction with the genome, and how, as a network these factors contribute to adaptation to environmental challenges.

Chapter 4 Pathway analysis of hippocampal genome-wide ChIP-seq and RNA-seq following acute stress and during the circadian rise

4.1 Abstract

GC hormones are critical regulators of many vital physiological processes and the genomic actions of GCs, via hippocampal MRs and GRs, are essential for adaptation to external stressors. Despite the importance of hippocampal GC hormone action in adaptation and survival, the genomic actions of MRs and GRs within the hippocampus at a genome-wide level remains yet to be fully elucidated. For the first time, MR and GR ChIP-seq has been integrated with RNA-seq, providing a comprehensive insight into the genomic actions of MRs and GRs in the rat hippocampus under physiological conditions of relevance for GC secretion. These ChIP- and RNA-seq analyses have revealed over 1,000 genome-wide loci to which MRs and/or GRs bind and many more genes exhibiting transcriptional responses under acute stress and circadian peak and trough conditions. Though the findings of ChIP- and RNA-seq have provided an unprecedented insight into the genomic actions of MRs and GRs in the hippocampus, the biological relevance of these findings require interpretation.

Ingenuity Pathway Analysis (IPA), a highly sophisticated pathway analysis programme, was used to analyse MR and GR ChIP-seq and RNA-seq datasets of rat hippocampus following acute stress and circadian conditions. Genes exhibiting MR and/or GR binding and/or changes in RNA expression were linked to signalling pathways such as circadian rhythm signalling and glucocorticoid receptor signalling, and upstream regulators such as heat shock proteins, circadian enzymes and circadian transcriptional regulators, underscoring the high specificity of the analyses. Biological processes involved in neurodevelopment, hippocampal functions and synaptic functions were predicted to be affected by genes in the target datasets, demonstrating the diversity of important neurobiological functions under GC hormone regulation. Moreover, neurological diseases such as Alzheimer's disease, epilepsy and Parkinson's disease were all predicted to be linked to genes in the target datasets, indicating a relevance for GC hormone action in these poorly understood diseases. The output of these pathway analyses provides a valuable resource in understanding how the genomic targets of MRs and GRs may relate to the biological processes and diseases influenced by GC hormones.

4.2 Introduction

Decades of research and thousands of publications have established the importance of GC hormone action in maintaining homeostasis, facilitating adaptation to external stressors and developing resilience to promote survival (Reul et al., 2015). A number of vital physiological processes are under GC regulation, while genomic GC hormone action in the hippocampus via MRs and GRs influences learning and memory formation and facilitates behavioural changes that allow adaptation following stressful events. Furthermore, GC hormones have been implicated in a wide range of devastating neuropsychiatric disorders that demonstrate hippocampal pathologies, such as depression (Sheline et al., 1996), post-traumatic stress disorder (Maes et al., 1998) and schizophrenia (Seo et al., 2018, Sinclair et al., 2011), however the link between GC hormone action in the hippocampus and the development of these disorders remains yet to be elucidated. In Chapter 3, genome wide ChIP- and RNA-seq has provided unprecedented insight into the genomic actions of MRs and GRs in the rat hippocampus under stress and circadian conditions. In this chapter, datasets generated in these studies were further examined to determine the biological relevance of these findings and to establish links between GC hormone action, biological processes and disease pathophysiology.

Pathway analysis has been developed to facilitate the meaningful biological interpretation of data arising from high throughput next generation sequencing experiments, that often generate an output of thousands of genes whose functions are unknown at a network level. A number of pathway analysis programmes are freely available, including Database for Annotation, Visualization and Integrated Discovery (DAVID), Gene Ontology (GO), Kyoto Encyclopaedia of Genes and Genomes (KEGG) and Protein Analysis Through Evolutionary Relationships (PANTHER). These programmes have offered insight when interpreting data from sequencing experiments, however they fail to provide detailed and directional molecular information regarding genomic targets. Ingenuity pathway analysis (IPA) “Core Analysis”, however, offers a far more comprehensive analysis and integration of sequencing data. From the reference dataset, IPA can identify upstream regulators, predicting downstream effects on biological and disease processes and generating networks of genes in the reference dataset. Pathway analysis performed on MR/GR ChIP-seq and RNA-seq data has so far been underwhelming, offering very limited insight to the consequences of GC hormone action at a network level. DAVID has been used to analyse GR ChIP-seq data derived from neuronal PC12 cells (Polman et al., 2012) and hippocampus of ADX rats (Polman et al., 2013), however the pathways highlighted were very general. Pathways linked to

genes arising from *in vitro* GR ChIP-seq included “metal ion binding” and “protein tyrosine kinase activity” (Polman et al., 2012), while pathway analysis of *in vivo* GR hippocampal ChIP-seq highlighted processes such as “enzyme binding”, “apoptosis” and “positive regulation of transcription” (Polman et al., 2013). GC hormones may be relevant for these processes; however, it is unclear how these results contribute to and improve our wider understanding of GC hormone action in the hippocampus. DAVID was also used to analyse the 7,000 enrichment sites found in rat hippocampus (Pooley et al., 2017), however the high number of peaks and low replicate number in the study causes concern regarding the interpretation of the pathway analysis. Many of these peaks may simply be artefacts as these 7,000 comprise the top 20% of each group, indicating that many more peaks were identified. The peaks were also aligned to Rnor_5.0, an outdated version of the rat genome, therefore it is possible that certain genes have moved location thus the annotations are not the most up to date possible. Pathway analysis of MR and GR ChIP-seq datasets of ADX rats by DAVID did enable the identification of pathways specific to or shared between both receptors, however terms were yet again quite general, such as “cell adhesion” and “sodium channel activity” (van Weert et al., 2017). Moreover, none of these studies have integrated ChIP-seq with RNA-seq and are based on the assumption that MR/GR bound genes are regulated by the receptor. Binding of MR and/or GR, however, does not always lead to a transcriptional response of the gene in closest proximity, therefore pathway analysis of genes annotated to MR/GR peaks is liable to misinterpretation. Clearly, current pathway analysis of hippocampal ChIP-seq and RNA-seq under physiological conditions of relevance for GC-secretion is lacking.

Datasets from our ChIP- and RNA-seq experiments described in Chapter 3 underwent “Core Analysis” by IPA software, which predicted canonical pathways, upstream regulators and diseases and functions associated with the genes in these datasets. Many predictions made by IPA validated the high specificity of our ChIP- and RNA-seq experiments, as the genes in these datasets were predicted to participate in well-established GC-regulated signalling pathways and biological processes including glucocorticoid receptor signalling, learning and memory. In addition to highlighting well known upstream regulators, such as heat shock proteins, IPA emphasised previously reported links between several transcription factor families, like the KLFs, and genes in our datasets. The analyses also highlighted neurodevelopmental processes such as neuritogenesis, development of neurons and differentiation of the nervous system, of which GC hormones have been shown to play a role in, however the molecular underpinnings are unclear. Associations were made between the genes in our sequencing datasets

and neurological diseases and neuropsychiatric disorders not yet strongly linked to GC hormone action, such as epilepsy and schizophrenia. Although HPA-axis irregularities and stressful experiences have been implicated in these disorders (Wolff and Huston, 1959, Nakken et al., 2005), it is unclear whether genomically acting MRs and GRs are involved in their aetiology. These data provide so far, the most in depth pathway analysis of the genes targeted following hippocampal stress or circadian input, and the biological process and diseases potentially influenced consequently. Many novel targets for further exploration have been highlighted and these data shall certainly provide a resource for future studies aiming to elucidate the genomic effects of GC hormone action on the brain.

4.3 Materials and Methods

4.3.1 Ingenuity Pathway Analysis

Ingenuity Pathway Analysis (IPA) software (QIAGEN Inc.,) was used to perform a “Core Analysis” on datasets from ChIP-seq and RNA-seq experiments to predict diseases and functions associated with genes becoming bound by MRs or GRs or exhibiting differential RNA expression after acute stress and during the circadian rise. Details regarding Core Analysis are described in Chapter 2.

4.3.2 ChIP-seq dataset preparation

ChIP-seq datasets comprising all genes annotated to an MR or GR peak included in DiffBind analysis were uploaded to IPA, as described in Chapter 2.

4.3.3 RNA-seq dataset preparation

RNA-seq datasets comprising all genes with significant (FDR<0.05) differential intronic RNA (inRNA) or exonic RNA (exRNA) expression following acute stress or the circadian rise was uploaded to IPA, as described in Chapter 2.

4.3.4 Core Analysis

A core analysis was performed on each dataset by IPA which identified canonical pathways, upstream regulators, diseases and functions and networks predicted to be associated with genes present in the dataset. The settings for all core analyses are described in Chapter 2. Core Analysis predicted canonical pathways, upstream regulators, diseases and functions and networks to be influenced by genes in our ChIP- and RNA-seq datasets. An “overlap *p*-value” and “z-score” were calculated as described in Chapter 2.

4.4 Results

4.4.1 Canonical pathways influenced by genes annotated to MR and GR peaks or differentially expressed genes following acute stress or during the circadian rise

Datasets comprising of genes annotated to MR and GR peaks or exhibiting differential inRNA or exRNA expression following acute stress and during the circadian rise were uploaded to IPA and a core analysis was performed. We found that a number of canonical pathways were predicted to be influenced by genes in these datasets.

Following acute stress and during the circadian rise, genes annotated to MR and GR peaks were predicted (p<0.05) to influence 118 and 92 canonical pathways, respectively, while genes exhibiting differential inRNA and exRNA expression were predicted to be influence 266 and 181 canonical pathways, respectively.

Canonical pathways associated with each dataset were examined to identify relevant pathways associated with our experimental model. As expected, genes present in MR ChIP, GR ChIP, inRNA and exRNA sequencing datasets following both acute stress and the circadian rise (Figure 4.1) were linked to glucocorticoid receptor signalling, circadian rhythm signalling and corticotropin releasing hormone signalling. The statistical significance (p-value), predicted activation state, activation z-score and number of genes associated with each canonical pathway and the corresponding dataset are depicted in Table 4.1.

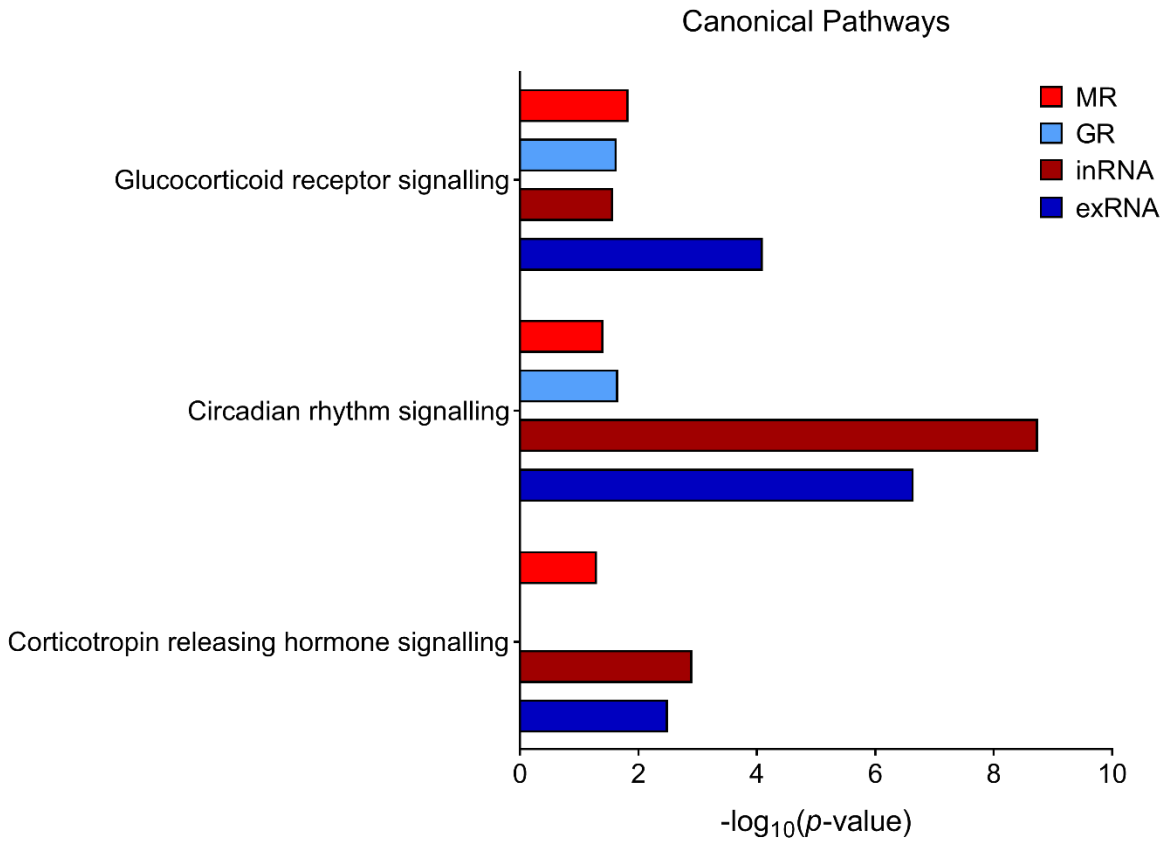

Figure 4.1 Canonical pathways predicted to be related to genes present in ChIP-seq and RNA-seq datasets

IPA Core analysis identified canonical pathways associated with genes present in MR and GR ChIP-seq datasets and inRNA and exRNA RNA-seq datasets. Among these signalling pathways were glucocorticoid receptor signalling, circadian rhythm signalling and corticotropin releasing hormone signalling. Data is expressed as the antilog of the *p*-value.

Canonical Pathway	Dataset	Predicted activation state	Activation z-score	*p*-value of overlap	# Target genes in dataset
Glucocorticoid receptor signalling	MR			0.0148	29
	GR			0.0234	18
	inRNA			0.030	35
	exRNA			6.9e-03	15
Circadian rhythm signalling	MR			0.0389	5
	GR			0.0219	4
	inRNA			2.089e-06	15
	exRNA			2.239e-07	7
CRH signalling	MR	Activated	3.000	0.050	8
	inRNA		-0.688		21
	exRNA		0.447		7

Table 4.1. GC-hormone associated signalling pathways influenced by genes annotated to MR and GR peaks and genes exhibiting differential RNA expression following acute stress or during the circadian rise

MR and GR ChIP-seq datasets and intronic and exonic RNA-seq datasets underwent "Core Analysis" by IPA. GC-hormone associated signalling pathways, such as glucocorticoid receptor signalling, circadian rhythm signalling and corticotropin releasing hormone (CRH) signalling pathways were predicted to be influenced by genes in these datasets. Activation z-scores ≥ +2 significantly predict pathway activation, while z-scores of ≤ -2 significantly predict pathway inhibition. Activation z-scores < +2 or > -2 indicate a trend towards activation or inhibition, however the prediction is not statistically significant. Statistical analysis: Right-tailed Fisher's exact test, $p<0.05$.

4.4.2 Upstream Regulators of genes annotated to MR and GR peaks or genes exhibiting differential expression following acute stress or during the circadian rise

IPA predicted 915 upstream regulators of MR- and GR-annotated genes, while 3323 upstream regulators were predicted for genes exhibiting differential inRNA and/or exRNA expression.

Molecules previously known to be associated with GC-hormone signalling were identified among the predicted upstream regulators of genes present in ChIP- and RNA-seq datasets, such as GC cochaperones and receptors (Table 4.2), circadian enzymes and circadian transcriptional regulators (Table 4.3).

Findings of upstream regulator prediction were examined for the corresponding transcription factors of the top transcription factor binding motifs present in MR and/or GR binding sites, as discussed in Chapter 3. Notably, EGR family members (Table 4.4), KLF family members (Table 4.5) SP family members (Table 4.6), ZNF family members (Table 4.7) were predicted as upstream regulators of genes in the ChIP-seq and RNA-seq datasets.

Based on experimental evidence of an interaction between GR and the NMDA-R activated MAPK-ERK pathway as reported previously by this lab group (Chandramohan et al., 2008, Gutierrez-Mecinas et al., 2011), results of upstream regulator prediction were searched for glutamate receptor family members, as shown in Table 4.8.

The statistical significance (*p*-value), predicted activation state, activation z-score and number of genes associated with each upstream regulator and the corresponding dataset are depicted in Tables 4.2 – 4.8.

Upstream Regulator	Dataset	Predicted activation state	Activation z-score	*p*-value of overlap	# Target genes in dataset
Hsp70	MR		1.715	0.0377	4
	GR			0.0358	3
	inRNA		1.067	0.0228	5
Hsp27	inRNA			0.0476	7
	exRNA		0.365	4.33e-04	5
GR	MR	Activated	2.604	1.01e-06	69
	GR	Activated	3.84	2.08e-11	57
	inRNA	Activated	2.534	4.18e-07	97
	exRNA	Activated	2.024	5.38e-09	38
MR	MR		1.046	5.27e-03	14
	GR	Activated	2.359	3.98e-06	15
	inRNA	Activated	2.404	4.05e-03	17
	exRNA	Activated	3.396	3.02e-05	16

Table 4.2 Molecules associated with GC-hormone signalling are predicted upstream regulators of genes annotated to MR and/or GR peaks and genes exhibiting differential RNA expression following acute stress or during the circadian rise

IPA Core analysis was performed on ChIP-seq and RNA-seq datasets comprising genes annotated to MR and/or GR peaks and genes exhibiting differential RNA expression following acute stress or during the circadian rise. Molecules known to interact with MRs and GRs, such as heat shock proteins and glucocorticoid receptors themselves were predicted as upstream regulators of genes in these datasets. Heat shock protein 27 (Hsp27), heat shock protein 70 (Hsp70), Glucocorticoid receptor (GR), Mineralocorticoid receptor (MR). Activation z-scores ≥ +2 significantly predict pathway activation, while z-scores of ≤ -2 significantly predict pathway inhibition. Activation z-scores < +2 or > -2 indicate a trend towards activation or inhibition, however the prediction is not statistically significant. Statistical analysis: Right-tailed Fisher's exact test, $p<0.05$.

Upstream regulator	Dataset	Predicted activation state	Activation z-score	*p*-value of overlap	# Target genes in dataset
CLOCK	MR		1.925	9.98e-03	16
	GR		1.925	08.50e-03	11
	inRNA	Activated	3.185	7.51e-10	49
	exRNA		1.421	4.17e-09	21
CRY1	MR			0.0334	3
	GR			7.32e-03	3
	inRNA		-1.205	0.0118	4
	exRNA		-1.000	5.54e-07	6
CRY2	MR			0.0334	3
	GR			7.32e-03	3
	inRNA		-0.152	0.0118	5
	exRNA		-0.124	1.09e-08	6

Table 4.3 Circadian associated enzymes and transcriptional regulators are predicted upstream regulators of genes annotated to MR and GR peaks and genes exhibiting differential RNA expression following acute stress or during the circadian rise

Datasets comprising genes annotated to significant MR and GR peaks and genes exhibiting differential RNA expression following acute stress or during the circadian rise were analysed by IPA. Core analysis predicted circadian enzymes and circadian transcriptional regulators as upstream regulators of genes in these datasets. Clock circadian regulator (CLOCK), cryptochrome circadian regulator 1 (CRY1), cryptochrome circadian regulator (CRY2). Activation z-scores ≥ +2 significantly predict pathway activation, while z-scores of ≤ -2 significantly predict pathway inhibition. Activation z-scores < +2 or > -2 indicate a trend towards activation or inhibition, however the prediction is not statistically significant. Statistical analysis: Right-tailed Fisher's exact test, $p<0.05$.

Upstream regulator	Dataset	Predicted Activation state	Activation z-score	*p*-value of overlap	# Target genes in dataset
EGR1	inRNA		0.923	9.15e-05	29
	exRNA		1.979	1.71e-11	19
EGR2	MR	Activated	3.203	2.31e-03	18
	GR	Activated	3.274	3.6e-03	12
	inRNA		0.793	8.51e-05	26
	exRNA		1.094	3.7e-07	13
EGR3	GR		-1.000	0.0297	4
	inRNA		-1.091	0.0132	8
	exRNA			0.0232	3

Table 4.4 EGR transcription factor family members are predicted upstream regulators of genes present in datasets produced by MR/GR ChIP-seq and intronic/exonic RNA-seq

EGR transcription factor family members were predicted, by IPA core analysis, as upstream regulators of genes annotated to MR and GR peaks and genes exhibiting differential RNA expression following acute stress or during the circadian rise. Early growth response (EGR). Activation z-scores ≥ +2 significantly predict pathway activation, while z-scores of ≤ -2 significantly predict pathway inhibition. Activation z-scores < +2 or > -2 indicate a trend towards activation or inhibition, however the prediction is not statistically significant. Statistical analysis: Right-tailed Fisher's exact test, $p<0.05$.

Upstream regulator	Dataset	Predicted Activation state	Activation z-score	*p*-value of overlap	# Target genes in dataset
KLF1	inRNA			0.0476	7
KLF2	inRNA		1.219	0.018	19
	exRNA		-0.831	2.57e-07	13
KLF3	GR		-1.739	0.043	17
	exRNA	Inhibited	-2.345	0.0455	9
KLF4	inRNA		-1.366	6.62e-03	31
	exRNA		1.639	5.27e-06	15
KLF5	GR		1.070	7.34e-03	6
	exRNA			0.049	3
KLF6	MR		-0.392	0.0491	8
	GR		0.513	0.0275	6
	inRNA		-0.417	4.99e-03	12
	exRNA		-0.77	6.05e-07	9
KLF10	exRNA			0.0228	2
KLF15	exRNA			0.0232	3
KLF16	exRNA			0.0411	1

Table 4.5 KLF transcription factor family members are predicted upstream regulators of genes annotated to MR and GR peaks and genes exhibiting differential RNA expression following acute stress or during the circadian rise

Datasets comprising genes annotated to MR and GR peaks and genes exhibiting differential RNA expression following acute stress or during the circadian rise were analysed by IPA. Core analysis predicted KLFs as upstream regulators of genes in these datasets. Krüppel-like factor (KLF). Activation z-scores ≥ +2 significantly predict pathway activation, while z-scores of ≤ -2 significantly predict pathway inhibition. Activation z-scores < +2 or > -2 indicate a trend towards activation or inhibition, however the prediction is not statistically significant. Statistical analysis: Right-tailed Fisher's exact test, $p<0.05$.

Upstream regulator	Dataset	Predicted Activation state	Activation z-score	*p*-value of overlap	# Target genes in dataset
SP1	MR	Activated	3.182	0.0448	41
	inRNA		-0.14	1.10e-05	70
	exRNA		0.641	3.18e-08	27
SP2	exRNA			1.07e-03	3
SP3	inRNA		1.299	0.0272	24
	exRNA		1.404	2.3e-06	14
SP4	exRNA			7.45e-03	3
SP6	inRNA			0.0289	2

Table 4.6 SP transcription factor family members are predicted upstream regulators of genes annotated to MR peaks and genes exhibiting differential RNA expression following acute stress or during the circadian rise

Datasets comprising genes annotated to MR peaks and genes exhibiting differential RNA expression following acute stress or during the circadian rise were analysed by IPA. Core analysis predicted SP transcription factors as upstream regulators of genes in these datasets. Specificity Protein (SP). Activation z-scores ≥ +2 significantly predict pathway activation, while z-scores of ≤ -2 significantly predict pathway inhibition. Activation z-scores < +2 or > -2 indicate a trend towards activation or inhibition, however the prediction is not statistically significant. Statistical analysis: Right-tailed Fisher's exact test, $p<0.05$.

Upstream regulator	Dataset	Predicted Activation state	Activation z-score	*p*-value of overlap	# Target genes in dataset
ZNF43	inRNA			8.25e-04	4
ZNF148	MR			8.31e-03	4
	GR			0.0111	3
ZNF503	inRNA			0.0233	3
	exRNA			6.51e-03	2

Table 4.7 ZNF transcription factor family members are predicted upstream regulators of genes annotated to MR and GR peaks and genes exhibiting differential RNA expression following acute stress or during the circadian rise

Upstream regulators of genes in MR and GR ChIP-seq datasets and intronic/exonic RNA-seq datasets were predicted by IPA Core analysis. ZNF transcription factors were identified as upstream regulators of genes in these datasets. Zinc finger protein (ZNF). Activation z-scores ≥ +2 significantly predict pathway activation, while z-scores of ≤ -2 significantly predict pathway inhibition. Activation z-scores < +2 or > -2 indicate a trend towards activation or inhibition, however the prediction is not statistically significant. Statistical analysis: Right-tailed Fisher's exact test, $p<0.05$.

Upstream regulator	Dataset	Predicted activation state	Activation z-score	*p*-value of overlap	# Target genes in dataset
NMDAR	MR	Activated	2.425	3.24e-04	6
	GR		1.982	2.23e-03	4
GRIA2	MR			6.84e-04	3
	GR			5.87e-03	2
GRIN1	MR			0.021	3
	GR			0.0464	2
GRIN2B	MR			0.0283	2

Table 4.8 Glutamate receptor family members are predicted upstream regulators of genes annotated to MR and GR peaks following acute stress or during the circadian rise

Genes annotated to MR and GR peaks following acute stress or during the circadian rise were analysed by IPA. Core analysis predicted members of the glutamate receptor family as upstream regulators of genes in these datasets. *N*-methyl-*D*-aspartate receptor (NMDAR), Glutamate ionotropic receptor AMPA type subunit 2 (GRIA2), glutamate ionotropic receptor NMDA type subunit 1 (GRIN1), glutamate ionotropic receptor NMDA type subunit 2B (GRIN2B). Activation z-scores ≥ +2 significantly predict pathway activation, while z-scores of ≤ -2 significantly predict pathway inhibition. Activation z-scores < +2 or > -2 indicate a trend towards activation or inhibition, however the prediction is not statistically significant. Statistical analysis: Right-tailed Fisher's exact test, $p<0.05$.

4.4.3 Biological functions influenced by genes annotated to MR and GR peaks or differentially expressed genes following acute stress or during the circadian rise

IPA made significant predictions between biological functions and genes in our MR, GR, inRNA and exRNA datasets. Biological processes of relevance to GC hormone action in the brain were selected for further examination and categorised into subgroups. The statistical significance (*p*-value), predicted activation state, activation z-score and number of genes associated with each category of biological functions and the corresponding dataset are depicted in Tables 4.9 – 4.11.

Many hippocampal dependent processes (Figure 4.2) were associated with genes in our ChIP- and RNA-seq datasets including memory, spatial memory, conditioning, learning and cognition. The hippocampal dependent function predicted with the highest statistical significance to be associated with genes in our datasets; Cognition, is depicted in Figure 4.3. The subcellular localisation of MR and/or GR annotated genes related to cognition are shown.

Genes present in our ChIP- and RNA-seq datasets were linked to a number of neurodevelopmental processes (Figure 4.4) such as neuronal maturation, branching of neurites, branching of neurons, neuronal morphology, nervous system differentiation, nervous system morphology, neurite growth, neuritogenesis, neuronal cell proliferation and neuronal development. Neuronal development was the most significantly predicted neurodevelopmental process associated with genes in our dataset and the subcellular localisation of MR and/or GR annotated genes related to this pathway can be seen in Figure 4.5.

Synaptic signalling processes (Figure 4.6) were shown to be linked with genes annotated to MR and/or GR peaks or genes exhibiting differential inRNA expression following elevations in GC hormones. Such processes included NMDA-mediated synaptic current, long-term depression, synaptic depression, synaptic plasticity, long-term potentiation and synaptic transmission. The most significant prediction was made between genes in our datasets and synaptic transmission, therefore Figure 4.7 shows the subcellular localisation of MR and/or GR annotated genes related to this pathway.

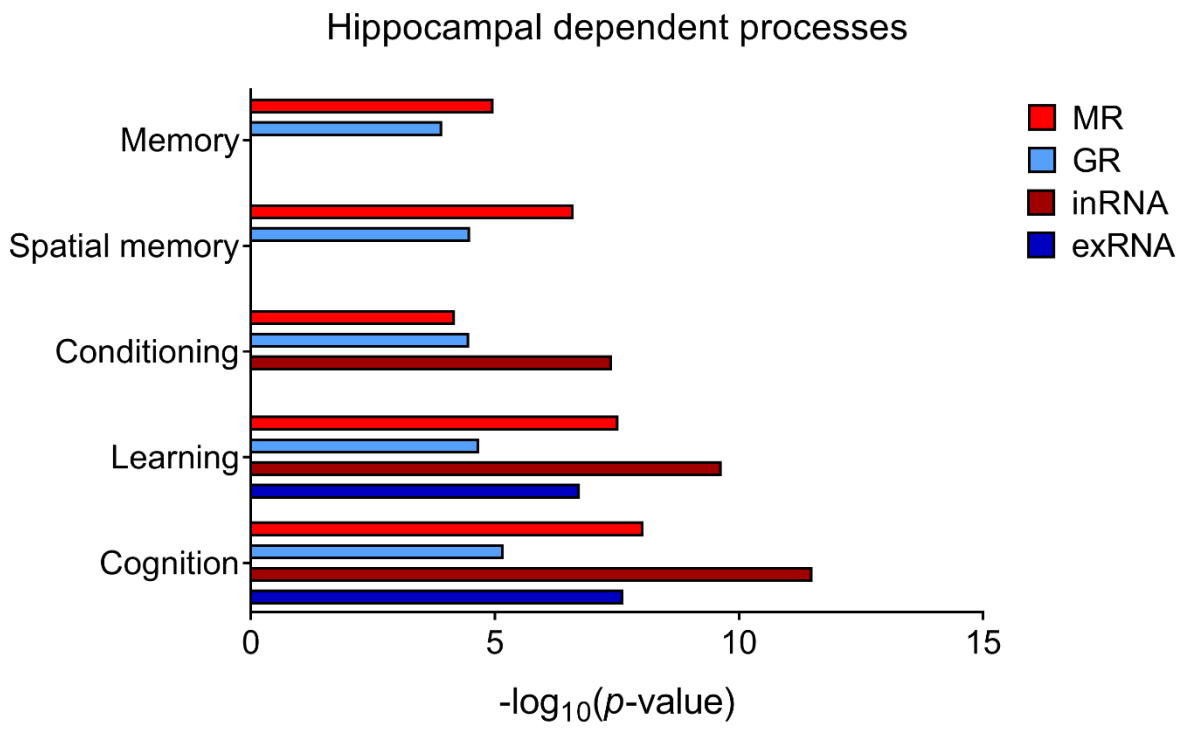

Figure 4.2 Hippocampal-dependent processes influenced by genes bound by MRs and/or GRs or exhibiting differential RNA expression following acute stress or during the circadian rise

Hippocampal-dependent processes were predicted, by IPA, to be associated with genes in our ChIP- and RNA-seq datasets. Such processes included hippocampal dependent processes, such as memory, spatial memory, conditioning, learning and cognition, and genes in our ChIP- and RNA-seq datasets. Data is expressed as the antilog of the *p*-value.

Biological function	Dataset	Predicted Activation state	Activation z-score	*p*-value of overlap	# Target genes in dataset
Memory	MR	Activated	2.012	1.06e-05	40
	GR	Activated	2.149	1.2e-04	25
Spatial memory	MR		1.706	2.41e-07	23
	GR			3.24e-05	14
Conditioning	MR	Activated	3.515	6.51e-05	31
	GR	Activated	3.365	3.39e-05	22
	inRNA		0.65	4.04e-08	46
Learning	MR	Activated	2.817	2.91e-08	66
	GR	Activated	3.088	2.10e-05	38
	inRNA		0.718	2.23e-10	87
	exRNA		1.622	1.80e-07	26
Cognition	MR	Activated	2.525	8.99e-09	72
	GR	Activated	2.969	6.67e-06	42
	inRNA		0.224	3.13e-12	98
	exRNA		1.721	2.32e-08	29

Table 4.9 Genes associated with MR and/or GR binding or exhibiting differential RNA expression following acute stress or during the circadian rise are associated with hippocampal dependent processes

Datasets comprising genes annotated to significant MR and GR peaks and genes exhibiting differential RNA expression following acute stress or during the circadian rise were predicted by IPA Core analysis to be linked to hippocampal dependent processes. Activation z-scores ≥ +2 significantly predict pathway activation, while z-scores of ≤ -2 significantly predict pathway inhibition. Activation z-scores < +2 or > -2 indicate a trend towards activation or inhibition, however the prediction is not statistically significant. Statistical analysis: Right-tailed Fisher's exact test, $p<0.05$.

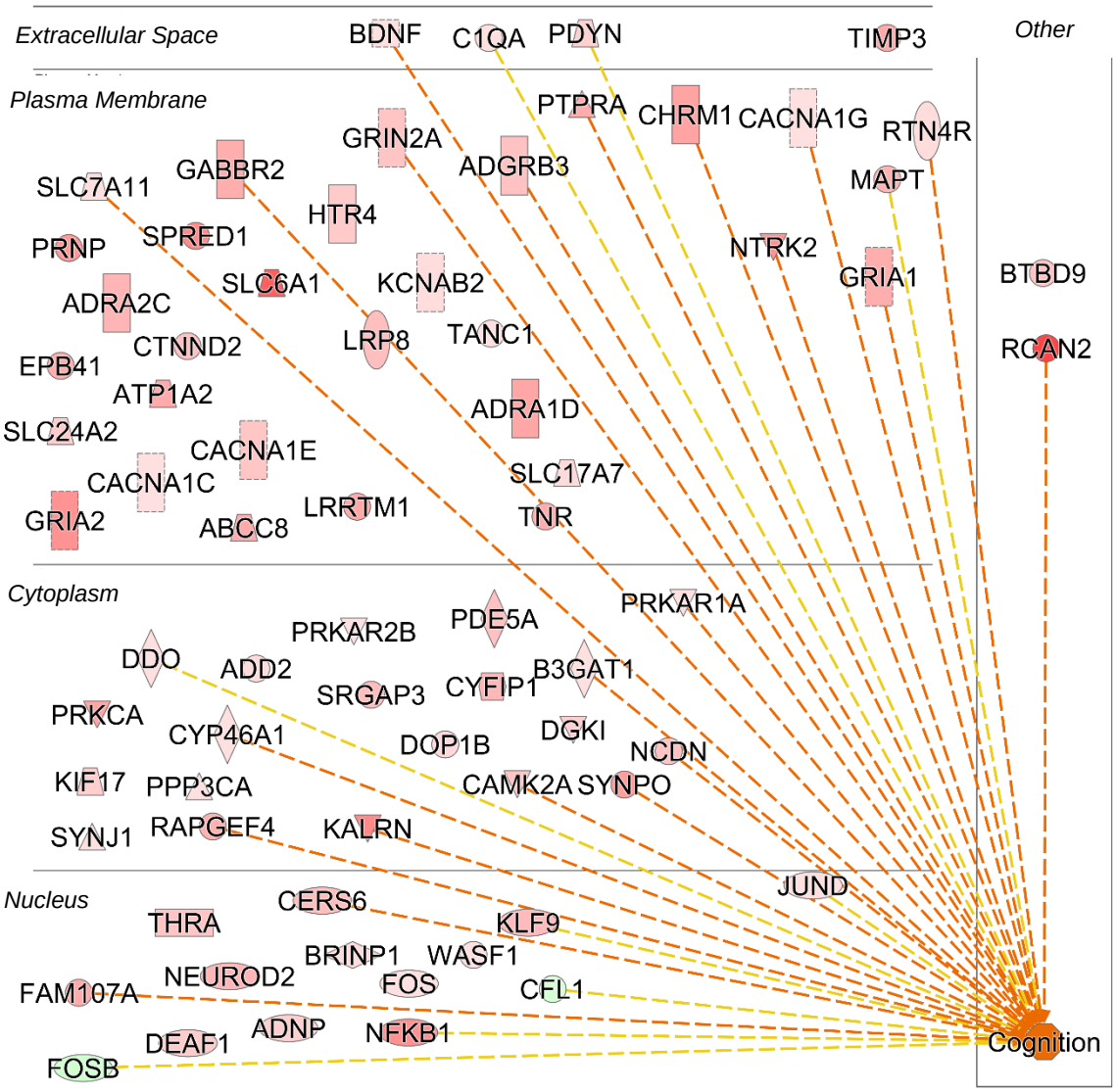

Figure 4.3 The hippocampal dependent process "Cognition" is strongly linked with genes exhibiting MR and/or GR binding following acute stress or during the circadian rise

A highly significant prediction was made by IPA Core analysis between cognition and genes annotated to significant MR and/or GR binding peaks following acute stress or during the circadian rise. The subcellular localisation of 72 MR- and/or GR-annotated genes associated with the hippocampal dependent process; cognition, are shown. Genes highlighted in red indicate increased MR and/or GR binding, while genes highlighted in green indicate decreased MR and/or GR binding, with the intensity of the shade corresponding to the fold change in binding. Orange connections represent a significant prediction of enhanced cognition. Yellow connections indicate that experimental findings are inconsistent with the state of the downstream molecule, therefore an effect cannot be significantly predicted.

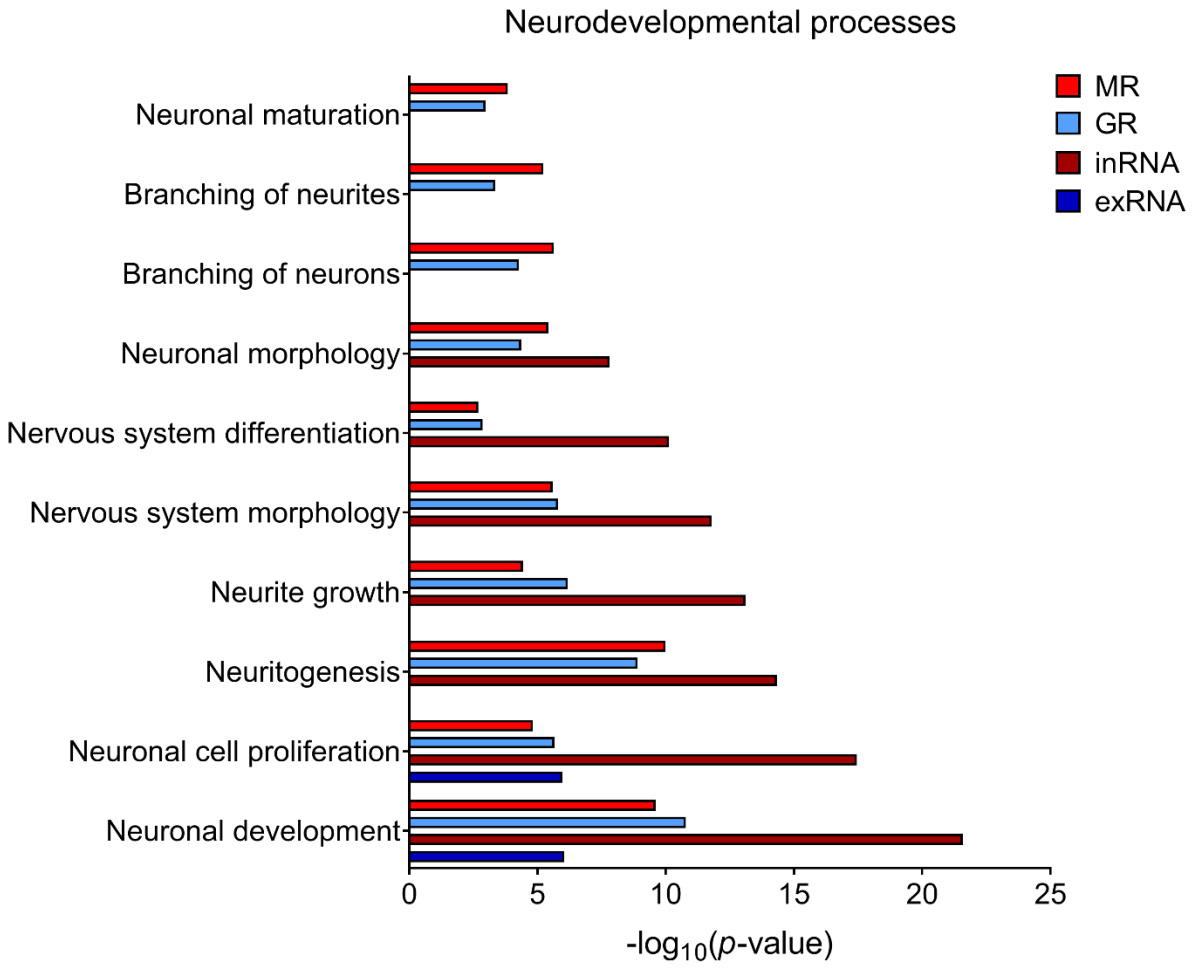

Figure 4.4 Neurodevelopmental processes associated with genes annotated to MR and GR peaks or genes exhibiting differential RNA expression following acute stress or during the circadian rise

Genes bound by MRs and/or GRs or exhibiting differential RNA expression following acute stress or during the circadian rise were linked, by IPA, to neurodevelopmental processes. These processes included neuronal maturation, branching of neurites, branching of neurons, neuronal morphology, nervous system differentiation, nervous system morphology, neurite growth, neuritogenesis, neuronal cell proliferation and neuronal development, and genes in our datasets. Data is expressed as the antilog of the *p*-value.

Biological function	Dataset	Predicted Activation state	Activation z-score	*p*-value of overlap	# Target genes in dataset
Neuronal maturation	MR	Activated	2.137	1.42e-04	14
	GR	Activated	2.236	1.04e-03	9
Branching of neurites	MR	Activated	2.792	5.84e-06	45
	GR	Activated	2.568	4.47e-04	26
Branching of neurons	MR	Activated	2.300	2.33e-06	47
	GR	Activated	1.756	5.18e-05	29
Neuronal morphology	MR			3.70e-06	73
	GR			4.29e-05	45
	inRNA			1.54e-08	109
Nervous system differentiation	MR	Activated	4.265	2.06e-03	57
	GR	Activated	3.646	1.38e-03	37
	inRNA		0.753	7.42e-11	100

Table 4.10.a Neurodevelopmental functions influenced by genes annotated to MR and GR peaks or genes differentially expressed following acute stress or during the circadian rise

IPA Core analysis highlighted a relationship between genes in our ChIP-seq and RNA-seq datasets and many neurodevelopmental functions. Neuronal maturation, branching of neurites, branching of neurons, neuronal morphology and nervous system differentiation were among these functions. Activation z-scores ≥ +2 significantly predict pathway activation, while z-scores of ≤ -2 significantly predict pathway inhibition. Activation z-scores < +2 or > -2 indicate a trend towards activation or inhibition, however the prediction is not statistically significant. Statistical analysis: Right-tailed Fisher's exact test, $p<0.05$.

Biological function	Dataset	Predicted Activation state	Activation z-score	*p*-value of overlap	# Target genes in dataset
Nervous system morphology	MR			2.59e-06	114
	GR			1.59e-06	74
	inRNA			1.60e-12	177
Neurite growth	MR	Activated	3.638	3.78e-05	61
	GR	Activated	2.397	6.59e-07	45
	inRNA		0.848	7.71e-14	103
Neuritogenesis	MR	Activated	3.411	1.01e-10	95
	GR	Activated	2.457	1.23e-09	62
	inRNA		0.656	4.59e-15	130
Neuronal cell proliferation	MR	Activated	3.779	1.48e-05	71
	GR	Activated	2.443	2.21e-06	49
	inRNA		0.239	3.51e-18	127
	exRNA		0.077	1.07e-06	29
Neuronal development	MR	Activated	4.239	2.49e-10	117
	GR	Activated	3.270	1.66e-11	81
	inRNA		0.396	2.63e-22	181
	exRNA		0.077	1.07e-06	29

Table 4.10.b Neurodevelopmental functions influenced by genes annotated to MR and GR peaks or genes differentially expressed following acute stress or during the circadian rise

IPA Core analysis highlighted a relationship between genes in our ChIP-seq and RNA-seq datasets and many neurodevelopmental functions. Nervous system morphology, neurite growth, neuritogenesis, neuronal cell proliferation, neuronal development. Activation z-scores ≥ +2 significantly predict pathway activation, while z-scores of ≤ -2 significantly predict pathway inhibition. Activation z-scores < +2 or > -2 indicate a trend towards activation or inhibition, however the prediction is not statistically significant. Statistical analysis: Right-tailed Fisher's exact test, $p<0.05$.

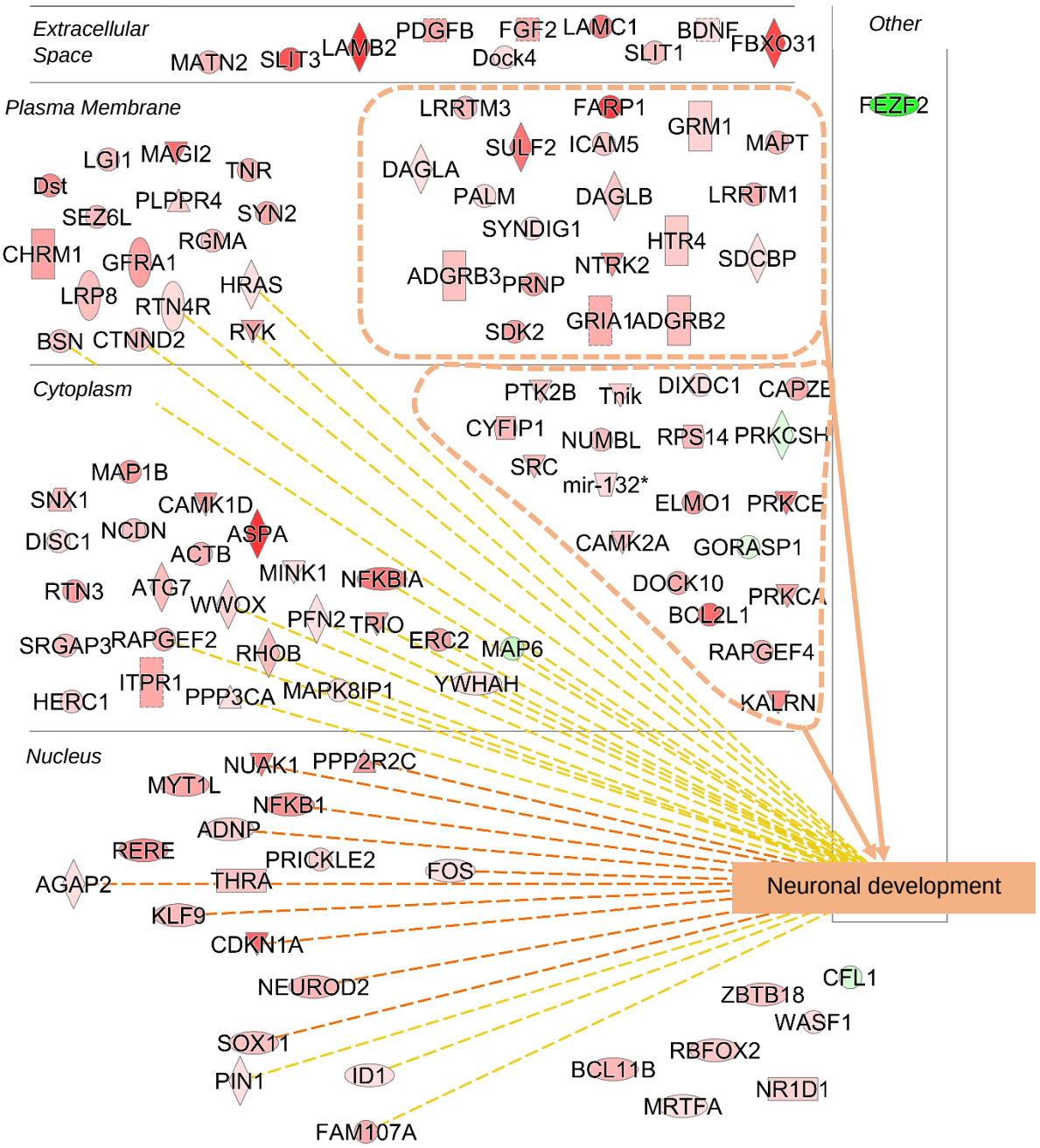

Figure 4.5 Neuronal development is strongly linked to genes bound by MRs and/or GRs following acute stress or during the circadian rise

IPA Core analysis predicted, with high statistical significance, an association between neuronal development and genes annotated to MR and/or GR peaks following elevations in GC hormones. The subcellular localisation of these 117 MR- and/or GR-annotated genes linked to neuronal development can be seen. Genes highlighted in red indicate increased MR and/or GR binding, while genes highlighted in green indicate decreased MR and/or GR binding, with the intensity of the shade corresponding to the fold change in binding. Orange connections represent a significant prediction of enhanced neuronal development. Dashed lines represent predicted enhanced neuronal development of all genes within the boxed region. Yellow connections indicate that experimental findings are inconsistent with the state of the downstream molecule, therefore an effect cannot be predicted.

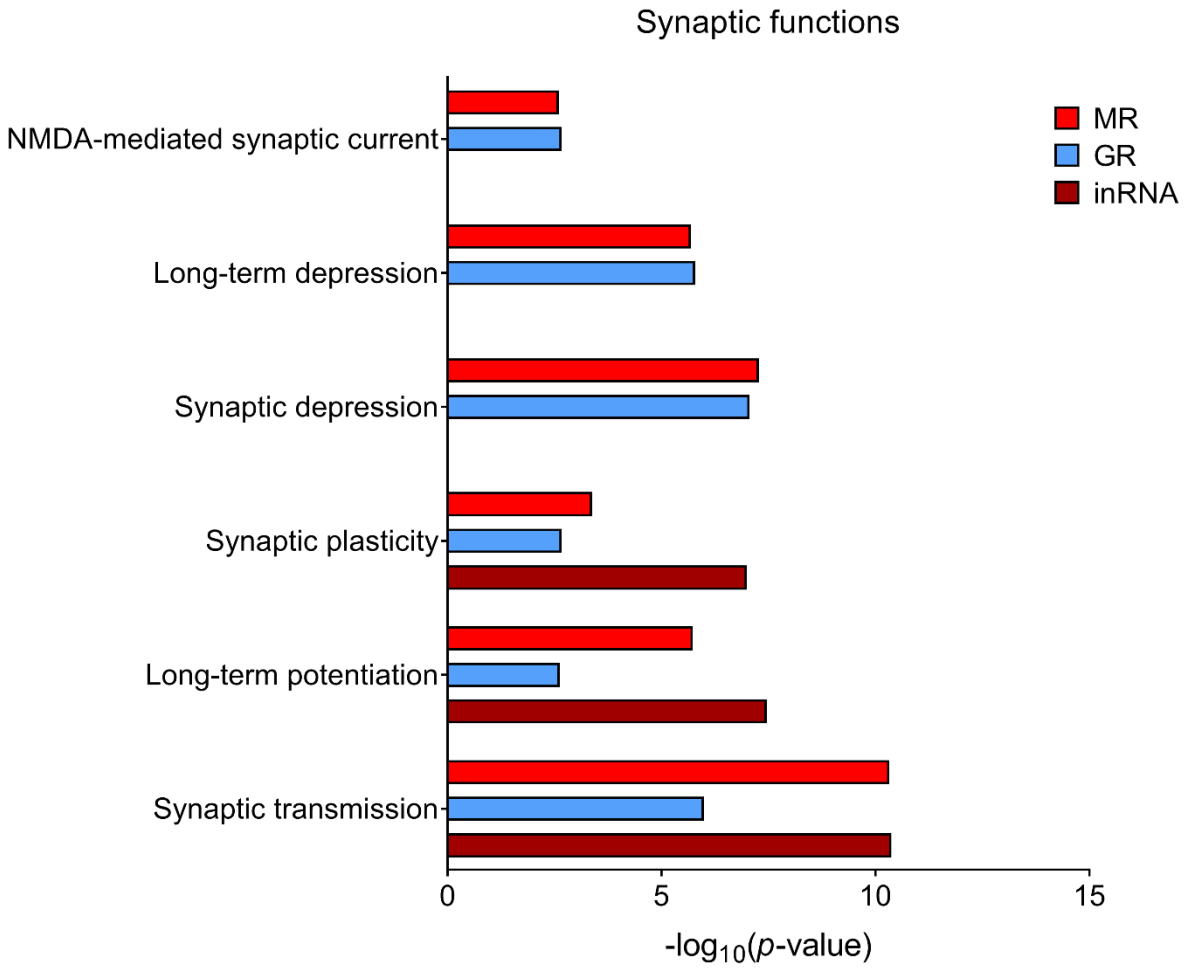

Figure 4.6 Genes bound by MRs and/or GRs or differentially expressed genes following acute stress and during the circadian rise are linked to synaptic functions

Several synaptic functions were highlighted by IPA core analysis to be associated with genes in our ChIP-seq and RNA-seq datasets. Among the synaptic related functions were NMDA-mediated synaptic current, long-term depression, synaptic depression, synaptic plasticity, long-term potentiation and synaptic transmission. Data is expressed as the antilog of the *p*-value.

Biological function	Dataset	Predicted Activation state	Activation z-score	*p*-value of overlap	# Target genes in dataset
NMDA-mediated synaptic current	MR			2.49e-03	5
	GR			2.14e-03	4
Long-term depression	MR	Activated	2.512	1.82e-03	23
	GR	Activated	3.037	1.62e-06	17
Synaptic depression	MR	Activated	1.674	5.22e-08	29
	GR	Activated	2.410	8.68e-08	21
Synaptic plasticity	MR		1.756	4.18e-04	19
	GR		1.982	2.13e-04	12
	inRNA		-0.488	9.98e-08	31
Long-term potentiation	MR	Activated	3.287	1.84e-06	41
	GR	Activated	2.984	2.35e-03	21
	inRNA		-0.260	3.48e-08	53
Synaptic transmission	MR	Activated	1.389	4.65e-11	60
	GR	Activated	2.342	1.01e-06	34
	inRNA	Activated	2.412	4.26e-11	74

Table 4.11 Synaptic functions influenced by genes annotated to MR and GR peaks or genes exhibiting differential inRNA expression following acute stress or during the circadian rise

IPA predicted an association between a number of synaptic functions and genes annotated to significant MR and GR binding peaks or exhibiting differential inRNA expression following elevations in GC hormones. Synaptic functions included NMDA-mediated synaptic current, long-term depression, synaptic depression, synaptic plasticity, long-term potentiation and synaptic transmission. Activation z-scores ≥ +2 significantly predict pathway activation, while z-scores of ≤ -2 significantly predict pathway inhibition. Activation z-scores < +2 or > -2 indicate a trend towards activation or inhibition, however the prediction is not statistically significant. Statistical analysis: Right-tailed Fisher's exact test, $p<0.05$.

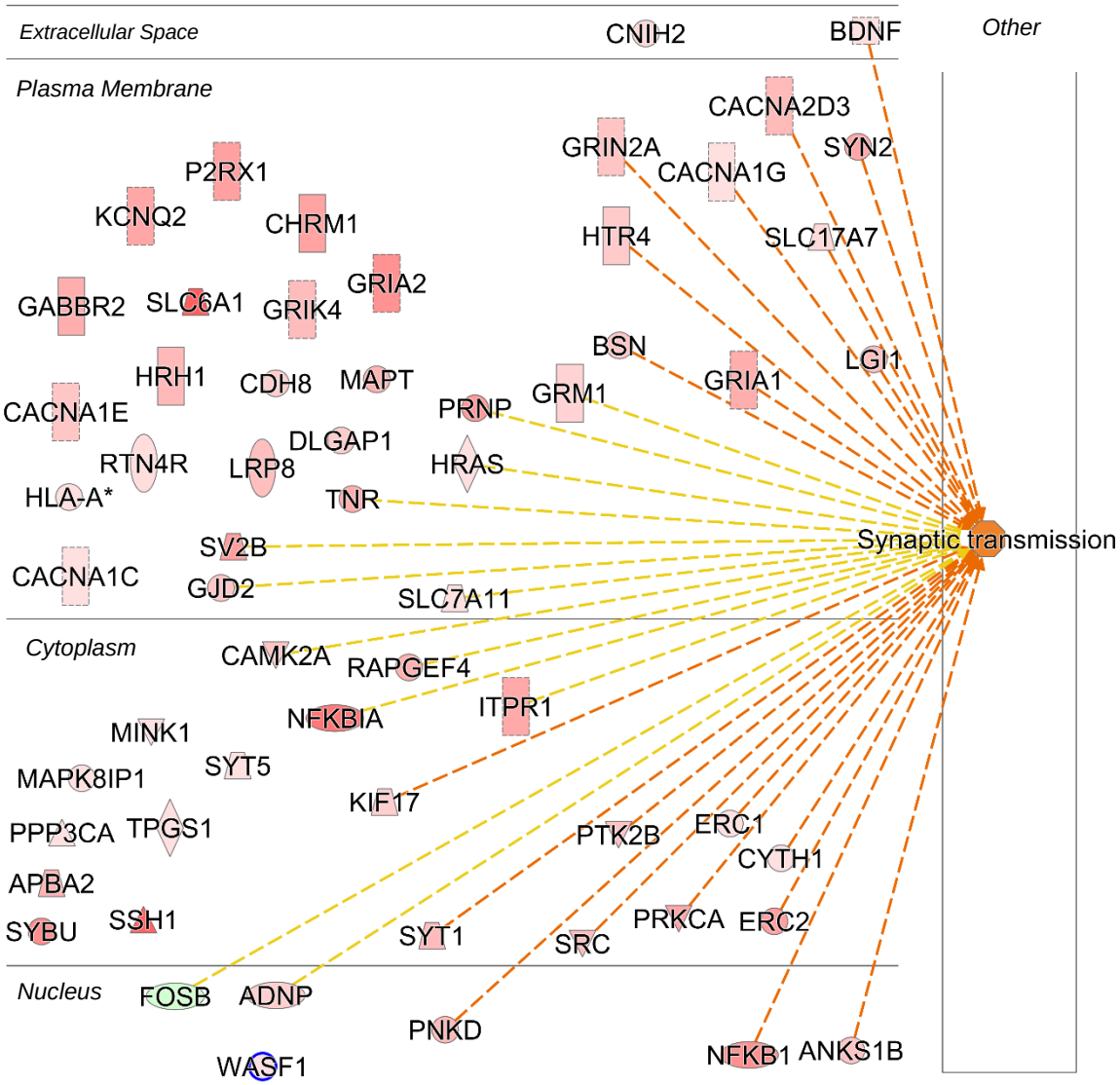

Figure 4.7 Synaptic transmission is strongly linked to genes bound by MRs and/or GRs following stress or circadian driven elevations in GC hormone secretion

A strong significant association was made, by IPA, between synaptic transmission and genes bound by MRs and/or GRs following acute stress or during the circadian rise. The subcellular localisation of the 60 MR and/or GR bound genes associated with synaptic transmission is shown. Genes highlighted in red indicate increased MR and/or GR binding, while genes highlighted in green indicate decreased MR and/or GR binding, with the intensity of the shade corresponding to the fold change in binding. Orange connections represent a significant prediction of enhanced synaptic transmission. Yellow connections indicate that experimental findings are inconsistent with the state of the downstream molecule, therefore an effect cannot be predicted.

4.4.4 Neurological diseases and psychological disorders influenced by MR and/or GR bound genes and differentially expressed genes following acute stress or during the circadian rise

IPA made significant predictions between diseases and genes in the reference MR, GR, inRNA and exRNA datasets. Diseases of relevance to GC hormone action in the brain were examined further and were categorised into neurological diseases and psychological disorders. The statistical significance (*p*-value), predicted activation state, activation z-score and number of genes associated with each category of neurological disease or psychological disorder and the corresponding dataset are depicted in Table 4.12 and Table 4.13.

Neurological diseases (Figure 4.10) linked to genes in our ChIP- and RNA-seq datasets included Huntington's disease, epilepsy, Parkinson's disease, cognitive impairment and Alzheimer's disease. A strong association was made between genes in our ChIP- and RNA-seq datasets and epilepsy, thus the subcellular localisation of MR- and/or GR-annotated genes predicted to be involved in this neurological disease can be seen in Figure 4.9.

Genes in our ChIP- and RNA-seq datasets were associated with psychological disorders (Figure 4.12) such as anxiety, depressive disorder and schizophrenia spectrum disorder. Schizophrenia spectrum disorder was predicted with the highest statistical significance to be linked with genes in our ChIP- and RNA-seq datasets, therefore the subcellular localisation of MR and/or GR annotated genes associated with this psychological disorder are depicted in Figure 4.11.

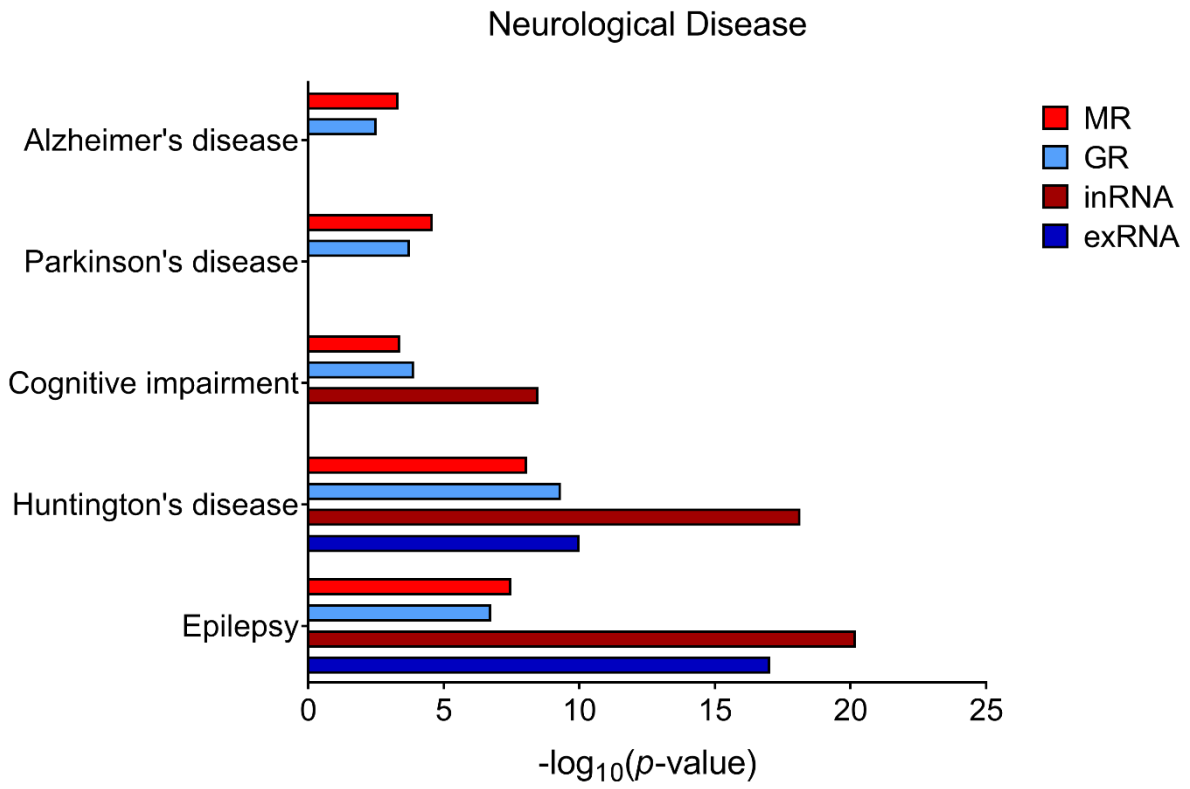

Figure 4.8 Neurological diseases are linked to genes bound by MRs and/or GRs or genes exhibiting differential expression following stress or circadian driven elevations in GC hormone secretion

A number of neurological diseases were shown to be related to genes annotated to MR and GR peaks and differentially expressed genes following acute stress or during the circadian rise. Such diseases included Alzheimer's disease, Parkinson's disease, cognitive impairment, Huntington's disease and epilepsy. Data is expressed as the antilog of the *p*-value.

Disease	Dataset	Predicted Activation state	Activation z-score	*p*-value of overlap	# Target genes in dataset
Alzheimer's disease	MR			4.76e-04	69
	GR			2.94e-03	41
Parkinson's disease	MR			2.50e-05	38
	GR			1.77e-04	37
Cognitive impairment	MR		-0.365	4.13e-04	56
	GR		1.342	1.25e-04	38
	inRNA		0.283	3.28e-09	112
Huntington's disease	MR			8.56e-09	83
	GR			4.87e-10	59
	inRNA			7.13e-19	127
	exRNA			9.81e-11	36
Epilepsy	MR		0.194	3.30e-08	54
	GR		0.218	1.80e-07	36
	inRNA		-1.599	6.44e-21	97
	exRNA			9.52e-18	37

Table 4.12 Genes annotated to MR and/or GR peaks or genes differentially expressed following acute stress or during the circadian rise are associated with neurological diseases

A relationship was shown by IPA between genes in our ChIP- and RNA-seq datasets and neurological diseases such as Alzheimer's disease, Parkinson's disease, cognitive impairment, Huntington's disease and epilepsy. Activation z-scores ≥ +2 significantly predict pathway activation, while z-scores of ≤ -2 significantly predict pathway inhibition. Activation z-scores < +2 or > -2 indicate a trend towards activation or inhibition, however the prediction is not statistically significant. Statistical analysis: Right-tailed Fisher's exact test, $p<0.05$.

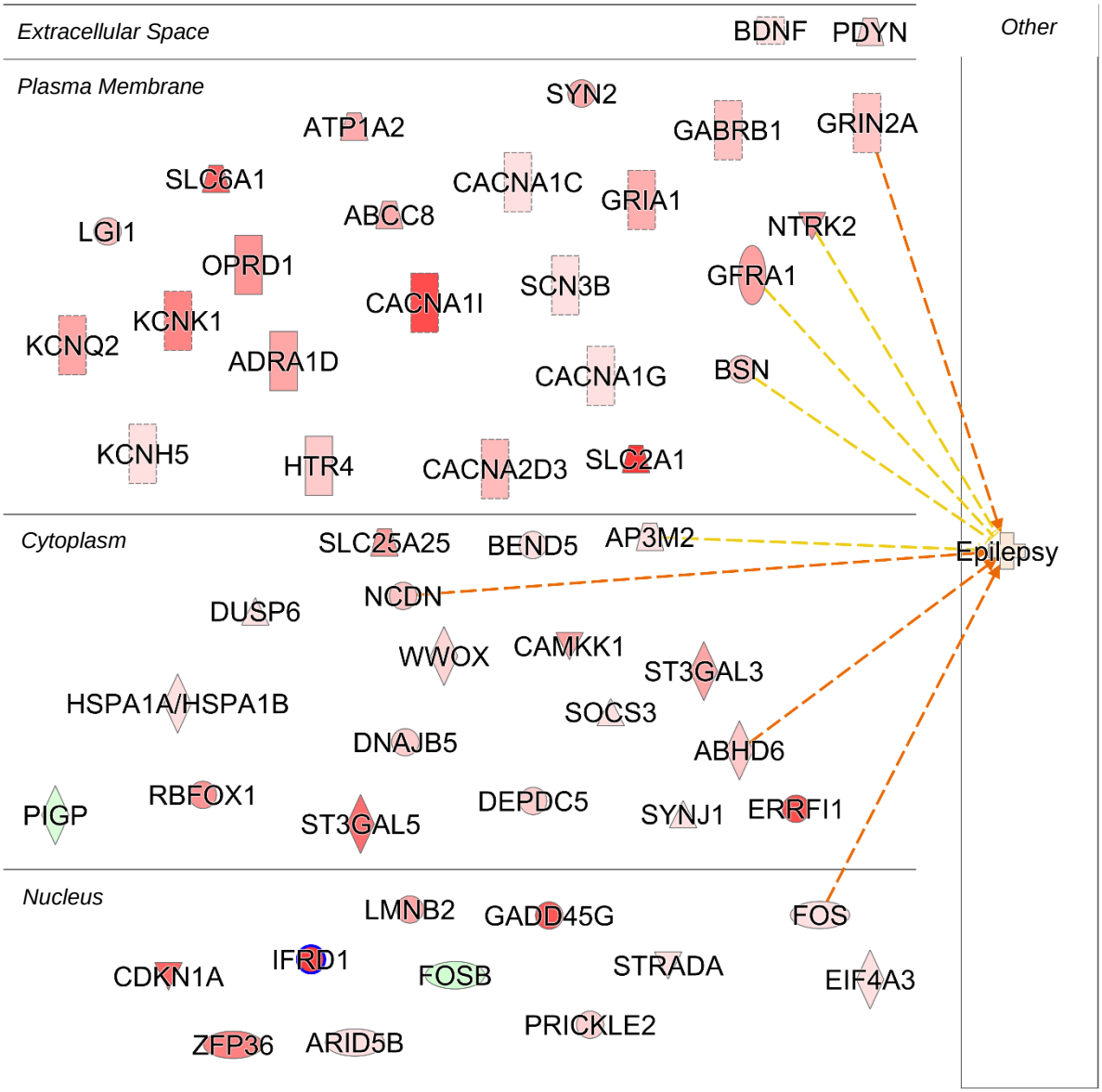

Figure 4.9 Epilepsy is highly associated with genes bound by MRs and/or GRs and genes exhibiting differential RNA expression following acute stress or during the circadian rise

A strong link was predicted by IPA between epilepsy and genes in our ChIP-seq and RNA-seq datasets. The subcellular localisation of 54 genes bound by MRs and/or GRs following stress or circadian driven elevations in GC hormone secretion is depicted. Genes highlighted in red indicate increased Mr and/or GR binding, while genes highlighted in green indicate decreased Mr and/or GR binding, with the intensity of the shade corresponding to the fold change in binding. Orange connections represent activation of epilepsy. Yellow connections indicate that experimental findings are inconsistent with the state of the downstream molecule, therefore an effect cannot be predicted.

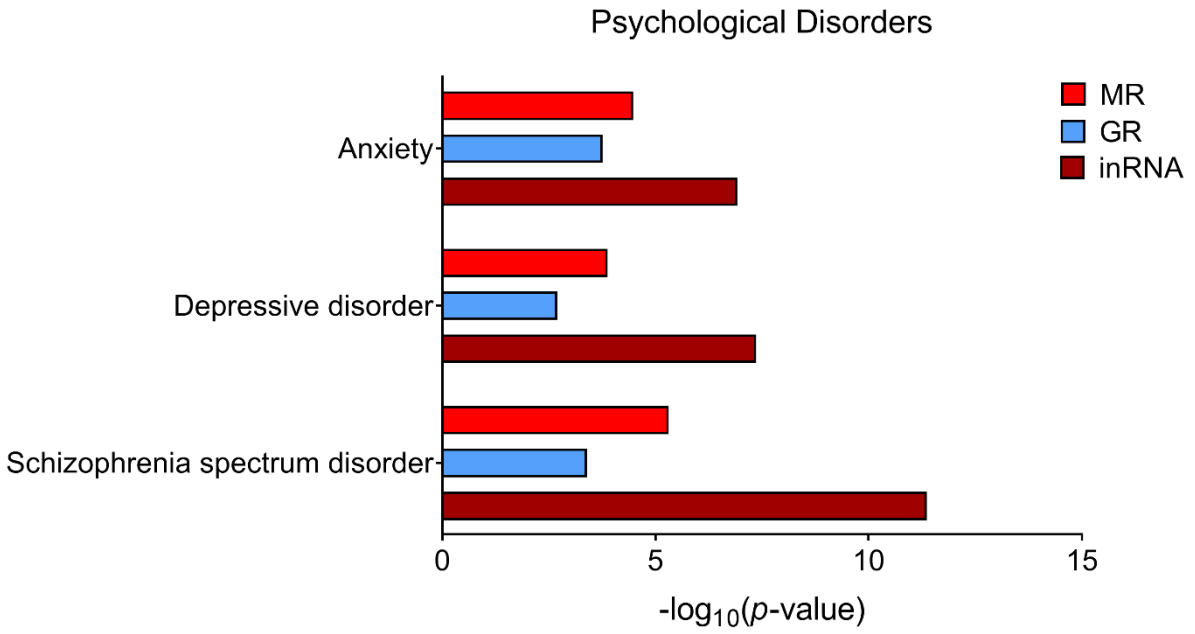

Figure 4.10 Psychological disorders are linked to genes annotated to MR and GR peaks and differentially expressed genes following acute stress or during the circadian rise

Psychological disorders, such as anxiety, depressive disorder and Schizophrenia spectrum disorder are associated with and genes bound by MRs and/or GRs and genes exhibiting differential inRNA expression following stress or circadian driven elevations in GC hormone secretion. Data is expressed as the antilog of the *p*-value.

Disorder	Dataset	Predicted Activation state	Activation z-score	*p*-value of overlap	# Target genes in dataset
Anxiety	MR		0.465	3.33e-05	31
	GR		0.492	1.73e-04	20
	inRNA		1.425	1.22e-07	44
Depressive disorder	MR		-0.987	1.33e-04	39
	GR			1.99 e-03	23
	inRNA		0.769	4.32e-08	58
Schizophrenia spectrum disorder	MR			4.91 e-06	66
	GR			3.99e-04	38
	inRNA			4.34e-12	100

Table 4.13 Psychological disorders related to genes bound by MRs and/or GRs or genes exhibiting differential inRNA expression following stress or circadian driven elevations in GC hormone secretion

IPA highlighted a relationship between the psychological disorders; anxiety, depressive disorder and schizophrenia spectrum disorder and genes in our ChIP- and RNA-seq datasets. Activation z-scores ≥ +2 significantly predict pathway activation, while z-scores of ≤ -2 significantly predict pathway inhibition. Activation z-scores < +2 or > -2 indicate a trend towards activation or inhibition, however the prediction is not statistically significant. Statistical analysis: Right-tailed Fisher's exact test, $p<0.05$.

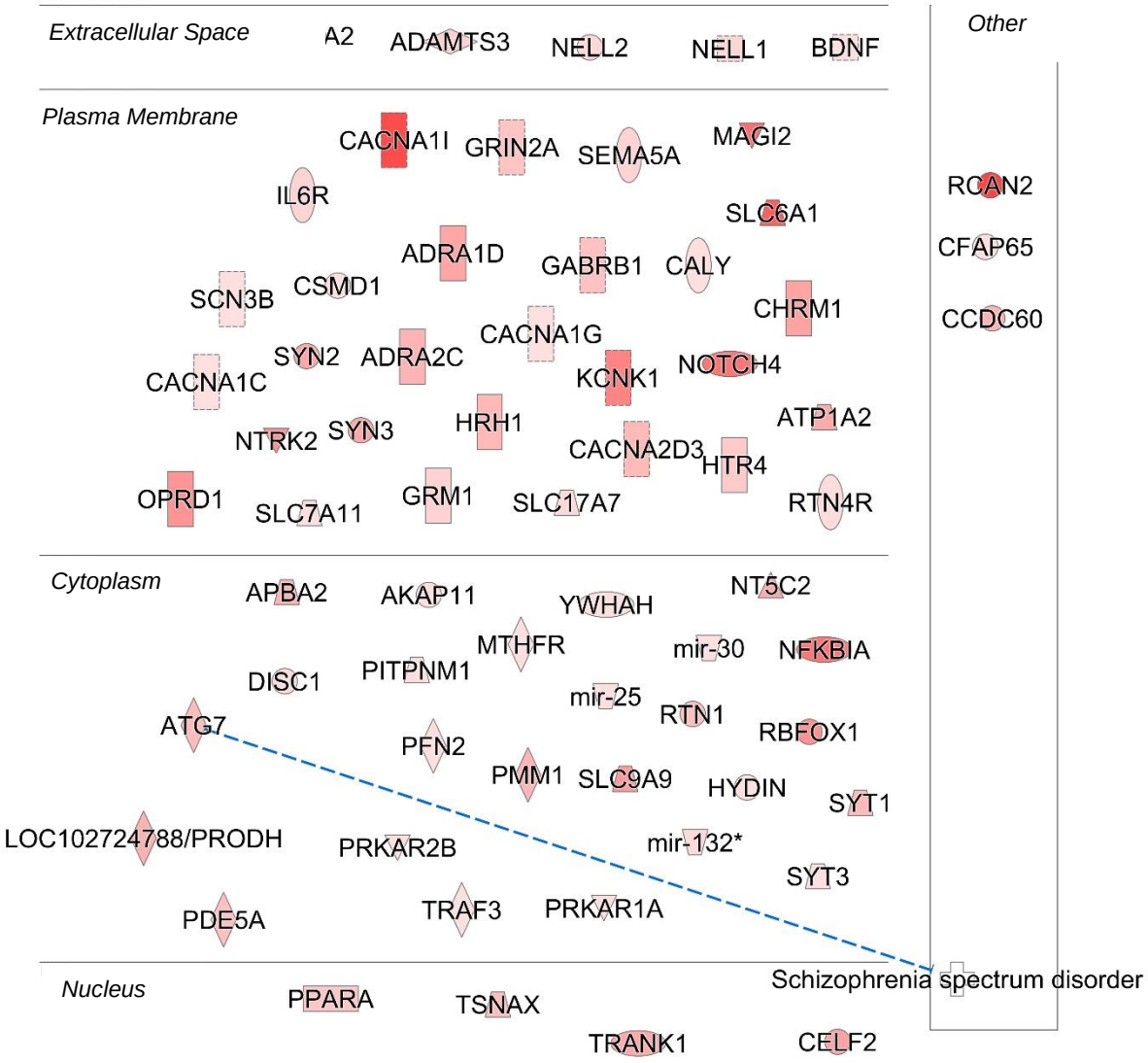

Figure 4.11 Schizophrenia spectrum disorder is strongly linked to genes bound by MRs and/or GRs and genes exhibiting differential inRNA expression following acute stress or during the circadian rise

A highly significant association was made by IPA between schizophrenia spectrum disorder and genes in our ChIP- and RNA-seq datasets. The subcellular localisation of 64 genes annotated to MR and/or GR peaks following stress and circadian driven elevations in GC hormone secretion is shown. Genes highlighted in red indicate increased MR and/or GR binding, with the intensity of the shade corresponding to the magnitude of increased binding. Blue connections represent a significant prediction of schizophrenia spectrum disorder inhibition.

4.5 Discussion

"Core analysis" of ChIP- and RNA-seq datasets by IPA has provided a detailed, comprehensive insight into the biological processes and diseases which may be under GC hormone regulation in the hippocampus under stress and circadian conditions. Several upstream regulators of genes within the reference datasets were also predicted by IPA, allowing for the identification of molecules potentially acting as coregulators of MRs and GRs in orchestrating the genomic response to stress and the circadian rise. Furthermore, numerous biological processes and diseases not specifically associated with the hippocampus have been highlighted, enabling the extrapolation of these predictions to GC hormone action throughout the brain. These findings have confirmed the high specificity of the ChIP- and RNA-seq analyses, while highlighting previously unknown genes and molecular targets for further exploration and validation.

The significant associations made between the genes in all four datasets with glucocorticoid receptor signalling, circadian rhythm signalling and CRH signalling highlights the specificity of the ChIP- and RNA-seq analyses under both stress and circadian conditions. Glucocorticoid receptor signalling is logical when looking at MR and GR. Nevertheless, inRNA and exRNA are also linked with this pathway, underlining an overall importance of GCs in the RNA response to stress. Our experimental model is consistent with circadian rhythm signalling, while CRH signalling is noteworthy as this hormone is the central stress mediator in the brain (Gjerstad et al., 2018). Moreover, the MR and GR were predicted as upstream regulators of genes in our datasets, and for both ChIP datasets, the GR was the most highly significant upstream regulator predicted by IPA. Well established GC receptor cochaperones were also identified as upstream regulators of genes in the target datasets, such as heat-shock proteins Hsp70 and Hsp90. These proteins play an essential regulatory role in the assembly and activity of MRs and GRs. Hsp70 regulates the folding of *de novo* synthesised GR, while Hsp90 is essential for the processing of GR to its mature form capable of binding GC hormones (Grad and Picard, 2007). Hsp90 also regulates GRs affinity for ligand (Nemoto et al., 1990) and the interactions between GR and DNA (Cadepond et al., 1991).

Regarding the circadian rhythm, IPA predicted the circadian transcriptional regulators CLOCK, CRY1 and CRY2 as upstream regulators of genes in our ChIP- and RNA-seq datasets. CLOCK is a key TF which plays a central role, alongside brain-muscle-arnt-like protein 1 (BMAL1), in the circadian

regulation of GC action at local target tissues by increasing the sensitivity of target tissues to GC hormones in the active phase and decreasing tissue sensitivity to GCs during the inactive phase (Nicolaides et al., 2014). CLOCK has been demonstrated to reduce the ability of human GR (hGR) to influence target gene expression by inducing post-translational modifications within the hGR hinge region, thus attenuating hGR binding to GREs. GC-target gene expression was shown to fluctuate in a circadian fashion, mirroring in reverse phase the *Clock/Bmal1* expression (Nader et al., 2009). CLOCK and BMAL1 have also been shown to induce the expression of the circadian co-regulators, *Cry1* and *Cry2* (Oster et al., 2017), which can interact with the GR resulting in genome wide transcriptional responses, including the induction of *Per1* and *Sgk1* (Lamia et al., 2011).

As previously discussed in Chapter 3, genome-wide MR and GR peaks were highly associated with TF binding motifs other than the classical GRE. Interestingly, a number of the corresponding TFs associated with these motifs, specifically EGRs, KLFs, SPs and ZNFs, were predicted as upstream regulators of genes in the reference datasets. Thus, these TFs share many downstream genomic targets with MRs and GRs. The observations from the motif analyses and pathway analyses suggest that MRs and GRs may interact with these TFs, thereby indirectly binding to the corresponding motif in order to coregulate the transcription of shared target genes. Many findings of *in vitro* experiments support these observations as: 1. The GR has been shown to physically interact with EGR1 at an EGR response element (Chen et al., 2019); 2. Co-localisation of GR and ZNF764 binding sites (Fadda et al., 2017) and KLF binding sites (Chinenov et al., 2014) has been reported; and 3. An indirect interaction between GRs and SP1 at Sp-1 binding sites has been demonstrated (Ou et al., 2006).

Downstream biological processes highlighted by IPA were examined for TFs predicted as upstream regulators of genes in our ChIP- and RNA-seq datasets. Although EGR and SP genes were not found to be associated with a biological pathway of interest, a number of KLF and ZNF genes were. *Klf9* and *Klf15* were highlighted in neurodevelopmental processes, synaptic plasticity, anxiety, learning, and cognition. *Klf9* homozygous knockout mice have been found to show impaired differentiation of dendritic spines in the DG, impaired maturation of adult-born DG neurons, reduced synaptic plasticity and impairments in anxiety-like behaviours and contextual fear discrimination learning (Scobie et al., 2009). KLF15 has been implicated in the regulation of glial development, with an overexpression of the protein resulting in the induction of Glial fibrillary acidic protein (GFAP) expression in astrocytes of mouse spinal cord explant cultures (Fu et al., 2009). *Znf24* and *Znf365* are both linked to neuronal morphology. The

ZFP191 protein, which is encoded by the *Znf24* gene, was shown to play a critical regulatory role in the myelination of CNS oligodendrocytes in mice (Howng et al., 2010), while the absence of DISC1-binding zinc finger protein encoded by the *Znf365* gene resulted in an irregular morphology of cortical basket cells (Koyama et al., 2013).

Glutamate receptor family members were predicted as upstream regulators of the genes in the reference datasets. Their corresponding ligand, glutamate, is the primary excitatory neurotransmitter found in the brain. It is likely that a finely tuned balance of glutamatergic and GABAergic signalling may serve to potentiate and dampen neuronal activity following the stress response or the circadian drive. IPA made a prediction between the upstream regulator, NMDAR, and downstream *Fos* activation. This prediction agrees with previous work of our research group, which has demonstrated an interaction between activated GRs and the NMDAR-activated MAPK-ERK pathway, resulting in induction of *Fos* expression within the DG and the consolidation of long-lasting behavioural responses in response to an acutely stressful challenge (Chandramohan et al., 2007, Gutierrez-Mecinas et al., 2011). Glutamate receptor genes, including *Gria1, Gria2, Grin2a* and *Grin2b* were linked to downstream biological processes enriched for genes in our ChIP- and RNA-seq datasets, such as synaptic transmission and LTP, which have been strongly linked with GC hormone activity (Diamond et al., 1992). The strong electrophysiological effects of GC hormones are well-established, yet the underpinning mechanisms are unclear. One mechanism is via rapidly acting membrane GC receptors (Hua and Chen, 1989, Tasker et al., 2005) while the other is via slower genomically mediated effects. The latter are still poorly characterised; however, our work contributes to the elucidation of electrophysiological activities of genomically acting GC receptors, by identifying GC target genes potentially participating in LTP and synaptic transmission.

Gria1 and *Gria2* genes encode for AMPA receptor subunits GluR1 and GluR2, respectively, that form heterocomplexes in the hippocampus and mediate synaptic transmission (Shi et al., 2001). GluR1 (also known as GluA1) has been implicated in LTP and memory formation, and was shown to regulate the activity pattern of LTP in CA1 pyramidal neurons (Frey et al., 2009). *Grin2a* and *Grin2b* genes encode for the GluN2A and GluN2B proteins, respectively, which have been shown to play a role in hippocampal LTP and LTD, while GluN2B may regulate spatial memory consolidation (Ge et al., 2010). A number of neurological diseases and psychological disorders were also associated with these genes, such as anxiety, Alzheimer's disease, and major depression (Finsterwald and Alberini, 2014).

Decreased anxiety-like behaviour has been observed in *Grin2a* homozygous KO mice (Ryan et al., 2013). The link between *Gria1* and anxiety is unclear, however, as homozygous KO mice have exhibited both increased (Fitzgerald et al., 2010) and decreased anxiety-like behaviours (Vekovischeva et al., 2004). Impairments in spatial learning were observed in homozygous KO *Grin2a* mice (Sakimura et al., 1995). Alzheimer's disease in humans has been associated with a downregulation of *Grin2a* mRNA and GRIN2A protein levels in the hippocampus, motor cortex and cingulate gyrus (Hynd et al., 2004) and upregulated *Gria2* mRNA in the PFC (Williams et al., 2009). Downregulated levels of *Gria1 and Grin2a* mRNA have been observed in the PFC and perirhinal cortex, respectively, in humans suffering with major depression (Beneyto and Meador-Woodruff, 2008).

A number of genes encoding for synapse-related proteins, such as *Syn1, Syn2, Synj1* and *Synpo* were also among genes enriched for biological processes such as synaptic transmission and LTP, and neurological diseases such as Alzheimer's disease. Exposure to chronically high GC levels led to significantly lower hippocampal levels of synaptopodin, the protein product of *Synpo* in the mouse brain (Cohen et al., 2011). Chronically stressed rats show decreased hippocampal expression of synapsin, the protein product of *Syn1* (Schmidt et al., 2015). As GCs strongly regulate LTP, it is possible that these synapse-related proteins may be genomic targets participating in this regulation. *Syn2* plays a critical role in maintaining a balance between synaptic excitation and inhibition, as homozygous KO of this gene results in an over-excitable phenotype, with increased spontaneous synaptic activity in the hippocampal CA1 region (Feliciano et al., 2013). Expression of synaptopodin, the protein encoded by *Synpo* was shown to be critical for hippocampal LTP in the developing mouse (Zhang et al., 2013) and *Synpo* KO mice demonstrated impaired LTP and spatial learning (Deller et al., 2003). In a mouse model of Alzheimer's disease, heterozygous KO of *Synj1* has been shown to decrease cognitive impairment (Zhu et al., 2013) and suppress the inhibitory effect of amyloid-β (Aβ), a peptide linked to cognitive defects in Alzheimer's disease, on hippocampal LTP (Berman et al., 2008). Chronic stress exposure has also been linked to increased expression of *Bace1*, which produces a protein involved in Aβ cleavage (Cordner and Tamashiro, 2016).

The potent brain neurotrophin, *Bdnf,* was also amongst the genes in the target datasets predicted to play a role in biological process such as synaptic transmission and learning and memory formation. *Bdnf* expression has been implicated in both short- and long-term memory (Suzuki et al., 2011), and pathways activated by BDNF are also regulated by GRs during memory consolidation (Finsterwald and

Alberini, 2014). Moreover, interactions between GR and EGR1 have been shown to critically regulate the expression of the *Bdnf* isoform *Bdnf4* (Chen et al., 2019). BDNF has also been shown to play a role in synaptic transmission (Pattwell et al., 2012) and dendritic development (Martin and Finsterwald, 2011). In the hippocampus, GRs were shown to mediate memory consolidation via neural plasticity pathways activated by BDNF (Chen et al., 2012). These findings suggest that MRs and GRs may regulate hippocampal memory formation via targeting *Bdnf,* and the signalling pathways regulated by BDNF.

An association was made by IPA between genes in the reference datasets and neurological disorders which have not (yet) been directly linked to GC hormone action, such as epilepsy and schizophrenia. Among the genes predicted to play a role in epilepsy were synaptic protein coding genes *Syn2* and *Synj1*, the neurotrophin *Bdnf* and glutamate receptor subunit gene *Gria2*. GC hormones are not widely implicated in the aetiology of epilepsy, however the observation that MRs and GRs target epilepsy-related genes suggests a potential link. Moreover, the frequent co-occurrence of depression, a disorder strongly associated with HPA axis activity, alongside epilepsy has initiated exploration of the role GCs may play in this disorder. In rat models of epilepsy, plasma CORT levels were elevated during the period between seizures (Mazarati et al., 2009) and in humans experiencing stress-sensitive seizures, levels of cortisol were shown to correlate positively with the incidence of epileptiform discharges (van Campen et al., 2016). Epilepsy in humans has been associated with increases in neocortical *Bdnf* mRNA (Beaumont et al., 2012) and genetic mutations in *Gria2* (Lesca et al., 2013), *Synj1* (Hardies et al., 2016) and *Syn2* (Lakhan et al., 2010).

A prediction was also made between schizophrenia and genes in our ChIP- and RNA-seq datasets by IPA, including *Bdnf, Grin2a, Syn2, Syn3* and most notably the *Disrupted-In-Schizophrenia 1 (Disc1)* gene. At present it is unclear whether a link between schizophrenia and HPA activity exists, however a number of observations support the possibility. In particular, changes in neuronal morphology (Brown et al., 2005, Cook and Wellman, 2004, Luczynski et al., 2015) and reductions in hippocampal volumes (Starkman et al., 1992) reported following exposure to elevated GC levels, following chronic stress exposure or in disorders such as Cushing's disease, have also been observed in schizophrenia (Nelson et al., 1998). Changes in the mRNA expression of *Bdnf* (Paz et al., 2006, Pillai, 2008, Wong et al., 2010) and *Grin2a* (Beneyto and Meador-Woodruff, 2008, Dracheva et al., 2001) have been reported in many brain regions of humans with schizophrenia, while downregulated *Syn2* mRNA expression in the PFC

(Hurko and Ryan, 2005) and hippocampal expression of the *Syn3* protein (Vawter et al., 2002) have been associated with schizophrenia in humans.

Interactions between the DISC1 scaffold protein and several proteins involved in dopaminergic signalling is thought to underlie the role of the *Disc1* gene in schizophrenia, as dopamine has been widely implicated in the aetiology of psychotic disorders (Dahoun et al., 2017). Mutations in the *Disc1* gene have been strongly associated with schizophrenia in humans (Ayala et al., 2007, Callicott et al., 2005, Hurko and Ryan, 2005) and the gene has been used as a biomarker in the diagnosis of schizophrenia (Pangalos et al., 2007). The neurodevelopmental hypothesis of schizophrenia proposes that a disruption of brain development during early life underlies the manifestation of the disorder in early adulthood (McGrath et al., 2003), and, interestingly, IPA predicted a relationship between *Disc1* and many other GC target genes with neurodevelopmental processes. In particular, *Disc1* was shown to play a central role in adult hippocampal neurogenesis (Duan et al., 2007), a process also strongly influenced by GC hormone action (Anacker et al., 2013).

In conclusion, the results of these pathway analyses by IPA has contributed to filling an enormous gap in our knowledge regarding the consequences of GC hormone genomic activity in the brain. This analysis has highlighted many promising MR and GR target genes for further exploration, including the KLFs, synaptic-related genes and neurotrophins such as *Bdnf.* Several neurological diseases and psychological disorders have also been highlighted by these analyses, which is in agreement with the importance of HPA axis regulation in the maintenance of brain health and mental well-being. Many genes, pathways and putative disease relationships were unknown until this point. It must be emphasised, however, that these links are purely predictive and require extensive validation in animal models and human studies.

Chapter 5 The genomic regulation of the Krüppel-like factors by MRs and GRs throughout the brain following acute stress or circadian influences

5.1 Abstract

Our genome-wide hippocampal ChIP- and RNA-sequencing experiments described in Chapter 3 identified a number of KLF family members as targets of GC hormone action. KLFs comprise a family of transcription factors that play a role in various neurobiological processes, such as neurogenesis, neuronal migration and neuronal differentiation. Following elevations in GC hormones increased binding of MRs and GRs to responsive elements within KLF genes was accompanied by elevated intronic RNA (inRNA) and exonic RNA (exRNA) expression. Transcription factor-binding motif analysis showed a high prevalence of KLF motifs within genomic loci bound by MRs and GRs, while pathway analysis predicted a number of KLF family members as upstream regulators of MR and GR target genes. These observations strongly indicate that KLFs may be important GC hormone target genes and potential coregulators of MR and GR genomic action in the hippocampus.

Previous studies showed that the hippocampus is a principal region of MR and GR co-expression in the brain and that MR expression is barely detectable in neocortical regions. Consequently, the majority of studies investigating the genomic actions of MRs and GRs have centred upon the hippocampus and neglected many other brain regions. GC hormones, however, have been shown to act upon brain regions such as the amygdala, PFC and neocortex and changes in gene expression have been observed in these regions following exposure to stress. In this chapter, studies are reported describing MR and GR binding to GREs within *Klf2, Klf9* and *Klf15* in the hippocampus, amygdala, PFC and neocortex under acute stress and circadian conditions. Changes in the expression of the respective hnRNAs and mRNAs are also examined under these conditions. These experiments validated results of our sequencing experiments while demonstrating increased MR and GR binding to GREs within the *Klfs* accompanied by changes in RNA expression throughout all brain regions following stress and circadian input. Our observations suggest that MRs may play a greater role in GC action in extra-hippocampal brain regions than previously thought. Overall, these observations have highlighted the KLFs as significant GC hormone targets following acute stress and the circadian rise.

5.2 Introduction

A number of KLF family members have been identified, by genome-wide hippocampal ChIP- and RNA-seq studies, as targets of MR and GR genomic activity during the acute stress response and the circadian rise. The KLFs comprise a family of transcription factors characterised by their zinc finger containing DNA-binding domain (Pearson et al., 2008) of which 11 genes can be found in the rat (Kaczynski et al., 2003). Family members are categorised into three distinct subgroups according to homology and transcriptional activity (McConnell and Yang, 2010) and are abundantly expressed in the brain where they have been shown to regulate processes such as neural development and repair in response to brain injury (Yin et al., 2015). Our MR and GR ChIP-seq studies (Chapter 3) detected MR- and GR-binding peaks in the promoter regions of *Krüppel-like factor 2 (Klf2), Krüppel-like factor 9 (Klf9)* and *Krüppel-like factor 15 (Klf15)*, with binding of both receptors significantly increasing following both acute stress and the circadian rise. Differential RNA expression of *Klf2, Klf9* and *Klf15* was also observed under these conditions. Furthermore, many other KLFs, including *Klf4, Klf7* and *Klf13* exhibited differential RNA expression following acute stress and the circadian rise, however in the absence of MR or GR binding within these genes. Transcription factor-binding motif analysis revealed that within the entire hippocampal genome, a high proportion of MR and GR bound loci contain KLF motifs. Moreover, pathway analysis by IPA (see Chapter 4) predicted a number of KLF genes as upstream regulators of genes present in the ChIP- and RNA-seq datasets and also predicted a relationship between *Klf9* and *Klf15* and biological functions such as neurodevelopment, synaptic plasticity, learning and cognition. These observations indicate that KLFs are important MR and GR target genes during the acute stress response and circadian rise, and that KLFs may act as coregulators of MR and GR genomic actions in the hippocampus.

The actions of MRs and GRs within the hippocampus have undergone extensive investigation; however, it is presently unknown whether they regulate gene expression in a similar manner throughout the brain. According to early radioligand binding studies, the hippocampus is the primary site of MR and GR co-expression. Moreover, MR expression was reported as very low within cortical regions and the (central) amygdala, while GR expression was shown throughout the brain (Reul and de Kloet, 1985, Reul and de Kloet, 1986). Following these initial findings, very few studies have examined the binding of MRs and GRs to DNA in regions such as the amygdala, PFC and neocortex, despite GC hormones exerting a number of effects on these brain regions. While the amygdala has been suggested to play a role in

potentiating the stress response (Shepard et al., 2003), the prefrontal cortex has been suggested to play a role in negative feedback of the HPA-axis (Diorio et al., 1993) and differential gene expression has been reported in both regions following exposure to acute (Sillivan et al., 2019) and chronic (Andrus et al., 2012, Calabrese et al., 2016, Nava et al., 2017) stress. The role of the neocortex in the stress response is poorly characterised, however immobilisation stress has been shown to elicit changes in gene expression in this brain region (Kurumaji et al., 2008, Park et al., 2009). Clearly, further studies are required to expand our knowledge of genomic GC hormone action beyond the hippocampus.

Therefore, the aims of the following experiments were to validate the findings of genome-wide hippocampal ChIP- and RNA-seq regarding the *Klfs* and to extend this investigation to other brain regions influenced by HPA-axis activation, such as the amygdala, prefrontal cortex and neocortex. The expression of the MR in neocortical brain regions was of interest, in view of early experiments reporting a localised expression of the receptor to hippocampal and amygdalar areas. Rats were killed following acute stress or under circadian peak or trough conditions and the binding of MRs and GRs and transcriptional responses were examined in the hippocampus, amygdala, prefrontal cortex and neocortex. Findings of hippocampal ChIP- and RNA-qPCR validated results of our hippocampal ChIP- and RNA- seq, while our observations of increased MR and GR binding to *Klf* GREs in the amygdala, PFC and neocortex following elevations in GCs indicated that co-expression of both receptors is not limited to the hippocampus. Changes in receptor binding were accompanied by increased expression of hnRNA and mRNA at various timepoints after FS or during the circadian rise in GC secretion. These findings indicate that MRs and GRs regulate the expression of KLF genes throughout the brain following elevations in GC hormones, and suggest that the KLF family of transcription factors may be of significance in the brain's response to stress.

5.3 Materials and Methods

5.3.1 Animals

A separate cohort of male Wistar rats (150-175g) were purchased from Envigo (Oxon, UK) and group housed (two to three animals per cage). Animals were kept under standard light (lights on 5:00–19:00; 80–100 Lux) and environmentally controlled conditions (temperature 21 ± 1 °C; relative humidity 40–60%) with food and water available *ad libitum*. Until the day of the experiment all rats were handled (2 min per rat per day; min. 5 days) to reduce any nonspecific stress effects. A separate cohort of rats were used for sequencing and validation studies.

5.3.2 Animal Experiments

Baseline rats were killed straight from their home-cages between either 7-9am (circadian trough, baseline AM (BLAM)) or 5-7pm (circadian peak, baseline PM (BLPM)). Alternatively, rats were killed 30 min (FS30), 60 min (FS60) or 120 min (FS120) after the start of a FS challenge (15 min at 25 ± 1 °C).

5.3.3 Measurement of corticosterone by Radioimmunoassay (RIA)

Plasma CORT concentrations were measured using a commercial CORT RIA Kit (MP Biomedicals) as described previously in Chapter 2.

5.3.4 ChIP-seq and RNA-seq

Data from ChIP-seq and RNA-seq experiments described in Chapter 3 are presented in this Chapter. Experimental methods and statistical analysis pertaining to these data are found in Chapter 2.

5.3.5 ChIP-qPCR

Standard ChIP was performed as described in Chapter 2. The following antibodies were used: MR (MR ab64457; Abcam, Cambridge, UK) or GR (GR 24050-1-AP antibody; Proteintech, Manchester, UK). All samples (bounds and inputs) were diluted to a standardized concentration with nuclease-free water for analysis by qPCR using primers/probes listed in Table 2.6. Data (i.e. enrichment) are expressed as quantity of bound DNA divided by the respective quantity of input DNA (i.e., B/I), which is a measure of the enrichment of steroid receptor bound to specific genomic sequences.

5.3.6 RNA-qPCR

RNA was extracted and RNA-qPCR was performed as described in Chapter 2 using primers and probes listed in Table 2.7 (hnRNA) and Table 2.8 (mRNA). Expression of hnRNA and mRNA in each sample was calculated based on the Pfaffl method of relative quantification (Pfaffl, 2001) and standardized to the expression of house- keeping genes listed in Table 2.9.

5.3.7 Statistical Analysis

ChIP-qPCR and RNA-qPCR data were statistically analysed using GraphPad Prism software 7.04. Results are presented as group means ± SEM; sample sizes are indicated in the figures. Multiple statistical comparisons were conducted with one-way ANOVA or Kruskal-Wallis, and if significant, a Dunnett's or Dunn's post hoc test was performed. Statistical results are provided in the figures. $P<0.05$ was considered statistically significant.

5.4 Results

5.4.1 Acute stress and the circadian rise evoke enhanced MR and GR to KLF GRE binding and RNA transcription, as revealed by ChIP- and RNA-seq

To determine the binding of MRs and GRs to GREs within *Klfs*, rats were killed under early morning baseline conditions (BLAM), 30 min (FS30) after the start of an acute 15 min FS challenge or under late afternoon baseline conditions (BLPM). Previous work of our group had shown that MR and GR binding at GREs is maximal at 30 min post-stress (Mifsud and Reul, 2016).

As described in Chapter 3, MR and GR ChIP-seq on hippocampal tissue was followed by Peak calling (PeakAnalyser) and differential binding (DiffBind) analysis (see Chapters 2 and 3). Significant MR and GR binding peaks were identified within *Klf2, Klf9* and *Klf15* at FS30 and BLPM (Figure 5.1). Following acute stress, the enrichment of MR and GR was increased at GREs within *Klf2*, *Klf9, Klf15* GRE1 and *Klf15* GRE2 in the hippocampus (Figure 5.2). Under late afternoon baseline conditions, MR enrichment was elevated at GREs within *Klf2, Klf9* and *Klf15* GRE2, while GR binding was increased at GREs within *Klf2, Klf9, Klf15* GRE1 and *Klf15* GRE2.

To assess changes in hippocampal RNA expression of *Klf* genes under stress and circadian conditions, rats were killed under BLAM conditions, 30 min (FS30), 60 min (FS60), 120 min (FS120), 180 min (FS180) or 360 min (FS360) after the start of an acute 15 min FS challenge or under BLPM conditions. RNA-seq on hippocampal tissue was followed by differential expression (EdgeR) analysis. Following FS stress, a time-dependent increase in the transcription of *Klf2*, *Klf4*, *Klf9* and *Klf15* was observed in the hippocampus (Figure 5.3). At FS30, increased inRNA levels of *Klf2*, *Klf4, Klf9* and *Klf15* were observed. *Klf9* inRNA remained elevated at FS60, rising again at FS180 and FS360, while *Klf15* inRNA was increased at all timepoints following FS.

exRNA transcripts of *Klf2* and *Klf4* rose at FS30, remaining elevated at FS60. At FS360, inRNA levels of *Klf4* decreased. *Klf9* exRNA levels rose at FS60 and remained higher throughout the remainder of the timecourse. *Klf15* exRNA levels were elevated at all timepoints following FS. Under BLPM conditions, *Klf2* exRNA, *Klf9* inRNA and exRNA and *Klf15* inRNA and exRNA were increased.

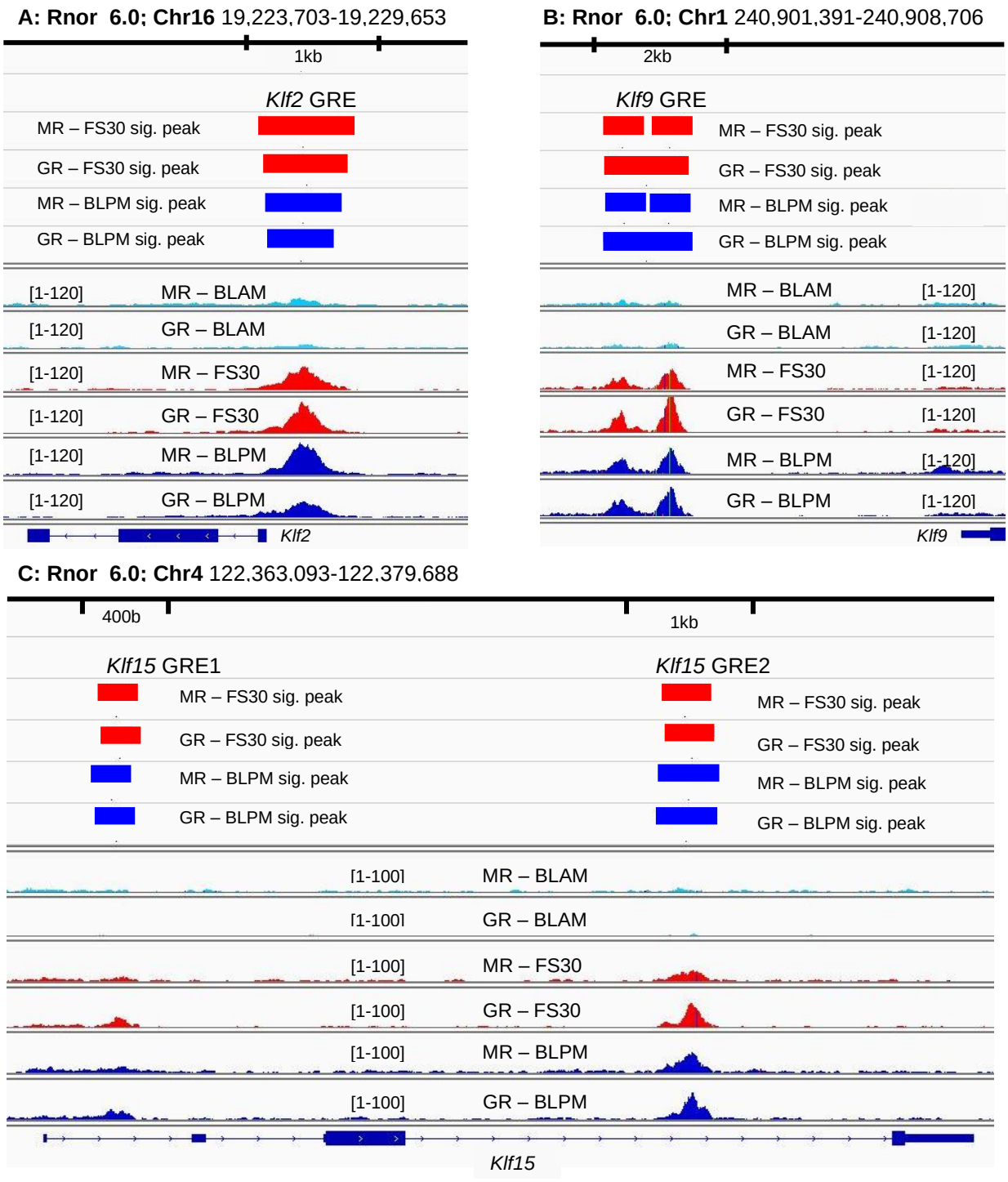

Figure 5.1 MR and GR peaks within *Klf2, Klf9* and *Klf15* under baseline and stress conditions
Rats were killed under early morning (BLAM) or late afternoon (BLPM) baseline conditions or 30 min (FS30) after the start of FS (15 min, 25 ºC water). Peak calling identified genomic loci bound by MRs and GRs. IG Viewer images show MR and GR peaks within *Klf2* (A), *Klf9* (B) and *Klf15* (C) at BLAM, FS30 and BLPM. Significant peaks (i.e. above input level) are indicated by the presence of a horizontal red (FS30) or blue (BLPM) bar. Note that there are no significant peaks within these genes under BLAM conditions. Numbers between square brackets indicate the y-axis range. Rnor_6.0, Rattus norvegicus genome version 6.0. These images represent data from experiments carried out in Chapter 3.

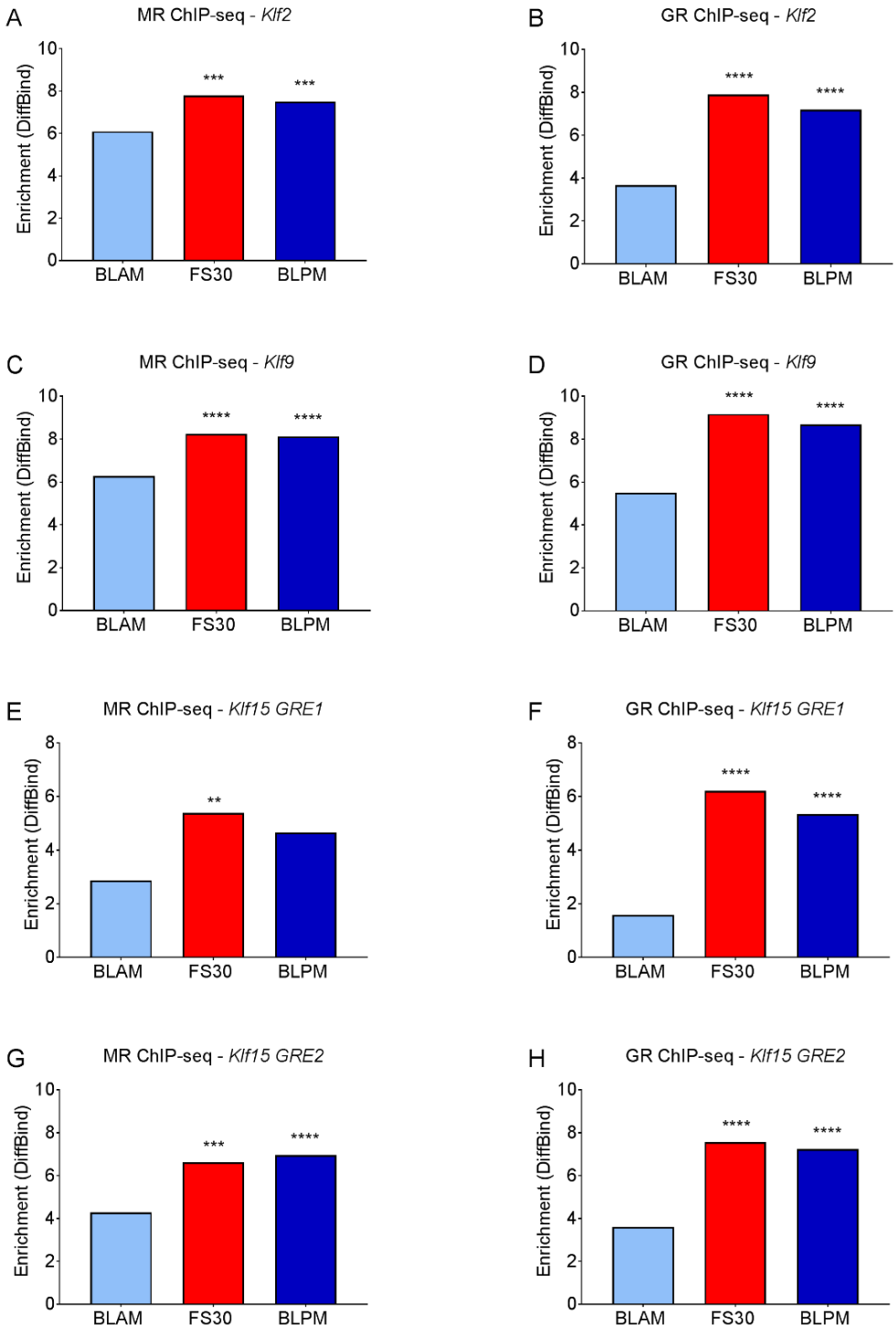

Figure 5.2 Hippocampal MR and GR ChIP-seq shows binding of MRs and GRs at GREs within *Klf2, Klf9* and *Klf15* under baseline and stressed conditions

Rats were killed under early morning (BLAM) or late afternoon (BLPM) baseline conditions or 30 min (FS30) after the start of FS (15 min, 25 ºC water). Graphs show enrichment of MR and GR at GREs within *Klf2* (A and B), *Klf9* (C and D) and *Klf15* GRE1 (E – H) was calculated by Differential binding (DiffBind) analysis. ** $P<0.01$, *** $P<0.001$, **** $P<0.0001$ significantly different from BLAM.

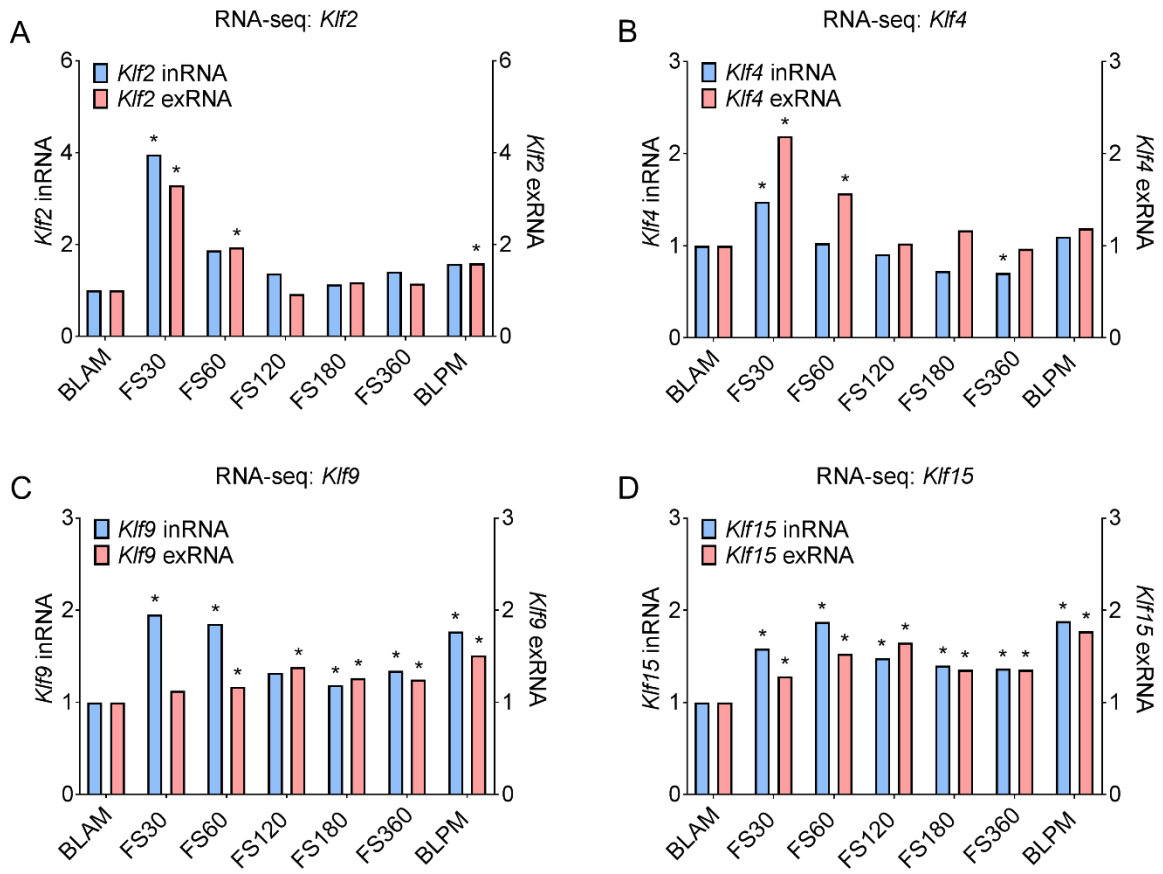

Figure 5.3 Hippocampal inRNA and exRNA transcript counts of KLFs under baseline conditions and following stress

Rats were killed under early morning (BLAM) or late afternoon (BLPM) baseline conditions, or 30 min (FS30), 60 min (FS60), 120 min (FS120), 180 min (FS180) or 360 min (FS360) after the start of FS (15 min, 25 ºC water. Graphs show inRNA (blue bars) and exRNA (red bars) counts of *Klf2* (A), *Klf4* (B) *Klf9* (C) and *Klf15* (D). Data are shown as percentage of transcripts per million at BLAM. Differential expression analysis, corrected for multiple comparisons with Benjamini-Hochberg procedure, * $P<0.05$, significantly different from BLAM.

5.4.2 Validation of hippocampal ChIP- and RNA-seq findings regarding KLF-genes in a separate cohort of rats with hippocampal ChIP- and RNA-qPCR

To validate findings of the ChIP- and RNA-seq experiments described in Chapter 3, a separate cohort of rats were killed under BLAM conditions, at FS30, FS60, FS120 or under BLPM conditions. Plasma CORT levels were examined to determine the similarity of the plasma CORT profile between the validation cohort and the sequencing cohort used in experiments described in Chapter 3. The plasma CORT profile of the validation cohorts (Figure 5.4) was very similar to that of the sequencing cohort, with plasma CORT levels elevated at FS30 and under BLPM conditions.

The binding of hippocampal MRs and GRs to GREs within *Klf* genes was subsequently examined in the validation cohort of rats under BLAM, FS30 and BLPM conditions. Results of ChIP-qPCR closely mirrored that of ChIP-seq. Following FS and under BLPM conditions, MR and GR enrichment increased at GREs within *Klf2*, *Klf9*, *Klf15* GRE1 and *Klf15* GRE2 (Figure 5.5).

Hippocampal transcriptional responses of *Klf* genes were examined under BLAM conditions, at FS30, FS60, FS120 or under BLPM conditions. Similar to results shown by RNA-seq, FS resulted in hippocampal transcriptional activation of *Klf2, Klf4*, *Klf9* and *Klf15* (Figure 5.6). *Klf2* hnRNA levels were elevated at FS30, while mRNA levels increased at FS30 and FS60. *Klf4* hnRNA levels did not change, while mRNA levels rose at FS30 and FS60. *Klf9* hnRNA levels were elevated at FS30 and at FS60, while mRNA levels rose at FS60 and FS120. *Klf15* hnRNA levels were increased at FS30, FS60 and FS120, while mRNA levels were elevated at FS120. Under late baseline conditions, hnRNA and mRNA levels of *Klf9* and *Klf15* were higher compared with early baseline conditions.

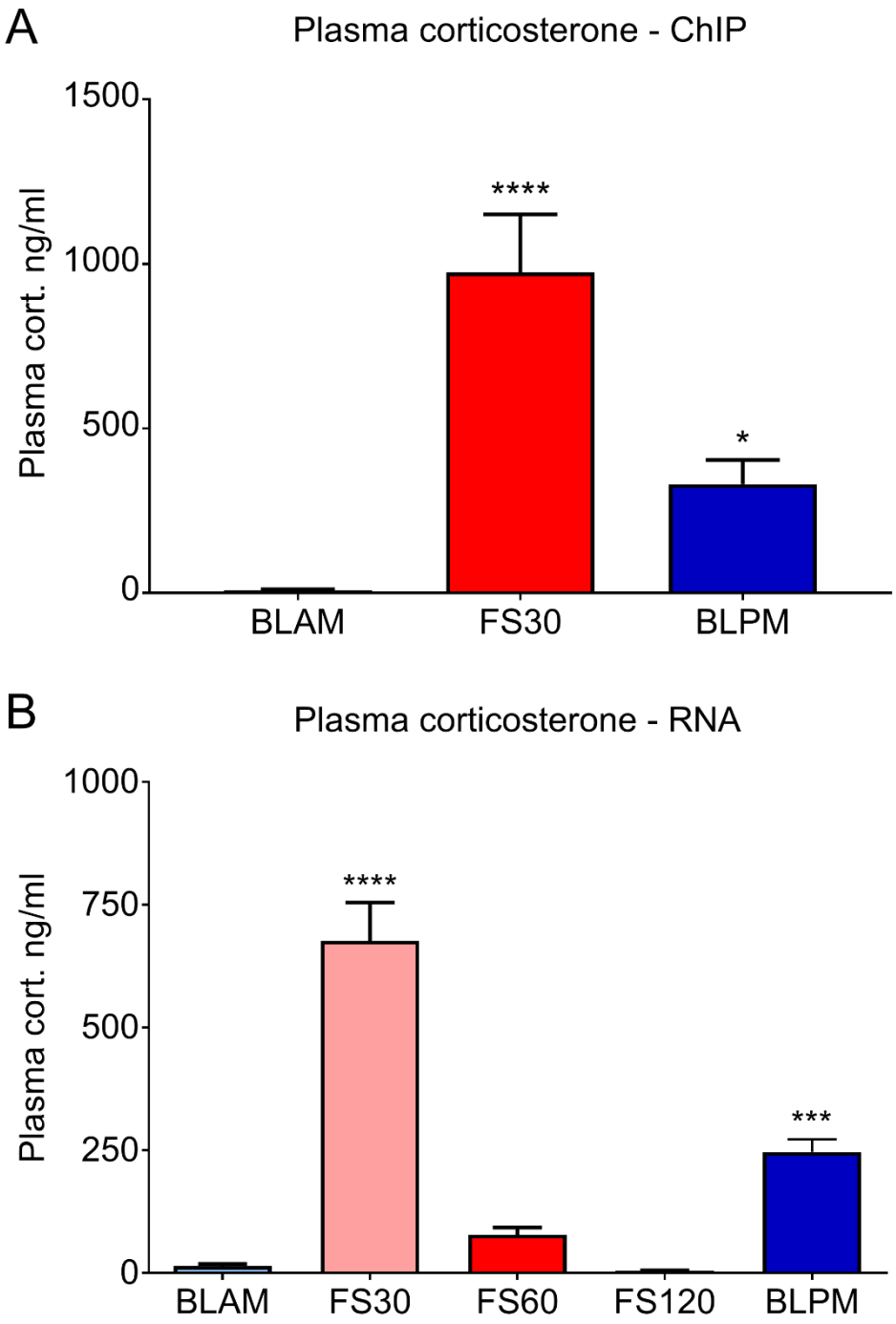

Figure 5.4 Plasma corticosterone levels under baseline and stressed conditions

Rats were killed under early morning (BLAM) or late afternoon (BLPM) baseline conditions or 30 min (FS30), 60 min (FS60) or 120 min (FS120) after the start of FS (15 min, 25ºC water). Plasma CORT levels for ChIP (A) and RNA (B) are expressed as ng/ml (mean ± SEM, n=8 per group). Average CORT concentration at BLAM for ChIP animals, 8.86 ng/ml (A) and for RNA animals, 10.32 ng/ml (B). Statistical analysis: one-way ANOVA, (A) $F_{(2,\ 21)}$=19.87, p<0.0001, (B) $F_{(2,\ 37)}$=51.12, p<0.0001, Dunnett's post hoc test, *P<0.05, ***P<0.001, ****P<0.0001 significantly different from BLAM. Inter-assay coefficient of variation; 2.68%, intra-assay coefficient of variation for (A) 5.3%, (B) 7.4%.

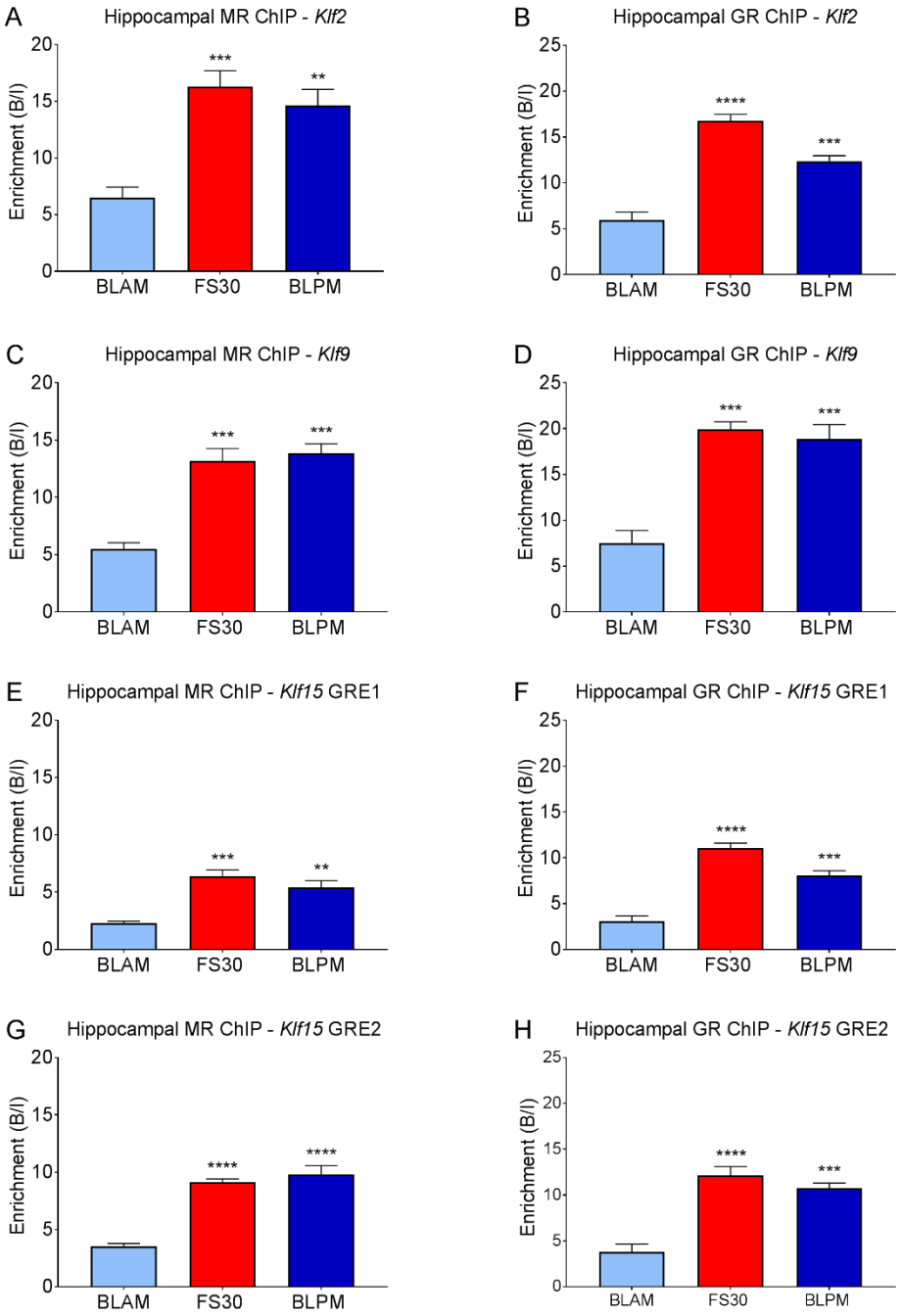

Figure 5.5 Hippocampal MR and GR binding at GREs within *Klf2 Klf9* and *Klf15* under baseline and stressed conditions

Rats were killed under early morning (BLAM) or late afternoon (BLPM) baseline conditions or 30 min (FS30) after the start of FS (15 min, 25 ºC water). Graphs show enrichment of MR and GR, expressed as bound/input (mean ± SEM, n = 4 per group), at GREs within *Klf2* (A and B), *Klf9* (C and D), *Klf15* (E-H) as determined by MR and GR ChIP-qPCR. Statistical analysis; One-way ANOVA (A) $F_{(2, 9)}$=17.14, p=0.0009, (B) $F_{(2, 9)}$=55.18, p<0.0001, (C) $F_{(2, 9)}$=30.22, p<0.001, (D) $F_{(2, 9)}$=28.05, p<0.001, (E) $F_{(2, 9)}$=19.62, p=0.0005, (F) $F_{(2, 9)}$=52.65, p<0.0001, (G) $F_{(2, 9)}$=50.43, p<0.0001, (H) $F_{(2, 9)}$=31.39, p<0.0001. Dunnett's post hoc test, ***P*<0.01, ****P*<0.001, *****P*<0.0001 significantly different from BLAM.

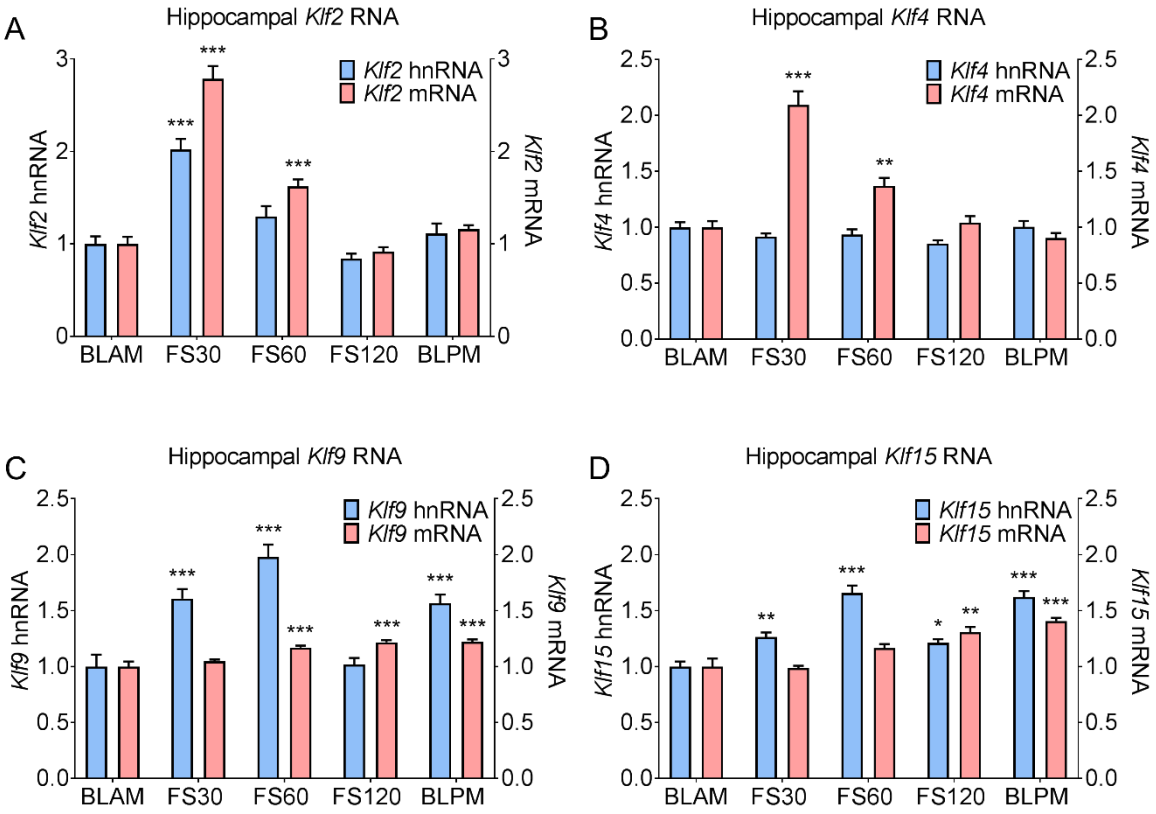

Figure 5.6 Hippocampal hnRNA and mRNA of KLF genes under baseline conditions and following stress

Rats were killed under early morning (BLAM) or late afternoon (BLPM) baseline conditions or 30 min (FS30), 60 min (FS60) or 120 min (FS120) min after the start of FS (15 min, 25 ºC water). Graphs show hnRNA (blue bars) and mRNA (red bars) levels of *Klf2* (A), *Klf4* (B) *Klf9* (C) and *Klf15* (D). Data are shown as relative RNA copy number calculated using the Pfaffl method of analysis, standardised to the expression of the house keeping genes *Hprt1* and *Ywhaz* (mean ± SEM, n = 8-9 per group). Statistical analysis: one-way ANOVA; (A) *Klf2* hnRNA $F_{(4,\ 39)}$=21.91, p<0.0001, *Klf2* mRNA $F_{(4,\ 39)}$=81.88, p<0.0001, (B) *Klf4* hnRNA $F_{(4,\ 39)}$=2.178, p=0.0895, *Klf4* mRNA $F_{(4,\ 39)}$=41.14, p<0.0001, (C) *Klf9* hnRNA $F_{(4,\ 39)}$=21.38, p <0.0001, *Klf9* mRNA $F_{(4,\ 39)}$=16.7, p<0.0001, (D) *Klf15* hnRNA $F_{(4,\ 39)}$=31.41, p<0.0001. Dunnett's post hoc test, **P*<0.05, ***P*<0.01, ****P*< 0.001, compared with BLAM group. Kruskal-Wallis; (D) *Klf15* mRNA χ^2 (4) = 27.72, p<0.0001. Dunn's post hoc test, ***P*<0.01, ****P*<0.001 significantly different from BLAM.

5.4.3 Brain-region investigation into MR and GR binding at GREs within KLFs and associated transcriptional responses following acute stress and during the circadian rise

The binding of MRs and GRs within *Klf* genes and the associated transcriptional responses of these genes was subsequently investigated in the amygdala, PFC and neocortex under identical experimental conditions (BLAM, FS30 and BLPM).

Following FS and under BLPM conditions, MR and GR enrichment was increased in the amygdala (Figure 5.7) and PFC (Figure 5.8) at GREs within *Klf2*, *Klf9*, *Klf15* GRE1 and *Klf15* GRE2. Within the neocortex (Figure 5.9), MR and enrichment was elevated at GREs within *Klf2*, *Klf9* and *Klf15* GRE2, while GR enrichment was also increased *Klf15* GRE2 (Figure 5.9.h). Under BLPM conditions, MR enrichment was higher at GREs within *Klf2* (Figure 5.9.a).

FS led to the transactivation of *Klf2, Klf4* and *Klf15* in the amygdala (Figure 5.10), PFC (Figure 5.11) and neocortex (Figure 5.12). *Klf2* hnRNA and mRNA levels were increased at FS30 in the amygdala (Figure 5.10.a), while mRNA was remained higher at FS60. In the PFC (Figure 5.11.a) and neocortex (Figure 5.12.a), *Klf2* hnRNA and mRNA rose at FS30 and remained elevated at FS60. hnRNA levels of *Klf4* did not significantly change within the amygdala (Figure 5.10.b) or neocortex (Figure 5.12.b), however within the PFC (Figure 5.11.b), *Klf4* hnRNA rose at FS30. *Klf4* mRNA levels were significantly increased at FS30 and FS60 within the amygdala (Figure 5.10.b), PFC (Figure 5.11.b) and neocortex (Figure 5.12.b). *Klf9* hnRNA were higher at FS30 and FS60 in the amygdala (Figure 5.10.c), PFC (Figure 5.11.c) and neocortex (Figure 5.12.c). mRNA of *Klf9* was increased at FS30-120 in the amygdala (Figure 5.10.c), while mRNA levels were higher at FS60 and FS120 in the PFC (Figure 5.11.c) and neocortex (Figure 5.12.c). Levels of *Klf15* hnRNA were elevated at FS30-FS120 in the amygdala (Figure 5.10.d) and increased at FS30 and FS60 in the neocortex (Figure 5.11.d) and PFC (Figure 5.12.d). *Klf15* mRNA was increased at FS120 in the amygdala (Figure 5.10.d) and PFC (Figure 5.11.d), however in the neocortex (Figure 5.12.d) no change in *Klf15* mRNA was detected at any timepoint.

BLPM conditions led to a rise in amygdala hnRNA and mRNA levels of *Klf9* and *Klf15* (Figure 5.10). Under late baseline conditions in the PFC (Figure 5.11), hnRNA and mRNA levels of all *Klfs* were increased. In the neocortex, *Klf2* mRNA levels, and hnRNA and mRNA levels of *Klf9* and *Klf15* were elevated at BLPM (Figure 5.12).

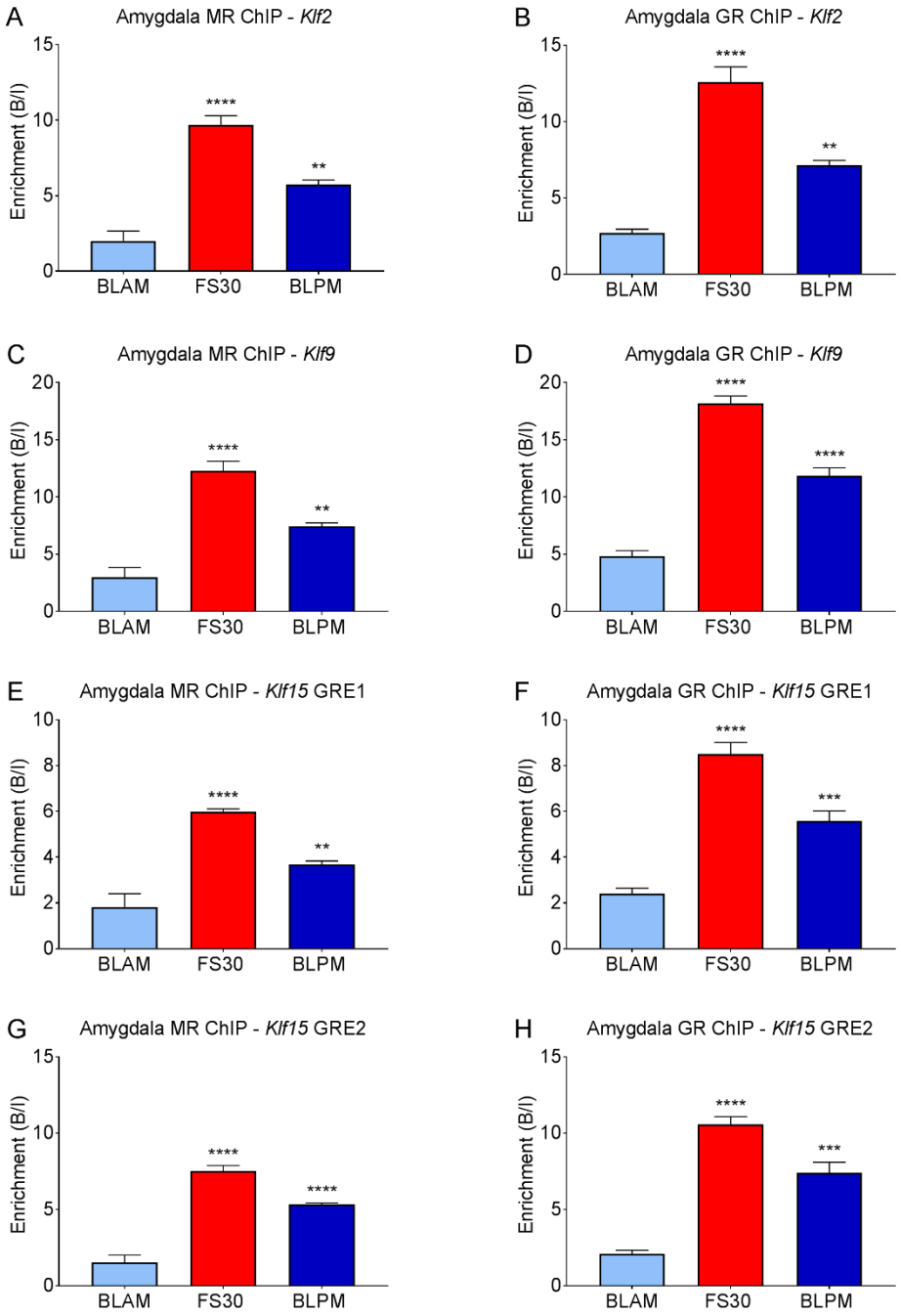

Figure 5.7 Amygdala MR and GR binding at GREs within *Klf2, Klf9* and *Klf15* under baseline and stressed conditions

Rats were killed under early morning (BLAM) or late afternoon (BLPM) baseline conditions or 30 min (FS30) after the start of FS (15 min, 25 ºC water). Graphs show enrichment of MR and GR, expressed as bound/input (mean ± SEM, n = 4 per group), at GREs within *Klf2* (A and B), *Klf9* (C and D), *Klf15* (E-H) as determined by MR and GR ChIP-qPCR. Statistical analysis; One-way ANOVA (A) $F_{(2, 9)}$=51.49, p<0.0001, (B) $F_{(2, 9)}$=63.46, p<0.0001, (C) $F_{(2, 9)}$=42.92, p<0.0001, (D) $F_{(2, 9)}$=114, p<0.0001, (E) $F_{(2, 9)}$=34.73, p<0.0001, (F) $F_{(2, 9)}$=56.24, p<0.0001, (G) $F_{(2, 9)}$ =72.83, p<0.0001, (H) $F_{(2, 9)}$=68.58, p<0.0001. Dunnett's post hoc test, ** P<0.01, *** P<0.001, **** P<0.0001 significantly different from BLAM.

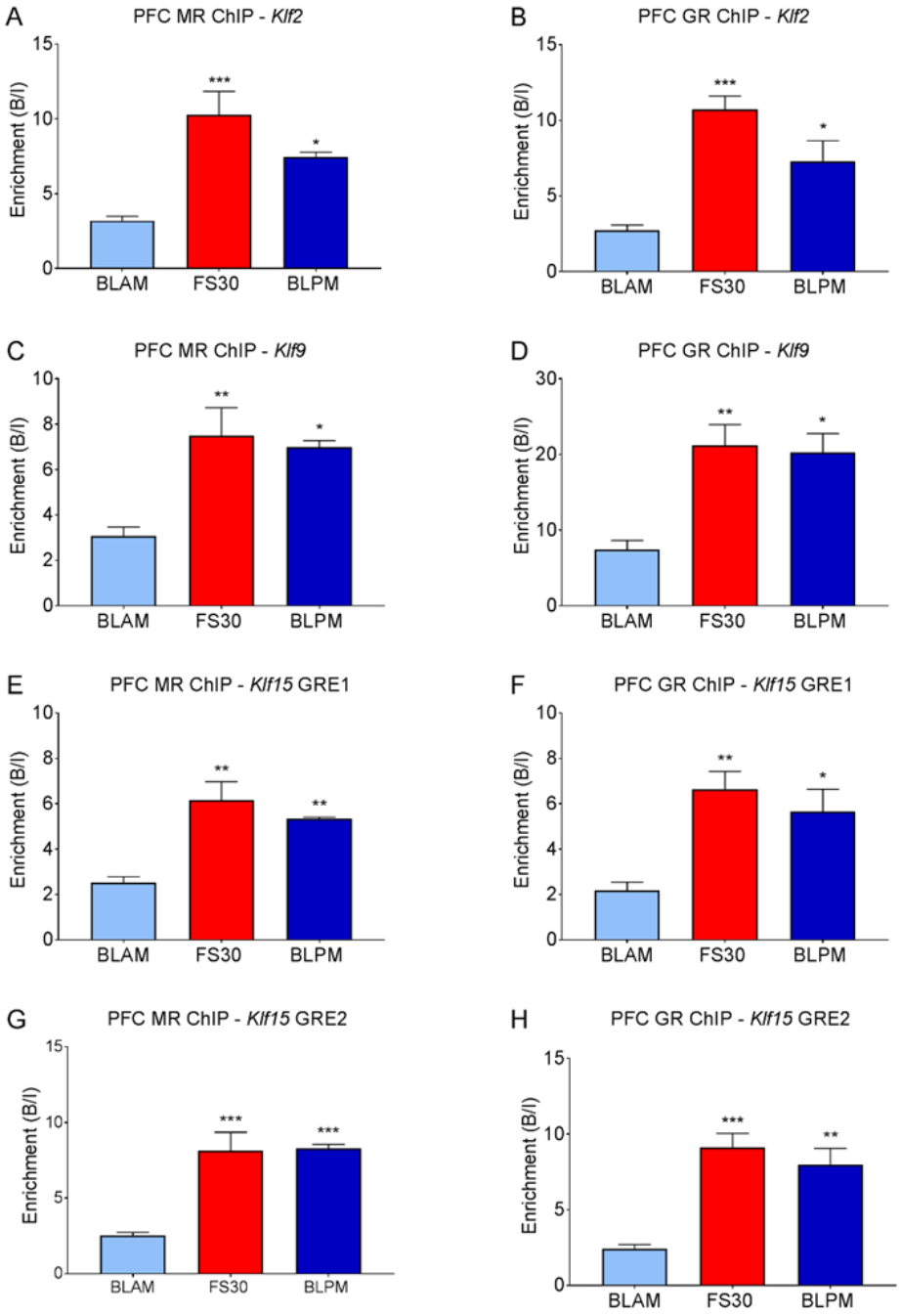

Figure 5.8 PFC MR and GR binding at GREs within *Klf2, Klf9* and *Klf15* under baseline and stressed conditions

Rats were killed under early morning (BLAM) or late afternoon (BLPM) baseline conditions or 30 min (FS30) after the start of FS (15 min, 25 ºC water). Graphs show enrichment of MR and GR, expressed as bound/input (mean ± SEM, n = 4 per group), at GREs within *Klf2* (A and B), *Klf9* (C and D), *Klf15* (E-H) as determined by MR and GR ChIP-qPCR. Statistical analysis; One-way ANOVA (A) $F_{(2, 9)}$=14.63, *p*=0.0015, (B) $F_{(2, 9)}$=17.82, *p*=0.0007, (C) $F_{(2, 9)}$=9.935, *p*=0.0053, (D) $F_{(2, 9)}$=11.84, *p*=0.0030, (E) $F_{(2, 9)}$=14.57, *p*=0.0015, (F) $F_{(2, 9)}$=9.89, *p*=0.00531, (G) $F_{(2, 9)}$=20.33, *p*=0.0005, (H) $F_{(2, 9)}$=18.46, *p*=0.0007. Dunnett's post hoc test, **P*<0.05 ***P*<0.01, ****P*<0.001 significantly different from BLAM.

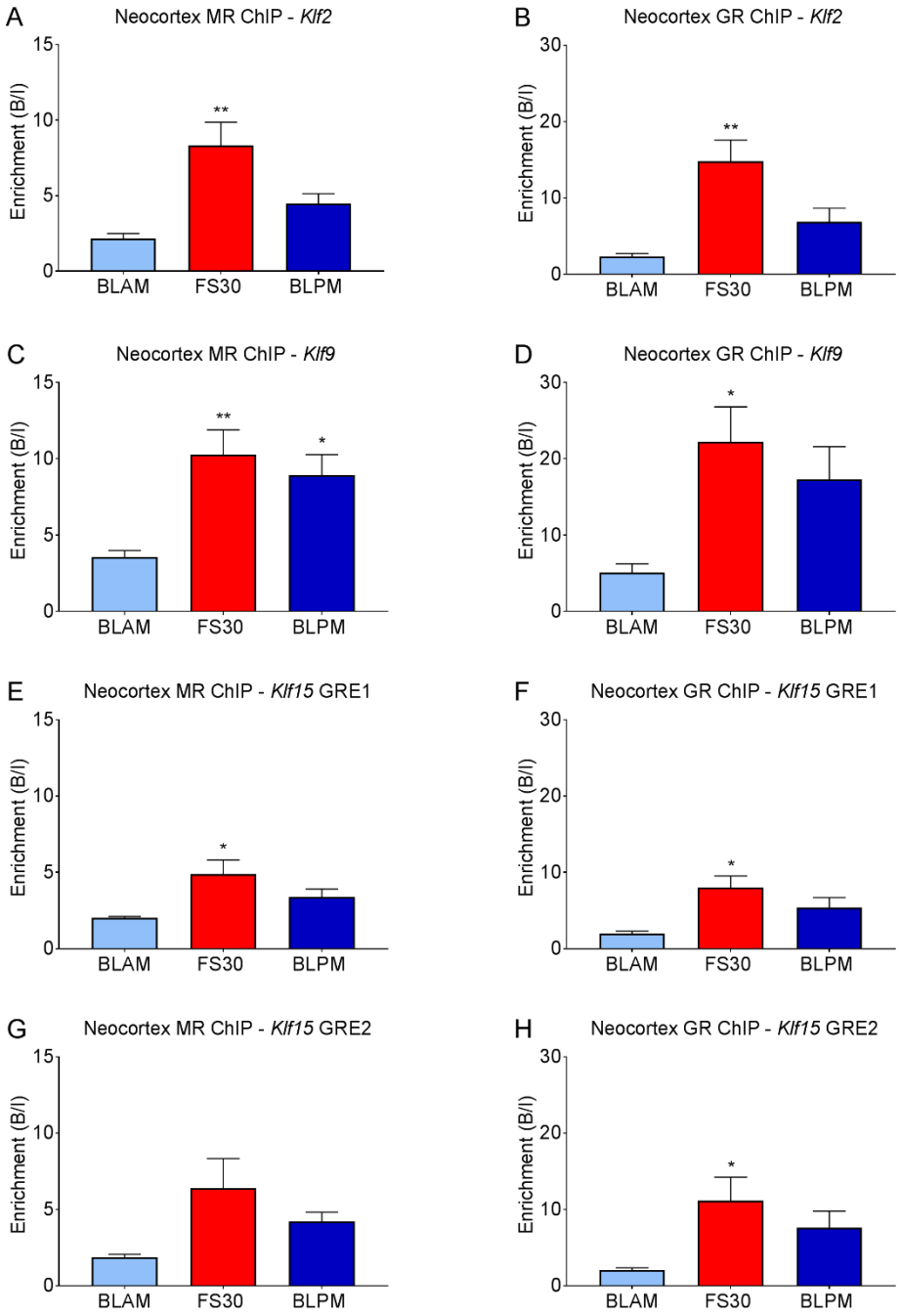

Figure 5.9 Neocortex MR and GR binding at GREs within *Klf2, Klf9* and *Klf15* under baseline and stressed conditions

Rats were killed under early morning (BLAM) or late afternoon (BLPM) baseline conditions or 30 min (FS30) after the start of FS (15 min, 25 ºC water). Graphs show enrichment of MR and GR, expressed as bound/input (mean ± SEM, n = 4 per group), at GREs within Klf2 (A and B), Klf9 (C and D), Klf15 (E-H) as determined by MR and GR ChIP-qPCR. Statistical analysis; One-way ANOVA (A) $F_{(2, 9)}$=10.07, p=0.0051, (B) $F_{(2, 9)}$=10.49, p=0.0045, (C) $F_{(2, 9)}$=7.987, p=0.0101, (D) $F_{(2, 9)}$=5.788, p=0.0242. (E) $F_{(2, 9)}$=5.267, p=0.0306, (F) $F_{(2, 9)}$=6.535, p=0.0177, (G) $F_{(2, 9)}$=3.71, p=0.066, (H) $F_{(2, 9)}$=4.49, p<0.0444. Dunnett's post hoc test, *P<0.05, **P<0.01 significantly different from BLAM.

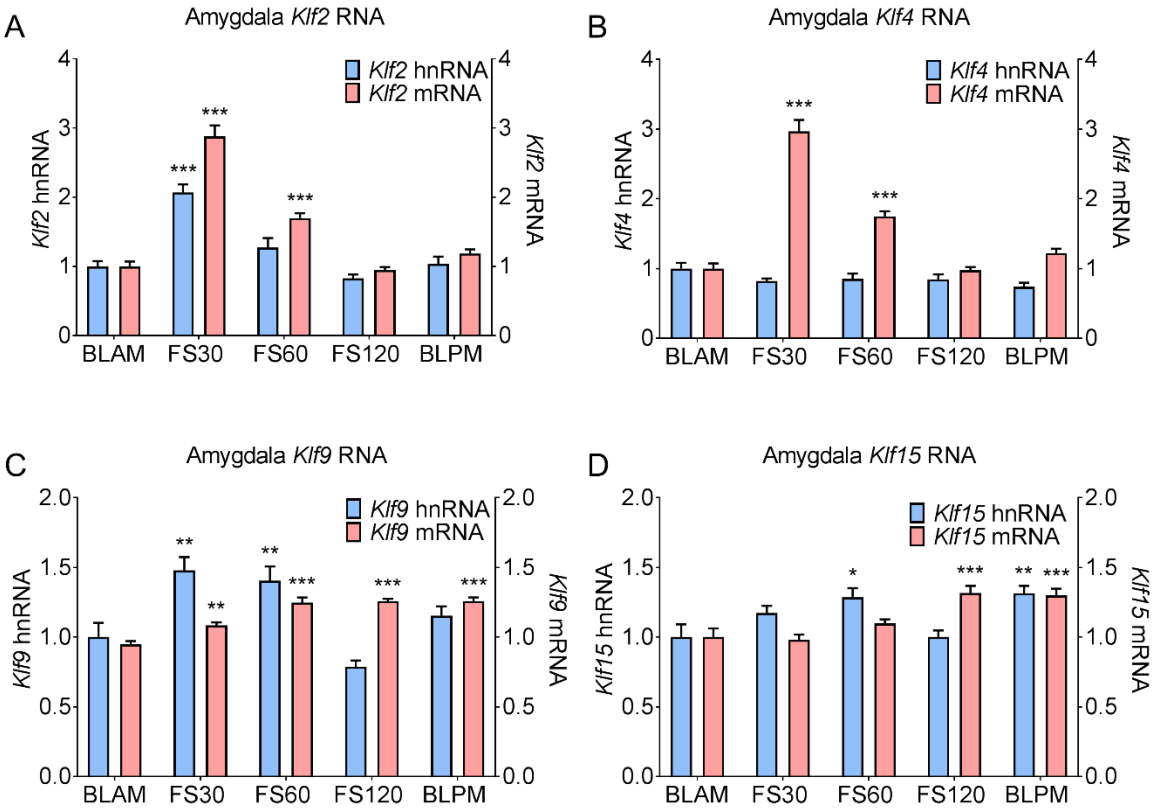

Figure 5.10 Amygdala hnRNA and mRNA of KLFs under baseline conditions and following stress

Rats were killed under early morning (BLAM) or late afternoon (BLPM) baseline conditions or 30 min (FS30), 60 min (FS60) or 120 min (FS120) min after the start of FS (15 min, 25 ºC water). Graphs show hnRNA (blue bars) and mRNA (red bars) levels of *Klf2* (A), *Klf4* (B) *Klf9* (C) and *Klf15* (D). Data are shown as relative RNA copy number calculated using the Pfaffl method of analysis, standardised to the expression of the house keeping genes *Hprt1* and *Gapdh* (mean ± SEM, n = 8-9 per group). Statistical analysis: one-way ANOVA; (A) *Klf2* hnRNA $F_{(4, 40)}$=23.36, p<0.0001, *Klf2* mRNA $F_{(4, 40)}$=79.11, p<0.0001, (B) *Klf4* hnRNA $F_{(4, 40)}$=2.04, p=0.35, *Klf4* mRNA $F_{(4, 40)}$=78.69, p<0.0001, (C) *Klf9* hnRNA $F_{(4, 40)}$=11.07, p<0.0001, *Klf9* mRNA $F_{(4, 40)}$=26.97, p<0.0001, (D) *Klf15* hnRNA $F_{(4, 40)}$=5.493, p=0.00131, *Klf15* mRNA $F_{(4, 39)}$=11.32, p<0.0001. Dunnett's post hoc test, *P<0.05, **P<0.01, *** P<0.001 significantly different from BLAM.

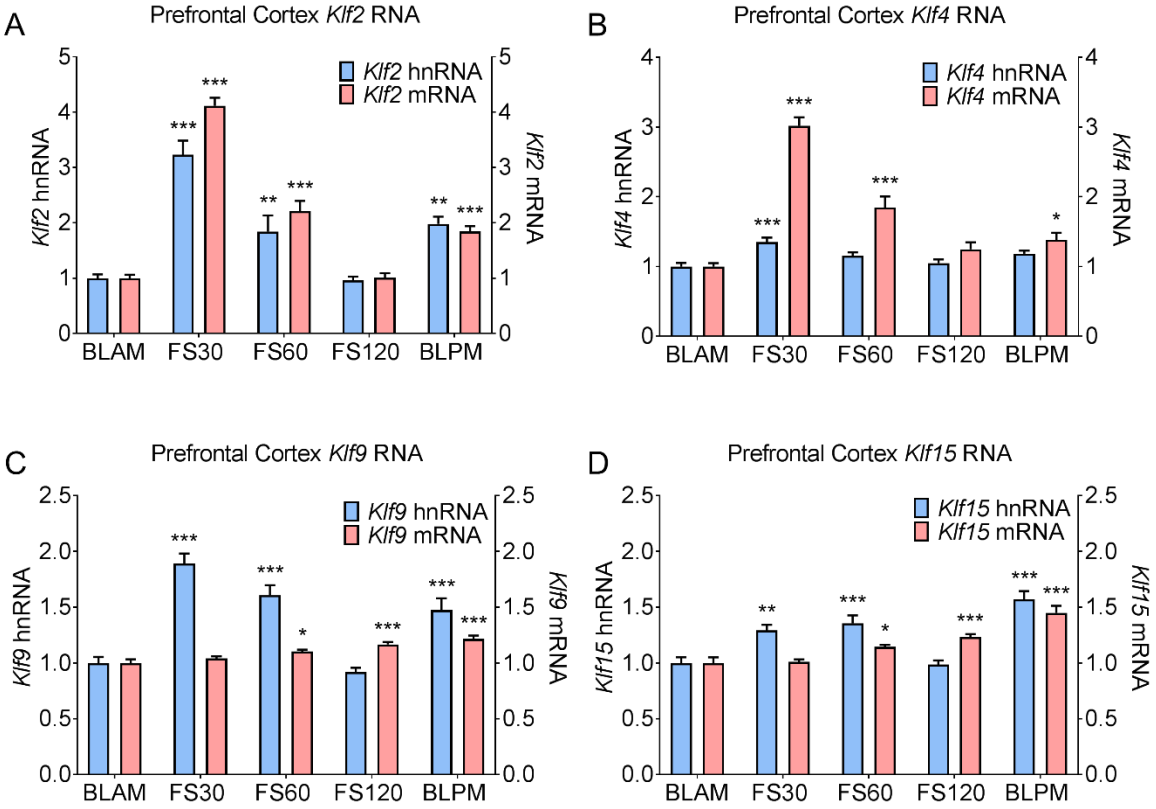

Figure 5.11 PFC hnRNA and mRNA of KLFs under baseline conditions and following stress

Rats were killed under early morning (BLAM) or late afternoon (BLPM) baseline conditions or 30 min (FS30), 60 min (FS60) or 120 min (FS120) min after the start of FS (15 min, 25 ºC water). Graphs show hnRNA (blue bars) and mRNA (red bars) levels of *Klf2* (A), *Klf4* (B) *Klf9* (C) and *Klf15* (D). Data are shown as relative RNA copy number calculated using the Pfaffl method of analysis, standardised to the expression of the house keeping genes *Hprt1* and *Ywhaz* (mean ± SEM, n = 8-9 per group). Statistical analysis: one-way ANOVA; (A) *Klf2* hnRNA $F_{(4,\ 40)}$=24.53, p<0.0001, *Klf2* mRNA $F_{(4,\ 40)}$=113.1, p<0.0001, (B) *Klf4* hnRNA $F_{(4,\ 40)}$=6.373, p<0.001, *Klf4* mRNA $F_{(4,\ 40)}$=62.04, p<0.0001, (C) *Klf9* hnRNA $F_{(4,\ 40)}$=27.81, p<0.0001, *Klf9* mRNA $F_{(4,\ 40)}$=12.88, p<0.0001, (D) *Klf15* hnRNA $F_{(4,\ 40)}$=18.54, p<0.0001, *Klf15* mRNA $F_{(4,\ 40)}$=22.03, p<0.0001. Dunnett's post hoc test, *P<0.05, **P<0.01, ***P<0.001 significantly different from BLAM.

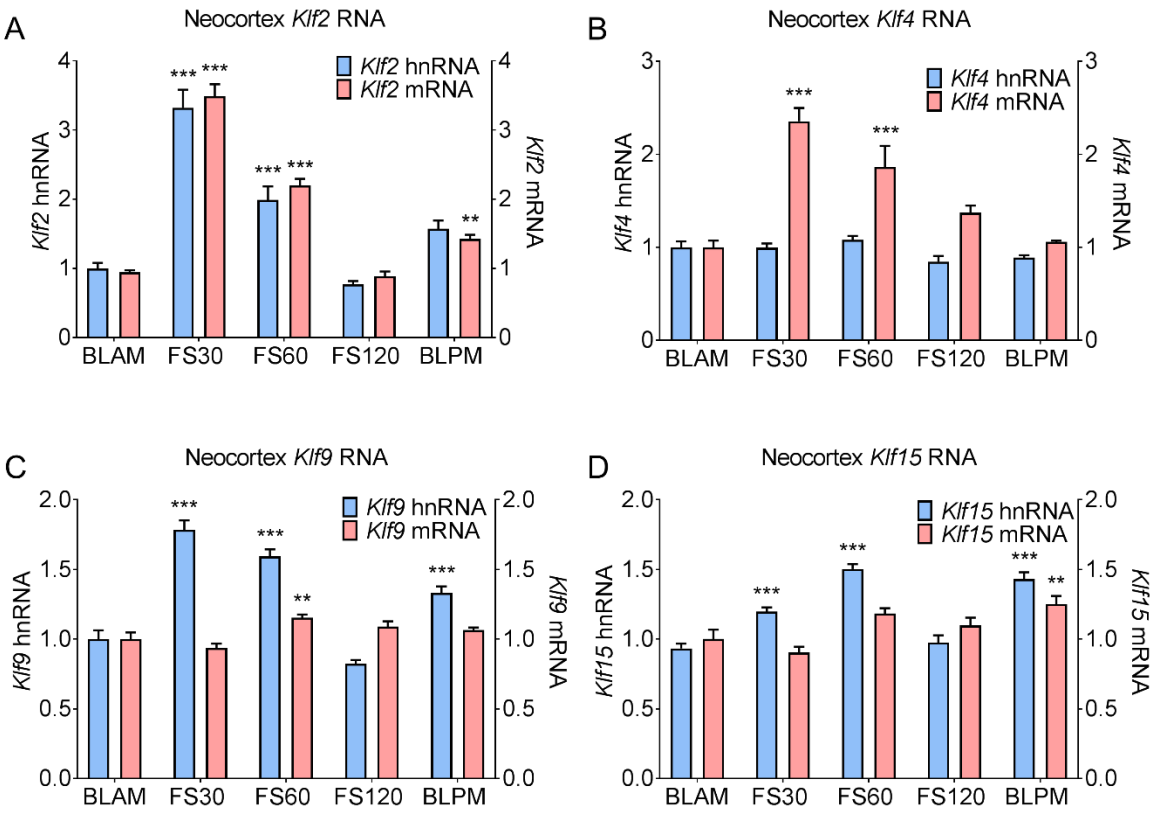

Figure 5.12 Neocortex hnRNA and mRNA of KLFs under baseline conditions and following stress

Rats were killed under early morning (BLAM) or late afternoon (BLPM) baseline conditions or 30 min (FS30), 60 min (FS60) or 120 min (FS120) min after the start of FS (15 min, 25 ºC water). Graphs show hnRNA (blue bars) and mRNA (red bars) levels of *Klf2* (A), *Klf4* (B) *Klf9* (C) and *Klf15* (D). Data are shown as relative RNA copy number calculated using the Pfaffl method of analysis, standardised to the expression of the house keeping genes *Rpl10a* and *Cyclophilin A* (mean ± SEM, n = 8-9 per group). Statistical analysis: one-way ANOVA; (A) *Klf2* hnRNA $F_{(4, 39)}$=37.63, *p*<0.0001, *Klf2* mRNA $F_{(4, 39)}$=119.4, *p*<0.0001, (B) *Klf4* hnRNA $F_{(4, 40)}$=3.659, *p*=0.0124, *Klf4* mRNA $F_{(4, 37)}$=17.19, <0.0001, (C) *Klf9* hnRNA $F_{(4, 39)}$=53.45, *p*<0.0001, *Klf9* mRNA $F_{(4, 40)}$=6.177, *p*<0.001, (D) *Klf15* hnRNA $F_{(4, 39)}$=38.56, *p*<0.0001, *Klf15* mRNA $F_{(4, 40)}$=6.2606, *p*=0.0006. Dunnett's post hoc test, **P*<0.05, ***P*<0.01, ****P*<0.001 significantly different from BLAM.

5.5 Discussion

These experiments have validated some of our novel genome-wide hippocampal ChIP- and RNA-seq findings presented in Chapter 3, which suggest that *Klfs* are important GC hormone target genes following acute stress and during the circadian rise. Furthermore, the high prevalence of KLF motifs within genome-wide loci bound by hippocampal MRs and GRs (Chapter 3) and the predictions that a number of KLFs may act as upstream regulators of downstream MR and GR target genes (Chapter 4) suggests that the KLFs may act as coregulators of genomically acting MRs and GRs. The KLFs encompass a family of transcription factors exhibiting diverse regulatory functions in the brain. Their role in the brain in relation to acute stress or the circadian drive has not been fully elucidated, however given their prominent role in neuronal development and regeneration (Yin et al., 2015) they provide interesting targets for further examination. This investigation was extended to elucidate the regulation of the *Klfs* by genomically acting MRs and GRs throughout the brain. We found that MRs and GRs indeed regulate the expression of *Klfs* in the amygdala, PFC and neocortex, indicating a brain-wide targeting of the *Klfs* by MRs and GRs following HPA axis activation. Furthermore, these findings reveal a more widespread expression of the MR than predicted based on previous radioligand binding studies (Reul and de Kloet, 1985, Reul and de Kloet, 1986). This observation may prompt further investigation into genomically acting MRs and GRs throughout the brain, as studies examining the genomic actions of MRs and GRs outside the hippocampus are currently lacking.

ChIP- and RNA-seq validation experiments involved an almost indistinguishable experimental design carried out in a different cohort of rats from those used for the sequencing experiments. For ChIP-seq validation, rats were killed under identical conditions; early morning baseline (BLAM), 30 min following FS (FS30) or under late baseline conditions (BLPM). Due to the discontinuation of the antibodies used in the original ChIP-seq experiments, new MR and GR antibodies were used in validation ChIP-qPCR experiments. The ability to reproduce the ChIP-seq results using different antibodies for ChIP-qPCR further strengthens the validation and confirms the high quality and robustness of the data. For RNA-seq validation, rats were killed under BLAM and BLPM conditions, however a compacted FS time course was carried out. No further validation was performed at the FS180 and FS360 timepoints as these were from a scientific point of view of less interest and because of our endeavour to reduce animal numbers. While the FS180 timepoint was removed simply because very few significant changes in RNA expression were detected under this condition, the FS360 timepoint was removed due to uncertainty

regarding the influence of the upcoming circadian rise. Despite a few minor changes in the experimental protocols for ChIP- and RNA-qPCR, the data was largely reproducible and strongly agreed with results of ChIP- and RNA-seq.

The pattern of MR and GR enrichment observed in the hippocampal ChIP-qPCR validation experiment was in agreement with the findings of hippocampal ChIP-seq. Hippocampal ChIP-qPCR revealed significantly increased binding of MRs and GRs at GREs within *Klf2, Klf9* and *Klf15* following both acute stress and during the circadian rise. MR enrichment at *Klf15* GRE1 was not found to be significantly increased under BLPM conditions by ChIP-seq, however there was a trend towards significance (p = 0.06) and enrichment was found to be significantly increased by ChIP-qPCR. This is likely due to the increased sensitivity of qPCR compared with sequencing; qPCR is less likely to suffer from background signal as the amplification is directed to a defined DNA sequence rather than an entire DNA library of genome-wide sequences. The results of the RNA-qPCR validation experiment closely mirrored results of RNA-seq and demonstrated inRNA and exRNA counts measured by RNA-seq to be a good representation of hnRNA and mRNA levels, respectively, measured by RNA-qPCR. In the majority of cases, levels of inRNA/hnRNA and exRNA/mRNA for all *Klfs* were shown to be significantly increased at the same timepoints in RNA-seq and RNA-qPCR experiments. Significantly elevated levels of *Klf2* exRNA at BLPM and of *Klf4* inRNA at FS30 shown by RNA-seq were not replicated by RNA-qPCR. It is unclear why these differences were observed under FS conditions, however as the BLPM timepoint represents a wide timeframe in which CORT levels are rising, it is possible that the precise point at which GC levels and changes in RNA levels are occurring may vary between animals.

Findings of ChIP-qPCR throughout the hippocampus, amygdala, PFC and neocortex indicate a more widespread expression of the MR than previously believed. Early radio-ligand binding studies demonstrated high levels of MRs in the hippocampus, with low to very low levels detected in the amygdala, PFC and neocortex (Reul and de Kloet, 1985). This may be the reason why MR binding to GREs within these brain regions has hardly been examined. Following stress or circadian input, enrichment levels of the MR were slightly lower in the PFC and neocortex compared with the hippocampus and the amygdala, however MR binding was found to significantly increase at GREs within *Klf2, Klf9* and *Klf15* in these regions. In the neocortex, however, levels of MR binding to GREs within *Klf15* did not significantly change following acute stress. During the circadian rise, no significant changes in MR binding were detected at *Klf2,* and *Klf15* GRE1 and GRE2. It is likely that the circadian

rise leads to a smaller change in MR binding compared with acute stress, and due to the lower levels of MR enrichment in this region, these changes may be harder to detect with a sample size of only 4 rats. GR binding to *Klf* GREs increased throughout all brain regions in a similar manner to the MR following elevations in GC hormones, however during the circadian rise, neocortex GR binding did not significantly increase at any *Klf* GRE. In some cases, such as for *Klf9,* this may be due to increased variation in neocortex GR enrichment levels observed within the BLPM group, while in other instances it may be due to lower overall levels of neocortex GR enrichment. As the neocortex consists of various layers that exhibit a heterogeneity of cell types (Hodge et al., 2019), it is likely that variations exist in MR and GR receptor expression within these layers.

Although a few studies have shown increased mRNA expression of *Klf4* and *Klf9* following increases in GCs (Datson et al., 2011, Reddy et al., 2009), until now, no study has investigated changes in hnRNA and mRNA expression of *Klf2, Klf4, Klf9* and *Klf15* throughout brain regions under acute stress and circadian conditions. Here, for the first time we show significantly increased levels of *Klf2* hnRNA and mRNA following acute stress or the circadian rise in multiple brain regions. KLF2 is highly expressed within endothelial cells (ECs) where it plays a central role in the regulation of EC function within the BBB (Wu et al., 2013); a structure essential for healthy CNS functioning (Salvador et al., 2014). Many CNS disorders are accompanied by compromised integrity of the BBB, including stroke (Shi et al., 2013) and Alzheimer's disease (Fang et al., 2017). In the cerebral cortex, KLF2 has been shown to regulate the function of the BBB following stroke, thus exerting a neuroprotective effect on the brain. Larger stroke volumes and increased permeability of the BBB following intracerebral injection of the pro-inflammatory cytokine TNF-α were observed in KLF2$^{-/-}$ mice, while KLF2 overexpressing mice had smaller stroke volumes and were protected against TNF-α-mediated BBB dysfunction (Shi et al., 2013). Decreased expression of *Klf2* mRNA and KLF2 protein was observed in a mouse model of Alzheimer's disease and in Human brain microvascular endothelial cells (HBMECs) treated with the amyloid beta protein fragment; $A\beta_{1\text{-}42.}$ Moreover, KLF2 overexpression attenuated the reduction in mRNA levels of *Occludin,* a vascular endothelial associated gene, observed in HBMEs treated with $A\beta_{1\text{-}42}$ (Wu et al., 2013). Decreased expression of *Klf2* mRNA and protein were reported in post-mortem tissue of Alzheimer's disease patients and primary mouse brain microvascular endothelial cells (mBMECs) incubated with $A\beta_{1\text{-}42}$, with (Fang et al., 2017).

Stress exposure and GCs have been linked to damage to the BBB in the hippocampus, amygdala and PFC. Morphological changes in tight junction structural proteins claudin-5 and occludin were accompanied by increased levels of the glucose transport protein GLUT-1in the frontal cortex and hippocampus following exposure to acute and chronic restraint stress (Santha et al., 2015). Rats exposed to restraint stress for up to 21 days exhibited hyperpermeability of the amygdala BBB and elevated expression of BBB permeability markers (Xu et al., 2019). GCs have been linked to improved BBB integrity and the regulation of the expression of many vascular endothelium genes encoding for proteins which maintain endothelial barrier structure such as Occludin, Claudin 1 and 2 and Vascular Endothelial Cadherin (Salvador et al., 2014). No evidence of MR or GR binding to GREs within these genes was seen in our ChIP-seq experiments or reported by other studies, therefore the regulation of these genes by GC hormones may involve a non-genomic mechanism and/or the induction of other (transcription) factors. Possibly, the upregulation in hnRNA and mRNA levels of *Klf2* following elevations in GC hormones serves to promote the integrity of the BBB after stress. However, protein expression levels and the localisation of KLF2 would need to be examined by western blot and immunohistochemistry to confirm whether this link exists.

Despite lacking significant MR or GR binding, RNA levels of *Klf4* were investigated to provide a negative control for further studies involving the manipulation of MR and GR binding. hnRNA levels of *Klf4* remained stable, apart from a small increase in the PFC at FS30, while mRNA levels were increased at FS30 in all brain regions examined. It is probable that hnRNA levels of *Klf4* have risen prior to the FS30 timepoint, and as there is no significant MR or GR binding occurring within *Klf4* it is likely that more rapidly acting transcription factors are regulating the expression of this gene. Interestingly, the application of NMDA to primary cortical neuron cultures induced a rapid upregulation of *Klf4* mRNA which was accompanied by upregulated KLF4 protein expression. Antagonism of the NMDAR by MK801 completely abolished the induction of *Klf4* mRNA expression, an effect that antagonists of AMPA or kainite receptors failed to produce (Zhu et al., 2009). Following exposure to an acute stressor, activated GRs have been shown to participate in the MAPK/ERK signalling cascade initiated by the NMDAR, resulting in changes of chromatin structure which expose target genes for transcription (Gutierrez-Mecinas et al., 2011). It is possible that the induction of *Klf4* hnRNA and mRNA observed in our study occurs via this mechanism, and unpublished findings of histone modification ChIP-seq experiments carried out by the Reul group have shown constitutive formation of the histone

modification, H3K9acS10p, within close proximity to *Klf4* following FS and during the circadian rise (Price et al., unpublished observations).

KLF4 has been shown to play a central role in a number of important physiological and pathological processes within the brain. *In vitro* studies have identified KLF4 as a transcriptional repressor of axon growth in retinal ganglion cells (RGCs) and embryonic day 18 (E18) hippocampal neurons. Overexpression of KLF4 reduced axon and dendrite length and decreased the number of neurites and branches of E18 hippocampal neurons. KLF4 overexpressing RGCs exhibited decreased neurite and branch numbers and a slower rate of neurite extension (Moore et al., 2009). An extensive study into the role of KLF4 during brain development has also demonstrated repressed neural growth following overexpression of the gene. High embryonic expression of KLF4 within the mouse forebrain was followed by postnatal downregulation by PND7, and neurons and astrocytes exhibited a dramatic decrease in KLF4 expression when compared with neural stem cells (NSCs). KLF4 overexpression within cultured NSCs resulted in structural abnormalities accompanied by reduced growth, differentiation and self-renewal. In transgenic mice, KLF4 overexpression led to a hydrocephalus phenotype characterised by ventricular enlargement and an excess of CSF. The hydrocephalus phenotype was accompanied by morphological abnormalities of the corpus callosum, hippocampus and cerebral cortex. The Subcommissural organ (SCO), a structure thought to regulate CSF reabsorption, was also reduced in these mice and fewer ependymal cilia were observed. Cilia comprise flagella-like projections made up of microtubules and are thought to facilitate the flow of CSF. Of the ependymal cilia that were detected, a shorter disorganised structure was seen (Qin et al., 2011). A central role of KLF4 in the neurogenesis and radial neuronal migration of developing cerebral cortex cells has also been shown in mice. Constitutive expression of KLF4 prevented the migration and differentiation of cells within the cerebral cortex and kept cells in a glia-like fate. Overexpression of KLF4 prevented the migration of cells to the cortical plate from the ventricular and subgranular zones and led to a round multipolar morphology of cells. When KLF4 was downregulated, increased cellular migration to the cortical plate was observed, cells exhibited more neuronal processes and more unipolar and bipolar cells were seen (Qin and Zhang, 2012).

These experiments show that a downregulation of KLF4 expression in the developing brain is of critical importance to allow the proper differentiation, migration and maturation of neurons. Interestingly, in the rodent the early postnatal “stress-hyporesponsive period” (approximately PND2-14) characterised by

low GC hormone levels coincides with the postnatal period at which cell birth and death is maximal within the DG (Gould et al., 1991). Early postnatal exposure to GCs has been shown to inhibit neurogenesis (Bohn, 1980) and decrease migration of pyknotic cells to the granule cell layer (Gould et al., 1991). As we have shown that a rise in GC levels results in upregulated hnRNA and mRNA of *Klf4,* it would be interesting to investigate whether postnatal exposure to GCs leads to increased levels of KLF4 expression and whether this upregulation is responsible for the inhibition of neurogenesis and migration of new-born cells.

Klf9, originally named *basic transcription element-binding protein* (*BTEB*), was the first member of the KLFs to be identified (Imataka et al., 1992) and despite ubiquitous tissue expression of the gene, the translation of *Klf9* mRNA appears be limited to the brain (Imataka et al., 1994). Early studies identified *Klf9* as a thyroid responsive gene in the developing rat brain. *Klf9* mRNA levels were shown to increase postnatally in the cerebral hemisphere between PND 15-30, remaining elevated in the adult rat. Hypothyroidism reduced *Klf9* mRNA levels significantly throughout PND 5-22, while T_3 treatment rescued *Klf9* mRNA expression. By postnatal day 30, *Klf9* mRNA levels remained elevated irrespective of thyroid levels. In mouse Neuro2a (N2a) cells, *Klf9* mRNA and protein levels were upregulated by T_3 and overexpression of KLF9 induced neurite outgrowth (Denver et al., 1999). In the developing mouse brain, KLF9 expression was observed in the hippocampal pyramidal cell layer and cerebellar cortical layer from PND6 and PND7, respectively. *Klf9* KO mice demonstrated impaired motor learning and motor coordination and deficits in contextual-dependent fear conditioning in behavioural paradigms involving the cerebellum and hippocampus, respectively (Morita et al., 2003). Developmental and behavioural deficits were also reported in *Klf9* KO mice, with impaired differentiation of dendritic spines in the DG, impaired maturation of adult-born DG neurons, reduced synaptic plasticity and impairments in anxiety-like behaviours and contextual fear discrimination learning (Scobie et al., 2009).

Klf9 was identified as a GC receptor target gene in later studies and exposure of frogs to shaking stress led to an increase in plasma CORT and KLF9 expression within the amygdala and optic areas. RU486 treatment attenuated the induction of *Klf9* mRNA *in vivo* and *in vitro,* while *in vitro* treatment with spironolactone caused only a slight reduction in CORT-induced mRNA levels of *Klf9,* indicating that induction of the gene is primarily GR-mediated. Forced expression of KLF9 *in vivo* resulted in an increased number of Golgi-stained cells, reflective of neuronal differentiation and maturation (Bonett et al., 2009). GREs have also been reported within close proximity to the TSS of *Klf9.* In the hippocampus,

mice injected postnatally with CORT exhibited increased *Klf9* hnRNA and mRNA levels, while treatment of mouse hippocampal-derived (HT-22) cell lines with CORT caused dose- and time-dependent increases in *Klf9* mRNA. RU486 abolished the induction of *Klf9* mRNA in HT-22 cells, while aldosterone caused a small but significant increase in *Klf9* mRNA, indicating that while both MR and GR contribute to the induction of *Klf9* mRNA expression, GR is the principal regulator. Electrophoretic mobility shift assay (EMSA) and ChIP experiments demonstrated CORT-dependent GR binding to two highly conserved GREs within *Klf9.* ChIP also showed a CORT-dependent increase in H3 acetylation at one of the two GREs (Bagamasbad et al., 2012). These GREs are reported to exhibit 100% homology between the mouse and rat, the two GREs described by (Bagamasbad et al., 2012) are found within the MR/GR peak identified by our hippocampal ChIP-seq experiment.

Klf9 clearly plays a role in early brain development, and in contrast with *Klf4,* mRNA levels are upregulated postnatally to facilitate processes such as neuronal differentiation and maturation (Bonett et al., 2009). The upregulation of *Klf9* mRNA, however, occurs after the stress-hyporesponsive period has ended (PND15-30) (Denver et al., 1999), therefore may be under GC hormone regulation. The observation that *Klf9* mRNA levels are maintained in the absence of thyroid hormone at PND30 further supports this hypothesis (Denver et al., 1999), however this would need to be assessed by additional experiments.

In comparison with *Klf2, Klf4* and *Klf9,* the role of *Klf15* has hardly been examined in the brain in relation to GC hormone activity. KLF15 expression is enriched within tissues such as skeletal muscle (Shimizu et al., 2011), kidney (Mallipattu et al., 2012), heart, adipose and liver tissue (McConnell and Yang, 2010). Evidence is emerging, however, for a role of KLF15 in the CNS. KLF15 was identified as a potential transcriptional regulator of rhodopsin in bovine retinal cells. *Klf15* mRNA expression was detected in multiple bovine neural tissues such as the cerebellum, visual cortex and ciliary epithelium of the iris. Transfection of cells with KLF15 led to transcriptional repression of the Rhodopsin promoter (Otteson et al., 2004). KLF15 has been implicated as a regulator of glial development, with overexpression of the protein resulting in the induction of Glial fibrillary acidic protein (GFAP) expression in astrocytes of mouse spinal cord explant cultures (Fu et al., 2009). Gene expression profiling of cells from mouse embryos revealed upregulated expression of KLF15 within the dorsolateral telencephalon at embryonic day 17. Overexpression of KLF15 inhibited neuronal differentiation, while KLF15 knockdown led to premature neuronal differentiation and inhibited radial migration to the cortical plate

(Ohtsuka et al., 2011). Microarray and qPCR revealed a strong induction of *Klf15* mRNA expression following DEX treatment of primary human airway smooth muscle (ASM) cells, an effect thought to be mediated by the GR (Masuno et al., 2011). Within rat skeletal muscle, *Klf15* was identified as a direct target of GR as increased mRNA levels were observed following DEX administration, while RU486 inhibited DEX-induction of *Klf15* within myoblasts. GREs were also identified within the promoter of *Klf15* and RU486 attenuated DEX induced activity within these GREs. ChIP also demonstrated significantly increased GR binding at two GREs within *Klf15* following DEX treatment (Shimizu et al., 2011). The *Klf15* GRE2 identified by (Shimizu et al., 2011) lies within the MR and GR binding peak detected by our hippocampal ChIP-seq study which was labelled as *Klf15* GRE1.

The lack of studies investigating the role of *Klf15* in the brain may be due to low expression levels in this region. Although MR and GR binding at *Klf15* GREs did significantly increase throughout all brain regions following acute stress and in the circadian rise, enrichment levels were slightly lower compared with levels seen at *Klf2* and *Klf9* GREs. RNA of *Klf15* did rise in all brain regions at multiple timepoints following acute stress and during the circadian rise, however in contrast with the other *Klfs,* the induction of *Klf15* RNA did not exceed 2-fold in any brain region. It is also possible, however, that *Klf15* is expressed in relatively few cells, hence the low MR and GR enrichment and RNA expression observed. A more distinct pattern of *Klf15* expression, however, may have an underlying functional significance, thus expression of *Klf15* in relatively few cells may be worth pursuing. Quantification of the absolute expression levels of *Klf15* and the expression pattern could provide further insight into whether the gene is a target warranting further examination in the brain.

Overall, the results of the validation experiments mirrored findings of the hippocampal genome-wide ChIP- and RNA-seq, confirming the reproducibility and robustness of the data. These findings also show MR expression occurring in brain regions such as the PFC and neocortex, in which expression of the receptor was originally believed to be very low (Reul and de Kloet, 1985). Members of the KLF family of transcription factors have also been identified as targets of genomically acting MRs and GRs throughout the brain. Many studies have highlighted an important role of the KLFs in a number of neurobiological processes, however it is unclear whether GC hormone activity regulates KLF expression with regard to these processes. A number of KLFs have also been implicated in neurological and psychiatric disorders that are linked to GC hormones, such as Alzheimer's disease (Fang et al., 2017, Wu et al., 2013), hydrocephalus (Qin et al., 2011), anxiety and cognitive impairment (Scobie et

al., 2009). These observations indicate that future studies are needed to elucidate whether a connection exists between GC hormone regulation of the KLFs and the aetiology of these disorders.

Chapter 6 The effects of MR and GR antagonism on the genomic regulation of KLFs in the hippocampus under early morning baseline conditions and following acute stress

6.1 Abstract

Genomically acting MRs and GRs target a number of KLF family members following elevations in GC hormone levels throughout the brain. These KLFs have been shown to play a role in various neurobiological processes under GC hormone regulation and are implicated in neurological disorders linked to stress, suggesting these genes to be important targets of genomically acting MRs and GRs. In Chapter 5, we showed that increased MR and GR binding to GREs within *Klf2, Klf9* and *Klf15* was accompanied by elevated hnRNA and mRNA expression of these genes in the hippocampus, amygdala, PFC and neocortex following acute stress and during the circadian rise. It has not been shown yet, however, whether MRs and GRs are mediators of the circadian- and stress-induced effects on transcriptional activity of the *Klfs*.

In this chapter, the effect of the MR and GR antagonists, spironolactone (SPIRO) and RU486 (RU), respectively, on hippocampal MR and GR binding to GREs within the *Klfs* and associated transcriptional responses of these genes are investigated under early circadian trough conditions and following acute stress. For a comparison, hippocampal transcriptional responses were also examined in ADX rats under identical conditions. Under baseline conditions, drug treatment appeared to have an effect on receptor binding, whereas RNA levels of the *Klfs* were mainly unaffected. Drug treatment had no influence on FS-induced MR and GR binding to GREs within the *Klfs*. After FS, at the dose of 30 mg/kg, RU alone did not change the FS-induced transcriptional response of *Klf2, Klf9* and *Klf15.* A combination of SPIRO and RU, however, attenuated the transactivation of *Klf2, Klf9* and *Klf15* following FS stress. ADX completely abolished the transcriptional responses of *Klf9* and *Klf15* to stress*.* The transactivation of *Klf2,* however, was only partially inhibited by ADX. These findings confirm genomically acting MRs and GRs as transcriptional regulators of the *Klfs. O*ther coregulators are likely participating in MR/GR regulation of the *Klfs*, therefore further studies are needed to elucidate the regulation of the *Klfs* under acute stress conditions.

6.2 Introduction

The genomic action of MRs and GRs is thought to underlie many GC-dependent behavioural and physiological changes observed after stress or associated with circadian rhythm (Mifsud and Reul, 2018, Reul, 2014). In Chapter 3 and 5, ChIP-qPCR and RNA-qPCR have identified the KLF family members *Klf2, Klf9* and *Klf15* as transcriptional targets of genomically acting MRs and GRs following conditions under which GC levels are elevated (i.e. acute stress and the circadian rise in GC secretion). These KLFs have been linked to numerous neurobiological processes, such as BBB function (Shi et al., 2013), neurogenesis (Qin and Zhang, 2012), synaptic plasticity (Scobie et al., 2009) and neuronal differentiation and migration (Ohtsuka et al., 2011).

As described in chapter 5, acute stress and circadian influences led to increased binding of MRs and GRs to GREs within *Klf2, Klf9* and *Klf15* in the hippocampus, amygdala, PFC and neocortex. Increased hnRNA and mRNA levels of these *Klfs* were also observed, suggesting that increased MR and GR binding to GREs within *Klfs* leads to enhanced transcriptional activity of these genes. Despite the absence of MR or GR binding, mRNA levels of *Klf4* were significantly elevated following acute stress throughout all brain regions examined, and in the PFC during the circadian rise. Constitutive formation of the chromatin relaxing-dual histone modification H3K9acS10p within close proximity to *Klf4* has also been shown under acute stress and circadian conditions (Price E.M. et al., unpublished observations, Gutierrez-Mecinas et al., 2011), indicating that a non-genomic GC-regulated mechanism may play a part in the transcriptional regulation of this gene. Thus, it is unclear whether the binding of MR and GR to GREs within *Klfs* is directly leading to transcriptional activation of these genes, or whether alternative TFs or non-genomic mechanisms may be involved as well.

As the transcriptional effects of MRs and GRs are ligand-dependent, an effective (pharmacological) intervention strategy for elucidating their genomic actions would involve blocking these receptors with competitive antagonists. SPIRO and RU486 are widely used antagonists that compete with ligand for the occupancy of MR (Rogerson et al., 2003) and GR (Nordeen et al., 1995), respectively. SPIRO has been shown to compete with DEX for the LBD of the MR *in vitro* (Rogerson et al., 2003), but also displays a very weak affinity for the GR (Couette et al., 1992). MR antagonism by SPIRO has been shown to inhibit the transcriptional activity of MRs in ADX rats (Herman and Spencer, 1998). RU486 emulates many of the agonist actions of CORT, including dissociation of the GR from HSPs and DNA

binding, however, prevents the induction of transcriptional responses (Nordeen et al., 1995), likely by preventing interactions of DNA-bound GRs with transcriptional machinery (Baulieu, 1991). RU486 can exhibit partial GR agonistic activity (Bachmann et al., 2003) depending on interactions between coactivators and corepressors (Liu et al., 2002). In mouse cell lines, RU486 has been shown to fully attenuate DEX-induced GR-mediated transcriptional activity (Qin et al., 2014).

The aim of the following experiments was to determine whether MR and GR binding to *Klf* GREs leads to changes in RNA expression of the corresponding *Klf* gene. Moreover, for sake of comparison. We also investigated the effects of CORT removal by ADX on stress-induced RNA expression of the *Klfs*. To prevent non-specific binding of by GR by SPIRO (Couette et al., 1992), RU486 was administered alongside SPIRO as it displays no affinity for the MR (Baulieu, 1991). Rats were voluntarily dosed with a combination of SPIRO and RU486 or RU486 alone and killed under early baseline conditions (BLAM) or at various timepoints after FS. In a second experiment, rats underwent sham surgery or bilateral ADX and were killed, alongside an intact group, under early baseline conditions (BLAM) or at various timepoints after FS. ChIP-qPCR and RNA-qPCR were performed on the hippocampus to investigate the effects of MR and/or GR antagonism, or removal of endogenous CORT, on MR and GR binding and RNA expression.

Following exposure to stress, plasma CORT secretion and MR/GR to GRE binding was unaffected by drug treatment. Plasma CORT levels remained elevated, however, over an extended period in drug treated animals, indicating impaired negative feedback of the HPA-axis. Despite an enhanced plasma CORT profile, drug treatment with a combination of both antagonists partially attenuated the transcriptional response of *Klf2, Klf9* and *Klf15.* The observation that *Klf4* RNA levels were left unaffected by drug treatment demonstrated that neither drug elicited effects on transcription independently of their effects on MRs and GRs. ADX abolished the FS-induced transcriptional responses of *Klf9* and *Klf15.* RNA levels of *Klf2* were only partially attenuated, however, indicating that alternative TFs may be regulating the transcription of this gene independently of GC hormone action. Levels of *Klf4* RNA were attenuated by ADX, suggesting that this gene is regulated by a non-genomic GC-dependent mechanism. These findings show that the *Klfs* are regulated by both MRs and GRs following acute stress, however alternative transcription factors are also likely contributing to the transcriptional regulation of the *Klfs.* Further investigation, however, is required to identify the mediators of *Klf* expression in the hippocampus.

6.3 Materials and Methods

6.3.1 Animals

Adult male Wistar rats (150-175g on arrival) were purchased from Envigo (Oxon, UK) and group-housed (2-3 per cage). Rats were housed under standard lighting (lights on 05:00– 19:00 h, approximately 80-100 Lux) and environmentally controlled conditions (temperature 21 ± 1°C; relative humidity 40–60%) with food and water available *ad libitum*. All rats were handled daily (2 min per rat per day; min. 5 days) to reduce any nonspecific stress effects.

6.3.2 Drug treatment

To block MR and GR mediated effects, rats were voluntarily dosed with the MR antagonist SPIRO (Sigma, Dorset, UK) or the GR antagonist RU486 (RU, 'Mifepristone', Sigma, Dorset, UK) as described in Chapter 2.

6.3.3 Surgical procedures

Rats underwent bilateral underwent bilateral ADX or sham surgery as described in Chapter 2.

6.3.4 Animal experiments

For the antagonist ChIP study, baseline rats were voluntarily dosed in their home cage 90 min before being killed between 9-11am (circadian trough (BLAM)). For the acute stress groups, rats were voluntarily dosed 60 min before FS (15 min, 25 °C (±1) water) and killed 30 minutes after. For the antagonist RNA study, baseline rats were voluntarily dosed in their home cages 120 min before being under BLAM conditions. Stressed rats were voluntarily dosed 60 min before FS and killed 60 minutes after. For the ADX study, intact, sham and ADX rats were killed straight from their home-cages under BLAM conditions or 60 min after the start of FS as described in Chapter 2.

6.3.5 Measurement of corticosterone by RIA

Plasma CORT concentrations were measured using a commercial CORT RIA Kit (MP Biomedicals) as described in Chapter 2.

6.3.6 ChIP-qPCR

Standard ChIP was performed as previously described in Chapter 2, using the antibodies listed in Table 2.5. All samples (bounds and inputs) were diluted to a standardized concentration with nuclease-free water and analysed by qPCR using primers/probes listed in Table 2.6. Data are expressed as quantity of bound DNA divided by the respective quantity of input DNA (i.e., B/I), which is a measure of the enrichment of steroid receptor bound to specific genomic sequences.

6.3.7 RNA-qPCR

RNA was extracted as previously described in Chapter 2. RNA-qPCR was performed as described in Chapter 2 using primers and probes listed in Table 2.7 (hnRNA) and Table 2.8 (mRNA). Expression of hnRNA and mRNA in each sample was calculated based on the Pfaffl method of relative quantification (Pfaffl, 2001) and standardized to the expression of house- keeping genes listed in Table 2.9.

6.3.8 Statistical analysis

Data were statistically analysed using GraphPad Prism software 7.04. Results are presented as group means ± SEM; sample sizes are indicated in the figures. Multiple statistical comparisons were conducted with one-way or two-way ANOVA, and if significant, a Dunnett's or Sidak's post hoc test was performed. Statistical results are provided in the legends of the figures. $P<0.05$ was considered statistically significant.

6.4 Results

6.4.1 The effects of SPIRO and/or RU on hippocampal MR and GR binding to GREs within *Klfs* under BLAM conditions and following acute stress

To determine the effect of SPIRO and/or RU on the binding of MRs and GRs to GREs within *Klf* genes, rats were administered vehicle, a combination of SPIRO (50 mg/kg) and RU (30 mg/kg) or RU only (30 mg/kg) and killed at BLAM or FS30. Under BLAM conditions, plasma CORT levels were unaffected by drug treatment. Following FS, plasma CORT levels were significantly elevated in all groups (Figure 6.1).

Drug treatment had no effect on MR enrichment at *Klf2*, *Klf9*, *Klf15* GRE1 and *Klf15* GRE2 (Figure 6.2) under BLAM or stress conditions. In vehicle-treated rats, FS resulted in increased MR enrichment at *Klf2* and *Klf15* GRE1 (Figure 6.2). Rats treated with a combination of SPIRO/RU showed elevated levels of MR binding at *Klf2* and *Klf15* GRE1 (Figure 6.2) following FS.

Treatment with SPIRO/RU and RU increased baseline levels of GR enrichment at *Klf2*, *Klf9* and *Klf15* GRE2 (Figure 6.3) compared with the vehicle controls. In vehicle-treated rats, FS stress resulted in increased GR binding at *Klf2*, *Klf9* (Fig. 6.3), *Klf15* GRE1 and *Klf15* GRE2 (Figure 6.3). GR enrichment at *Klf2* was elevated at FS30 in rats which had received SPIRO/RU and RU, while RU-treated rats exhibited enhanced GR binding at *Klf15* GRE1 (Figure 6.3.c) following FS. It appeared that the effect of drug treatment on GR binding at these GREs depended on the experimental conditions (BLAM vs FS) which is underlined by the significant interaction term in the two-way ANOVA analysis (see legend to Fig. 6.3).

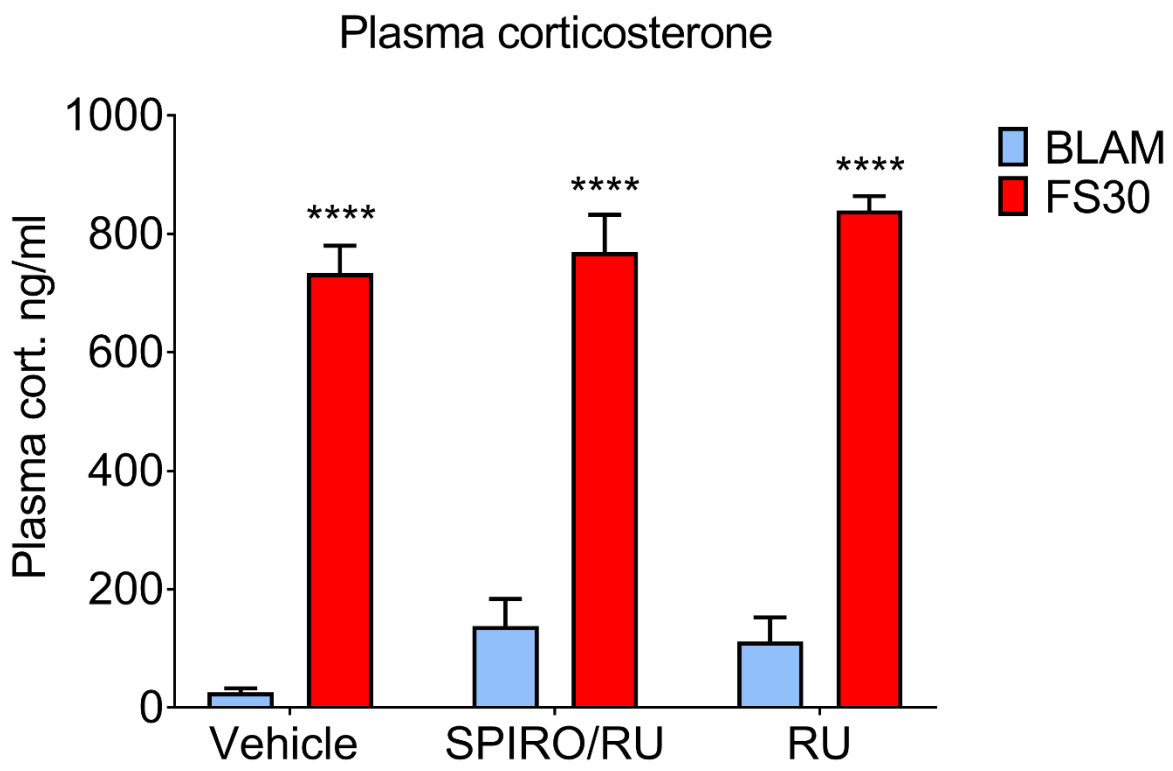

Figure 6.1 The effect of SPIRO and RU on plasma CORT levels under BLAM conditions and following acute FS stress

Rats were voluntarily dosed with vehicle, a combination of SPIRO (50 mg/kg) and RU (30mg/kg) or RU only (30mg/kg). Baseline rats were killed 90 minutes after voluntary dosing under early morning baseline conditions (~9:00 am (BLAM)). Stressed rats were voluntarily dosed 60 minutes before the onset of FS and killed 30 min after the start of FS (15 min, 25°C water). Plasma CORT levels are expressed as ng/ml (mean ± SEM, n=6-8 per group). Statistical analysis: two-way ANOVA, effect of drug: $F_{(2, 38)}$=2.724, p=0.0785, effect of stress: $F_{(1, 38)}$=372.5, p<0.0001, interaction drug x stress: $F_{(2, 38)}$ =0.648, p=0.528, Sidak's post hoc tests, ****P<0.0001 significantly different from BL within the same vehicle/drug treatment group. Inter-assay coefficient of variation; 2.68%, intra-assay coefficient of variation; 3.46%.

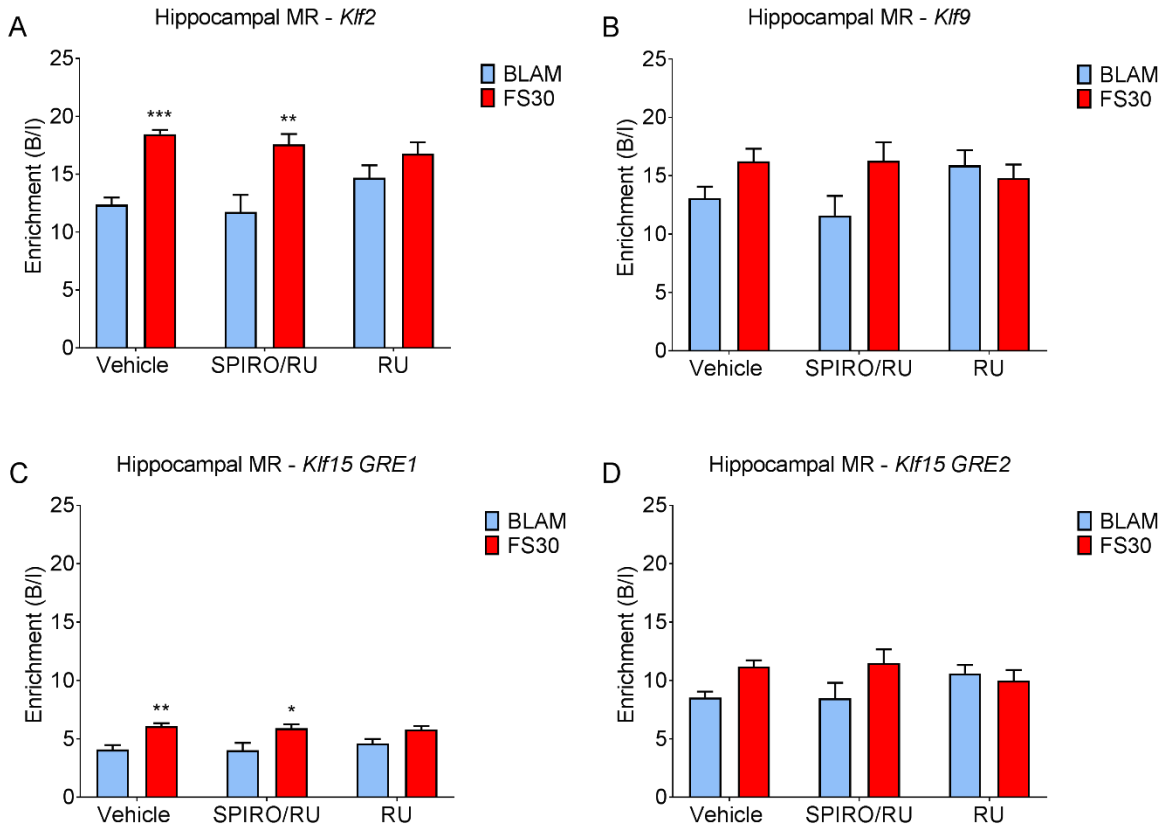

Figure 6.2 The effect of SPIRO and RU on hippocampal MR binding to GREs within *Klf2, Klf9* and *Klf15* under BLAM conditions and following acute FS stress

Rats were voluntarily dosed with vehicle, a combination of SPIRO (50 mg/kg) and RU (30mg/kg) or RU only (30mg/kg). Baseline rats were killed 90 minutes after voluntary dosing under early morning baseline conditions (~9:00 am (BLAM)). Stressed rats were voluntarily dosed 60 minutes before the onset of FS and killed 30 min after the start of FS (15 min, 25°C water). Graphs show enrichment of MR, expressed as bound/input (mean ± SEM, n=4 per group), at GREs within *Klf2* (A) and *Klf9* (B) and *Klf15* (C and D). Statistical analysis: two-way ANOVA; (A) effect of drug: $F_{(2, 18)} = 0.647$, $p = 0.535$, effect of stress: $F_{(1, 18)} = 34.68$, $p < 0.0001$, interaction drug x stress: $F_{(2, 18)} = 2.701$, $p = 0.094$, (B) effect of drug: $F_{(2, 18)} = 0.566$, $p = 0.577$, effect of stress: $F_{(1, 18)} = 4.338$, $p = 0.0518$, interaction drug x stress: $F_{(2, 18)} = 2.559$, $p = 0.105$, (C) effect of drug: $F_{(2, 18)} = 0.184$, $p = 0.833$, effect of stress: $F_{(1, 18)} = 27.07$, $p < 0.0001$, interaction drug x stress: $F_{(2, 18)} = 0.588$, $p = 0.565$, (D) effect of drug: $F_{(2, 18)} = 0.112$, $p = 0.895$, effect of stress: $F_{(1, 18)} = 4.994$, $p = 0.0384$, interaction drug x stress: $F_{(2, 18)} = 2.34$ $p = 0.125$. Sidak's post hoc tests, $^{*}P < 0.05$, $^{**}P < 0.01$, $^{***}P < 0.001$ significantly different from BL within the same vehicle/drug treatment group.

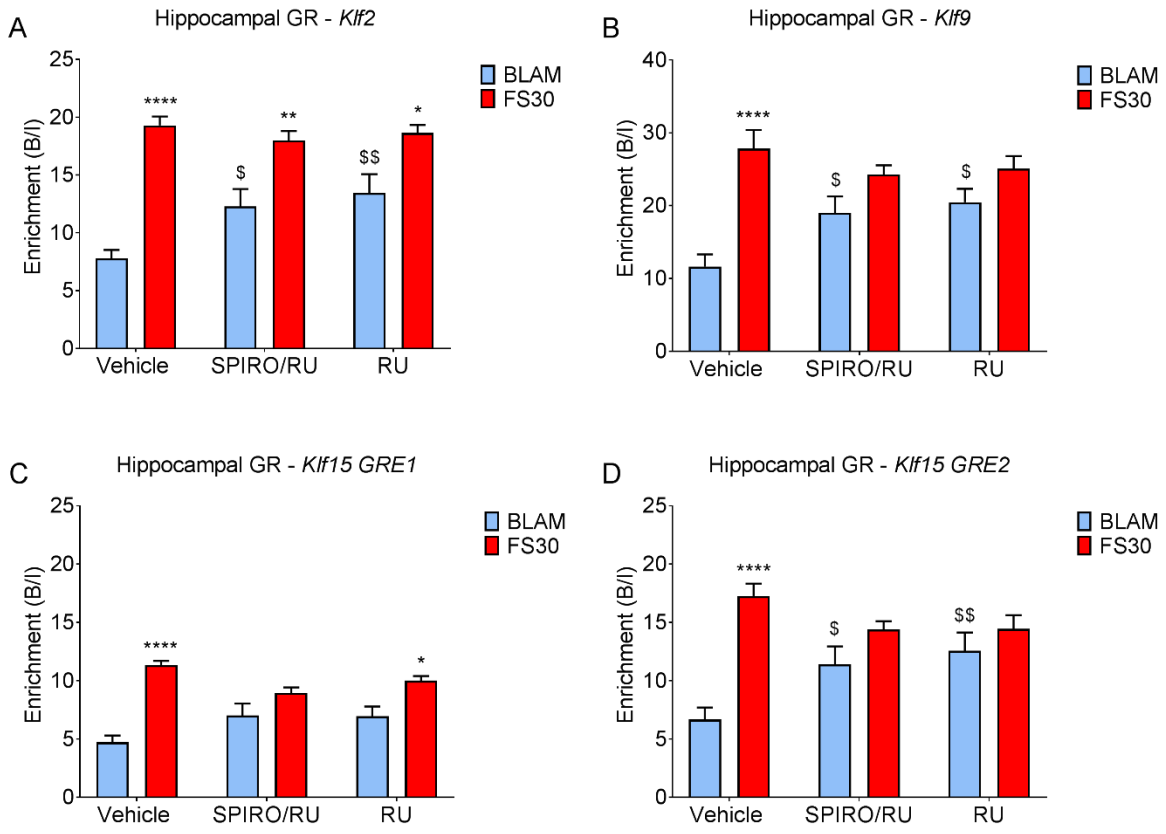

Figure 6.3 The effect of SPIRO and RU on hippocampal GR binding to GREs within *Klf2, Klf9* and *Klf15* under BLAM conditions and following acute FS stress

Rats were voluntarily dosed with vehicle, a combination of SPIRO (50 mg/kg) and RU (30mg/kg) or RU only (30mg/kg). Baseline rats were killed 90 minutes after voluntary dosing under early morning baseline conditions (~9:00 am (BLAM)). Stressed rats were voluntarily dosed 60 minutes before the onset of FS and killed 30 min after the start of FS (15 min, 25°C water). Graphs show enrichment of GR, expressed as bound/input (mean ± SEM, n=4 per group), at GREs within *Klf2* (A) and *Klf9* (B) and *Klf15* (C and D). Statistical analysis: two-way ANOVA; (A) effect of drug: $F_{(2, 18)}$=2.702, p=0.094, effect of stress: $F_{(1, 18)}$=70.16, p<0.0001, interaction drug x stress: $F_{(2, 18)}$=5.148, p=0.0171, (B) effect of drug: $F_{(2, 18)}$=1.256, p=0.309, effect of stress: $F_{(1, 18)}$=30.42, p<0.0001, interaction drug x stress: $F_{(2, 18)}$ = 5.68, p=0.0122, (C) effect of drug: $F_{(2, 18)}$=0.358, p=0.704, effect of stress: $F_{(1, 18)}$=51.12, p<0.0001, interaction drug x stress: $F_{(2, 18)}$=6.877, p=0.0060, (D) effect of drug: $F_{(2, 18)}$=0.809, p=0.461, effect of stress: $F_{(1, 18)}$=26.62, p<0.0001, interaction drug x stress: $F_{(2, 18)}$=7.53, p=0.0042. Sidak's post hoc tests, **P*<0.05, ***P*<0.01, *****P*<0.0001 significantly different from BL within the same vehicle/drug treatment group. $*P*<0.05, $$*P*<0.01 significantly different from vehicle within same BLAM or FS group.

6.4.2 The effects of SPIRO and/or RU on hippocampal RNA expression of *Klf*s under BLAM conditions and following acute FS stress

Changes in hippocampal RNA expression of *Klf* genes were examined in rats receiving the same drug treatment with SPIRO and RU as previously described. Rats were killed under BLAM conditions or at FS60. Under baseline conditions, drug treatment appeared to have no effect on plasma CORT levels (Figure 6.4). At FS60, plasma CORT was significantly elevated in rats receiving SPIRO/RU and RU treatment. Furthermore, rats receiving RU alone had significantly higher stress-induced plasma CORT levels compared with rats receiving vehicle and SPIRO/RU.

Drug treatment had no effect on the hnRNA levels of *Klf2* or *Klf4*, however stress led to enhanced hnRNA levels of *Klf2* in all groups, and elevated *Klf4* hnRNA in vehicle-treated rats only (Fig. 6.5). Levels of *Klf9* hnRNA and *Klf15* hnRNA were significantly increased by stress in all groups (Fig. 6.5). Rats receiving SPIRO/RU exhibited significantly lower levels of *Klf9* hnRNA and *Klf15* hnRNA at FS60 compared with vehicle-treated rats (Figure 6.5).

Klf2 mRNA levels were significantly increased following acute stress in vehicle-, SPIRO/RU- and RU-treated rats (Figure 6.6). Treatment with SPIRO/RU attenuated the stress-induced levels of *Klf2* mRNA compared with vehicle-treated rats. Stress led to an increase in mRNA levels of *Klf4*, *Klf9* and *Klf15* (Figure 6.6) in all groups, while drug treatment had no effect.

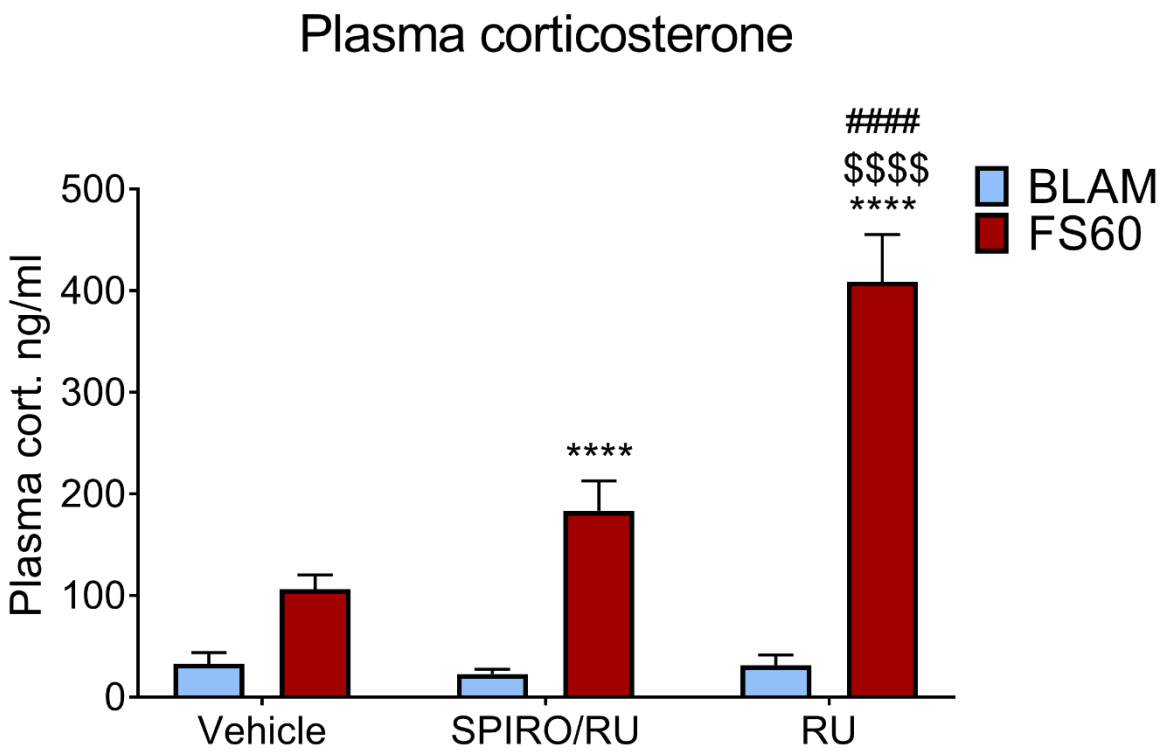

Figure 6.4 The effect of SPIRO and RU on plasma CORT levels under BLAM conditions and following acute FS stress

Rats were voluntarily dosed with vehicle, a combination of SPIRO (50 mg/kg) and RU (30mg/kg) or RU only (30mg/kg). Baseline rats were killed 120 minutes after voluntary dosing under early morning baseline conditions (~9:00 am (BLAM)). Stressed rats were voluntarily dosed 60 minutes before the onset of FS and killed 60 min after the start of FS (15 min, 25°C water). Plasma CORT levels are expressed as ng/ml (mean ± SEM, n=7-8 per group). Statistical analysis: two-way ANOVA, effect of drug: $F_{(2, 41)}$=20.98, p<0.0001, effect of stress: $F_{(1, 41)}$=104, <0.0001, interaction drug x stress: $F_{(2, 41)}$= 20.47, p<0.0001. Sidak's post hoc tests, ****P<0.0001 significantly different from BL within the same vehicle/drug treatment group. $$$$$P$<0.0001 significantly different from vehicle within the same BLAM or FS group, ####P<0.0001 significantly different from SPIRO/RU treated rats within the same BLAM or FS group. Inter-assay coefficient of variation; 2.68%, intra-assay coefficient of variation; 4.21%.

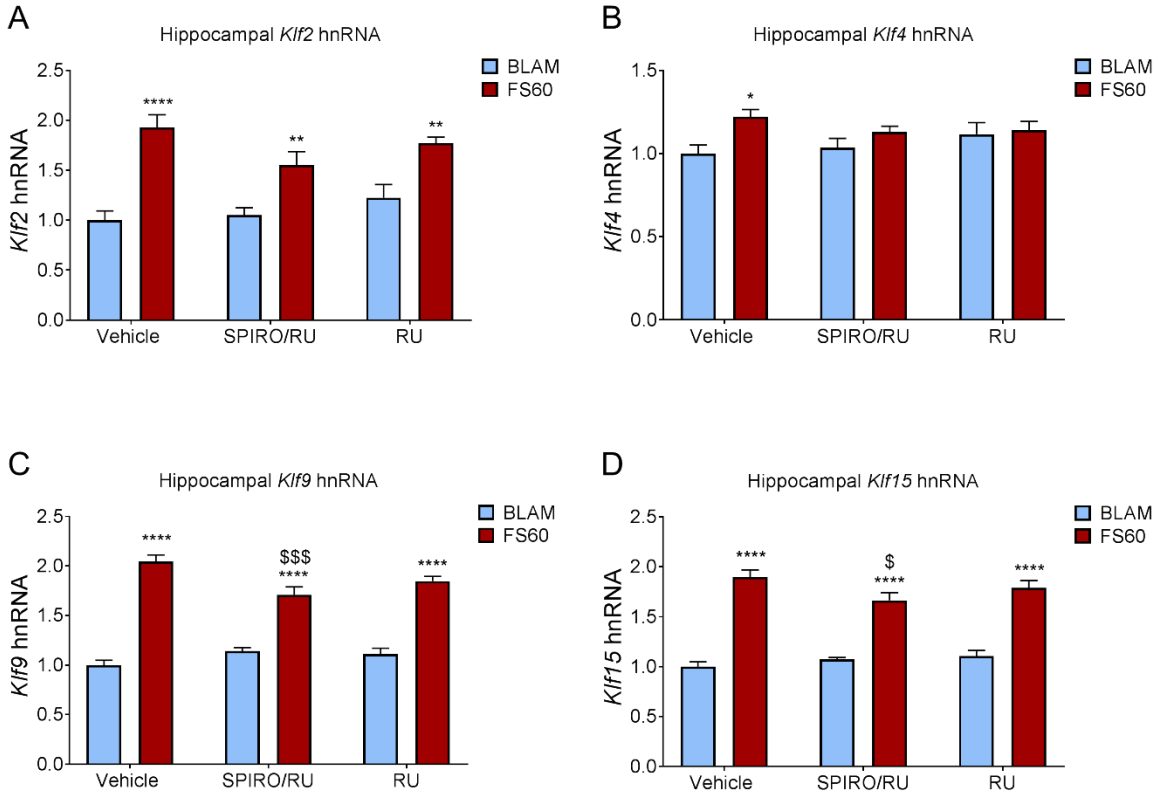

Figure 6.5 The effect of SPIRO and RU on hippocampal hnRNA expression of KLFs under BLAM conditions and following acute FS stress

Rats were voluntarily dosed with vehicle, a combination of SPIRO (50 mg/kg) and RU (30mg/kg) or RU only (30mg/kg). Baseline rats were killed 120 minutes after voluntary dosing under early morning baseline conditions (~9:00 am (BLAM)). Stressed rats were voluntarily dosed 60 minutes before the onset of FS and killed 60 min after the start of FS (15 min, 25°C water). Graphs show hnRNA levels of *Klf2* (A), *Klf4* (B) *Klf9* (C) and *Klf15* (D). Data are shown as relative RNA copy number calculated using the Pfaffl method of analysis, standardised to the expression of the house keeping genes *Hprt1* and *Gapdh* (mean ± SEM, n=7-8 per group). Statistical analysis: two-way ANOVA; (A) *Klf2* hnRNA effect of drug: $F_{(2, 41)}$ =1.975, p=0.1975, effect of stress: $F_{(1, 41)}$=57.38, p<0.0001, interaction drug x stress: $F_{(2, 41)}$ =2.454, p=0.0985, (B) *Klf4* hnRNA effect of drug: $F_{(2, 41)}$=0.4071, p=0.6683, effect of stress: $F_{(1, 41)}$ =7.37, p=0.0097, interaction drug x stress: $F_{(2, 41)}$=1.858, p=0.1688, (C) *Klf9* hnRNA effect of drug: $F_{(2, 41)}$=1.388, p=0.2612, effect of stress: $F_{(1, 41)}$=272.9, p<0.0001, interaction drug x stress: $F_{(2, 41)}$ =8.799, p=0.0007, (D) *Klf15* hnRNA effect of drug: $F_{(2, 41)}$=1.142, p=0.3292, effect of stress: $F_{(1, 41)}$=212.4, p<0.0001, interaction drug x stress: $F_{(2, 41)}$=3.474, p=0.0404. Sidak's post hoc tests, *P<0.05, **P<0.01, ***P<0.001, ****P<0.0001 significantly different from BL within the same vehicle/drug treatment group. \$$P$<0.05, \$\$\$$P$<0.001, \$\$\$\$$P$<0.0001 significantly different from vehicle within the same BLAM or FS group.

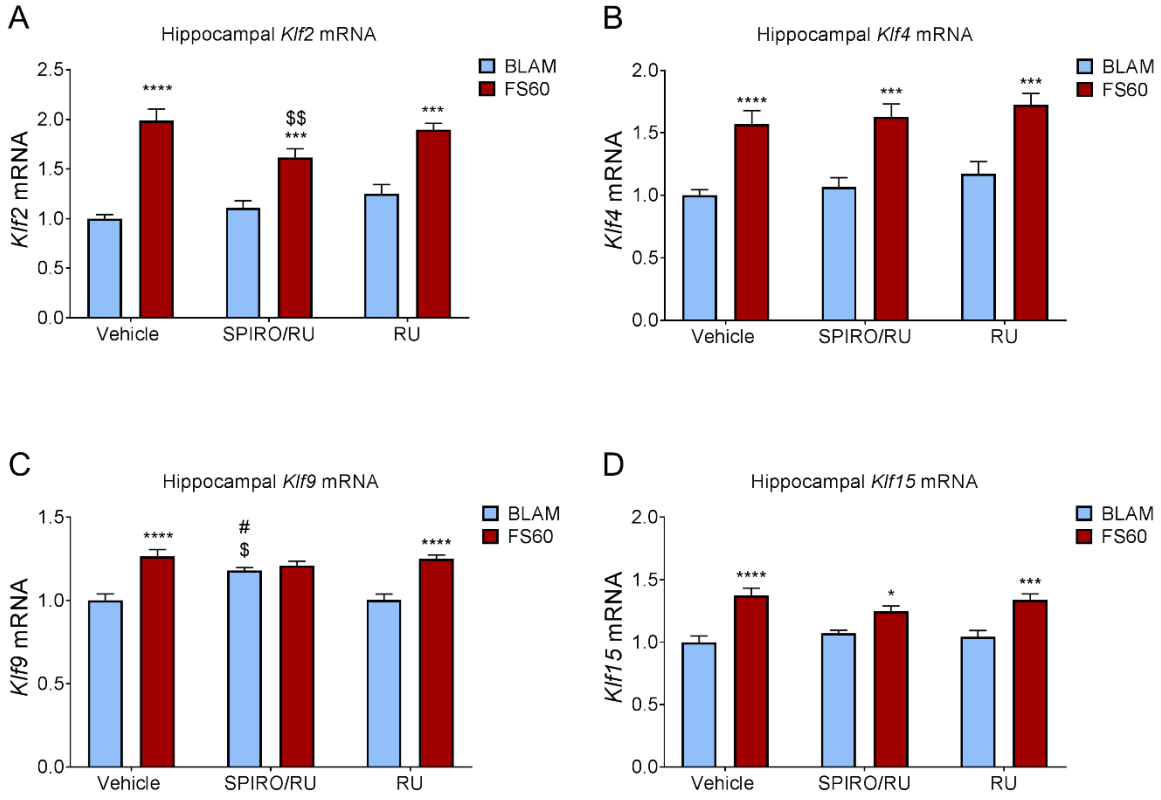

Figure 6.6 The effect of SPIRO and RU on hippocampal mRNA expression of KLFs under early baseline conditions and following acute stress

Rats were voluntarily dosed with vehicle, a combination of SPIRO (50 mg/kg) and RU (30mg/kg) or RU only (30mg/kg). Baseline rats were killed 120 minutes after voluntary dosing under early morning baseline conditions (~9:00 am (BLAM)). Stressed rats were voluntarily dosed 60 minutes before the onset of FS and killed 60 min after the start of FS (15 min, 25°C water). Graphs show mRNA levels of *Klf2* (A), *Klf4* (B) *Klf9* (C) and *Klf15* (D). Data are shown as relative RNA copy number calculated using the Pfaffl method of analysis, standardised to the expression of the house keeping genes *Hprt1* and *Gapdh* (mean ± SEM, n=7-8 per group). Statistical analysis: two-way ANOVA; (A) *Klf2* mRNA effect of drug: $F_{(2, 41)}$=3.287, p=0.0474, effect of stress: $F_{(1, 41)}$=112.1, p<0.0001, interaction drug x stress: $F_{(2, 41)}$=4.542, p=0.0165, (B) *Klf4* mRNA effect of drug: $F_{(2, 41)}$=1.763, p=0.1846, effect of stress: $F_{(1, 41)}$ = 62.31, <0.0001, interaction drug x stress: $F_{(2, 41)}$=0.006145, p=0.9939, (C) *Klf9* mRNA effect of drug: $F_{(2, 37)}$=2.802, p=0.0736, effect of stress: $F_{(1, 37)}$=47.84, p<0.0001, interaction drug x stress: $F_{(2, 37)}$=8.746, p=0.0008, (D) *Klf15* mRNA effect of drug: $F_{(2, 37)}$=0.25, p=0.7801, effect of stress: $F_{(1, 37)}$=52.55, p<0.0001, interaction drug x stress: $F_{(2, 37)}$=2.345, p=0.01100. Sidak's post hoc tests, **P*<0.05, ***P*<0.01, ****P*<0.001, *****P*<0.0001 significantly different from BL within the same vehicle/drug treatment group. $*P*<0.05, $$$*P*<0.001, $$$$*P*<0.0001 significantly different from vehicle within the same BLAM or FS group, #*P*<0.05 significantly different from RU treated within the same BLAM or FS group.

6.4.3 The effects of ADX on hippocampal RNA expression of *Klfs* under BLAM conditions and following acute FS stress

To examine the effects of the removal of endogenous CORT on downstream transcriptional responses following acute stress, rats underwent ADX or sham surgery. Alongside an intact group, sham and ADX rats were killed under BLAM conditions or at FS60. Plasma CORT levels and hippocampal transcriptional responses were determined. At FS60, plasma CORT levels (Figure 6.7) of sham rats were significantly increased compared with baseline sham and intact stressed rats. Following FS, ADX rats exhibited reduced levels of plasma CORT compared with rats undergoing sham surgery.

FS led to significant increases in hnRNA levels of *Klf2*, *Klf9* and *Klf15* in intact and sham rats but not in hnRNA Levels of *Klf4* (Figure 6.8). Under BLAM conditions and at FS60, hnRNA levels of *Klf9* (Figure 6.8.c) and *Klf15* (Figure 6.8.d) were lower in sham operated rats compared with intact rats. ADX abolished the stress-induced rises in hnRNA levels of *Klf2*, *Klf9* and *Klf15* observed in the intact and sham groups (Figure 6.8).

Intact and sham groups showed elevated mRNA levels of *Klf2*, *Klf4*, *Klf9* and *Klf15* at FS60 (Figure 6.9). In ADX rats, the FS effects on *Klf9* and *Klf15* mRNA were abolished but an attenuated, albeit significant effect of the stressor was retained regarding *Klf2* mRNA (figure 6.9). In contrast, ADX had no effect on the FS-evoked increase in *Klf4* mRNA (Figure 6.9).

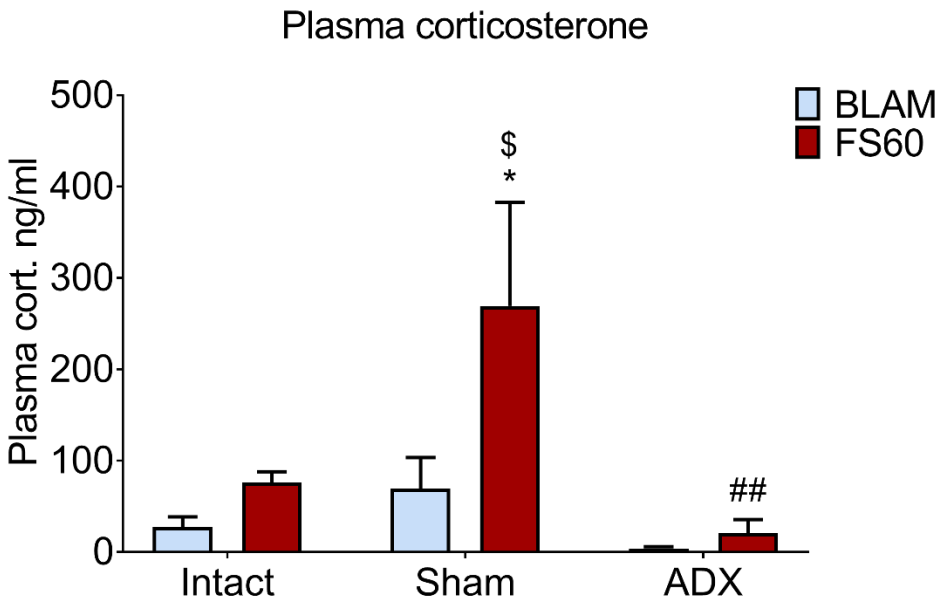

Figure 6.7 The effect of sham and ADX surgery on plasma CORT levels under BLAM conditions and following acute FS stress

Rats underwent sham surgery or adrenalectomy (ADX) and 1 week later, alongside an intact group, were killed under early morning baseline conditions (~9:00 am (BLAM)) or 30 min after the onset of FS (15 min, 25°C water). Plasma CORT levels are expressed as ng/ml (mean ± SEM, n=6 per group). Average CORT levels of ADX rats under baseline conditions; 3.92 ng/ml, and at FS60; 20.69 ng/ml. Statistical analysis: two-way ANOVA, effect of surgery: $F_{(2, 29)}$=5.196, p<0.05, effect of stress: $F_{(1, 29)}$ = 4.54, p<0.05, interaction stress x surgery: $F_{(2, 29)}$=1.874, p=0.172, Sidak's post hoc test *P<0.05 significantly different from BL within the same treatment group, \$$P$<0.05, significantly different from intact within same behaviour group, ##P <0.01, significantly different from sham within same behaviour group. Inter-assay coefficient of variation; 2.68%, intra-assay coefficient of variation; 5%.

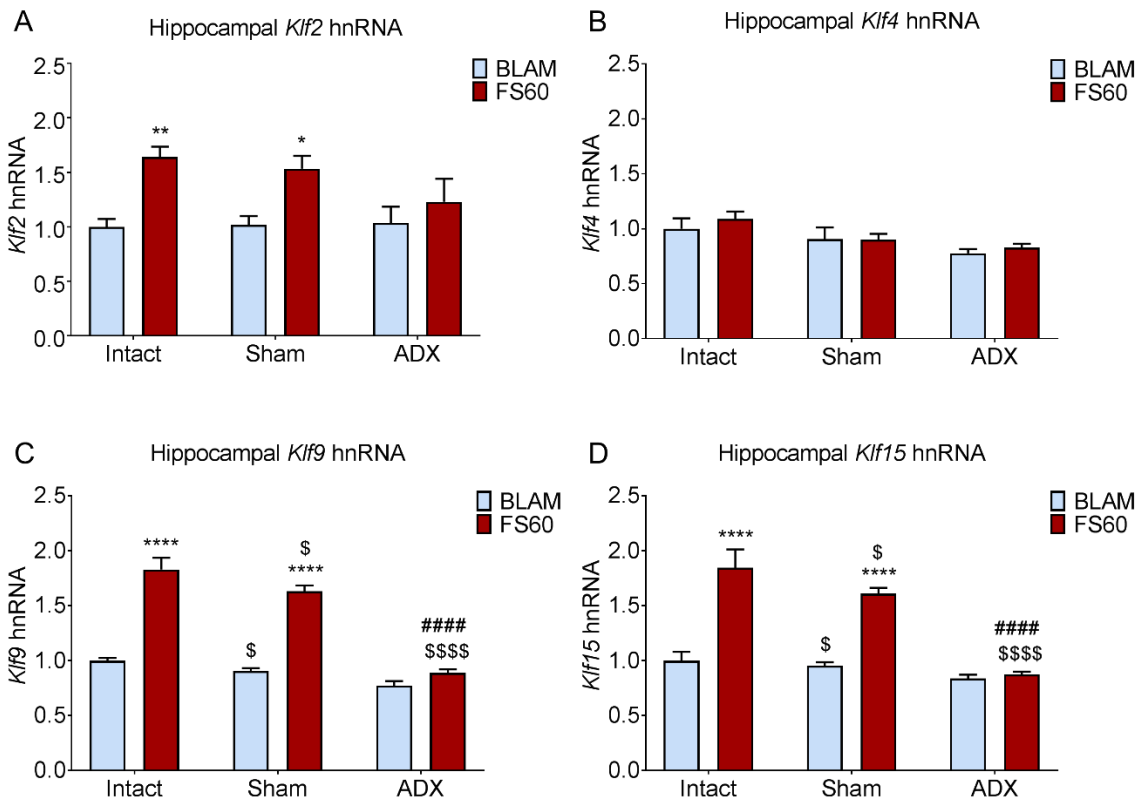

Figure 6.8 The effect of ADX on hippocampal hnRNA expression of KLF genes under BLAM conditions and following acute FS stress

Rats underwent sham surgery or adrenalectomy (ADX) and 1 week later, alongside an intact group, were killed under early morning baseline conditions (~9:00 am (BLAM)) or 60 min after the onset of FS (15 min, 25 °C water). Graphs show hnRNA levels of *Klf2* (A), *Klf4* (B) *Klf9* (C) and *Klf15* (D). Data are shown as relative RNA copy number calculated using the Pfaffl method of analysis, standardised to the expression of the house keeping genes *Hprt1* and *Ywhaz* (mean ± SEM, n = 6 per group). Statistical analysis: two-way ANOVA; (A) effect of surgery: $F_{(2, 29)}$=1.215, p=0.311, effect of stress: $F_{(1, 29)}$=19.6, p<0.001, interaction surgery x stress: $F_{(2, 29)}$=1.655, p=0.209, (B) effect of surgery: $F_{(2, 29)}$=5.529, p =0.0092, effect of stress: $F_{(1, 29)}$=0.620, p=0.438, interaction surgery x stress: $F_{(2, 29)}$=0.211, p=0.810, (C) effect of surgery: $F_{(2, 29)}$=57.44, p<0.0001, effect of stress: $F_{(1, 29)}$=148.5, p<0.0001, interaction surgery x stress: $F_{(2, 29)}$=23.09, p<0.0001, (D) effect of surgery: $F_{(2, 29)}$=24.17, p<0.0001, effect of stress: $F_{(1, 29)}$ =55.88, p<0.0001, interaction surgery x stress: $F_{(2, 29)}$=12.37, p=0.0001, Sidak's post hoc tests, *P<0.05, **P<0.01, ****P<0.0001 significantly different from BLAM within the same surgery group. $$P$<0.05, $$$P$<0.01, $$$$P$<0.001, $$$$$P$<0.0001 significantly different from intact within same behaviour group, ####P<0.0001 significantly different from sham within the same behaviour group.

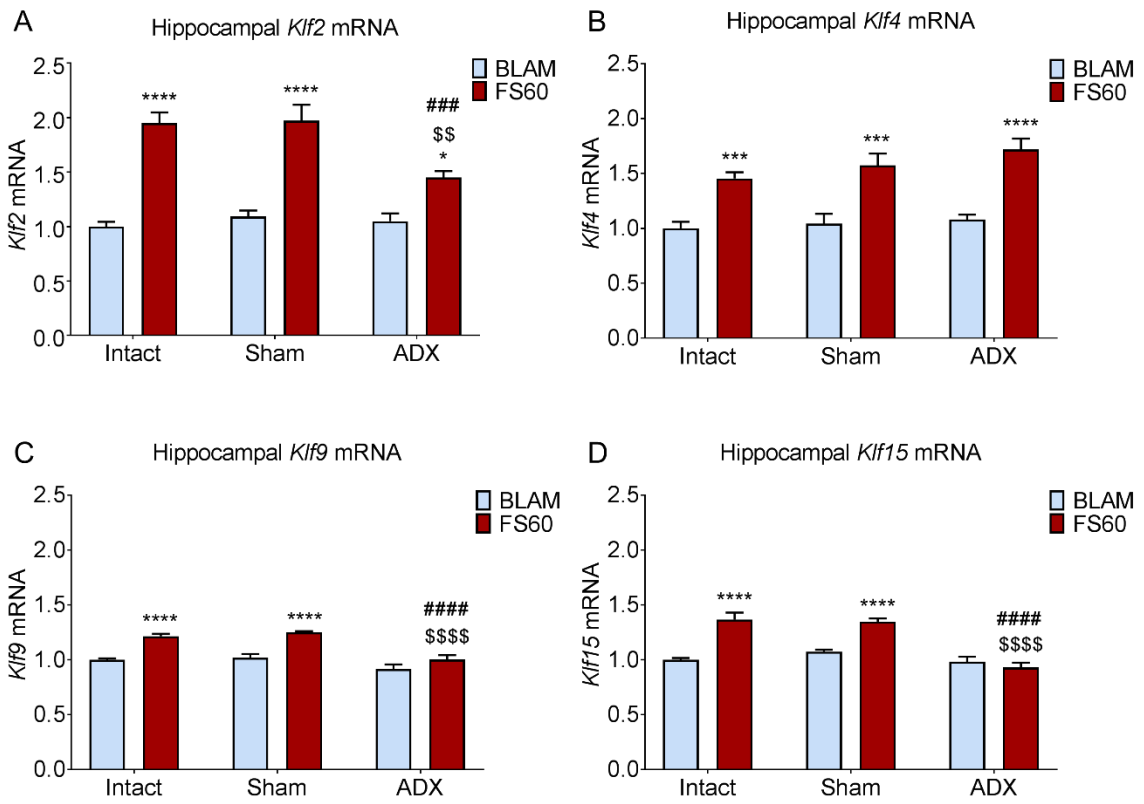

Figure 6.9 The effect of ADX on hippocampal mRNA expression of KLF genes under BLAM and following acute FS stress

Rats underwent sham surgery or adrenalectomy (ADX) and 1 week later, alongside an intact group, were killed under early morning baseline conditions (~9:00 am (BLAM)) or 60 min after the onset of FS (15 min, 25 °C water). Graphs show mRNA levels of *Klf2* (A), *Klf4* (B) *Klf9* (C) and *Klf15* (D). Data are shown as relative RNA copy number calculated using the Pfaffl method of analysis, standardised to the expression of the house keeping genes *Hprt1* and *Ywhaz* (mean ± SEM, n = 6 per group). Statistical analysis: two-way ANOVA; (A) effect of surgery: $F_{(2, 29)}$=5.624, p=0.0087, effect of stress: $F_{(1, 29)}$=107.4, p <0.0001, interaction surgery x stress: $F_{(2, 29)}$=5.615, p<0.01, (B) effect of surgery: $F_{(2, 29)}$=2.304, p =0.118, effect of stress: $F_{(1, 29)}$=69.78, p<0.0001, interaction surgery x stress: $F_{(2, 29)}$=0.663, p=0.523, (C) effect of surgery: $F_{(2, 29)}$=21.59, p<0.0001, effect of stress: $F_{(1, 29)}$=58.54, p<0.0001, interaction surgery x stress: $F_{(2, 29)}$=3.738, p=0.0359, (D) effect of surgery: $F_{(2, 29)}$=23.71, p<0.0001, effect of stress: $F_{(1, 29)}$=36.28, p<0.0001, interaction surgery x stress: $F_{(2, 29)}$=14.66, p<0.0001, Sidak's post hoc tests, *P<0.05, ***P<0.001, ****P<0.0001 significantly different from BLAM within the same surgery group. $$P$<0.05, $$$P$<0.01, $$$$$P$<0.0001 significantly different from intact within same behaviour group, #### P<0.0001 significantly different from sham within the same behaviour group.

6.5 Discussion

Findings of these experiments have shown, for the first time, the effects of antagonising genomically acting MRs and GRs on receptor binding to GREs within *Klfs* and associated transcriptional responses under acute stress and circadian conditions. Under baseline conditions, SPIRO and RU486 enhanced GR binding, and quite possibly MR binding, to *Klf* GREs. RNA expression was for the most part unaffected, however SPIRO/RU treatment did lead to higher *Klf9* mRNA expression at baseline. Following an acute FS stressor, SPIRO and RU486 had no effect on MR and GR binding to GREs within the *Klfs*, however RNA expression of the *Klfs* was attenuated by the combined SPIRO/RU treatment. Meanwhile, ADX fully abolished the FS-induced rise in RNA expression of *Klf9* and *Klf15,* while partially reducing the FS-triggered rise of *Klf2* mRNA expression. These results indicate that genomically acting MRs and GRs coregulate the expression of *Klfs* following an acute FS stressor. Blockade of MR and GR action (at the used dosages), however, is insufficient to fully abolish *Klf* induction, therefore alternative TFs appear to be contributing to the *Klf* transcriptional response. Removal of CORT by ADX fully abrogated the changes in *Klf9* and *Klf15* RNA transcription and partially attenuated changes in *Klf2* transcription, thus confirming the *Klfs* as GC-hormone target genes during the acute stress response.

Rats were administered a combination of SPIRO and RU486 rather than SPIRO alone. SPIRO has been shown to display a weak affinity for the GR (Couette et al., 1992), while RU486 displays no affinity for the MR (Baulieu, 1991). Therefore, administration of RU486 in combination with SPIRO would prevent potential GR binding by SPIRO from occurring. Preliminary data regarding the well characterised GC target genes, *Fkbp5, Per1* and *Sgk1,* indicated that administration of SPIRO alone was insufficient to attenuate the FS-induced transcriptional response. Moreover, administration of RU486 at a higher dose (100mg/kg), resulted in a much more potent antagonism of transcriptional responses. Here, we chose a dose of 30mg/kg of RU486 to co-administer alongside SPIRO, to determine whether an interaction was present between MR and GR antagonism. From a technical point of view, we had decided, to avoid potential flaws due to injection stress, to choose voluntary dosing to administer the MR and GR antagonists. A vehicle control group was also included to control for any effects of voluntary dosing. Under baseline conditions and at the peak of the stress-evoked rise in GC secretion (FS30), plasma CORT levels were virtually identical among all groups. Interestingly, at FS60, while plasma CORT levels had fallen in vehicle control rats as expected, plasma CORT levels remained

significantly elevated in SPIRO/RU486 and RU486 treated rats. It is possible that antagonism of the MR and GR by SPIRO and RU486 prevented MR- and GR-mediated negative feedback on the HPA-axis, thus prolonging CORT secretion by the adrenals (De Kloet and Reul, 1987). It is unclear, however, why selective blockade of the GR leads to higher plasma CORT in comparison with MR and GR blockade. It appears that MR antagonism is interfering with antagonism of the GR, however the precise mechanism needs to be investigated in the future.

The absence of an effect of SPIRO and/or RU486 on FS-induced hippocampal MR or GR binding to GREs within *Klf2, Klf9* or *Klf15* was not surprising. Both drugs behave as antagonists that compete with endogenous ligand (in this case CORT) for receptor binding. SPIRO competes with CORT for the LBD of MR (Corvol et al., 1981), while RU486 competes with CORT for the LBD of GR. Once bound by SPIRO or RU486, conformational changes ensue that allow DNA binding however without resulting in transcriptional activation (Baulieu, 1991). Under baseline conditions, however, levels of MR enrichment appear higher in vehicle-treated rats in comparison to the enrichment levels observed at baseline in hippocampus of rats in Chapter 5. Moreover, the lack of a FS-induced rise in MR binding to *Klf9* and *Klf15* GRE2 strongly suggested that baseline enrichment levels were elevated. It is possible that the act of voluntary dosing has an arousing/stimulating effect on the rat, inducing a small CORT response sufficient to occupy the high affinity MR (Reul et al., 1987) and lead to DNA-binding. As a no-treatment group was not included in the experiment, however, it is presently not possible to deduce whether MR binding levels were actually higher in vehicle-treated control rats. Enrichment levels may simply vary between cohorts of rats or between ChIP experiments. When investigating the MR, future experiments should include a non-vehicle control, as the receptor displays a high sensitivity to even small changes in CORT.

In vehicle-treated controls, GR enrichment levels under baseline conditions appear similar to those observed in previous experiments (Chapter 5). Moreover, in the control rats, a significant FS-induced rise in GR binding was seen at all *Klfs,* indicating that GR binding is unaffected by voluntary dosing under baseline conditions. In comparison to the MR, the GR is much less sensitive to small changes in CORT levels. This is due to the low affinity of GR for CORT, and as a result, GR occupancy and DNA binding is barely detectable under low CORT conditions (Reul et al., 1987). GR binding was, however, significantly increased under baseline conditions following SPIRO and/or RU486 treatment at *Klf2, Klf9* and *Klf15* GRE2. This is likely due to the GR becoming occupied by RU486, resulting in nuclear

translocation and DNA binding (Baulieu, 1991). For *Klf2* and *Klf15,* elevated levels of GR binding at baseline did not elicit a transcriptional response of these genes. *Klf9* mRNA levels in the SPIRO/RU-treated rats were, however, increased under baseline conditions compared with vehicle and RU486 treated rats, indicating that RU486 was behaving as an agonist rather than an antagonist under these conditions. Alternatively, the dose we chose in these experiments may explain our observations, as preliminary data indicated that 100mg/kg of RU486 elicited a far stronger attenuation of the FS-induced transcriptional response. It is possible that SPIRO was also exerting agonistic activity on *Klf9* under baseline conditions, however a non-vehicle control is needed to assess whether MR binding to *Klf9* was elevated during the circadian trough.

Treatment with RU486 alone had no effect on the RNA levels of any *Klf* examined, while combination of SPIRO and RU486 resulted in a partial attenuation of the FS-induced transcriptional activation of *Klf2* mRNA*, Klf9* hnRNA and *Klf15* hnRNA*.* The observation that antagonism of both receptors is required to induce an inhibitory effect on transcription suggests that heterodimerisation of receptors are taking place at GREs within *Klfs.* Compelling evidence for MR and GR heterodimerisation following FS has previously been shown at *Fkbp5, Per1* and *Sgk1* (Mifsud and Reul, 2016). It is possible that in the presence of RU alone (selective GR-blockade), MR may coregulate *Klf* expression by interacting with other co-factors, such as other members of the KLF family. Findings of transcription factor binding site motif analysis described in Chapter 3 indicated a high presence of KLF motifs within genomic loci bound by MRs and GRs, while pathway analysis predicted the KLFs as upstream regulators of genes in our ChIP-seq and RNA-seq datasets. Moreover, KLF15 has been shown to promote the transcription of *Klf3* in adipocytes. ChIP showed binding of KLF15 in the promoter of *Klf3* which was accompanied by increased mRNA expression of *Klf3* (Guo et al., 2018). KLF4 was shown, *in vitro,* to activate the promoter of the *Klf4* gene, while KLF5 exerted inhibitory effects via binding to the promoter of the *Klf4* gene (Dang et al., 2002). It is also possible that MR binding alone may lead to *Klf* transactivation, therefore examining the effects of SPIRO alone on *Klf* transactivation is needed. To establish whether heterodimerisation is occurring between MRs and GRs at *Klf* GREs, tandem ChIP could be employed as described by (Mifsud and Reul, 2016). ChIP for KLFs at KLF motifs in close proximity to GREs would enable the identification of candidate TFs that may be acting as coregulators of MR/GR regarding the transcriptional regulation of the *Klfs.*

Another explanation for our observations may be that RU486 is acting as an agonist at the concentration administered in these experiments (30 mg/kg). Many studies have reported agonistic and antagonistic effects of RU486 *in vitro*. Stimulation of cAMP signalling has been shown to result in agonistic activity of RU486 (Beck et al., 1993). Cell- and coactivator-specific agonistic effects of RU486 have also been demonstrated, with RU486 activating transcription in T47D breast cancer cell lines while negatively regulating transcription in HeLa cervical cancer cell lines. Agonistic activity of RU486 was further shown in the presence of the coactivator SRC-1, while the corepressor complexes SMRT inhibited RU486-induced transcription (Liu et al., 2002). At a dose of 200nM, RU486 was shown to reduce *Klf9* mRNA under baseline conditions and fully abolished CORT-induced transcriptional responses *in vivo*. SPIRO induced only a small attenuation in baseline and CORT-induced *Klf9* mRNA expression (Bonett et al., 2009). In foetal hippocampal neurons, RU486 (10µM) abolished DEX-mediated repression of total *Bdnf* mRNA, consistent with GR antagonism (Chen et al., 2017). Higher doses of RU486 than that used in our study may be required *in vivo* in order to elicit the antagonist effects required.

Although our results demonstrate an antagonistic effect of SPIRO, studies have reported agonistic effects. Cell- and promoter-specific agonist effects of SPIRO were demonstrated in hMR expressing HepG2 cells, H5 cell and CV1 cell lines. In HepG2 and H5 cell lines, SPIRO enhanced MMTV transcriptional activity in the presence of the MR ligand aldosterone. In CV1 cell lines, however, SPIRO demonstrated full antagonist activity at the highest concentration used (100 nM). The agonistic effects of SPIRO were shown to be promoter-dependent and of comparable efficiency to aldosterone (Massaad et al., 1997). The antagonistic effects of SPIRO may be gene-dependent, as the drug was shown to affect the transcripts of over 1,000 genes in activated mononuclear cells, leading to the downregulation of 831 genes and the upregulation of the remainder (Sonder et al., 2006). It is likely that the upregulation observed is due to antagonism of MR activity at negative GREs.

The absence of any effect of drug treatment on *Klf2* hnRNA expression and *Klf15* mRNA expression is likely due to the timepoint chosen to examine RNA levels. The results of our RNA-seq time course described in Chapter 3 indicated FS60 to be the timepoint at which the highest number of changes in gene expression are occurring, therefore this timepoint was chosen for these experiments. Based on findings of our FS timecourse in Chapter 5, however, we know that *Klf2* hnRNA levels have fallen considerably by FS60, therefore FS30 may have been a more suitable timepoint to detect the effects of drug treatment on *Klf2* hnRNA transcription. For *Klf9* and *Klf15,* a more optimal timepoint to examine

changes in transcription would be FS120, during which mRNA levels have risen significantly. Meanwhile, ADX fully attenuated the FS-induced rise of hnRNA and mRNA levels of *Klf9* and *Klf15.* mRNA levels of *Klf2,* however, were only partially attenuated by ADX, indicating that alternative coregulators acting independently of CORT regulate the transcription of this gene. Potential coregulators include the KLFs themselves, as pathway analysis described in Chapter 4 predicted a number of KLF family members to regulate the expression of MR and GR target genes.

RNA levels of *Klf4* were also investigated, as our ChIP-seq and RNA-seq experiments indicated that FS-induced changes in *Klf4* RNA expression was not regulated by genomically acting MRs and GRs. hnRNA and mRNA levels of *Klf4* were unaffected by SPIRO and/or RU486, thus indirectly confirming that the effects of SPIRO and RU486 on the RNA expression of the other investigated *Klf*s are a result of blocking MR and GR action. ADX also had no effect on the FS-induced rise in *Klf4* mRNA. Unpublished data from histone modification ChIP-seq shows constitutive formation of the histone modification H3S10p-14ac (which is associated with active, open chromatin) in proximity to *Klf4* (Price EM et al., unpublished observations). GRs have been shown to contribute to the formation of H3S10p-14ac via a non-genomic mechanism following FS stress (Bilang-Bleuel et al., 2005, Gutierrez-Mecinas et al., 2011). It is possible that in the absence of CORT, alternative coregulators contribute to H3S10p-14ac formation and subsequent induction of *Klf4.*

Overall, findings of these experiments contribute to the presently lacking knowledge regarding genomic regulation of the *Klfs* by MRs and GRs following acute stress. Clearly, MR and GR coregulate transcription of the *Klfs*, possibly by heterodimerisation at GREs. Other coregulators, however, are likely contributing to MR/GR regulation of *Klf* transactivation, as receptor antagonism induced only a partial attenuation of the transcriptional response. Probable candidates are the KLFs themselves, due to our observations of KLF motifs within MR and GR binding sites and predictions made by pathway analysis. Further exploration is required, however, to identify the coregulatory factors interacting with MRs and GRs to regulate *Klf* transactivation. Immunohistochemistry would allow the identification of candidate KLFs, while ChIP and tandem ChIP would enable the investigation of KLF binding and MR/GR co-binding following stress. KLF inhibitors or *Klf* KO animal models may facilitate further elucidation of the genomic regulation of the *Klfs* following exposure to acute stress.

Chapter 7 Unexpected effects of metyrapone on genomically acting MRs and GRs and GC target gene transcription in the rat hippocampus

7.1 Abstract

Genomically acting MRs and GRs bind to GREs within the DNA, exerting transcriptional responses of target genes following an acute stressful challenge. Antagonism of the MR and/or the GR, however, does not fully abrogate transcriptional responses. In chapter 6, the effects of administering antagonists of the MR and GR on receptor to GRE binding and associated transcriptional responses was examined in the rat hippocampus under acute stress conditions. We showed that antagonism of genomically acting MRs and GRs led to partial attenuation of the transcriptional responses of GC target genes. Removal of CORT by ADX, however, abrogated FS-induced transactivation of the *Klfs.* An alternative pharmacological mechanism of blocking CORT is using the CORT-synthesis blocker metyrapone (MET). How MET affects GC action at the genomic level, however, is still unclear.

Therefore, in this chapter, the effects of MET on plasma CORT levels and hippocampal MR and GR binding to GREs within the GC target genes *Fkbp5*, *Per1* and *Sgk1* as well as transcriptional responses of these genes are investigated under baseline and acute stress conditions in rats. For comparison, these endpoints were also examined in ADX rats. Results of these experiments revealed effects of metyrapone, which were contradictory to the expected GC-reducing effects of the drug. As a comparison, the effects of complete removal of endogenous GCs by bilateral ADX were additionally investigated. ADX completely abolished the effects of stress on MR/GR GRE-binding and *Fkbp5*, *Per1* and *Sgk1* transcriptional responses. This work shows that when using metyrapone unexpected effects at the genomic level need to be considered that may preclude proper interpretation of the data on the paradigm under investigation.

7.2 Introduction

Stress and circadian input were shown, in Chapter 3, to elicit transactivation and transrepression of thousands of genes in the rat hippocampus. The binding of genomically acting MRs and GRs to GREs in close proximity to or within these genes is believed to underlie the observed transcriptional responses, however the expression of many genes is activated/inhibited in the absence of receptor binding. Thus, it is unclear whether MR/GR binding is responsible for changes in RNA expression following exposure to stress or during the circadian drive. The genomic action of MRs and GRs is thought to underlie many GC-dependent behavioural and physiological changes observed following stress or circadian input. Thus, elucidating the mechanisms by which MRs and GRs regulate transcription is of critical importance.

In Chapter 6, we addressed this question by antagonising MRs and GRs and examining RNA levels under early morning baseline and stress conditions. Antagonism of both the MR and GR partially attenuated the FS-induced transcriptional responses of *Klf2, Klf9* and *Klf15*. ADX was shown to fully abolish the transcriptional responses of *Klf9* and *Klf15,* indicating that the removal of the endogenous source of CORT is required to block the effects of genomically acting MRs and GRs. ADX, however, is an invasive surgical procedure which has been shown to result in neuronal cell death (Sloviter et al., 1989) and behavioural changes such as increased anxiety levels (File et al., 1979). An alternative strategy would be to block or remove GC secretion from the adrenal glands. Metyrapone (MET), an inhibitor of the enzyme 11-β-hydroxylase (thus, preventing the conversion of deoxycorticosterone to CORT (Strashimirov and Bohus, 1966)), has been used to block endogenous GC synthesis in behavioural paradigms (Roozendaal et al., 1996, Liu et al., 1999). Until now, however, the consequences of metyrapone administration on the molecular effects of GCs at the genomic level have not been investigated.

Recently, an acute stressful challenge was shown to result in a substantial rise in the binding of MRs and GRs to GREs in *Fkbp5*, *Per1* and *Sgk1,* leading to enhanced transcriptional activity of the GC target genes (Mifsud & Reul, 2016). These findings were validated by our ChIP-seq and RNA-seq experiments described in Chapter 3, where we observed MR and GR peaks within GREs of *Fkbp5, Per1* and *Sgk1* in addition to changes in inRNA and exRNA expression. In contrast to *Klfs* investigated in Chapter 5 and 6, these genes are well-characterised in regards to GC hormone activity. *Fkbp5* is involved in the

regulation of GR binding by ligand by encoding for the steroid receptor immunophilin FKBP51; a negative regulator of GR sensitivity for CORT (Binder, 2009). *Per1* encodes for the PER1 protein; a member of the clock gene family essential for the circadian regulation of learning-induced histone modifications and hippocampal plasticity (Rawashdeh et al., 2014) while *Sgk1* is essential for spatial memory consolidation (Tsai et al., 2002). Given the important neurobiological roles of these genes, it is astonishing that the mechanisms underlying their transcriptional regulation following stress have hardly been examined.

Therefore, the aim of this final chapter was to study the effects of the enzyme inhibitor metyrapone on MR and GR binding to GREs within *Fkbp5*, *Per1* and *Sgk1* and transcriptional responses of these genes in the hippocampus under early morning baseline conditions and acute stress conditions. Although MET had no effect on (unstressed) control levels of CORT, the drug increased MR and GR to GRE binding within the GC target genes and the transcriptional activity of these genes. Acute FS stress as expected strongly increased plasma CORT levels, hippocampal MR and GR to GRE binding within *Fkbp5*, *Per1* and *Sgk1*, and transcriptional activity (mainly hnRNA levels) of these genes. MET attenuated, but not abolished, these effects of stress on plasma CORT and MR and GR to GRE binding. The drug effects on FS-induced transcriptional activity were gene-dependent with a reduction seen in *Fkbp5* hnRNA (but not *Fkbp5* mRNA), an enhancement in *Per1* hnRNA (but not *Per1* mRNA), and no effect on both *Sgk1* hnRNA and mRNA levels. In contrast, ADX completely abrogated the effects of FS stress on plasma CORT as well as hippocampal MR and GR to GRE binding and transcriptional responses. These results indicate that when aiming to elucidate genomic action of MRs and GRs via CORT suppression, ADX may be a more appropriate intervention than MET.

7.3 Materials and Methods

7.3.1 Animals

Adult male Wistar rats (150-175g on arrival) were purchased from Envigo (Oxon, UK) and group-housed (2-3 per cage). Rats were housed under standard lighting (lights on 05:00– 19:00 h, approximately 80-100 Lux) and environmentally controlled conditions (temperature 21 ± 1°C; relative humidity 40–60%) with food and water available *ad libitum*. All rats were handled daily (2 min per rat per day) for at least 5 days prior to experimentation to reduce non-specific handling stress on the day of the experiment.

7.3.2 Drug treatment

To block CORT mediated effects, rats were intraperitoneally (i.p.) injected with the 11-β-hydroxylase inhibitor metyrapone, or with the same amount of vehicle, as previously described in Chapter 2.

7.3.3 Surgical procedures

Rats underwent bilateral underwent bilateral ADX or sham surgery as described in Chapter 2. For RNA-qPCR, the group of rats are the same as described in Chapter 6.

7.3.4 Animal experiments

Metyrapone experiments were conducted between 7:00 am and 1:00 pm. Baseline rats received treatment with metyrapone or the respective vehicle and were killed 2 hrs later under baseline conditions. Rats received treatment with metyrapone or the respective vehicle 90 min prior to FS (15 min, 25 °C (±1) water) and were killed 30 min (FS30) or 60 min (FS60) after the start of FS. Full schedules of the metyrapone dosing experiments are shown in Table 2.1, Table 2.2 and Table 2.3.

ADX experiments were conducted between 9:00 am and 11:30 am. Rats were killed straight from the home cage under baseline conditions (~9:00 am (BLAM)) or following FS (15 min, 25 °C (±1) water). For ChIP, rats were killed 30 min (FS30) after the start of FS, for RNA rats were killed 60 min (FS60) after the start of FS.

7.3.5 Measurement of corticosterone by RIA

Plasma CORT concentrations were measured using a commercial CORT RIA Kit (MP Biomedicals) as described previously in Chapter 2.

7.3.6 ChIP-qPCR

Standard ChIP was performed as previously described in Chapter 2, from hippocampal tissues of single rats. The following antibodies; MR (MR H-300 antibody; sc11412X; Santa Cruz) or GR (GR H-300 antibody, sc8992X; Santa Cruz) were used. All samples (bounds and inputs) were diluted to a standardized concentration with nuclease-free water and analysed by qPCR using primers/probes listed in Table 2.6. Data are expressed as quantity of bound DNA divided by the respective quantity of input DNA (i.e., B/I), which is a measure of the enrichment of steroid receptor bound to specific genomic sequences.

7.3.7 RNA-qPCR

RNA was extracted as previously described in Chapter 2. RNA-qPCR was performed as described in Chapter 2 using primers and probes listed in Table 2.7 (hnRNA) and Table 2.8 (mRNA). Expression of hnRNA and mRNA in each sample was calculated based on the Pfaffl method of relative quantification (Pfaffl, 2001) and standardized to the expression of house- keeping genes listed in Table 2.9.

7.3.8 Statistical analysis

Data were statistically analysed using GraphPad Prism software. Results are presented as group means ± SEM; sample sizes are indicated in the figures. Multiple statistical comparisons were conducted with one-way or two-way ANOVA, and if significant, a Dunnett's or Sidak's post hoc test was performed. Significant differences within treatments group refers to drug treatment, while significant differences within behaviour groups refers to baseline or FS conditions. Statistical results are provided in the figures. $P<0.05$ was considered statistically significant.

7.4 Results

7.4.1 The effects of MET on plasma CORT levels under early morning baseline conditions and following acute FS stress

To determine the ability of MET to block CORT synthesis following exposure to an acute stressor, rats were killed at the peak of the stress-evoked plasma CORT rise 30 min after the start of an acute, 15 min FS challenge (FS30). Two doses of MET (75mg/kg or 100mg/kg) were administered to determine the optimal dose at which CORT synthesis is suppressed. Full details of the dosing schedule are shown in Table 2.1. At FS30, plasma CORT levels were significantly lower in rats receiving both doses of MET compared with non-injected and vehicle injected rats (Figure 7.1.a). Rats receiving vehicle injection had significantly higher plasma CORT levels compared with non-injected rats, indicating a potential injection stress. No significant difference between the two doses of MET were detected, however levels of CORT following 100mg/kg MET were observably lower than levels of CORT following 75mg/kg of MET.

Based on these results, a dose of 100mg/kg MET was selected for subsequent experiments as it produced maximal suppression of plasma CORT. Furthermore, to eliminate a potential CORT response due to injection stress, groups of rats received either a single or double injection of MET, with a 90-minute interval between repeated injections. Full details of the dosing schedule are shown in Table 2.2. Rats were injected once with vehicle, or once or twice with MET and killed under early baseline (BLAM) conditions or at FS30. At FS30, rats receiving both single and double injection of MET exhibited significantly decreased levels of CORT compared to vehicle-injected rats (Figure 7.1.b). Furthermore, rats receiving a double injection of metyrapone had significantly lower CORT levels at FS30 compared with rats receiving a single injection of MET, demonstrating that administration of a second dose is required to attenuate a CORT response due to injection stress. Levels of CORT, however, were significantly elevated at FS30 compared to BLAM in rats receiving both single and double injections of MET.

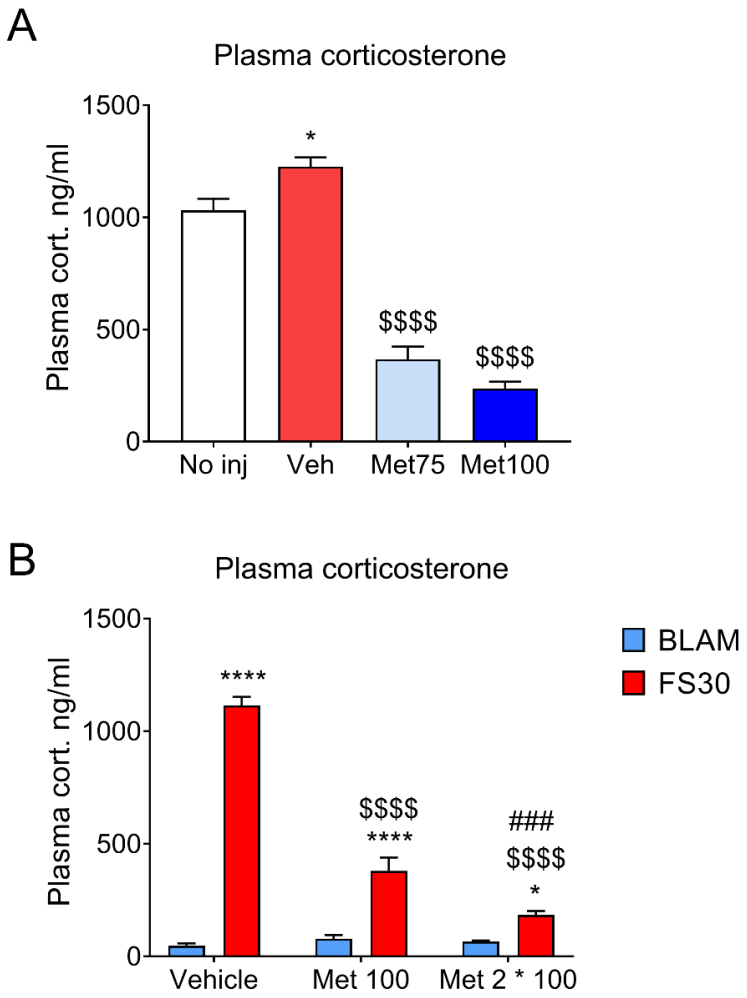

Figure 7.1 The effect of MET on plasma CORT levels under BLAM conditions and following acute FS stress

To determine the optimal dose of MET to suppress CORT synthesis following an acute stressor (A) rats were injected with vehicle, 75 mg/kg or 100 mg/kg MET, 90 minutes before the onset of FS. To prevent a potential CORT response due to injection stress (B) rats were injected with vehicle or MET (100mg/kg) and killed under early morning baseline conditions (BLAM) or underwent FS 90 minutes later. All rats were killed 30 min after the start of FS (15 min, 25 °C water). A second injection of MET (100mg/kg) was administered to a subset of rats, with a 90-minute interval between injections. Plasma CORT levels are expressed as ng/ml (mean ± SEM, n=6-8 per group). Statistical analysis: one-way ANOVA (A) $F_{(3, 19)}$=107.9, p<0.0001, Dunnett's post hoc test, *P <0.05, significantly different from non-injected control, $$$$ P <0.0001, significantly different from vehicle-injected control. Two-way ANOVA (B), effect of drug: $F_{(2, 42)}$=120.2 p<0.0001, effect of stress: $F_{(1, 42)}$=388.4, p<0.0001, interaction drug x stress: $F_{(2, 42)}$ =133.7, p<0.0001, Sidak's post hoc test, ****P<0.0001 significantly different from BL within the same vehicle/drug treatment group, $$$$$P$<0.0001 significantly different from vehicle within the same BLAM or FS group, ###P<0.001 significantly different from metyrapone single injection within the same BLAM or FS group. Inter-assay coefficient of variation; 2.68%, intra-assay coefficient of variation for (A) 3.94%, (B) 3.25%.

7.4.2 The effects of MET on hippocampal MR and GR binding to GREs in *Fkbp5, Per1* and *Sgk1* under early morning baseline conditions and following acute FS stress

To examine MR and GR binding to GREs, rats were injected once with vehicle, or once or twice with MET and killed under early baseline (BLAM) conditions or at FS30. Full details of the dosing schedule are shown in Table 2.2. In rats receiving vehicle injection, levels of MR binding at *Fkbp5*, *Per1* and *Sgk1* (Figure 7.2) were increased following FS. At FS30, rats receiving both single and double injections of MET had lower levels of MR binding at *Fkbp5* compared with rats receiving vehicle (Figure 7.2). At *Per1*, MR binding was decreased following both single and double injections of metyrapone (Figure 7.2). Rats receiving a single injection of metyrapone had decreased MR binding to *Sgk1* compared with vehicle injected rats at FS30 (Figure. 7.2). There were no differences in the binding of either receptor between rats receiving single or double injections of metyrapone.

In rats receiving vehicle injection, levels of GR binding at *Fkbp5*, *Per1* and *Sgk1* (Figure 7.3) were increased following FS. At FS30, rats receiving both single and double injections of MET had significantly lower levels GR binding at *Fkbp5* compared with rats receiving vehicle (Figure 7.3). At *Per1*, GR binding was decreased following double injection of MET only at FS30 compared with vehicle (Figure 7.3). GR binding to *Sgk1* was unaffected by either single or double injection of MET (Figure 7.3).

The FS effect was not completely abolished in either group, however, with a single injection of metyrapone resulting in increased binding of GR to all GREs tested (Figure 7.3) and MR at *Fkbp5* and *Per1* (Figure 7.2) while double injection of metyrapone led to elevated MR binding at *Fkbp5* and *Sgk1* following FS (Figure 7.2). There was also an increase in MR binding at *Sgk1* under baseline conditions following double injection of metyrapone compared to vehicle injection (Figure 7.2).

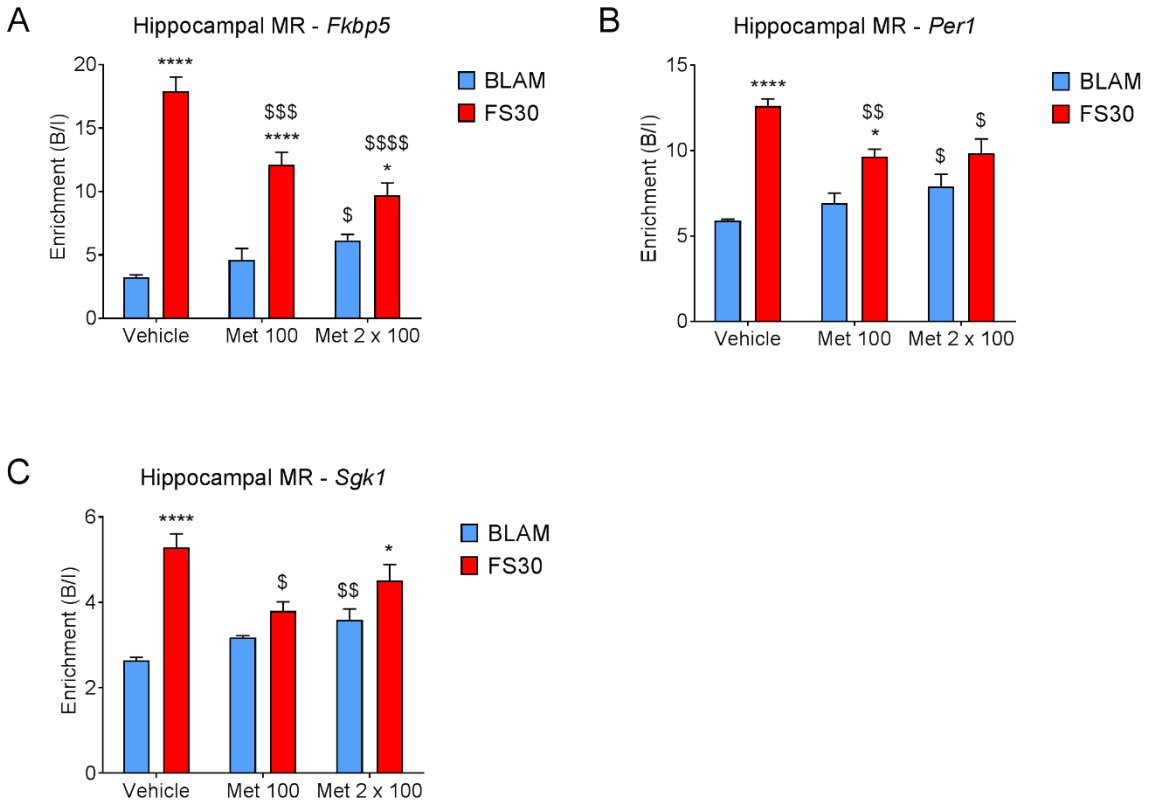

Figure 7.2 The effects of MET on hippocampal MR binding to GREs in *Fkbp5, Per1* and *Sgk1* under BLAM conditions and following acute FS stress

Rats were injected with vehicle or MET (100mg/kg) 90 minutes before the onset of FS. A second injection of MET (100mg/kg) was administered to a subset of rats, with a 90-minute interval between injections. Rats were killed under BLAM conditions or 30 min after the start of FS (15 min, 25 °C water). Graphs show enrichment of MR, expressed as bound/input (mean ± SEM, n=3-4 per group), at GREs within *Fkbp5* (A), *Per1* (B) and *Sgk1* (C). Statistical analysis: two-way ANOVA; (A) effect of drug: $F_{(2, 17)}$=5.603, p =0.0135, effect of stress: $F_{(1, 17)}$ =161.6, p<0.0001, interaction drug x stress: $F_{(2, 17)}$=22.43, p<0.0001, (B) effect of drug: $F_{(2, 17)}$=1.363, p=0.2825, effect of stress: $F_{(1, 17)}$=62.5, p<0.0001, interaction drug x stress: $F_{(2, 17)}$=9.143, p=0.0020, (C) effect of drug: $F_{(2, 17)}$=3.297, p=0.0616, effect of stress: $F_{(1, 17)}$=50.47, p<0.0001, interaction drug x stress: $F_{(2, 17)}$=9.787, p =0.0015. Sidak's post hoc test, **P* <0.05, *****P*<0.0001 significantly different from BL within the same treatment group, $*P*<0.05, $$*P*<0.01, $$$*P*<0.001, $$$$*P*<0.0001 significantly different from vehicle within the same behaviour group.

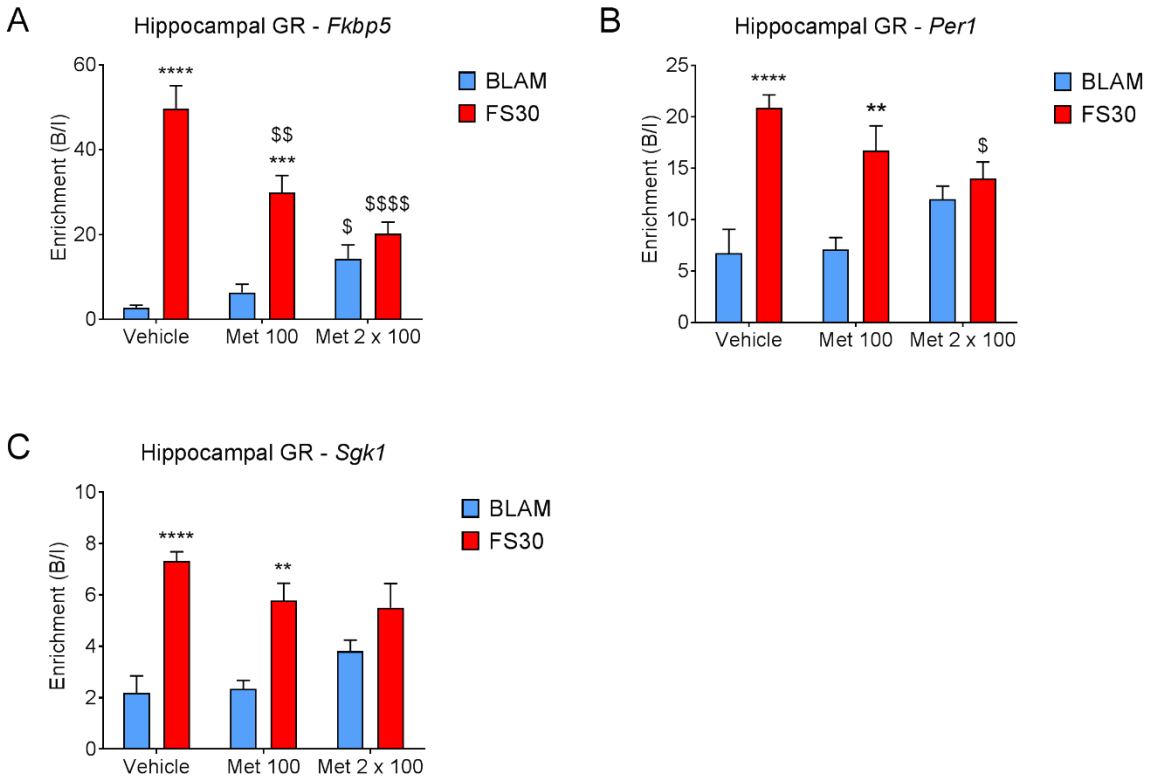

Figure 7.3 The effects of MET on hippocampal GR binding to GREs in *Fkbp5, Per1* and *Sgk1* under BLAM conditions and following acute FS stress

Rats were injected with vehicle or MET (100mg/kg) 90 minutes before the onset of FS. A second injection of MET (100mg/kg) was administered to a subset of rats, with a 90-minute interval between injections. Rats were killed under BLAM conditions or 30 min after the start of FS (15 min, 25 °C water). Graphs show enrichment of GR, expressed as bound/input (mean ± SEM, n=3-4 per group), at GREs within *Fkbp5* (A), *Per1* (B) and *Sgk1* (C). (A) effect of drug: $F_{(2, 16)}$=4.629, p=0.0259, effect of stress: $F_{(1, 16)}$=92.65, p<0.0001, interaction drug x stress: $F_{(2, 16)}$=20.54, p<0.0001, (B) effect of drug: $F_{(2, 18)}$ =0.6013, p=0.5587, effect of stress: $F_{(1, 18)}$ = 36.53, p<0.0001, interaction drug x stress: $F_{(2, 18)}$ = 6.187, p=0.0090, (C) effect of drug: $F_{(2, 18)}$=0.7892, p=0.4693, effect of stress: $F_{(1, 18)}$=48.13, p<0.0001, interaction drug x stress: $F_{(2, 18)}$=4.058, p=0.0351. Sidak's post hoc test, **P<0.01, ***P<0.001, ****P<0.0001 significantly different from BL within the same treatment group, \$$P$<0.05, \$\$$P$<0.01, \$\$\$\$$P$<0.0001 significantly different from vehicle within the same behaviour group.

7.4.3 The effects of MET on hippocampal RNA expression of *Fkbp5, Per1* and *Sgk1* under early morning baseline conditions and following acute FS stress

Rats were injected twice with vehicle or MET and killed under early morning baseline (BLAM) conditions or 60 minutes after the start of FS (FS60). Full details of the dosing schedule are shown in Table 2.3. Plasma CORT and RNA levels were examined to determine the effects of vehicle and MET injection under these conditions on plasma CORT levels and RNA transcription. Following acute stress, plasma CORT levels (Figure 7.4) were significantly elevated in vehicle injected rats, while a double injection of MET significantly attenuated the FS-induced rise in CORT secretion.

RNA levels of *Fkbp5, Per1* and *Sgk1* were subsequently examined following acute stress. Under baseline conditions, hnRNA levels of *Fkbp5, Per1*and *Sgk1* were elevated following MET injection (Figure 7.5), in comparison with vehicle injection. In vehicle injected rats, hnRNA levels of *Fkbp5*, *Per1* and *Sgk1* were elevated following acute stress (Figure 7.5). At FS60, levels of *Fkbp5* hnRNA were lower following MET injection (Figure 7.5), while levels of *Per1* hnRNA were higher following MET injection, in comparison with vehicle injection (Figure 7.5).

Under baseline conditions, mRNA levels of *Fkbp5, Per1*and *Sgk1*were elevated following MET injection, in comparison with vehicle injection (Figure 7.6). In vehicle injected rats, mRNA levels of *Per1* and *Sgk1* were elevated following acute stress (Figure 7.5). MET injection resulted in elevated mRNA levels of *Fkbp5* at FS60 compared with vehicle injected rats at FS60 (Figure 7.6). Levels of *Per1* mRNA were increased at FS60 compared to BLAM following MET injection (Figure 7.6).

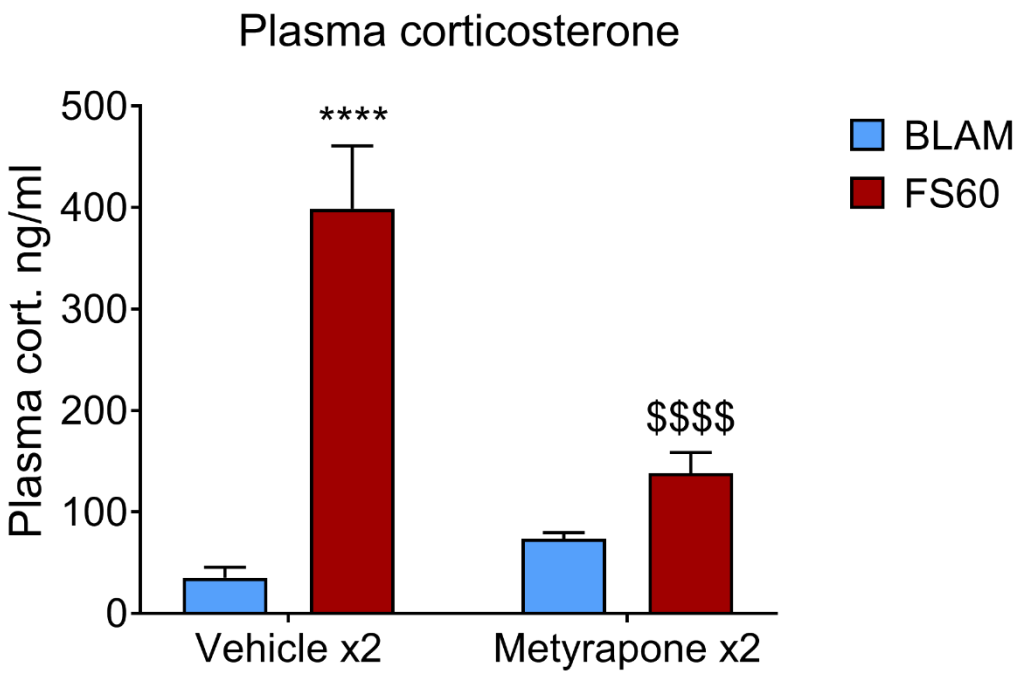

Figure 7.4 The effect of MET on plasma CORT levels under BLAM conditions and following acute FS stress

Rats were injected twice with vehicle or MET (100mg/kg) 90 minutes before the onset of FS, with a 90-minute interval between injections. Rats were killed under BLAM conditions or 60 min after the start of FS (15 min, 25 °C water). Plasma CORT levels are expressed as ng/ml (mean ± SEM, n=6 per group). Statistical analysis: two-way ANOVA; effect of drug: $F_{(1, 19)}$=10.31, p=0.0046, effect of stress: $F_{(1, 19)}$=38.39, p<0.0001, interaction drug x stress: $F_{(1, 19)}$=18.75, p=0.0004. Sidak's post hoc test, ****P<0.0001 significantly different from BL within the same treatment group, $$$$$P$<0.0001 significantly different from vehicle within the same behaviour group. Inter-assay coefficient of variation; 2.68%, intra-assay coefficient of variation; 2.44%

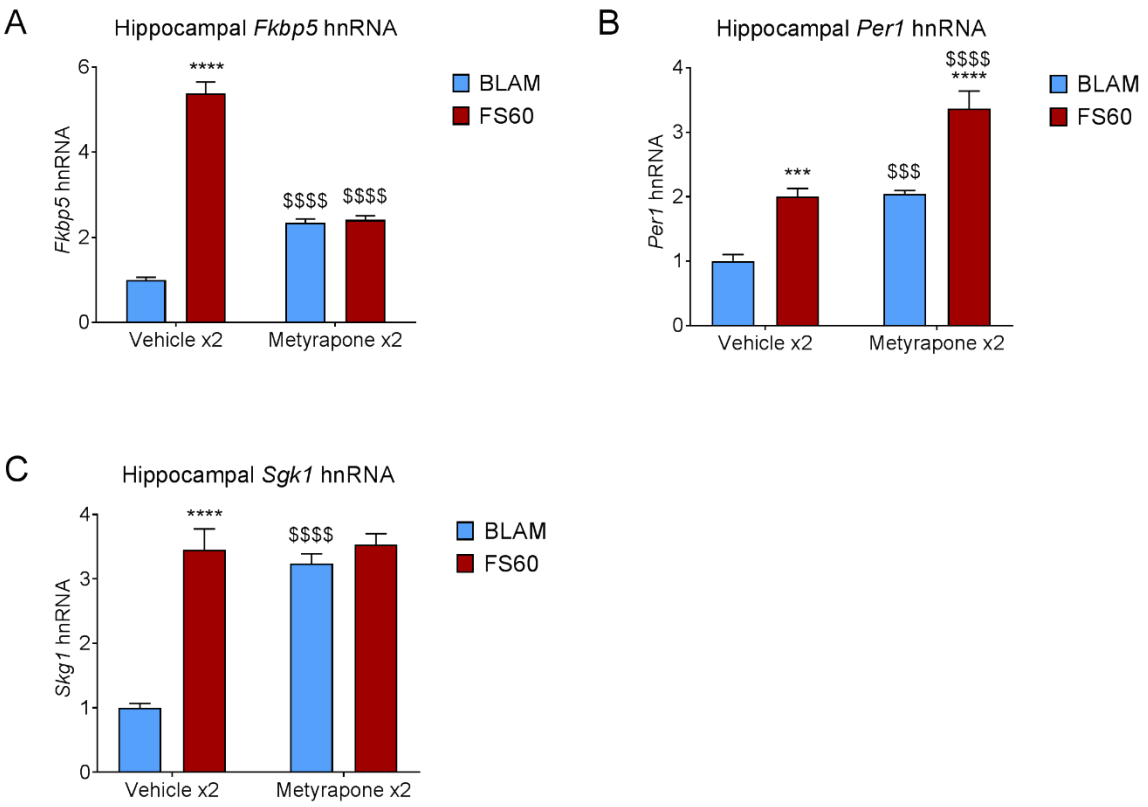

Figure 7.5 The effect of MET on hnRNA levels of *Fkbp5, Per1* and *Sgk1* under BLAM conditions and following acute FS stress

Rats were injected twice with vehicle or MET (100mg/kg) 90 minutes before the onset of FS, with a 90-minute interval between injections. Rats were killed under BLAM conditions or 60 min after the start of FS (15 min, 25 °C water). Graphs show hnRNA levels of *Fkbp5* (A), *Per1* (B) and *Sgk1* (C). Data are shown as relative RNA copy number calculated using the Pfaffl method of analysis, standardised to the expression of the house keeping genes *Hprt1* and *Ywhaz* (mean ± SEM, n=6 per group). (A) effect of drug: $F_{(1, 20)}$=28.42, p<0.0001, effect of stress: $F_{(1, 20)}$=212.9, p<0.0001, interaction drug x stress: $F_{(1, 20)}$ =199.6, p<0.0001, (B) effect of drug: $F_{(1, 20)}$=56.49, p<0.0001, effect of stress: $F_{(1, 20)}$=52.48, p<0.0001, interaction drug x stress: $F_{(1, 20)}$=1.027, p=0.3229, (C) effect of drug: $F_{(1, 20)}$=33.13, p<0.0001, effect of stress: $F_{(1, 20)}$=46.63, p<0.0001, interaction drug x stress: $F_{(1, 20)}$=28.89, p<0.0001. Sidak's post hoc test, **P*<0.05, ****P*<0.001, *****P*<0.0001 significantly different from BL within the same treatment group, $*P*<0.05, $$$*P*<0.001, $$$$*P*<0.0001 significantly different from vehicle within the same behaviour group.

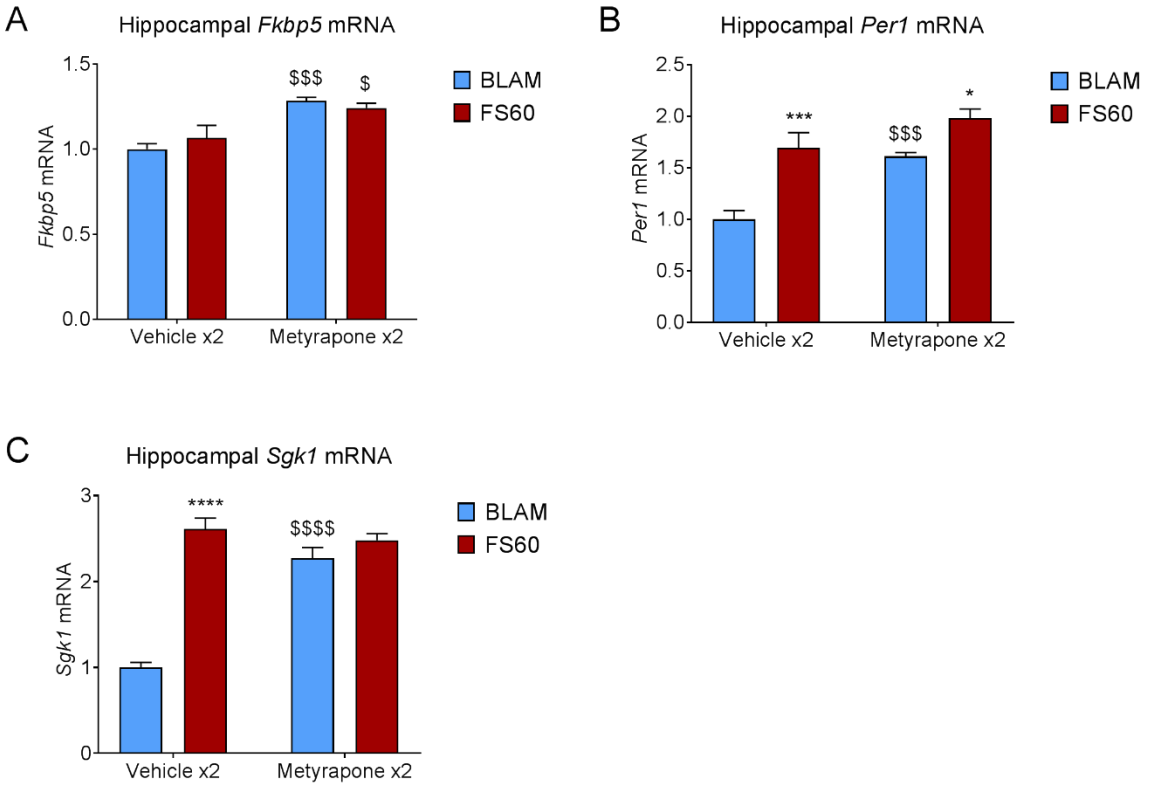

Figure 7.6 The effect of MET on mRNA levels of *Fkbp5, Per1* and *Sgk1* under BLAM conditions and following acute FS stress

Rats were injected twice with vehicle or MET (100mg/kg) 90 minutes before the onset of FS, with a 90-minute interval between injections. Rats were killed under BLAM conditions or 60 min after the start of FS (15 min, 25 °C water). Graphs show mRNA levels of *Fkbp5* (A), *Per1* (B) and *Sgk1* (C). Data are shown as relative RNA copy number calculated using the Pfaffl method of analysis, standardised to the expression of the house keeping genes *Hprt1* and *Ywhaz* (mean ± SEM, n=6 per group). (A) effect of drug: $F_{(1, 20)}$=27.48, p<0.0001, effect of stress: $F_{(1, 20)}$=0.07551, p=0.7863, interaction drug x stress: $F_{(1, 20)}$=1.527, p=0.2309, (B): effect of drug: $F_{(1, 20)}$=21.13, p=0.0002, effect of stress: $F_{(1, 20)}$=29.65, p<0.0001, interaction drug x stress: $F_{(1, 20)}$=2.762, p=0.1122, (C) effect of drug: $F_{(1, 20)}$=32.04, p<0.0001, effect of stress: $F_{(1, 20)}$=81.45, p<0.0001, interaction drug x stress: $F_{(1, 20)}$=48.42, p<0.0001. Sidak's post hoc test, ***P<0.001, ****P<0.0001 significantly different from BL within the same treatment group, $$$$P$<0.001, $$$$$P$<0.0001 significantly different from vehicle within the same behaviour group.

7.4.4 The effects of ADX on plasma CORT levels under early morning baseline conditions and following acute FS stress

Rats underwent ADX to determine whether the removal of the bodies endogenous source of CORT would prevent the genomic activity of MRs and GRs following acute stress. A group of rats underwent sham surgery which involved an identical surgical procedure to ADX without removal of the adrenals, to determine whether surgery alone had any effect on the CORT response and subsequent receptor activity. An intact group was also included for comparison. Rats were killed under early morning baseline conditions (~9:00 am (BLAM)) or 30 min after the onset of FS (FS30).

At FS30, plasma CORT was increased in intact and sham rats (Figure 7.7). ADX completely abolished the FS induced rise in plasma CORT at FS30 and under baseline conditions, no differences in plasma CORT levels were observed between ADX, sham or intact rats.

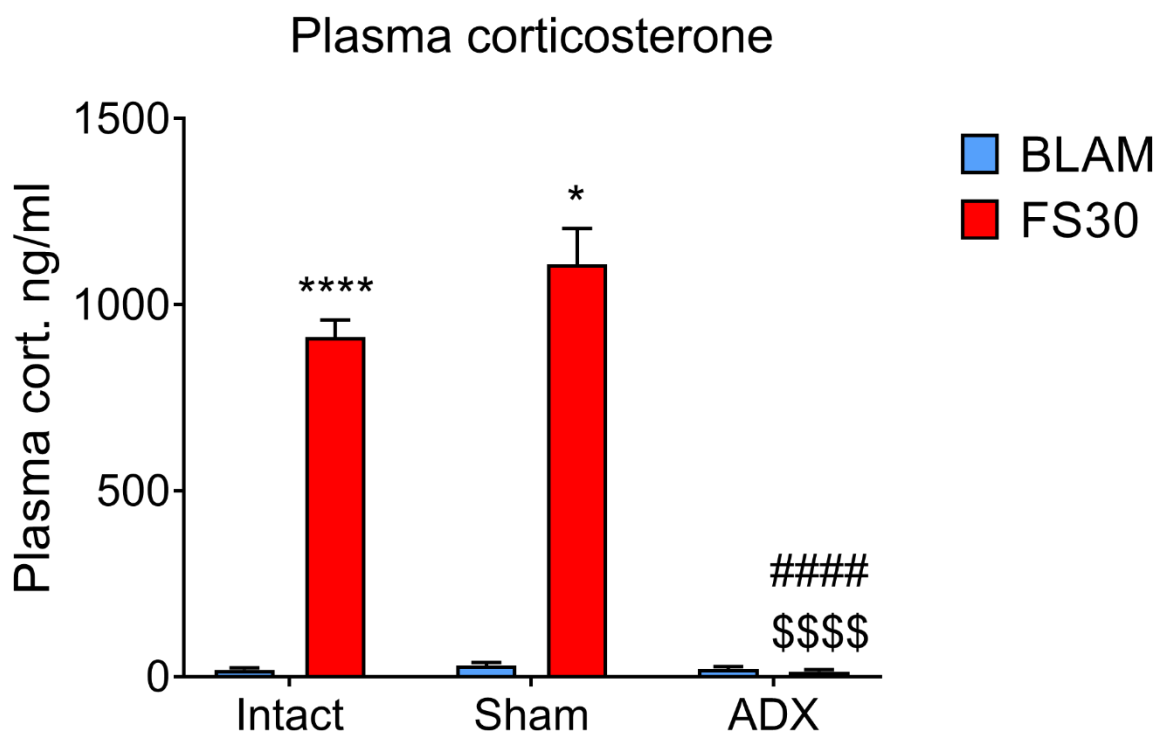

Figure 7.7 The effect of ADX on plasma CORT levels under BLAM conditions and following acute FS stress

Rats underwent sham or ADX surgery and alongside an intact group, were killed under early morning baseline conditions (~9:00 am (BLAM)) or killed 30 min after the start of FS (15 min, 25 °C water). Plasma CORT levels are expressed as ng/ml (mean ± SEM, n=4 per group). Average CORT levels for intact rats; 17.51 ng/ml and sham rats; 29.51 ng/ml at baseline, and ADX rats at baseline; 20.17 ng/ml and FS60; 12.72 ng/ml. Statistical analysis: two-way ANOVA; effect of surgery: $F_{(2, 18)}$=87.11, p<0.0001, effect of stress: $F_{(1, 18)}$=325.8, p<0.0001, interaction surgery x stress: $F_{(2, 18)}$=85.4, p<0.0001. Average levels under BLAM conditions, Sidak's post hoc test, *P<0.05, ***P<0.001 significantly different from BL within the same treatment group, $$$$$P$<0.0001 significantly different from intact within the same behaviour group, ####P<0.0001 significantly different from sham within the same behaviour group. Inter-assay coefficient of variation; 2.68%, intra-assay coefficient of variation; 3.68%.

7.4.5 The effects of ADX on hippocampal MR and GR binding to GREs within *Fkbp5, Per1* and *Sgk1* under early morning baseline conditions and following acute FS stress

Rats underwent ADX to determine whether the removal of the bodies endogenous source of CORT would prevent the genomic activity of MRs and GRs following acute stress. Intact, sham and ADX rats were killed under early baseline conditions (~9:00 am (BLAM)) or 30 min after the onset of FS (FS30).

MR and GR binding to GREs within *Fkbp5, Per1* and *Sgk1* following FS was subsequently examined. At FS30, MR binding was increased at *Fkbp5* and *Per1* in intact and sham animals (Figure 7.8). At *Sgk1,* MR binding was increased following acute stress in intact rats only (Figure 7.8). ADX abolished the FS-induced rise in MR binding at *Fkbp5*, *Per1* and *Sgk1* (Figure 7.8). Under baseline conditions, levels of MR enrichment were lower in ADX rats compared with intact and sham rats at *Per1* and *Sgk1* (Figure 7.8). Following acute stress, GR binding was increased at *Fkbp5*, *Per1* and *Sgk1* (Figure 7.9) in intact and sham rats. ADX abolished the FS-induced rise in GR binding at *Fkbp5*, *Per1* and *Sgk1* (Figure 7.9).

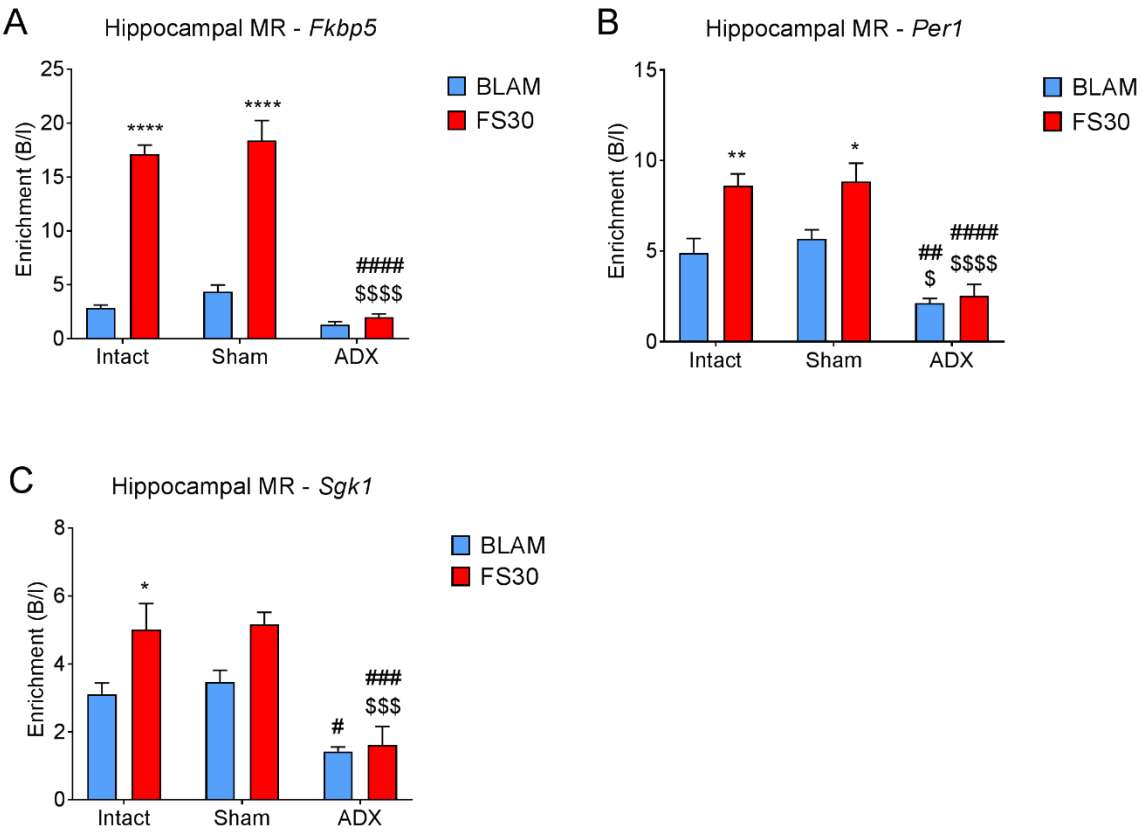

Figure 7.8 The effects of ADX on hippocampal MR binding to GREs in *Fkbp5, Per1* and *Sgk1* under BLAM conditions and following acute FS stress

Rats underwent sham or ADX surgery and alongside an intact group, were killed under early baseline conditions (~7:00 am (BLAM)) or killed 30 min after the start of FS (15 min, 25 °C water). Graphs show enrichment of MR, expressed as bound/input (mean ± SEM, n=3-4 per group), at GREs within *Fkbp5* (A), *Per1* (B) and *Sgk1* (C). Statistical analysis: two-way ANOVA; (A) effect of surgery: $F_{(2, 18)}$=69.81, p<0.0001, effect of stress: $F_{(1, 18)}$=177.3, p<0.0001, interaction surgery x stress: $F_{(2, 18)}$=38.41, p<0.0001, (B) effect of surgery: $F_{(2, 18)}$=31.32, p<0.0001, effect of stress: $F_{(1, 18)}$=18.77, p=0.0004, interaction surgery x stress: $F_{(2, 18)}$=3.366, p=0.0573, (C) effect of surgery: $F_{(2, 18)}$=22.11, p<0.0001, effect of stress: $F_{(1, 18)}$=10.79, p=0.0044, interaction surgery x stress: $F_{(2, 18)}$=1.99, p=0.1673. Sidak's post hoc test, **P*<0.05, ***P*<0.01, *****P*<0.0001 significantly different from BL within the same treatment group, $*P*<0.05, $$$*P*<0.001, $$$$*P*<0.0001 significantly different from intact within the same behaviour group, #*P*<0.05, ##*P*<0.01, ###*P*<0.001, ####*P*<0.0001 significantly different from sham within the same behaviour group.

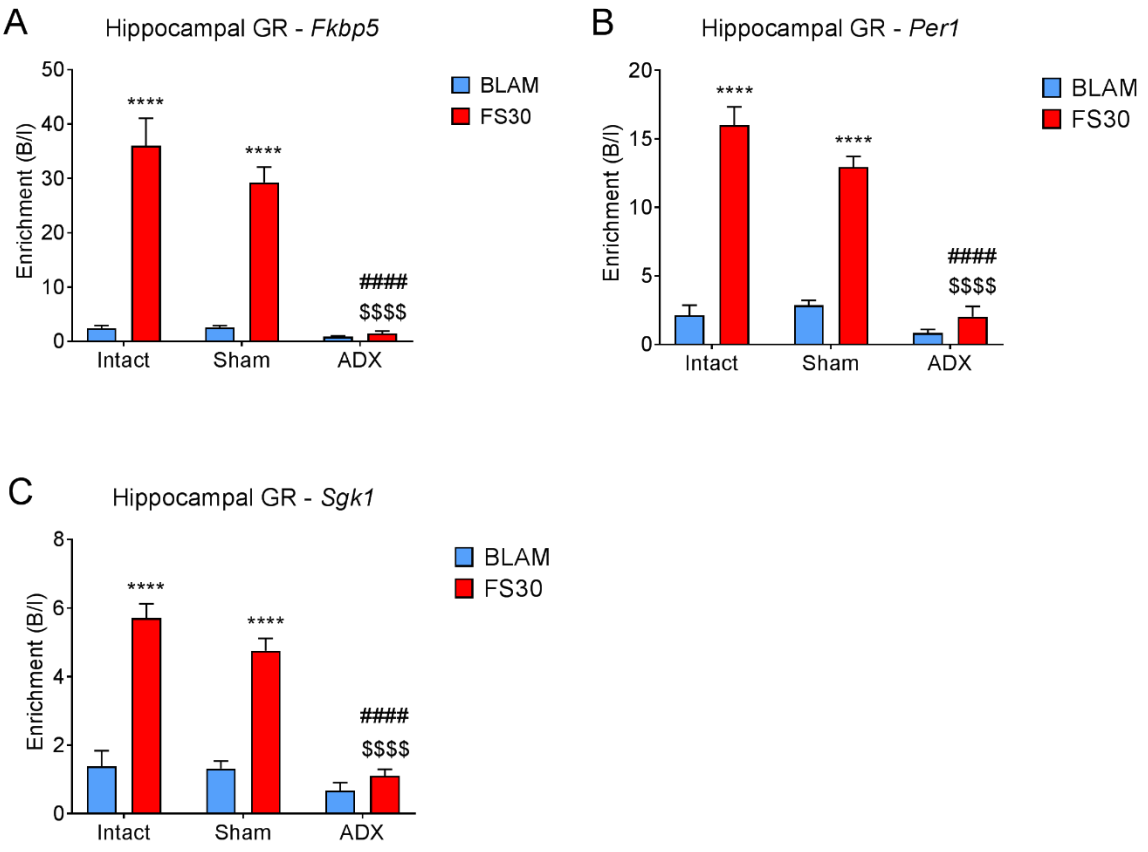

Figure 7.9 The effects of ADX on hippocampal GR binding to GREs in *Fkbp5, Per1* and *Sgk1* under BLAM conditions and following acute FS stress

Rats underwent sham or ADX surgery and alongside an intact group, were killed under early baseline conditions (~7:00 am (BLAM)) or killed 30 min after the start of FS (15 min, 25 °C water). Graphs show enrichment of GR, expressed as bound/input (mean ± SEM, n=3-4 per group), at GREs within *Fkbp5* (A), *Per1* (B) and *Sgk1* (C). Statistical analysis: two-way ANOVA; (A) effect of surgery: $F_{(2, 18)}$=32.31, p<0.0001, effect of stress: $F_{(1, 18)}$=108, p<0.0001, interaction surgery x stress: $F_{(2, 18)}$=26.47, p<0.0001, (B) effect of surgery: $F_{(2, 18)}$=54.47, p<0.0001, effect of stress: $F_{(1, 18)}$=169, p <0.0001, interaction surgery x stress: $F_{(2, 18)}$=34.12, p<0.0001, (C) effect of surgery: $F_{(2, 18)}$=36.01, p<0.0001, effect of stress: $F_{(1, 18)}$=107.3, p<0.0001, interaction surgery x stress: $F_{(2, 18)}$=18.86, p<0.0001. Sidak's post hoc test, ****P<0.0001 significantly different from BL within the same treatment group, $$$$$P$<0.0001 significantly different from intact within the same behaviour group, ####P<0.0001 significantly different from sham within the same behaviour group.

7.4.6 The effects of ADX on hippocampal RNA expression of *Fkbp5, Per1* and *Sgk1* under early morning baseline conditions and following acute stress

As described in Chapter 6, rats underwent ADX to determine whether the removal of the bodies endogenous source of CORT would prevent the FS-induced rise in hippocampal RNA expression of *Fkbp5, Per1* and *Sgk1*. Intact, sham and ADX rats were killed under early baseline conditions (~9:00 am (BLAM)) or 60 min after the onset of FS (FS60).

At FS60, plasma CORT levels were not increased in intact or ADX rats (Chapter 6 – Figure 6.7). There was, however, an increase in CORT levels in sham rats at FS60, indicating a potential effect of surgery. Removal of the adrenals abolished the potential stress effect of surgery, however, as plasma CORT levels were decreased in ADX rats compared with sham rats.

Following FS, hnRNA levels of *Fkbp5*, *Per1* and *Sgk1* hnRNA were increased in both intact and sham rats (Figure 7.10). ADX completely abolished the FS-induced rise in hnRNA levels of *Fkbp5*, *Per1* and *Sgk1.* At FS60, ADX rats had lower hnRNA levels of *Fkbp5*, *Per1* and *Sgk1* compared with intact and sham rats (Figure 7.10).

Under baseline conditions and following acute stress, mRNA levels of *Fkbp5* were lower in ADX rats compared with intact and sham rats (Figure 7.11). Following FS, mRNA levels of *Per1* and *Sgk1* hnRNA were increased in both intact and sham rats (Figure 7.11). ADX completely abolished the FS-induced rise in mRNA levels of *Per1* and *Sgk1*. At FS60, ADX rats had lower mRNA levels of *Per1* and *Sgk1* compared with intact and sham rats (Figure 7.11).

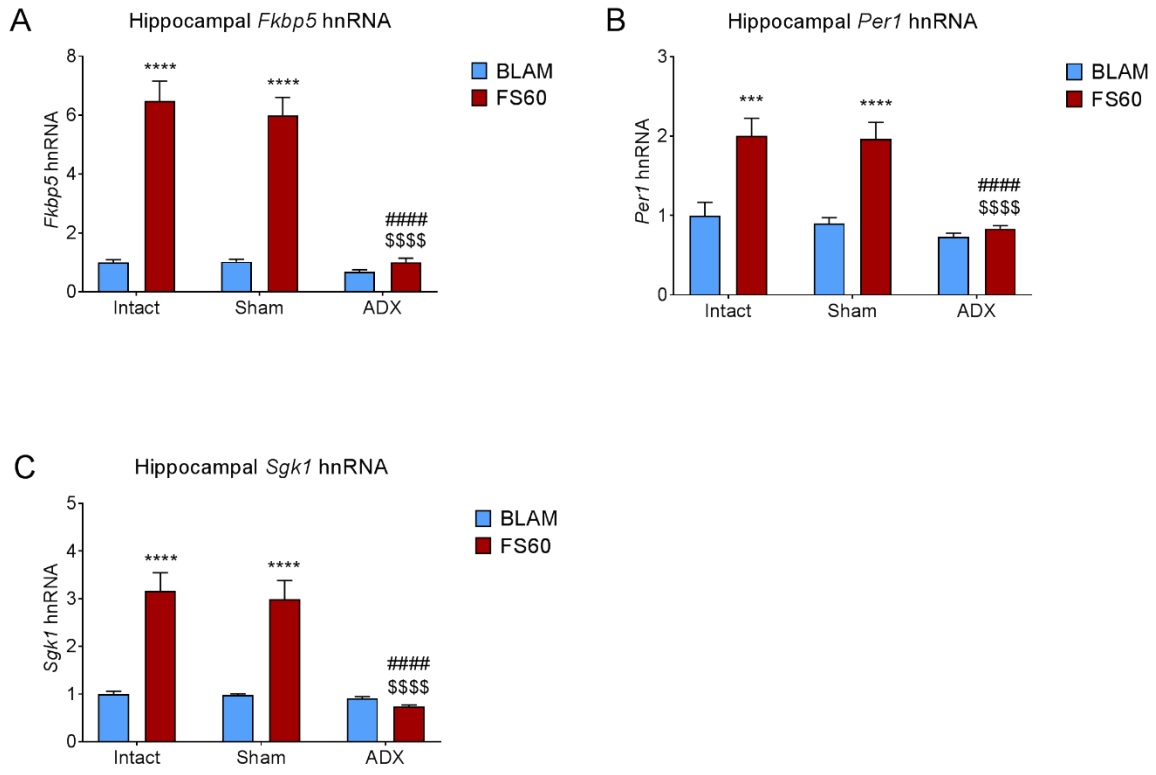

Figure 7.10 The effect of ADX on hnRNA levels of *Fkbp5, Per1* and *Sgk1* under BLAM conditions and following acute FS stress

Rats underwent sham or ADX surgery and alongside an intact group, were killed under early baseline conditions (~7:00 am (BLAM)) or killed 60 min after the start of FS (15 min, 25 °C water). Graphs show hnRNA levels of *Fkbp5* (A), *Per1* (B) and *Sgk1* (C). Data are shown as relative RNA copy number calculated using the Pfaffl method of analysis, standardised to the expression of the house keeping genes *Hprt1* and *Gapdh* (mean ± SEM, n=6 per group). Statistical analysis: two-way ANOVA; (A) effect of surgery: $F_{(2, 29)}$=32.8, p<0.0001, effect of stress: $F_{(1, 29)}$=126.4, p<0.0001, interaction surgery x stress: $F_{(2, 29)}$=25.47, p<0.0001, (B): effect of surgery: $F_{(2, 29)}$=13.42, p<0.0001, effect of stress: $F_{(1, 29)}$=34.27, p<0.0001, interaction surgery x stress: $F_{(2, 29)}$=6.069, p=0.0063, (C) effect of surgery: $F_{(2, 29)}$=17.45, p<0.0001, effect of stress: $F_{(1, 29)}$=49.3, p<0.0001, interaction surgery x stress: $F_{(2, 29)}$=15.18, p<0.0001. Sidak's post hoc test, ***P<0.001, ****P<0.0001 significantly different from BL within the same treatment group, $$$$$P$<0.0001 significantly different from intact within the same behaviour group, #### P<0.0001 significantly different from sham within the same behaviour group.

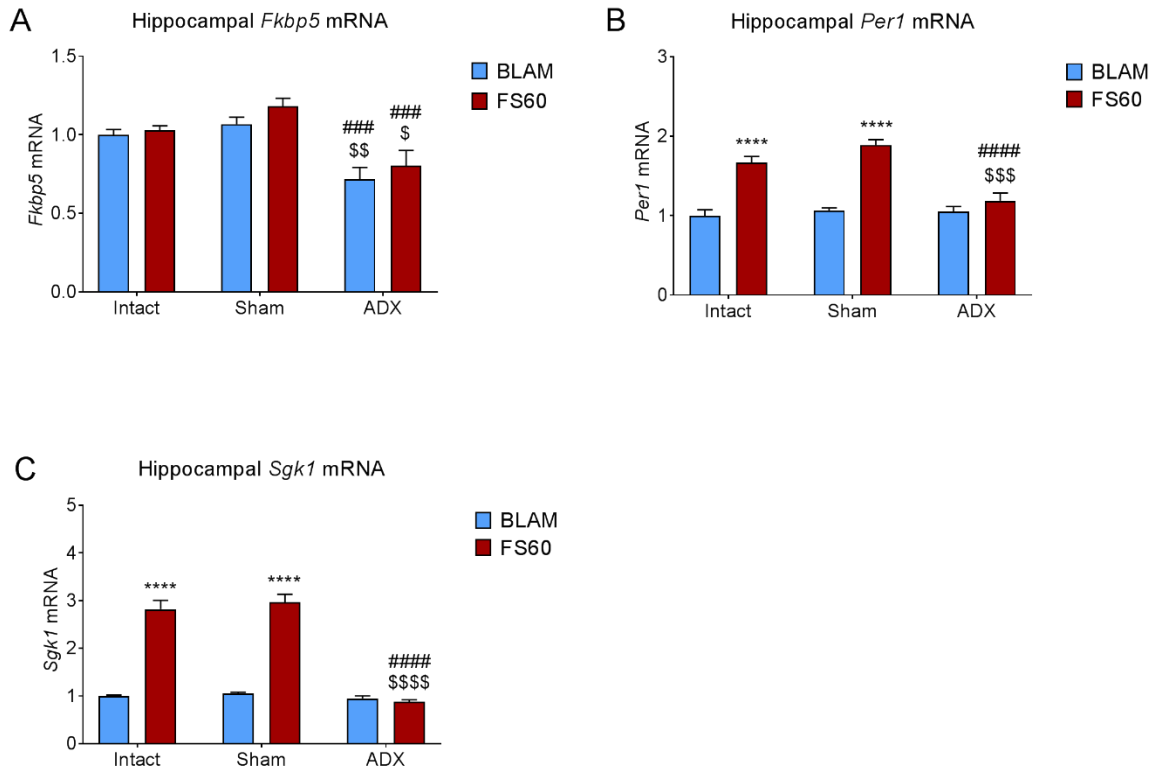

Figure 7.11 The effect of ADX on mRNA levels of *Fkbp5, Per1* and *Sgk1* under BLAM conditions and following acute FS stress

Rats underwent sham or ADX surgery and alongside an intact group, were killed under early baseline conditions (~7:00 am (BLAM)) or killed 60 min after the start of FS (15 min, 25 °C water). Graphs show mRNA levels of *Fkbp5* (A), *Per1* (B) and *Sgk1* (C). Data are shown as relative RNA copy number calculated using the Pfaffl method of analysis, standardised to the expression of the house keeping genes *Hprt1* and *Gapdh* (mean ± SEM, n=6 per group). Statistical analysis: two-way ANOVA; (A) effect of surgery: $F_{(2, 29)}$=21.02, p<0.0001, effect of stress: $F_{(1, 29)}$=2.089, p=0.1045, interaction surgery x stress: $F_{(2, 29)}$=0.3, p=0.7431, (B): effect of surgery: $F_{(2, 29)}$=13.29, p<0.0001, effect of stress: $F_{(1, 29)}$=91.85, p<0.0001, interaction surgery x stress: $F_{(2, 29)}$=13.26, p<0.0001, (C) effect of surgery: $F_{(2, 29)}$=60, p<0.0001, effect of stress: $F_{(1, 29)}$=189.7, p<0.0001, interaction surgery x stress: $F_{(2, 29)}$=51.26, p<0.0001. Sidak's post hoc test, ****P<0.0001 significantly different from BL within the same treatment group, $$P$<0.05, $$$P$<0.01, $$$$P$<0.001, $$$$$P$<0.0001 significantly different from intact within the same behaviour group, ###P<0.001, ####P<0.0001 significantly different from sham within the same behaviour group.

7.5 Discussion

This study reveals unexpected genomic effects in the hippocampus following metyrapone treatment which appear to be unrelated to the drug's effects on GC secretion. Despite failing to exert any effect on CORT levels under baseline conditions, metyrapone treatment resulted in enhanced MR and GR to GRE binding within the GC target genes and increased transcriptional activity of these genes. Metyrapone reduced stress-induced GC levels, however failed to fully attenuate the stress response. Following exposure to acute stress, drug treatment led to a partial inhibition of MR and GR to GRE binding and transcriptional activation in some cases. Thus, under stress conditions, the observed changes in MR and GR binding and transcriptional activity after metyrapone treatment appear to be the combined result of unspecific, GC-unrelated effects (apparent under early baseline conditions) and GC-reducing effects. In particular regarding effects on transcriptional activity, the drug effects were gene dependent. In contrast, ADX abolished the stress effects on plasma CORT as well as hippocampal MR and GR to GRE binding and transcriptional responses. These clear-cut genomic effects directly correspond with the absence of endogenous GCs as a result of the removal of the adrenals.

ChIP data show that vehicle-treated control rats as well as intact and sham-ADX rats present very low MR and GR binding to GREs within the classical GC target genes *Fkbp5*, *Per1* and *Sgk1*. FS resulted in significant increases in receptor binding to these GREs. These results are highly consistent with previously reported findings in (untreated) intact rats (Mifsud and Reul, 2016). Similarly, the FS-induced RNA responses in the vehicle-treated, intact and sham-operated rats paralleled previously published data (Mifsud & Reul, 2016). This present study shows that ADX completely abolished the stress-evoked responses in receptor binding and gene transcription indicating that the presence of endogenous GCs is crucial for these responses. Earlier work has shown that CORT is metabolized rapidly and MRs and GRs become unoccupied within a few hours post-ADX (Reul et al., 1987) . Thus, similarly, in the present study in the case of ADX, MRs and GRs will have become devoid of ligand shortly after withdrawal of CORT from the drinking water. This data shows for the first time that these receptors indeed require ligand binding in order to interact with GREs *in vivo* after stress.

The purpose of this study was to investigate the role of endogenous GCs in baseline and stress-induced genomic responses in GC target genes by using the CORT-synthesis inhibitor metyrapone. Treatment with this drug, however, produced contradictory results with regard to plasma CORT levels versus MR and GR to GRE binding and RNA responses concerning the genes *Fkbp5*, *Per1* and *Sgk1*. Metyrapone attenuated, albeit not abolished, the stress-induced increases in plasma CORT and GRE-binding of MR and GR. In view of the drug's effect on GC levels, a reduction in stress-induced receptor binding was expected but was not as stark as may have been predicted given the strong reduction in stress-evoked CORT levels. Surprisingly, however, although metyrapone produced no detectable changes in circulating GC levels in the unstressed control rats, drug treatment resulted in significant increases in MR binding and also to some extent GR binding (i.e. *Fkbp5*) to GREs within the target genes. These observations are rather surprising as CORT levels were unchanged. A possible reason for the elevated MR binding after metyrapone treatment may be 11-deoxycorticosterone (DOC), the CORT precursor known to accumulate after inhibition of 11β-hydroxylase (Daniel and Newell-Price, 2015). DOC is a mineralocorticoid with very high affinity for binding to MR (Funder, 2010) and is thought to be responsible for some of the side effects of metyrapone treatment (e.g. hypertension, hypokalaemia, oedema) observed in humans treated for instance for Cushing's disease (Juszczak et al., 2016). As metyrapone has been shown to increase plasma levels of ACTH in a dose-dependent manner (Rotllant et al., 2002), increases in plasma ACTH may potentiate the build-up of DOC.

As hippocampal MRs are at least 75-80% occupied under early morning baseline conditions (Reul et al., 1987, Reul and de Kloet, 1985), DOC could bind to the 20-25% rest-capacity in MR binding potentially resulting in the enhanced MR to GRE binding observed after metyrapone. Whilst this perhaps may be an explanation for the increased MR to GRE binding after metyrapone under control conditions, it fails to explain the elevated GR to GRE binding after drug administration under these conditions. Increased DOC levels after metyrapone may not be as relevant for GR, as this steroid has been reported to possess very low affinity for binding to GRs. DOC has been shown to occupy the GR in mouse fibroblasts (Brookes et al., 2012), however further evidence is needed to determine whether DOC is binding GR in this instance. Based on our recent study (Mifsud and Reul, 2016), it may be argued that possibly increased GR to GRE binding may be indirectly brought about through heterodimerization with MR whose GRE-binding is found to be enhanced after metyrapone. This is however an unlikely possibility as, under these control conditions, the occupancy of GRs by CORT will be very low and thus

the receptor would not be in a GRE-binding state (Reul et al., 1987, Reul and de Kloet, 1985). Thus, presently, the mechanisms underlying the increased MR and GR to GRE binding are unclear. Elevated post-metyrapone DOC levels can partially provide an explanation. Most likely, other, as yet unknown, effects of the enzyme inhibitor are very likely to play a role in the observations made in the drug-treated control rats.

In view of the diverse effects of metyrapone on the binding of MR and GR to *Fkbp5*, *Per1* and *Sgk1* GREs under control and stress conditions, it is difficult to explain the effects of the drug on the responses in hnRNA and mRNA of these genes. The increased hnRNA and mRNA levels observed under baseline conditions following metyrapone administration appear to correspond with the enhanced MR and GR to GRE binding under these conditions. The stress-induced responses in hnRNA after metyrapone treatment are highly varied. The drug inhibited, enhanced, or had no effects on the stress-induced changes in *Fkbp5* hnRNA, *Per1* hnRNA, and *Sgk1* hnRNA, respectively. These results appear not to point to a single, consistent mechanism underpinning the gene transcriptional effects of metyrapone. Factors contributing to these distinct effects may include differences in the relative contribution of MR and GR to gene activity, inherent differences between genes regarding transcriptional regulation (e.g. multiple GREs within genes or in enhancer regions, chromatin looping mechanisms), and differences in the timeline of transcriptional activation and RNA processing. ADX, in contrast, produced highly consistent effects on both receptor to GRE binding as well as gene transcriptional responses.

It is also plausible that metyrapone could activate other transcription factors (TFs) which bind to responsive elements within *Fkbp5, Per1* and *Sgk1* leading to enhanced gene transcription under baseline conditions and following acute stress. A likely candidate is the progesterone receptor (PR); a member of the steroid and nuclear hormone receptor superfamily alongside the MR and GR. PRs share many structural similarities with the MR and GR (Conneely et al., 1986, Jeltsch et al., 1986) and their expression in the hippocampus has been reported (Guerra-Araiza et al., 2001). Furthermore, PRs recognize GREs (Shaffer et al., 2004) and a study on cell lines expressing inducible chimeric PR demonstrated transcriptional activity of the PR with increased levels of *Fkbp5* and *Sgk1* RNA following treatment with the PR agonist R5020 (Trevino et al., 2016). Levels of the endogenous PR ligand, progesterone, has been shown to significantly increase in male rats following exposure to certain stressors (Andersen et al., 2004) while metyrapone treatment has been shown to increase progesterone

levels in males, an observation which is thought to be due to altered steroid synthesis indicating the drug to have extra-adrenal effects on central corticosteroid metabolism (Jahn et al., 2003).

Surgical intervention was also investigated as a method of modulating HPA-axis activity. ADX involves removal of the adrenal gland thus removing the bodies endogenous source of CORT. In addition to the synthesis of CORT, the adrenal gland also responsible for the synthesis of small amounts of progesterone (Wagner, 2006). Removal of the adrenals prevents steroidogenesis from occurring thus eliminating the possibility that by-products of the steroidogenic pathway may acting as MR or GR ligands. Despite the benefits of ADX when investigating HPA-axis activity, it has been shown that ADX results in the loss of hippocampal dentate granule cells (McNeill et al., 1991, Sloviter et al., 1989). CORT replacement can, however, completely prevent ADX-induced granule cell apoptosis (Hu et al., 1997) and in this study, rats were supplemented with CORT in their drinking water following surgery. Removal of CORT 1 day prior to experimentation for 24 hours only avoided the oxidative stress and cell loss reported in many experiments.

At FS30, ADX completely abolished the FS-induced rise in plasma CORT, resulting in levels comparable to those seen at baseline which was not achieved with either dose of metyrapone or repeated injections. At FS60, plasma CORT levels of sham rats were significantly elevated compared with intact rats. It is known that peri-operative stress can lead to an increase of adrenal CORT secretion persisting several days following surgery (Hogan et al., 2011). At baseline, CORT levels appeared to be unaffected, therefore sham surgery may have led to a heightened or sensitized stress response in these rats which was activated by FS. ADX fully attenuated MR and GR binding to GREs following acute stress and, in some cases, reduced levels of MR binding at baseline. This observation further supports early studies which report MR occupancy (Reul and de Kloet, 1985) in the presence of low circulating CORT, and indicates the ADX surgery has reduced levels of CORT sufficiently to prevent even basal levels of MR occupancy and binding. In a study investigating MR and GR binding to a subset of GREs in the rat hippocampus following ADX, CORT replacement revealed a dose-dependent effect on GR binding and MR binding occurring at lower CORT concentrations (Polman et al., 2013).

An examination of transcriptional responses revealed that following acute stress, ADX rats had significantly lower hnRNA and mRNA levels of all genes compared with both intact and sham rats. These findings are in agreement with early studies showing reduced levels of hippocampal 5-HT_{1A}

receptor mRNA expression following both short- and long-term ADX (Liao et al., 1993, Meijer and de Kloet, 1994) and a more recent study using ChIP and RNA-seq which has also shown ADX to abolish acute-stress induced mitochondrially transcribed mRNA (mtRNA) of genes involved in the electron transport chain in the rat (Hunter et al., 2016). Some studies have reported ADX to affect the expression of MR and GR mRNA and protein levels, with increased levels of hippocampal MR and GR mRNA reported following short-term ADX in developing rats (Vazquez et al., 1993) and a significant increase in hippocampal MR and GR protein reported in ADX rats compared to sham rats at various timepoints following surgery (Kalman and Spencer, 2002). These observations were present when rats were not supplemented with CORT, however, and hippocampal MR protein levels were significantly reduced in rats receiving a 45-minute CORT treatment 24 hrs after ADX (Kalman and Spencer, 2002).

Despite having significantly higher plasma levels of CORT compared to intact rats, there were no significant differences in gene expression between sham and intact rats indicating surgery did not have any effect on gene transcriptional responses at that timepoint. It is possible, however, the hnRNA and mRNA expression of these genes may remain significantly elevated for a longer period of time due to the prolonged increase in CORT levels observed. Previous timecourse analysis has revealed that hnRNA levels of *Per1* and *Sgk1* returns to levels similar to that at baseline 120 minutes following FS (FS120), while *Fkbp5* hnRNA levels return by 180 minutes following FS (FS180) (Mifsud and Reul, unpublished observations).

Interestingly, in ADX rats, *Fkbp5* mRNA was significantly lower under early baseline conditions and following acute stress. This observation may be due to the role the FKBP5 protein plays in an intracellular negative feedback loop for GR activity. In the absence of CORT, unligated GRs are sequestered in the cytosol as part of a complex with heat shock proteins and FKBP5. Once GR becomes bound by CORT, FKBP5 is replaced by FKBP4 allowing the nuclear translocation of GR, where it increases the transcription of *Fkbp5* RNA by binding GREs. Increased *Fkbp5* transcription and translation of *Fkbp5* RNA to FKBP5 protein thus decreases GR sensitivity for CORT (Binder, 2009, Mifsud and Reul, 2018). Following ADX, the complete absence of CORT may result in depleted levels of *Fkbp5* mRNA due to a reduction in the translation to FKBP5 protein. Many studies have investigated the effect of FKBP5 overexpression on the stress response (Scammell et al., 2001, Westberry et al., 2006, Buchmann et al., 2014, Ising et al., 2008), however very few have examined the effects of CORT levels on *Fkbp5* transcription and translation. In a study examining the effect of chronic CORT exposure

on *Fkbp5* expression in mice, increased levels of *Fkbp5* RNA were reported in the hippocampus, hypothalamus and blood (Peeters et al., 2004). Another study has shown decreased levels of *Fkbp5* RNA in the prefrontal cortex of ADX mice compared to SHAM mice (Costin et al., 2013), however it is worth noting that ADX mice did not receive CORT replacement and had been habituated to saline injections over 2 days. These observations further support the important role of FKBP5 in the stress response and suggest ADX may be an interesting model to further explore these relationships.

The aim of the present study was to investigate the role of endogenous GCs in the effects of an acute stressful challenge (FS) on MR and GR binding to GC target genes and the transcriptional responses of these genes. To block endogenous GCs, the CORT-synthesis inhibitor metyrapone was used in order to determine whether this pharmacological approach would be an appropriate alternative to the surgical procedure of ADX. These data show that the drug produces diverse genomic effects that can only partially be explained by its CORT-reducing activity and accumulation of DOC. In particular, its effects on gene transcriptional activity were highly diverse. In contrast, the effects of ADX on the GC-dependent genomic endpoints were clear. Importantly, the genes *Fkbp5*, *Per1* and *Sgk1* in the hippocampus play important roles in GC sensitivity and negative feedback regulation, circadian regulation of physiological and behavioural activities, and neuroplasticity processes underlying learning and memory, respectively (Mifsud and Reul, 2016). Moreover, these genes as well as many other GC-regulated genes play important roles in many organs throughout the entire body. Therefore, evidently the unexpected genomic effects of metyrapone question its suitability for conducting studies on the GC dependency of physiological and behavioural processes. These observations indicate that results on such processes may be difficult to interpret or may be liable to misinterpretation. In conclusion, ADX remains the method of choice to elucidate the role of endogenous GC secretion in physiology and behaviour.

Chapter 8 General Discussion

8.1 Summary

The purpose of this thesis was to expand our knowledge regarding the genomic actions of MRs and GRs throughout the brain, particularly in the hippocampus, under physiological conditions of relevance for GC secretion. Previous work carried out by this research group has led to the characterisation of MR/GR GRE-binding and transcriptional responses following exposure to FS and during the circadian rise. Although this work has provided invaluable insight into the regulation of well-established GC-target genes by genomically acting MRs and GRs, these experiments were limited by the ability to examine the regulation of a handful of genes at a time. Investigations undertaken by other research groups in the field have characterised MR and GR binding throughout the entire genome, however this work was carried out in animal models that do not represent true physiological conditions. Moreover, these studies neglect to investigate the transcriptional responses of the corresponding MR or GR bound gene; therefore the data is interpreted based on the assumption that receptor binding initiates a transcriptional response. Therefore, the aim of this thesis was to expand on previous work carried out by our research group and others, by identifying the loci to which MRs and GRs bind throughout the entire genome under acute stress and circadian conditions and to examine the transcriptional responses associated with MR and/or GR binding.

ChIP- and RNA-seq experiments described in Chapter 3 fulfilled the initial aim of this thesis and revealed striking differences in the manner by which MRs and GRs bind to the genome in response to stress and circadian input. This data underwent extensive transcription factor binding site motif analysis and was integrated with RNA-seq findings. Comprehensive pathway analysis (Chapter 4) enabled the identification of novel targets for further investigation, which was carried out in Chapter 5. The regulation of the KLFs by hippocampal GC hormone action was validated in a separate cohort of rats, thus confirming findings of ChIP- and RNA-seq. In addition, this investigation was extended to other brain regions of relevance for GC action, including the amygdala, PFC and neocortex. These brain regions have not received nearly as much attention as the hippocampus regarding MR and GR genomic actions; however our findings indicate further endeavours to be worthwhile. Finally, to fully determine whether GC receptor binding led to a transcriptional response, we explored

pharmacological and surgical interventions to interfere with genomically acting MRs and GRs in Chapter 6 and 7.

8.2 Genome-wide targets of hippocampal GC hormone action and their associated biological functions

In Chapter 3, ChIP-seq identified over 1000 genome-wide loci becoming differentially bound by MRs and GRs following elevations in GC hormone levels. A unique aspect of our study was the decision to examine MR and GR binding under both acute stress and circadian conditions, which enabled us to characterise peaks based on the physiological condition under which they became receptor bound. Moreover, we identified a subset of constitutively bound genomic loci, largely associated with the MR. Traditionally, the main focus of ChIP-seq studies is to identify changes in receptor binding, therefore the exploration of constitutive binding has been entirely neglected. For the MR, the concept of constitutive DNA binding is in agreement with the high degree of ligand occupancy exhibited by the MR under all physiological conditions (Reul et al., 1987, Reul and de Kloet, 1985). Our data suggests that constitutive receptor binding is as physiologically relevant as dynamic receptor binding and warrants further investigation.

We constructed a comprehensive transcription factor binding motif profile of MR and GR bound loci, which differed depending on the physiological conditions leading to receptor binding. We showed that while GREs were found in the majority of stress and/or circadian responsive peaks, a far lower proportion of constitutively bound loci were associated with GREs. Alternative transcription factor motifs such as ZNF, SP, KLF, EGR and RFX were seen to be most prominent within these constitutively bound loci. These findings were to some extent in agreement with previous ChIP-seq studies on ADX rat hippocampus, that showed an association between SP motifs and non-GRE containing GR peaks (Polman et al., 2013) and reported the presence of ZNF and EGR sites in MR and GR bound loci (van Weert et al., 2017). The NeuroD transcription factor motif has been a focal point of MR and/or GR ChIP-seq studies (Pooley et al., 2017, van Weert et al., 2017), and although a marked proportion of our MR and GR peaks did contain the NeuroD motif (also known as ATOH1), other transcription factor motifs were far more prominent. It is possible that ADX leads to changes in chromatin architecture influencing the accessibility of DNA-sequences for binding, thus physiological

conditions present a different transcription factor binding motif profile. Thus far, KLF and RFX motifs have received no attention in regard to genomically acting MRs and GRs.

We conducted an extensive RNA-seq timecourse which enabled us to examine transcriptional responses of genes at various timepoints following exposure to FS stress. Furthermore, the sequencing of inRNA and exRNA transcripts, which are a good representative of hnRNA and mRNA respectively, enabled us to identify more subtle changes in transcription. Far more genes responded with changes in inRNA transcripts compared with exRNA transcripts, therefore had we not sequenced inRNA, GC hormone regulation of these genes may never have been shown. The majority of inRNA changes occurred at FS60, while FS120 was the timepoint at which the majority of exRNA changes were seen, which corresponds with the timeframe of hnRNA transcription from the genome and splicing to produce mRNA. For the first time, RNA-seq data was cross-correlated with ChIP-seq data to determine whether MR and/or GR binding elicited a transcriptional response in the corresponding gene. We showed that a very small proportion of MR and/or GR GRE-binding led to a transcriptional response of the gene in closest proximity, however a significant correlation was still seen between changes in receptor binding and changes in RNA expression. The small overlap between genes containing binding sites and genes exhibiting transcriptional changes likely reflects the 3-D architecture of the genome, in which binding of a transcription factor at one site may lead to a conformational change precipitating transcriptional response of a gene at a completely different location (Matharu and Ahituv, 2015, Rajarajan et al., 2016).

Overall, this study provides the most in-depth analysis of genomically acting MRs and GRs in the hippocampus under physiological conditions to date. Compared with other studies, which may be confounded by the effects of ADX, our experimental model best represents the situation of stress *in vivo.* In terms of technicality, our study was carried out using the highest number of biological replicates per timepoint, at the highest sequencing depth and aligned to the most current version of the rat genome in contrast with other studies (Polman et al., 2012, Pooley et al., 2017, van Weert et al., 2017). A potential limitation of our study was that ChIP-seq was carried out on whole hippocampus tissue, and that both left and right hippocampi were combined for sequencing. Differences in gene expression has been demonstrated among hippocampal subfields (Datson et al., 2004), between the left and right hippocampi (Klur et al., 2009) and within different cell types (McKenzie et al., 2018). Therefore, it is possible that the regulation of gene expression by genomically

acting MRs and GRs differs dependent on these conditions. Future experiments could involve MR and GR ChIP-seq on more specific hippocampal cell populations, to determine whether differences exist in the genomic regulation of transcriptional responses following stress or circadian input.

Pathway analysis of ChIP- and RNA-seq datasets, as described in Chapter 4, further contributed to our elucidation of GC hormone action in the hippocampus. Results of DAVID pathway analysis performed on ChIP-seq data has so far have lacked novelty and clarity regarding GC hormone action in the hippocampus (Polman et al., 2012, Polman et al., 2013, Pooley et al., 2017, van Weert et al., 2017). IPA Core analysis of our datasets, however, has provided extensive insight into the biological consequences of GC hormone genomic action. In addition to confirming the robust nature of the data by highlighting pathways consistent with our experimental model, a number of novel relationships were unearthed by our pathway analysis. A limitation of our pathway analysis was the requirement by IPA of large reference datasets (ideally 200 genes or more) to perform predictions. This meant that although we had previously categorised the ChIP-seq peaks and RNA-seq genes based on physiological response, pathway analysis was performed on the entire dataset, as low n numbers for some peak/RNA categories impeded proper interpretation of the data.

The ability to predict upstream regulators of genes in our datasets was highly beneficial, as we could search for the corresponding TFs of the most prominent TF binding motifs found within MR and GR bound loci, described in Chapter 3. Strikingly, many of these TFs, including the KLFs, were predicted to regulate the genes in our datasets; indicating a potential coregulatory role alongside MRs and GRs at non-GRE containing sites. Neurodevelopmental and synaptic functions were linked to genes in our sequencing datasets, suggesting that the transactivation of these genes by genomically acting MRs and GRs may underlie GC hormone regulation of these processes. Neurological diseases scarcely linked to GC hormone action appeared with high significance in our analyses. The aetiology of many of these disorders, such as Schizophrenia, is currently poorly characterised; therefore, these findings may provide novel targets for further exploration in the elucidation of these illnesses. The observation that neurological disorders not traditionally associated with the hippocampus, such as Huntington's disease, were reported by IPA indicates the potential to extrapolate our findings to predict GC hormone action within other brain regions.

8.3 KLFs are transcriptional targets of genomically acting MRs and GRs throughout the brain following stress and circadian input

Findings of Chapter 4 led us to select the KLFs as GC hormone targets with which to validate results of our sequencing experiments. The purpose of the experiments described in Chapter 5 was to not only to confirm the validity of our ChIP- and RNA-seq data, but to also further investigate the KLFs as potentially significant targets of GC hormone action. We maintained a consistent experimental design between sequencing and validation experiments, however validation experiments described in Chapter 5 were carried out in an entirely separate cohorts of animals and ChIP-qPCR was conducted using different MR and GR antibodies to those used for ChIP-seq. From a technical point of view, the validation was a complete success as the results of our hippocampal ChIP and RNA-qPCR experiments mirrored findings of our ChIP- and RNA-seq data, thus confirming the high quality and reproducibility of our sequencing data. As we chose to sequence a substantial number of biological replicates (n = 4) compared with previous studies, it allowed us to determine with higher confidence whether the changes in receptor binding or RNA expression we observed were in fact true changes.

From an experimental perspective, our findings were the first to establish the *Klfs* as transcriptional targets of genomically acting MRs and GRs in the hippocampus. The KLF family of TFs exhibit structural similarity accompanied by considerable functional diversity (Pearson et al., 2008), and have been proposed to play important roles in processes such as BBB function (Wu et al., 2013), neurogenesis (Qin and Zhang, 2012), synaptic plasticity (Scobie et al., 2009) and glial development (Fu et al., 2009). Elevations in GC hormones had previously been shown to result in the transcriptional activation of *Klf4* and *Klf9* (Datson et al., 2011, Reddy et al., 2009), however no links between GC hormone action and *Klf2* or *Klf15* have so far been established. Our findings that hippocampal MRs and GRs bind to GREs within *Klfs* resulting in transcriptional activation suggests that GC hormone regulation of these genes may underlie important neurodevelopmental and neurophysiological functions.

This investigation was extended to other brain regions known to be influenced by GC hormone action in which the genomic actions of MRs and GRs have hardly been examined. Interestingly, the manner with which MRs and GRs regulated *Klf* expression throughout the hippocampus, amygdala, PFC and neocortex was very similar. These genes are clearly of importance in the brain-wide response to

stress and circadian input. It is possible that due to the sensitivity of the entire brain to changes in GC hormone levels, many genes are regulated in a similar fashion throughout the brain. On the other hand, the characterisation of tissue-specific changes in gene expression would be of interest, to identify functional roles for certain genes dependent on the function of the brain region. Future work may involve identifying potential tissue-specific genes based on the pathway analysis findings described in Chapter 4 and conducting brain-wide ChIP-qPCR for validation. The hippocampus has been the most extensively studied brain region regarding both GC hormone action and the genomic actions of MRs and GRs, however we have clearly shown that other brain regions such as the amygdala, PFC and neocortex should be the focus of future studies. Surprisingly, MR binding was shown in the PFC and neocortex, despite the widespread belief that MR is scarcely expressed in these regions (Reul and de Kloet, 1985). Hardly any MR ChIP has been published in neocortical regions, however our findings will hopefully encourage more investigations of this type.

8.4 Elucidating the genomic actions of MRs and GRs via pharmacological and surgical interventions

Following Chapter 5, we decided to antagonise the MR and/or the GR and examine the resultant transcriptional responses of the *Klfs*, to determine whether the ligand-activation of MRs and GRs was in fact responsible for the observed elevations in *Klf* RNA levels. Based on our own pilot data, that showed blockade of the MR alone was insufficient to affect transcriptional responses, we decided to co-administer the MR and GR antagonists; spironolactone and RU486. Our rationale was based on the hypothesis that MR and GR heterodimerisation may be occurring at GREs within the *Klfs*; therefore blockade of both receptors would be required to prevent initiation of transcription. Indeed, in our ChIP-seq findings, the MR and GR binding sites appeared to overlap considerably within the *Klf*s. We also selected an intermediary dose of RU486, to prevent a maximal dose from concealing any effect of spironolactone. In terms of CORT response, our findings were astonishing, as RU486 alone was shown to result in prolonged significant elevations CORT levels; even more so than spironolactone and RU486 combined. Previous experiments reported in the literature could not provide a rationale behind this finding; clearly our understanding of the HPA-axis needs to be improved.

Our receptor binding results were in agreements with the antagonists mechanism of action, as MRs and GRs could still bind to GREs within the *Klfs* upon antagonist occupancy (Baulieu, 1991). The transcriptional response of the corresponding gene, however, was only attenuated when both the MR and GR were antagonised. It is possible that MR and GR heterodimerisation at *Klf* GREs is required to initiate a transcriptional response, however the partial attenuation of the rise in RNA indicates other coregulatory factors to be playing a role. The observation that blockade of the GR alone was insufficient to have any effect on transcription suggests that the MR may be able to interact with alternative co-regulators and initiate transcription in the absence of GR activity. Again, we have shown that the genomic actions of MRs and GRs are not as clear cut as we may have previously believed. Alternatively, our decision to administer an intermediary dose of RU486 may be underlying this observation, as other studies have demonstrated antagonistic activity of RU486 (Qin et al., 2014). Testing the effects of a maximal dose of RU486 (100mg/kg) on the transcriptional responses of the *Klfs* is a future experiment planned by our lab. No currently published studies have examined MR and GR binding under such conditions, therefore interpretation of our results by comparison to other studies is not presently possible. Removal of endogenous CORT by ADX led to a far stronger attenuation of *Klf* transcriptional responses, with the RNA responses of *Klf9* and *Klf15* completely abolished; suggesting any potential co-regulators to be GC hormone dependent. Levels of *Klf2* RNA, however, were attenuated in ADX animals, indicating GC independent mechanisms to be involved in the transcriptional regulation of this gene. Our observations that ADX had no effect on *Klf4* acted as a negative control; as the gene is not associated with any MR or GR binding.

In light of our findings, it was clear that surgical removal of CORT led to a far more reliable blockade of MR and GR genomic activity. Thus, we decided to explore the effects of a pharmacological alternative to ADX, the CORT synthesis blocker; metyrapone, on the MR and GR genomic activity in the hippocampus. We took advantage of our recent characterisation of *Fkbp5, Per1* and *Sgk1* as genomic targets of MRs and GRs (Mifsud and Reul., 2016) by examining the transcriptional responses of these genes following metyrapone administration. Metyrapone has been widely used in many studies reporting effects of CORT blockade on behaviour (Liu et al., 1999, Roozendaal et al., 1996), however few studies have administered the drug with the aim of blocking MR- and GR-mediated transcriptional effects. Our results indicate the drug to be completely unsuitable to investigate the transcriptional activity of genomically acting MRs and GRs. One would expect to see a

reduction in the transcriptional activation of MR and GR target genes following a decrease in CORT levels, however we showed that metyrapone led to transcriptional activation of *Fkbp5, Per1* and *Sgk1* despite lowering CORT levels and reducing MR and GR binding to GREs. Explanations of our observations include the possibility of MR/GR occupancy by metyrapone by-products (DOC) (Funder, 2010) or alternative GC hormones (progesterone) (Jahn et al., 2003); however the bottom line of these findings is that metyrapone should be avoided when examining the transcriptional responses of MR and GR target genes. Again, we have shown the HPA axis and the genomic actions of MRs and GRs to be far more complex than originally thought and demonstrated that pharmacological manipulations of the HPA axis require extensive validation to ensure no unwanted effects on transcription are occurring.

We have provided strong evidence for the *Klfs* as significant GC target genes warranting further investigation. A next step would be to identify the co-regulators interacting with MRs and GRs to initiate *Klf* transcription and observe the effects of blocking these processes on processes such as neurogenesis or neuronal migration. ChIP-qPCR would identify whether KLFs themselves are binding at KLF motifs in close proximity to MR and GR binding sites within the *Klfs,* exerting a coregulatory role. Administration of GC receptor antagonists to rats during the early postnatal phase, followed by immunohistochemistry for markers of cell proliferation such as BrdU (Wojtowicz and Kee, 2006) would determine whether GC-induced expression of the *Klfs* was required for neurogenesis during development, and FS followed by a 24 hour or 4-week retest would determine whether this blockade had a negative or positive effect on learning and memory.

8.5 Conclusion and future directions

Work carried out during this PhD study has contributed substantially to the wider understanding of the mechanisms underlying GC hormone regulation of gene expression within the hippocampus and other brain regions. Many of the experiments undertaken are the first of their kind and will hopefully encourage the publication of studies of a similar nature. ChIP- and RNA-seq has provided the most thorough analysis of the genomic actions of MRs and GRs under physiological conditions of relevance for GC secretion to date. Once published, the datasets generated by these experiments shall provide an invaluable resource for research groups to select GC-target genes for validation and

further exploration. The manner in which we analysed, categorised and interpreted our data is unique to our study, and may change the way bioinformaticians and scientists decide to present sequencing data in the future. These experiments have provided the basis regarding NGS work conducted by our lab and future endeavours may further elucidate the genomic actions of MRs and GRs within more distinct hippocampal populations and potentially within other brain regions such as the amygdala, PFC or neocortex. Our data has also identified a plethora of novel genomic targets, biological pathways and diseases that our research group and others may pursue.

Words: 3378

BAULIEU, E. E. 1991. The antisteroid RU486: its cellular and molecular mode of action. *Trends Endocrinol Metab,* 2**,** 233-9.

DATSON, N. A., MEIJER, L., STEENBERGEN, P. J., MORSINK, M. C., VAN DER LAAN, S., MEIJER, O. C. & DE KLOET, E. R. 2004. Expression profiling in laser-microdissected hippocampal subregions in rat brain reveals large subregion-specific differences in expression. *Eur J Neurosci,* 20**,** 2541-54.

DATSON, N. A., POLMAN, J. A., DE JONGE, R. T., VAN BOHEEMEN, P. T., VAN MAANEN, E. M., WELTEN, J., MCEWEN, B. S., MEILAND, H. C. & MEIJER, O. C. 2011. Specific regulatory motifs predict glucocorticoid responsiveness of hippocampal gene expression. *Endocrinology,* 152**,** 3749-57.

FU, H., CAI, J., CLEVERS, H., FAST, E., GRAY, S., GREENBERG, R., JAIN, M. K., MA, Q., QIU, M., ROWITCH, D. H., TAYLOR, C. M. & STILES, C. D. 2009. A genome-wide screen for spatially restricted expression patterns identifies transcription factors that regulate glial development. *J Neurosci,* 29**,** 11399-408.

FUNDER, J. W. 2010. Minireview: Aldosterone and mineralocorticoid receptors: past, present, and future. *Endocrinology,* 151**,** 5098-102.

JAHN, H., KIEFER, F., SCHICK, M., YASSOURIDIS, A., STEIGER, A., KELLNER, M. & WIEDEMANN, K. 2003. Sleep endocrine effects of the 11-beta-hydroxysteroiddehydrogenase inhibitor metyrapone. *Sleep,* 26**,** 823-9.

KLUR, S., MULLER, C., PEREIRA DE VASCONCELOS, A., BALLARD, T., LOPEZ, J., GALANI, R., CERTA, U. & CASSEL, J. C. 2009. Hippocampal-dependent spatial memory functions might be lateralized in rats: An approach combining gene expression profiling and reversible inactivation. *Hippocampus,* 19**,** 800-16.

LIU, L., TSUJI, M., TAKEDA, H., TAKADA, K. & MATSUMIYA, T. 1999. Adrenocortical suppression blocks the enhancement of memory storage produced by exposure to psychological stress in rats. *Brain Res,* 821**,** 134-40.

MATHARU, N. & AHITUV, N. 2015. Minor Loops in Major Folds: Enhancer-Promoter Looping, Chromatin Restructuring, and Their Association with Transcriptional Regulation and Disease. *PLoS Genet,* 11**,** e1005640.

MCKENZIE, A. T., WANG, M., HAUBERG, M. E., FULLARD, J. F., KOZLENKOV, A., KEENAN, A., HURD, Y. L., DRACHEVA, S., CASACCIA, P., ROUSSOS, P. & ZHANG, B. 2018. Brain Cell Type Specific Gene Expression and Co-expression Network Architectures. *Sci Rep,* 8**,** 8868.

PEARSON, R., FLEETWOOD, J., EATON, S., CROSSLEY, M. & BAO, S. 2008. Kruppel-like transcription factors: a functional family. *Int J Biochem Cell Biol,* 40**,** 1996-2001.

POLMAN, J. A., WELTEN, J. E., BOSCH, D. S., DE JONGE, R. T., BALOG, J., VAN DER MAAREL, S. M., DE KLOET, E. R. & DATSON, N. A. 2012. A genome-wide signature of glucocorticoid receptor binding in neuronal PC12 cells. *BMC Neurosci,* 13**,** 118.

POLMAN, J. A. E., DE KLOET, E. R. & DATSON, N. A. 2013. Two Populations of Glucocorticoid Receptor-Binding Sites in the Male Rat Hippocampal Genome. *Endocrinology,* 154**,** 1832-1844.

POOLEY, J. R., FLYNN, B. P., GRONTVED, L., BAEK, S., GUERTIN, M. J., KERSHAW, Y. M., BIRNIE, M. T., PELLATT, A., RIVERS, C. A., SCHILTZ, R. L., HAGER, G. L., LIGHTMAN, S. L. & CONWAY-CAMPBELL, B. L. 2017. Genome-Wide Identification of Basic Helix-Loop-Helix and NF-1 Motifs Underlying GR Binding Sites in Male Rat Hippocampus. *Endocrinology,* 158**,** 1486-1501.

QIN, S. & ZHANG, C. L. 2012. Role of Kruppel-like factor 4 in neurogenesis and radial neuronal migration in the developing cerebral cortex. *Mol Cell Biol,* 32**,** 4297-305.

QIN, W., PAN, J., QIN, Y., LEE, D. N., BAUMAN, W. A. & CARDOZO, C. 2014. Identification of functional glucocorticoid response elements in the mouse FoxO1 promoter. *Biochem Biophys Res Commun,* 450**,** 979-83.

RAJARAJAN, P., GIL, S. E., BRENNAND, K. J. & AKBARIAN, S. 2016. Spatial genome organization and cognition. *Nat Rev Neurosci,* 17**,** 681-691.

REDDY, T. E., PAULI, F., SPROUSE, R. O., NEFF, N. F., NEWBERRY, K. M., GARABEDIAN, M. J. & MYERS, R. M. 2009. Genomic determination of the glucocorticoid response reveals unexpected mechanisms of gene regulation. *Genome Res,* 19**,** 2163-71.

REUL, J. M., VAN DEN BOSCH, F. R. & DE KLOET, E. R. 1987. Relative occupation of type-I and type-II corticosteroid receptors in rat brain following stress and dexamethasone treatment: functional implications. *J Endocrinol,* 115**,** 459-67.

REUL, J. M. H. M. & DE KLOET, E. R. 1985. Two receptor systems for corticosterone in rat brain: microdistribution and differential occupation. *Endocrinology,* 117**,** 2505-11.

ROOZENDAAL, B., BOHUS, B. & MCGAUGH, J. L. 1996. Dose-dependent suppression of adrenocortical activity with metyrapone: effects on emotion and memory. *Psychoneuroendocrinology,* 21**,** 681-93.

SCOBIE, K. N., HALL, B. J., WILKE, S. A., KLEMENHAGEN, K. C., FUJII-KURIYAMA, Y., GHOSH, A., HEN, R. & SAHAY, A. 2009. Kruppel-like factor 9 is necessary for late-phase neuronal maturation in the developing dentate gyrus and during adult hippocampal neurogenesis. *J Neurosci,* 29**,** 9875-87.

VAN WEERT, L., BUURSTEDE, J. C., MAHFOUZ, A., BRAAKHUIS, P. S. M., POLMAN, J. A. E., SIPS, H. C. M., ROOZENDAAL, B., BALOG, J., DE KLOET, E. R., DATSON, N. A. & MEIJER, O. C. 2017. NeuroD Factors Discriminate Mineralocorticoid From Glucocorticoid Receptor DNA Binding in the Male Rat Brain. *Endocrinology,* 158**,** 1511-1522.

WOJTOWICZ, J. M. & KEE, N. 2006. BrdU assay for neurogenesis in rodents. *Nat Protoc,* 1**,** 1399-405.

WU, C., LI, F., HAN, G. & LIU, Z. 2013. Abeta(1-42) disrupts the expression and function of KLF2 in Alzheimer's disease mediated by p53. *Biochem Biophys Res Commun,* 431**,** 141-5.

References

AMBROGINI, P., ORSINI, L., MANCINI, C., FERRI, P., BARBANTI, I. & CUPPINI, R. 2002. Persistently high corticosterone levels but not normal circadian fluctuations of the hormone affect cell proliferation in the adult rat dentate gyrus. Neuroendocrinology, 76, 366-72.

ANACKER, C., CATTANEO, A., LUONI, A., MUSAELYAN, K., ZUNSZAIN, P. A., MILANESI, E., RYBKA, J., BERRY, A., CIRULLI, F., THURET, S., PRICE, J., RIVA, M. A., GENNARELLI, M. & PARIANTE, C. M. 2013. Glucocorticoid-related molecular signaling pathways regulating hippocampal neurogenesis. Neuropsychopharmacology, 38, 872-83.

ANDERSEN, M. L., BIGNOTTO, M., MACHADO, R. B. & TUFIK, S. 2004. Different stress modalities result in distinct steroid hormone responses by male rats. Braz J Med Biol Res, 37, 791-7.

ANDRUS, B. M., BLIZINSKY, K., VEDELL, P. T., DENNIS, K., SHUKLA, P. K., SCHAFFER, D. J., RADULOVIC, J., CHURCHILL, G. A. & REDEI, E. E. 2012. Gene expression patterns in the hippocampus and amygdala of endogenous depression and chronic stress models. Mol Psychiatry, 17, 49-61.

ANGELINI, C. & COSTA, V. 2014. Understanding gene regulatory mechanisms by integrating ChIP-seq and RNA-seq data: statistical solutions to biological problems. Front Cell Dev Biol, 2, 51.

ARRIZA, J. L., WEINBERGER, C., CERELLI, G., GLASER, T. M., HANDELIN, B. L., HOUSMAN, D. E. & EVANS, R. M. 1987. Cloning of human mineralocorticoid receptor complementary DNA: structural and functional kinship with the glucocorticoid receptor. Science, 237, 268-75.

AYALA, R., SHU, T. & TSAI, L. H. 2007. Trekking across the brain: the journey of neuronal migration. Cell, 128, 29-43.

BACHMANN, C. G., LINTHORST, A. C., HOLSBOER, F. & REUL, J. M. H. M. 2003. Effect of chronic administration of selective glucocorticoid receptor antagonists on the rat hypothalamic-pituitary-adrenocortical axis. Neuropsychopharmacology, 28, 1056-67.

BAGAMASBAD, P., ZIERA, T., BORDEN, S. A., BONETT, R. M., ROZEBOOM, A. M., SEASHOLTZ, A. & DENVER, R. J. 2012. Molecular basis for glucocorticoid induction of the Krüppel-like factor 9 gene in hippocampal neurons. Endocrinology, 153, 5334-45.

BAILEY, T. L., JOHNSON, J., GRANT, C. E. & NOBLE, W. S. 2015. The MEME Suite. Nucleic Acids Res, 43, W39-49.

BANKI, C. M., KARMACSI, L., BISSETTE, G. & NEMEROFF, C. B. 1992. Cerebrospinal fluid neuropeptides in mood disorder and dementia. J Affect Disord, 25, 39-45.

BARNETT, D. W., GARRISON, E. K., QUINLAN, A. R., STROMBERG, M. P. & MARTH, G. T. 2011. BamTools: a C++ API and toolkit for analyzing and managing BAM files. Bioinformatics, 27, 1691-2.

BAULIEU, E. E. 1991. The antisteroid RU486: its cellular and molecular mode of action. Trends Endocrinol Metab, 2, 233-9.

BEAUMONT, T. L., YAO, B., SHAH, A., KAPATOS, G. & LOEB, J. A. 2012. Layer-specific CREB target gene induction in human neocortical epilepsy. J Neurosci, 32, 14389-401.

BECK, C. A., WEIGEL, N. L., MOYER, M. L., NORDEEN, S. K. & EDWARDS, D. P. 1993. The progesterone antagonist RU486 acquires agonist activity upon stimulation of cAMP signaling pathways. Proc Natl Acad Sci U S A, 90, 4441-5.

BENEYTO, M. & MEADOR-WOODRUFF, J. H. 2008. Lamina-specific abnormalities of NMDA receptor-associated postsynaptic protein transcripts in the prefrontal cortex in schizophrenia and bipolar disorder. Neuropsychopharmacology, 33, 2175-86.

BENJAMINI, Y. & HOCHBERG, Y. 1995. Controlling the False Discovery Rate: A Practical and Powerful Approach to Multiple Testing. Journal of the Royal Statistical Society. Series B (Methodological), 57, 289-300.

BERMAN, D. E., DALL'ARMI, C., VORONOV, S. V., MCINTIRE, L. B., ZHANG, H., MOORE, A. Z., STANISZEWSKI, A., ARANCIO, O., KIM, T. W. & DI PAOLO, G. 2008. Oligomeric amyloid-beta peptide disrupts phosphatidylinositol-4,5-bisphosphate metabolism. Nat Neurosci, 11, 547-54.

BESNARD, A., LANGBERG, T., LEVINSON, S., CHU, D., VICIDOMINI, C., SCOBIE, K. N., DWORK, A. J., ARANGO, V., ROSOKLIJA, G. B., MANN, J. J., HEN, R., LEONARDO, E. D., BOLDRINI, M. & SAHAY, A. 2018. Targeting Kruppel-like Factor 9 in Excitatory Neurons Protects against Chronic Stress-Induced Impairments in Dendritic Spines and Fear Responses. Cell Rep, 23, 3183-3196.

BEYLIN, A. V. & SHORS, T. J. 2003. Glucocorticoids are necessary for enhancing the acquisition of associative memories after acute stressful experience. Horm Behav, 43, 124-31.

BILANG-BLEUEL, A., RECH, J., DE CARLI, S., HOLSBOER, F. & REUL, J. M. H. M. 2002. Forced swimming evokes a biphasic response in CREB phosphorylation in extrahypothalamic limbic and neocortical brain structures in the rat. Eur J Neurosci, 15, 1048-60.

BILANG-BLEUEL, A., ULBRICHT, S., CHANDRAMOHAN, Y., DE CARLI, S., DROSTE, S. K. & REUL, J. M. H. M. 2005. Psychological stress increases histone H3 phosphorylation in adult dentate gyrus granule neurons: involvement in a glucocorticoid receptor-dependent behavioural response. Eur J Neurosci, 22, 1691-700.

BINDER, E. B. 2009. The role of FKBP5, a co-chaperone of the glucocorticoid receptor in the pathogenesis and therapy of affective and anxiety disorders. Psychoneuroendocrinology, 34 Suppl 1, S186-95.

BLOEM, L. J., GUO, C. & PRATT, J. H. 1995. Identification of a splice variant of the rat and human mineralocorticoid receptor genes. J Steroid Biochem Mol Biol, 55, 159-62.

BODNOFF, S. R., HUMPHREYS, A. G., LEHMAN, J. C., DIAMOND, D. M., ROSE, G. M. & MEANEY, M. J. 1995. Enduring effects of chronic corticosterone treatment on spatial learning, synaptic plasticity, and hippocampal neuropathology in young and mid-aged rats. J Neurosci, 15, 61-9.

BOHN, M. C. 1980. Granule cell genesis in the hippocampus of rats treated neonatally with hydrocortisone. Neuroscience, 5, 2003-12.

BONETT, R. M., HU, F., BAGAMASBAD, P. & DENVER, R. J. 2009. Stressor and glucocorticoid-dependent induction of the immediate early gene Krüppel-like factor 9: implications for neural development and plasticity. Endocrinology, 150, 1757-65.

BORRELL, J., DE KLOET, E. R., VERSTEEG, D. H. & BOHUS, B. 1983. Inhibitory avoidance deficit following short-term adrenalectomy in the rat: the role of adrenal catecholamines. Behav Neural Biol, 39, 241-58.

BOURDEAU, I., BARD, C., NOEL, B., LECLERC, I., CORDEAU, M. P., BELAIR, M., LESAGE, J., LAFONTAINE, L. & LACROIX, A. 2002. Loss of brain volume in endogenous Cushing's syndrome and its reversibility after correction of hypercortisolism. J Clin Endocrinol Metab, 87, 1949-54.

BRADY, L. S., WHITFIELD, H. J., JR., FOX, R. J., GOLD, P. W. & HERKENHAM, M. 1991. Long-term antidepressant administration alters corticotropin-releasing hormone, tyrosine hydroxylase, and mineralocorticoid receptor gene expression in rat brain. Therapeutic implications. J Clin Invest, 87, 831-7.

BROOKES, J. C., GALIGNIANA, M. D., HARKER, A. H., STONEHAM, A. M. & VINSON, G. P. 2012. System among the corticosteroids: specificity and molecular dynamics. J R Soc Interface, 9, 43-53.

BROWN, S. M., HENNING, S. & WELLMAN, C. L. 2005. Mild, short-term stress alters dendritic morphology in rat medial prefrontal cortex. Cereb Cortex, 15, 1714-22.

BUCHMANN, A. F., HOLZ, N., BOECKER, R., BLOMEYER, D., RIETSCHEL, M., WITT, S. H., SCHMIDT, M. H., ESSER, G., BANASCHEWSKI, T., BRANDEIS, D., ZIMMERMANN, U. S. & LAUCHT, M. 2014. Moderating role of FKBP5 genotype in the impact of childhood adversity on cortisol stress response during adulthood. Eur Neuropsychopharmacol, 24, 837-45.

BURD, C. J., WARD, J. M., CRUSSELLE-DAVIS, V. J., KISSLING, G. E., PHADKE, D., SHAH, R. R. & ARCHER, T. K. 2012. Analysis of chromatin dynamics during glucocorticoid receptor activation. Mol Cell Biol, 32, 1805-17.

CADEPOND, F., SCHWEIZER-GROYER, G., SEGARD-MAUREL, I., JIBARD, N., HOLLENBERG, S. M., GIGUERE, V., EVANS, R. M. & BAULIEU, E. E. 1991. Heat shock protein 90 as a critical factor in maintaining glucocorticosteroid receptor in a nonfunctional state. J Biol Chem, 266, 5834-41.

CAIAZZO, M., COLUCCI-D'AMATO, L., ESPOSITO, M. T., PARISI, S., STIFANI, S., RAMIREZ, F. & DI PORZIO, U. 2010. Transcription factor KLF7 regulates differentiation of neuroectodermal and mesodermal cell lineages. Exp Cell Res, 316, 2365-76.

CALABRESE, F., SAVINO, E., PAPP, M., MOLTENI, R. & RIVA, M. A. 2016. Chronic mild stress-induced alterations of clock gene expression in rat prefrontal cortex: modulatory effects of prolonged lurasidone treatment. Pharmacol Res, 104, 140-50.

CALLICOTT, J. H., STRAUB, R. E., PEZAWAS, L., EGAN, M. F., MATTAY, V. S., HARIRI, A. R., VERCHINSKI, B. A., MEYER-LINDENBERG, A., BALKISSOON, R., KOLACHANA, B., GOLDBERG, T. E. & WEINBERGER, D. R. 2005. Variation in DISC1 affects hippocampal structure and function and increases risk for schizophrenia. Proc Natl Acad Sci U S A, 102, 8627-32.

CAMERON, H. A., WOOLLEY, C. S. & GOULD, E. 1993. Adrenal steroid receptor immunoreactivity in cells born in the adult rat dentate gyrus. Brain Res, 611, 342-6.

CARROLL, B. J. 1982. The dexamethasone suppression test for melancholia. Br J Psychiatry, 140, 292-304.

CERQUEIRA, J. J., MAILLIET, F., ALMEIDA, O. F., JAY, T. M. & SOUSA, N. 2007. The prefrontal cortex as a key target of the maladaptive response to stress. J Neurosci, 27, 2781-7.

CHANDRAMOHAN, Y., DROSTE, S. K., ARTHUR, J. S. & REUL, J. M. H. M. 2008. The forced swimming-induced behavioural immobility response involves histone H3 phospho-acetylation and c-Fos induction in dentate gyrus granule neurons via activation of the N-methyl-D-aspartate/extracellular signal-regulated kinase/mitogen- and stress-activated kinase signalling pathway. Eur J Neurosci, 27, 2701-13.

CHANDRAMOHAN, Y., DROSTE, S. K. & REUL, J. M. H. M. 2007. Novelty stress induces phospho-acetylation of histone H3 in rat dentate gyrus granule neurons through coincident signalling via the N-methyl-D-aspartate receptor and the glucocorticoid receptor: relevance for c-fos induction. J Neurochem, 101, 815-28.

CHAPPELL, P. B., SMITH, M. A., KILTS, C. D., BISSETTE, G., RITCHIE, J., ANDERSON, C. & NEMEROFF, C. B. 1986. Alterations in corticotropin-releasing factor-like immunoreactivity in discrete rat brain regions after acute and chronic stress. J Neurosci, 6, 2908-14.

CHEN, D. Y., BAMBAH-MUKKU, D., POLLONINI, G. & ALBERINI, C. M. 2012. Glucocorticoid receptors recruit the CaMKIIalpha-BDNF-CREB pathways to mediate memory consolidation. Nat Neurosci, 15, 1707-14.

CHEN, H., AMAZIT, L., LOMBES, M. & LE MENUET, D. 2019. Crosstalk Between Glucocorticoid Receptor and Early-growth Response Protein 1 Accounts for Repression of Brain-derived Neurotrophic Factor Transcript 4 Expression. Neuroscience, 399, 12-27.

CHEN, H., LOMBES, M. & LE MENUET, D. 2017. Glucocorticoid receptor represses brain-derived neurotrophic factor expression in neuron-like cells. Mol Brain, 10, 12.

CHEUNG, P., ALLIS, C. D. & SASSONE-CORSI, P. 2000. Signaling to chromatin through histone modifications. Cell, 103, 263-71.

CHHAJLANI, V. & WIKBERG, J. E. 1992. Molecular cloning and expression of the human melanocyte stimulating hormone receptor cDNA. FEBS Lett, 309, 417-20.

CHINENOV, Y., COPPO, M., GUPTE, R., SACTA, M. A. & ROGATSKY, I. 2014. Glucocorticoid receptor coordinates transcription factor-dominated regulatory network in macrophages. BMC Genomics, 15, 656.

CHOREV, M. & CARMEL, L. 2012. The function of introns. Front Genet, 3, 55.

CHUNG, S., SON, G. H. & KIM, K. 2011. Circadian rhythm of adrenal glucocorticoid: its regulation and clinical implications. Biochim Biophys Acta, 1812, 581-91.

COHEN, J. W., LOUNEVA, N., HAN, L. Y., HODES, G. E., WILSON, R. S., BENNETT, D. A., LUCKI, I. & ARNOLD, S. E. 2011. Chronic corticosterone exposure alters postsynaptic protein levels of PSD-95, NR1, and synaptopodin in the mouse brain. Synapse, 65, 763-70.

CONNEELY, O., SULLIVAN, W., TOFT, D., BIRNBAUMER, M., COOK, R., MAXWELL, B., ZARUCKI-SCHULZ, T., GREENE, G., SCHRADER, W. & O'MALLEY, B. 1986. Molecular cloning of the chicken progesterone receptor. 233, 767-770.

COOK, S. C. & WELLMAN, C. L. 2004. Chronic stress alters dendritic morphology in rat medial prefrontal cortex. J Neurobiol, 60, 236-48.

CORDERO, M. I. & SANDI, C. 1998. A role for brain glucocorticoid receptors in contextual fear conditioning: dependence upon training intensity. Brain Res, 786, 11-7.

CORDNER, Z. A. & TAMASHIRO, K. L. 2016. Effects of chronic variable stress on cognition and Bace1 expression among wild-type mice. Transl Psychiatry, 6, e854.

CORVOL, P., CLAIRE, M., OBLIN, M. E., GEERING, K. & ROSSIER, B. 1981. Mechanism of the antimineralocorticoid effects of spirolactones. Kidney Int, 20, 1-6.

COSTIN, B. N., WOLEN, A. R., FITTING, S., SHELTON, K. L. & MILES, M. F. 2013. Role of adrenal glucocorticoid signaling in prefrontal cortex gene expression and acute behavioral responses to ethanol. Alcohol Clin Exp Res, 37, 57-66.

COUETTE, B., MARSAUD, V., BAULIEU, E. E., RICHARD-FOY, H. & RAFESTIN-OBLIN, M. E. 1992. Spironolactone, an aldosterone antagonist, acts as an antiglucocorticosteroid on the mouse mammary tumor virus promoter. Endocrinology, 130, 430-6.

CRUZ-TOPETE, D., HE, B., XU, X. & CIDLOWSKI, J. A. 2016. Krüppel-like Factor 13 Is a Major Mediator of Glucocorticoid Receptor Signaling in Cardiomyocytes and Protects These Cells from DNA Damage and Death. J Biol Chem, 291, 19374-86.

CUI, A., FAN, H., ZHANG, Y., ZHANG, Y., NIU, D., LIU, S., LIU, Q., MA, W., SHEN, Z., SHEN, L., LIU, Y., ZHANG, H., XUE, Y., CUI, Y., WANG, Q., XIAO, X., FANG, F., YANG, J., CUI, Q. & CHANG, Y.

2019. Dexamethasone-induced Krüppel-like factor 9 expression promotes hepatic gluconeogenesis and hyperglycemia. J Clin Invest, 129, 2266-2278.

CUMMINGS, S., ELDE, R., ELLS, J. & LINDALL, A. 1983. Corticotropin-releasing factor immunoreactivity is widely distributed within the central nervous system of the rat: an immunohistochemical study. J Neurosci, 3, 1355-68.

CUNNINGHAM, F., AMODE, M. R., BARRELL, D., BEAL, K., BILLIS, K., BRENT, S., CARVALHO-SILVA, D., CLAPHAM, P., COATES, G., FITZGERALD, S., GIL, L., GIRON, C. G., GORDON, L., HOURLIER, T., HUNT, S. E., JANACEK, S. H., JOHNSON, N., JUETTEMANN, T., KAHARI, A. K., KEENAN, S., MARTIN, F. J., MAUREL, T., MCLAREN, W., MURPHY, D. N., NAG, R., OVERDUIN, B., PARKER, A., PATRICIO, M., PERRY, E., PIGNATELLI, M., RIAT, H. S., SHEPPARD, D., TAYLOR, K., THORMANN, A., VULLO, A., WILDER, S. P., ZADISSA, A., AKEN, B. L., BIRNEY, E., HARROW, J., KINSELLA, R., MUFFATO, M., RUFFIER, M., SEARLE, S. M., SPUDICH, G., TREVANION, S. J., YATES, A., ZERBINO, D. R. & FLICEK, P. 2015. Ensembl 2015. Nucleic Acids Res, 43, D662-9.

DACHIR, S., KADAR, T., ROBINZON, B. & LEVY, A. 1993. Cognitive deficits induced in young rats by long-term corticosterone administration. Behav Neural Biol, 60, 103-9.

DAHOUN, T., TROSSBACH, S. V., BRANDON, N. J., KORTH, C. & HOWES, O. D. 2017. The impact of Disrupted-in-Schizophrenia 1 (DISC1) on the dopaminergic system: a systematic review. Transl Psychiatry, 7, e1015.

DANG, D. T., PEVSNER, J. & YANG, V. W. 2000. The biology of the mammalian Krüppel-like family of transcription factors. Int J Biochem Cell Biol, 32, 1103-21.

DANG, D. T., ZHAO, W., MAHATAN, C. S., GEIMAN, D. E. & YANG, V. W. 2002. Opposing effects of Krüppel-like factor 4 (gut-enriched Krüppel-like factor) and Krüppel-like factor 5 (intestinal-enriched Krüppel-like factor) on the promoter of the Krüppel-like factor 4 gene. Nucleic Acids Res, 30, 2736-41.

DANIEL, E. & NEWELL-PRICE, J. D. 2015. Therapy of endocrine disease: steroidogenesis enzyme inhibitors in Cushing's syndrome. Eur J Endocrinol, 172, R263-80.

DATSON, N. A., MEIJER, L., STEENBERGEN, P. J., MORSINK, M. C., VAN DER LAAN, S., MEIJER, O. C. & DE KLOET, E. R. 2004. Expression profiling in laser-microdissected hippocampal subregions in rat brain reveals large subregion-specific differences in expression. Eur J Neurosci, 20, 2541-54.

DATSON, N. A., POLMAN, J. A., DE JONGE, R. T., VAN BOHEEMEN, P. T., VAN MAANEN, E. M., WELTEN, J., MCEWEN, B. S., MEILAND, H. C. & MEIJER, O. C. 2011. Specific regulatory motifs predict glucocorticoid responsiveness of hippocampal gene expression. Endocrinology, 152, 3749-57.

DATSON, N. A., SPEKSNIJDER, N., MAYER, J. L., STEENBERGEN, P. J., KOROBKO, O., GOEMAN, J., DE KLOET, E. R., JOELS, M. & LUCASSEN, P. J. 2012. The transcriptional response to chronic stress and glucocorticoid receptor blockade in the hippocampal dentate gyrus. Hippocampus, 22, 359-71.

DE KLOET, E. R. & DERIJK, R. 2004. Signaling pathways in brain involved in predisposition and pathogenesis of stress-related disease: genetic and kinetic factors affecting the MR/GR balance. Ann N Y Acad Sci, 1032, 14-34.

DE KLOET, E. R., JOELS, M. & HOLSBOER, F. 2005. Stress and the brain: from adaptation to disease. Nat Rev Neurosci, 6, 463-75.

DE KLOET, E. R. & REUL, J. M. H. M. 1987. Feedback action and tonic influence of corticosteroids on brain function: a concept arising from the heterogeneity of brain receptor systems. Psychoneuroendocrinology, 12, 83-105.

DE PABLO, J. M., PARRA, A., SEGOVIA, S. & GUILLAMON, A. 1989. Learned immobility explains the behavior of rats in the forced swimming test. Physiol Behav, 46, 229-37.

DE SOUZA, E. B., INSEL, T. R., PERRIN, M. H., RIVIER, J., VALE, W. W. & KUHAR, M. J. 1985. Corticotropin-releasing factor receptors are widely distributed within the rat central nervous system: an autoradiographic study. J Neurosci, 5, 3189-203.

DENVER, R. J., OUELLET, L., FURLING, D., KOBAYASHI, A., FUJII-KURIYAMA, Y. & PUYMIRAT, J. 1999. Basic transcription element-binding protein (BTEB) is a thyroid hormone-regulated gene in the developing central nervous system. Evidence for a role in neurite outgrowth. J Biol Chem, 274, 23128-34.

DIAMOND, D. M., BENNETT, M. C., FLESHNER, M. & ROSE, G. M. 1992. Inverted-U relationship between the level of peripheral corticosterone and the magnitude of hippocampal primed burst potentiation. Hippocampus, 2, 421-30.

DIAMOND, D. M. & ROSE, G. M. 1994. Stress impairs LTP and hippocampal-dependent memory. Ann N Y Acad Sci, 746, 411-4.

DICKMEIS, T. 2009. Glucocorticoids and the circadian clock. J Endocrinol, 200, 3-22.

DIORIO, D., VIAU, V. & MEANEY, M. J. 1993. The role of the medial prefrontal cortex (cingulate gyrus) in the regulation of hypothalamic-pituitary-adrenal responses to stress. J Neurosci, 13, 3839-47.

DOUGHERTY, E. J., ELINOFF, J. M., FERREYRA, G. A., HOU, A., CAI, R., SUN, J., BLAINE, K. P., WANG, S. & DANNER, R. L. 2016. Mineralocorticoid Receptor (MR) trans-Activation of Inflammatory AP-1 Signaling: DEPENDENCE ON DNA SEQUENCE, MR CONFORMATION, AND AP-1 FAMILY MEMBER EXPRESSION. J Biol Chem, 291, 23628-23644.

DUNLAP, J. C. 1999. Molecular bases for circadian clocks. Cell, 96, 271-90.

DWIVEDI, Y., RIZAVI, H. S. & PANDEY, G. N. 2006. Antidepressants reverse corticosterone-mediated decrease in brain-derived neurotrophic factor expression: differential regulation of specific exons by antidepressants and corticosterone. Neuroscience, 139, 1017-29.

ENGBLOM, D., KORNFELD, J. W., SCHWAKE, L., TRONCHE, F., REIMANN, A., BEUG, H., HENNIGHAUSEN, L., MORIGGL, R. & SCHUTZ, G. 2007. Direct glucocorticoid receptor-Stat5 interaction in hepatocytes controls body size and maturation-related gene expression. Genes Dev, 21, 1157-62.

FADDA, A., SYED, N., MACKEH, R., PAPADOPOULOU, A., SUZUKI, S., JITHESH, P. V. & KINO, T. 2017. Genome-wide Regulatory Roles of the C2H2-type Zinc Finger Protein ZNF764 on the Glucocorticoid Receptor. Sci Rep, 7, 41598.

FANG, X., ZHONG, X., YU, G., SHAO, S. & YANG, Q. 2017. Vascular protective effects of KLF2 on Abeta-induced toxicity: Implications for Alzheimer's disease. Brain Res, 1663, 174-183.

FELICIANO, P., ANDRADE, R. & BYKHOVSKAIA, M. 2013. Synapsin II and Rab3a cooperate in the regulation of epileptic and synaptic activity in the CA1 region of the hippocampus. J Neurosci, 33, 18319-30.

FILE, S. E., VELLUCCI, S. V. & WENDLANDT, S. 1979. Corticosterone -- an anxiogenic or an anxiolytic agent? J Pharm Pharmacol, 31, 300-5.

FINSTERWALD, C. & ALBERINI, C. M. 2014. Stress and glucocorticoid receptor-dependent mechanisms in long-term memory: from adaptive responses to psychopathologies. Neurobiol Learn Mem, 112, 17-29.

FITZGERALD, P. J., BARKUS, C., FEYDER, M., WIEDHOLZ, L. M., CHEN, Y. C., KARLSSON, R. M., MACHADO-VIEIRA, R., GRAYBEAL, C., SHARP, T., ZARATE, C., HARVEY-WHITE, J., DU, J., SPRENGEL, R., GASS, P., BANNERMAN, D. & HOLMES, A. 2010. Does gene deletion of AMPA GluA1 phenocopy features of schizoaffective disorder? Neurobiol Dis, 40, 608-21.

FLEISCHER, J., METZ, S., DUSENBERG, M., GRIMM, S., GOLDE, S., ROEPKE, S., RENNEBERG, B., WOLF, O. T., OTTE, C. & WINGENFELD, K. 2019. Neural correlates of glucocorticoids effects on autobiographical memory retrieval in healthy women. Behav Brain Res, 359, 895-902.

FORGET, H., LACROIX, A. & COHEN, H. 2002. Persistent cognitive impairment following surgical treatment of Cushing's syndrome. Psychoneuroendocrinology, 27, 367-83.

FREY, M. C., SPRENGEL, R. & NEVIAN, T. 2009. Activity pattern-dependent long-term potentiation in neocortex and hippocampus of GluA1 (GluR-A) subunit-deficient mice. J Neurosci, 29, 5587-96.

FU, H., CAI, J., CLEVERS, H., FAST, E., GRAY, S., GREENBERG, R., JAIN, M. K., MA, Q., QIU, M., ROWITCH, D. H., TAYLOR, C. M. & STILES, C. D. 2009. A genome-wide screen for spatially restricted expression patterns identifies transcription factors that regulate glial development. J Neurosci, 29, 11399-408.

FUNDER, J. W. 2010. Minireview: Aldosterone and mineralocorticoid receptors: past, present, and future. Endocrinology, 151, 5098-102.

FURAY, A. R., BRUESTLE, A. E. & HERMAN, J. P. 2008. The role of the forebrain glucocorticoid receptor in acute and chronic stress. Endocrinology, 149, 5482-90.

GALIGNIANA, M. D., ECHEVERRIA, P. C., ERLEJMAN, A. G. & PIWIEN-PILIPUK, G. 2010. Role of molecular chaperones and TPR-domain proteins in the cytoplasmic transport of steroid receptors and their passage through the nuclear pore. Nucleus, 1, 299-308.

GALIGNIANA, M. D., HARRELL, J. M., MURPHY, P. J., CHINKERS, M., RADANYI, C., RENOIR, J. M., ZHANG, M. & PRATT, W. B. 2002. Binding of hsp90-associated immunophilins to cytoplasmic dynein: direct binding and in vivo evidence that the peptidylprolyl isomerase domain is a dynein interaction domain. Biochemistry, 41, 13602-10.

GE, Y., DONG, Z., BAGOT, R. C., HOWLAND, J. G., PHILLIPS, A. G., WONG, T. P. & WANG, Y. T. 2010. Hippocampal long-term depression is required for the consolidation of spatial memory. Proc Natl Acad Sci U S A, 107, 16697-702.

GESING, A., BILANG-BLEUEL, A., DROSTE, S. K., LINTHORST, A. C., HOLSBOER, F. & REUL, J. M. H. M. 2001. Psychological stress increases hippocampal mineralocorticoid receptor levels: involvement of corticotropin-releasing hormone. J Neurosci, 21, 4822-9.

GJERSTAD, J. K., LIGHTMAN, S. L. & SPIGA, F. 2018. Role of glucocorticoid negative feedback in the regulation of HPA axis pulsatility. Stress, 21, 403-416.

GOODSON, M., JONAS, B. A. & PRIVALSKY, M. A. 2005. Corepressors: custom tailoring and alterations while you wait. Nucl Recept Signal, 3, e003.

GOULD, E., BEYLIN, A., TANAPAT, P., REEVES, A. & SHORS, T. J. 1999. Learning enhances adult neurogenesis in the hippocampal formation. Nat Neurosci, 2, 260-5.

GOULD, E., CAMERON, H. A., DANIELS, D. C., WOOLLEY, C. S. & MCEWEN, B. S. 1992. Adrenal hormones suppress cell division in the adult rat dentate gyrus. J Neurosci, 12, 3642-50.

GOULD, E., WOOLLEY, C. S., CAMERON, H. A., DANIELS, D. C. & MCEWEN, B. S. 1991a. Adrenal steroids regulate postnatal development of the rat dentate gyrus: II. Effects of glucocorticoids and mineralocorticoids on cell birth. J Comp Neurol, 313, 486-93.

GOULD, E., WOOLLEY, C. S. & MCEWEN, B. S. 1991b. Adrenal steroids regulate postnatal development of the rat dentate gyrus: I. Effects of glucocorticoids on cell death. J Comp Neurol, 313, 479-85.

GRAD, I. & PICARD, D. 2007. The glucocorticoid responses are shaped by molecular chaperones. Mol Cell Endocrinol, 275, 2-12.

GRAY, J. D., RUBIN, T. G., HUNTER, R. G. & MCEWEN, B. S. 2014. Hippocampal gene expression changes underlying stress sensitization and recovery. Mol Psychiatry, 19, 1171-8.

GROENEWEG, F. L., KARST, H., DE KLOET, E. R. & JOELS, M. 2012. Mineralocorticoid and glucocorticoid receptors at the neuronal membrane, regulators of nongenomic corticosteroid signalling. Mol Cell Endocrinol, 350, 299-309.

GUERRA-ARAIZA, C., REYNA-NEYRA, A., SALAZAR, A. M., CERBON, M. A., MORIMOTO, S. & CAMACHO-ARROYO, I. 2001. Progesterone receptor isoforms expression in the prepuberal and adult male rat brain. Brain Res Bull, 54, 13-7.

GUO, H., KHAN, R., RAZA, S. H. A., NING, Y., WEI, D., WU, S., HOSSEINI, S. M., ULLAH, I., GARCIA, M. D. & ZAN, L. 2018. KLF15 promotes transcription of KLF3 gene in bovine adipocytes. Gene, 659, 77-83.

GUTIERREZ-MECINAS, M., TROLLOPE, A. F., COLLINS, A., MORFETT, H., HESKETH, S. A., KERSANTE, F. & REUL, J. M. H. M. 2011. Long-lasting behavioral responses to stress involve a direct interaction of glucocorticoid receptors with ERK1/2-MSK1-Elk-1 signaling. Proc Natl Acad Sci U S A, 108, 13806-11.

HADAD-OPHIR, O., ALBRECHT, A., STORK, O. & RICHTER-LEVIN, G. 2014. Amygdala activation and GABAergic gene expression in hippocampal sub-regions at the interplay of stress and spatial learning. Front Behav Neurosci, 8, 3.

HARDIES, K., CAI, Y., JARDEL, C., JANSEN, A. C., CAO, M., MAY, P., DJEMIE, T., HACHON LE CAMUS, C., KEYMOLEN, K., DECONINCK, T., BHAMBHANI, V., LONG, C., SAJAN, S. A., HELBIG, K. L., CONSORTIUM, A. R. W. G. O. T. E. R., SULS, A., BALLING, R., HELBIG, I., DE JONGHE, P., DEPIENNE, C., DE CAMILLI, P. & WECKHUYSEN, S. 2016. Loss of SYNJ1 dual phosphatase activity leads to early onset refractory seizures and progressive neurological decline. Brain, 139, 2420-30.

HARRELL, J. M., MURPHY, P. J., MORISHIMA, Y., CHEN, H., MANSFIELD, J. F., GALIGNIANA, M. D. & PRATT, W. B. 2004. Evidence for glucocorticoid receptor transport on microtubules by dynein. J Biol Chem, 279, 54647-54.

HEERY, D. M., KALKHOVEN, E., HOARE, S. & PARKER, M. G. 1997. A signature motif in transcriptional co-activators mediates binding to nuclear receptors. Nature, 387, 733-6.

HELMREICH, D. L., CULLINAN, W. E. & WATSON, S. J. 1996. The effect of adrenalectomy on stress-induced c-fos mRNA expression in the rat brain. Brain Res, 706, 137-44.

HENLEY, D., LIGHTMAN, S. & CARRELL, R. 2016. Cortisol and CBG - Getting cortisol to the right place at the right time. Pharmacol Ther, 166, 128-35.

HERMAN, J. P., PATEL, P. D., AKIL, H. & WATSON, S. J. 1989. Localization and regulation of glucocorticoid and mineralocorticoid receptor messenger RNAs in the hippocampal formation of the rat. Mol Endocrinol, 3, 1886-94.

HERMAN, J. P. & SPENCER, R. 1998. Regulation of hippocampal glucocorticoid receptor gene transcription and protein expression in vivo. J Neurosci, 18, 7462-73.

HITZEMANN, R., DARAKJIAN, P., WALTER, N., IANCU, O. D., SEARLES, R. & MCWEENEY, S. 2014. Introduction to sequencing the brain transcriptome. Int Rev Neurobiol, 116, 1-19.

HODGE, R. D., BAKKEN, T. E., MILLER, J. A., SMITH, K. A., BARKAN, E. R., GRAYBUCK, L. T., CLOSE, J. L., LONG, B., JOHANSEN, N., PENN, O., YAO, Z., EGGERMONT, J., HOLLT, T., LEVI, B. P., SHEHATA, S. I., AEVERMANN, B., BELLER, A., BERTAGNOLLI, D., BROUNER, K., CASPER, T., COBBS, C., DALLEY, R., DEE, N., DING, S. L., ELLENBOGEN, R. G., FONG, O., GARREN, E., GOLDY, J., GWINN, R. P., HIRSCHSTEIN, D., KEENE, C. D., KESHK, M., KO, A. L., LATHIA, K., MAHFOUZ, A., MALTZER, Z., MCGRAW, M., NGUYEN, T. N., NYHUS, J., OJEMANN, J. G., OLDRE, A., PARRY, S., REYNOLDS, S., RIMORIN, C., SHAPOVALOVA, N. V., SOMASUNDARAM, S., SZAFER, A., THOMSEN, E. R., TIEU, M., QUON, G., SCHEUERMANN, R. H., YUSTE, R., SUNKIN, S. M., LELIEVELDT, B., FENG, D., NG, L., BERNARD, A., HAWRYLYCZ, M., PHILLIPS, J. W., TASIC, B., ZENG, H., JONES, A. R., KOCH, C. & LEIN, E. S. 2019. Conserved cell types with divergent features in human versus mouse cortex. Nature.

HOGAN, B. V., PETER, M. B., SHENOY, H. G., HORGAN, K. & HUGHES, T. A. 2011. Surgery induced immunosuppression. Surgeon, 9, 38-43.

HOLLENBERG, S. M., WEINBERGER, C., ONG, E. S., CERELLI, G., ORO, A., LEBO, R., THOMPSON, E. B., ROSENFELD, M. G. & EVANS, R. M. 1985. Primary structure and expression of a functional human glucocorticoid receptor cDNA. Nature, 318, 635-41.

HOWNG, S. Y., AVILA, R. L., EMERY, B., TRAKA, M., LIN, W., WATKINS, T., COOK, S., BRONSON, R., DAVISSON, M., BARRES, B. A. & POPKO, B. 2010. ZFP191 is required by oligodendrocytes for CNS myelination. Genes Dev, 24, 301-11.

HU, Z., YURI, K., OZAWA, H., LU, H. & KAWATA, M. 1997. The in vivo time course for elimination of adrenalectomy-induced apoptotic profiles from the granule cell layer of the rat hippocampus. J Neurosci, 17, 3981-9.

HUA, S. Y. & CHEN, Y. Z. 1989. Membrane receptor-mediated electrophysiological effects of glucocorticoid on mammalian neurons. Endocrinology, 124, 687-91.

HUDSON, W. H., YOUN, C. & ORTLUND, E. A. 2013. The structural basis of direct glucocorticoid-mediated transrepression. Nat Struct Mol Biol, 20, 53-8.

HUNTER, R. G., SELIGSOHN, M., RUBIN, T. G., GRIFFITHS, B. B., OZDEMIR, Y., PFAFF, D. W., DATSON, N. A. & MCEWEN, B. S. 2016. Stress and corticosteroids regulate rat hippocampal mitochondrial DNA gene expression via the glucocorticoid receptor. Proc Natl Acad Sci U S A, 113, 9099-104.

HURKO, O. & RYAN, J. L. 2005. Translational research in central nervous system drug discovery. NeuroRx, 2, 671-82.

HYND, M. R., SCOTT, H. L. & DODD, P. R. 2004. Differential expression of N-methyl-D-aspartate receptor NR2 isoforms in Alzheimer's disease. J Neurochem, 90, 913-9.

IKEGAYA, Y., SAITO, H. & ABE, K. 1994. Attenuated hippocampal long-term potentiation in basolateral amygdala-lesioned rats. Brain Res, 656, 157-64.

ILLUMINA, I. 2017. An introduction to next-Generation Sequencing Technology [Online]. Available: https://www.illumina.com/content/dam/illumina-marketing/documents/products/illumina_sequencing_introduction.pdf [Accessed].

IMATAKA, H., NAKAYAMA, K., YASUMOTO, K., MIZUNO, A., FUJII-KURIYAMA, Y. & HAYAMI, M. 1994. Cell-specific translational control of transcription factor BTEB expression. The role of an upstream AUG in the 5'-untranslated region. J Biol Chem, 269, 20668-73.

IMATAKA, H., SOGAWA, K., YASUMOTO, K., KIKUCHI, Y., SASANO, K., KOBAYASHI, A., HAYAMI, M. & FUJII-KURIYAMA, Y. 1992. Two regulatory proteins that bind to the basic transcription element (BTE), a GC box sequence in the promoter region of the rat P-4501A1 gene. EMBO J, 11, 3663-71.

IOANNIDIS, A., ARVANITIDIS, K., FILIDOU, E., VALATAS, V., STAVROU, G., MICHALOPOULOS, A., KOLIOS, G. & KOTZAMPASSI, K. 2018. The Length of Surgical Skin Incision in Postoperative Inflammatory Reaction. JSLS, 22.

ISING, M., DEPPING, A. M., SIEBERTZ, A., LUCAE, S., UNSCHULD, P. G., KLOIBER, S., HORSTMANN, S., UHR, M., MULLER-MYHSOK, B. & HOLSBOER, F. 2008. Polymorphisms in the FKBP5 gene region modulate recovery from psychosocial stress in healthy controls. Eur J Neurosci, 28, 389-98.

JAASKELAINEN, T., MAKKONEN, H. & PALVIMO, J. J. 2011. Steroid up-regulation of FKBP51 and its role in hormone signaling. Curr Opin Pharmacol, 11, 326-31.

JAHN, H., KIEFER, F., SCHICK, M., YASSOURIDIS, A., STEIGER, A., KELLNER, M. & WIEDEMANN, K. 2003. Sleep Endocrine Effects of the 11-β-Hydroxysteroiddehydrogenase Inhibitor Metyrapone. Sleep, 26, 823-829.

JAY, T. M. & WITTER, M. P. 1991. Distribution of hippocampal CA1 and subicular efferents in the prefrontal cortex of the rat studied by means of anterograde transport of Phaseolus vulgaris-leucoagglutinin. J Comp Neurol, 313, 574-86.

JEFFERYS, D., COPOLOV, D., IRBY, D. & FUNDER, J. 1983. Behavioural effect of adrenalectomy: reversal by glucocorticoids or [D-Ala2,Met5]enkephalinamide. Eur J Pharmacol, 92, 99-103.

JEFFERYS, D. & FUNDER, J. W. 1987. Glucocorticoids, adrenal medullary opioids, and the retention of a behavioral response after stress. Endocrinology, 121, 1006-9.

JELTSCH, J. M., KROZOWSKI, Z., QUIRIN-STRICKER, C., GRONEMEYER, H., SIMPSON, R. J., GARNIER, J. M., KRUST, A., JACOB, F. & CHAMBON, P. 1986. Cloning of the chicken progesterone receptor. Proc Natl Acad Sci U S A, 83, 5424-8.

JIANG, H., LEI, R., DING, S. W. & ZHU, S. 2014. Skewer: a fast and accurate adapter trimmer for next-generation sequencing paired-end reads. BMC Bioinformatics, 15, 182.

JIN, R. O., MASON, S., MELLON, S. H., EPEL, E. S., REUS, V. I., MAHAN, L., ROSSER, R. L., HOUGH, C. M., BURKE, H. M., MUELLER, S. G. & WOLKOWITZ, O. M. 2016. Cortisol/DHEA ratio and hippocampal volume: A pilot study in major depression and healthy controls. Psychoneuroendocrinology, 72, 139-46.

JOHN, S., SABO, P. J., THURMAN, R. E., SUNG, M. H., BIDDIE, S. C., JOHNSON, T. A., HAGER, G. L. & STAMATOYANNOPOULOS, J. A. 2011. Chromatin accessibility pre-determines glucocorticoid receptor binding patterns. Nat Genet, 43, 264-8.

JOHNSON, T. A., ELBI, C., PAREKH, B. S., HAGER, G. L. & JOHN, S. 2008. Chromatin remodeling complexes interact dynamically with a glucocorticoid receptor-regulated promoter. Mol Biol Cell, 19, 3308-22.

JUSZCZAK, A., MORRIS, D. G., GROSSMAN, A. B. & NIEMAN, L. K. 2016. Cushing's syndrome. In: JAMESON, J. L., DE GROOT, L. J., DE KRETSER, D. M., GIUDICE, L. C., GROSSMAN, A. B., MELMED, S., POTTS, J. T. & WEIR, G. C. (eds.) Endocrinology: adult and pediatric Seventh ed.: Saunders.

KACZYNSKI, J., COOK, T. & URRUTIA, R. 2003. Sp1- and Krüppel-like transcription factors. Genome Biol, 4, 206.

KALMAN, B. A. & SPENCER, R. L. 2002. Rapid corticosteroid-dependent regulation of mineralocorticoid receptor protein expression in rat brain. Endocrinology, 143, 4184-95.

KAPLAN, M. S. & HINDS, J. W. 1977. Neurogenesis in the adult rat: electron microscopic analysis of light radioautographs. Science, 197, 1092-4.

KENNEDY, C. L. M., CARTER, S. D., MIFSUD, K. R. & REUL, J. 2019. Unexpected effects of metyrapone on corticosteroid receptor interaction with the genome and subsequent gene transcription in the hippocampus of male rats. J Neuroendocrinol, e12820.

KIM, D., LANGMEAD, B. & SALZBERG, S. L. 2015. HISAT: a fast spliced aligner with low memory requirements. Nat Methods, 12, 357-60.

KIM, J. J., LEE, H. J., HAN, J. S. & PACKARD, M. G. 2001. Amygdala is critical for stress-induced modulation of hippocampal long-term potentiation and learning. J Neurosci, 21, 5222-8.

KING, H. A., TROTTER, K. W. & ARCHER, T. K. 2012. Chromatin remodeling during glucocorticoid receptor regulated transactivation. Biochim Biophys Acta, 1819, 716-26.

KINO, T., NORDEEN, S. K. & CHROUSOS, G. P. 1999. Conditional modulation of glucocorticoid receptor activities by CREB-binding protein (CBP) and p300. J Steroid Biochem Mol Biol, 70, 15-25.

KITCHENER, P., DI BLASI, F., BORRELLI, E. & PIAZZA, P. V. 2004. Differences between brain structures in nuclear translocation and DNA binding of the glucocorticoid receptor during stress and the circadian cycle. Eur J Neurosci, 19, 1837-46.

KLUR, S., MULLER, C., PEREIRA DE VASCONCELOS, A., BALLARD, T., LOPEZ, J., GALANI, R., CERTA, U. & CASSEL, J. C. 2009. Hippocampal-dependent spatial memory functions might be lateralized in rats: An approach combining gene expression profiling and reversible inactivation. Hippocampus, 19, 800-16.

KOLBER, B. J., ROBERTS, M. S., HOWELL, M. P., WOZNIAK, D. F., SANDS, M. S. & MUGLIA, L. J. 2008. Central amygdala glucocorticoid receptor action promotes fear-associated CRH activation and conditioning. Proc Natl Acad Sci U S A, 105, 12004-9.

KORTE, S. M., DE KLOET, E. R., BUWALDA, B., BOUMAN, S. D. & BOHUS, B. 1996. Antisense to the glucocorticoid receptor in hippocampal dentate gyrus reduces immobility in forced swim test. Eur J Pharmacol, 301, 19-25.

KOYAMA, Y., HATTORI, T., SHIMIZU, S., TANIGUCHI, M., YAMADA, K., TAKAMURA, H., KUMAMOTO, N., MATSUZAKI, S., ITO, A., KATAYAMA, T. & TOHYAMA, M. 2013. DBZ (DISC1-binding zinc finger protein)-deficient mice display abnormalities in basket cells in the somatosensory cortices. J Chem Neuroanat, 53, 1-10.

KRETZ, O., SCHMID, W., BERGER, S. & GASS, P. 2001. The mineralocorticoid receptor expression in the mouse CNS is conserved during development. Neuroreport, 12, 1133-7.

KUMAR, R. & THOMPSON, E. B. 2012. Folding of the glucocorticoid receptor N-terminal transactivation function: dynamics and regulation. Mol Cell Endocrinol, 348, 450-6.

KURUMAJI, A., ITO, T., ISHII, S. & NISHIKAWA, T. 2008. Effects of FG7142 and immobilization stress on the gene expression in the neocortex of mice. Neurosci Res, 62, 155-9.

LADD, C. O., OWENS, M. J. & NEMEROFF, C. B. 1996. Persistent changes in corticotropin-releasing factor neuronal systems induced by maternal deprivation. Endocrinology, 137, 1212-8.

LAKHAN, R., KALITA, J., MISRA, U. K., KUMARI, R. & MITTAL, B. 2010. Association of intronic polymorphism rs3773364 A>G in synapsin-2 gene with idiopathic epilepsy. Synapse, 64, 403-8.

LAMBLE, S., BATTY, E., ATTAR, M., BUCK, D., BOWDEN, R., LUNTER, G., CROOK, D., EL-FAHMAWI, B. & PIAZZA, P. 2013. Improved workflows for high throughput library preparation using the transposome-based Nextera system. BMC Biotechnol, 13, 104.

LAMIA, K. A., PAPP, S. J., YU, R. T., BARISH, G. D., UHLENHAUT, N. H., JONKER, J. W., DOWNES, M. & EVANS, R. M. 2011. Cryptochromes mediate rhythmic repression of the glucocorticoid receptor. Nature, 480, 552-6.

LANDT, S. G., MARINOV, G. K., KUNDAJE, A., KHERADPOUR, P., PAULI, F., BATZOGLOU, S., BERNSTEIN, B. E., BICKEL, P., BROWN, J. B., CAYTING, P., CHEN, Y., DESALVO, G., EPSTEIN, C., FISHER-AYLOR, K. I., EUSKIRCHEN, G., GERSTEIN, M., GERTZ, J., HARTEMINK, A. J., HOFFMAN, M. M., IYER, V. R., JUNG, Y. L., KARMAKAR, S., KELLIS, M., KHARCHENKO, P. V., LI, Q., LIU, T., LIU, X. S., MA, L., MILOSAVLJEVIC, A., MYERS, R. M., PARK, P. J., PAZIN, M. J., PERRY,

M. D., RAHA, D., REDDY, T. E., ROZOWSKY, J., SHORESH, N., SIDOW, A., SLATTERY, M., STAMATOYANNOPOULOS, J. A., TOLSTORUKOV, M. Y., WHITE, K. P., XI, S., FARNHAM, P. J., LIEB, J. D., WOLD, B. J. & SNYDER, M. 2012. ChIP-seq guidelines and practices of the ENCODE and modENCODE consortia. Genome Res, 22, 1813-31.

LAUB, F., ALDABE, R., FRIEDRICH, V., JR., OHNISHI, S., YOSHIDA, T. & RAMIREZ, F. 2001. Developmental expression of mouse Krüppel-like transcription factor KLF7 suggests a potential role in neurogenesis. Dev Biol, 233, 305-18.

LEMAIRE, V., KOEHL, M., LE MOAL, M. & ABROUS, D. N. 2000. Prenatal stress produces learning deficits associated with an inhibition of neurogenesis in the hippocampus. Proc Natl Acad Sci U S A, 97, 11032-7.

LEWIS, J. G., BAGLEY, C. J., ELDER, P. A., BACHMANN, A. W. & TORPY, D. J. 2005. Plasma free cortisol fraction reflects levels of functioning corticosteroid-binding globulin. Clin Chim Acta, 359, 189-94.

LESCA, G., RUDOLF, G., BRUNEAU, N., LOZOVAYA, N., LABALME, A., BOUTRY-KRYZA, N., SALMI, M., TSINTSADZE, T., ADDIS, L., MOTTE, J., WRIGHT, S., TSINTSADZE, V., MICHEL, A., DOUMMAR, D., LASCELLES, K., STRUG, L., WATERS, P., DE BELLESCIZE, J., VRIELYNCK, P., DE SAINT MARTIN, A., VILLE, D., RYVLIN, P., ARZIMANOGLOU, A., HIRSCH, E., VINCENT, A., PAL, D., BURNASHEV, N., SANLAVILLE, D. & SZEPETOWSKI, P. 2013. GRIN2A mutations in acquired epileptic aphasia and related childhood focal epilepsies and encephalopathies with speech and language dysfunction. Nat Genet, 45, 1061-6.

LI, H., CHEN, D. & ZHANG, J. 2012. Analysis of intron sequence features associated with transcriptional regulation in human genes. PLoS One, 7, e46784.

LI, H. & DURBIN, R. 2009. Fast and accurate short read alignment with Burrows-Wheeler transform. Bioinformatics, 25, 1754-60.

LI, H., ZHANG, C., SHEN, H., SHEN, Z., WU, L., MO, F. & LI, M. 2017. Physiological stress-induced corticosterone increases heme uptake via KLF4-HCP1 signaling pathway in hippocampus neurons. Sci Rep, 7, 5745.

LIAO, B., MIESAK, B. & AZMITIA, E. C. 1993. Loss of 5-HT1A receptor mRNA in the dentate gyrus of the long-term adrenalectomized rats and rapid reversal by dexamethasone. Brain Res Mol Brain Res, 19, 328-32.

LIAO, Y., SMYTH, G. K. & SHI, W. 2013. The Subread aligner: fast, accurate and scalable read mapping by seed-and-vote. Nucleic Acids Res, 41, e108.

LIAO, Y., SMYTH, G. K. & SHI, W. 2014. featureCounts: an efficient general purpose program for assigning sequence reads to genomic features. Bioinformatics, 30, 923-30.

LIU, L., TSUJI, M., TAKEDA, H., TAKADA, K. & MATSUMIYA, T. 1999. Adrenocortical suppression blocks the enhancement of memory storage produced by exposure to psychological stress in rats. Brain Res, 821, 134-40.

LIU, Z., AUBOEUF, D., WONG, J., CHEN, J. D., TSAI, S. Y., TSAI, M. J. & O'MALLEY, B. W. 2002. Coactivator/corepressor ratios modulate PR-mediated transcription by the selective receptor modulator RU486. Proc Natl Acad Sci U S A, 99, 7940-4.

LUCZYNSKI, P., MOQUIN, L. & GRATTON, A. 2015. Chronic stress alters the dendritic morphology of callosal neurons and the acute glutamate stress response in the rat medial prefrontal cortex. Stress, 18, 654-67.

LUISI, B. F., XU, W. X., OTWINOWSKI, Z., FREEDMAN, L. P., YAMAMOTO, K. R. & SIGLER, P. B. 1991. Crystallographic analysis of the interaction of the glucocorticoid receptor with DNA. Nature, 352, 497-505.

MAES, M., LIN, A., BONACCORSO, S., VAN HUNSEL, F., VAN GASTEL, A., DELMEIRE, L., BIONDI, M., BOSMANS, E., KENIS, G. & SCHARPE, S. 1998. Increased 24-hour urinary cortisol excretion in patients with post-traumatic stress disorder and patients with major depression, but not in patients with fibromyalgia. Acta Psychiatr Scand, 98, 328-35.

MALLIPATTU, S. K., LIU, R., ZHENG, F., NARLA, G., MA'AYAN, A., DIKMAN, S., JAIN, M. K., SALEEM, M., D'AGATI, V., KLOTMAN, P., CHUANG, P. Y. & HE, J. C. 2012. Krüppel-like factor 15 (KLF15) is a key regulator of podocyte differentiation. J Biol Chem, 287, 19122-35.

MARTIN, J. L. & FINSTERWALD, C. 2011. Cooperation between BDNF and glutamate in the regulation of synaptic transmission and neuronal development. Commun Integr Biol, 4, 14-6.

MASSAAD, C., LOMBES, M., AGGERBECK, M., RAFESTIN-OBLIN, M. E. & BAROUKI, R. 1997. Cell-specific, promoter-dependent mineralocorticoid agonist activity of spironolactone. Mol Pharmacol, 51, 285-92.

MASUNO, K., HALDAR, S. M., JEYARAJ, D., MAILLOUX, C. M., HUANG, X., PANETTIERI, R. A., JR., JAIN, M. K. & GERBER, A. N. 2011. Expression profiling identifies Klf15 as a glucocorticoid target that regulates airway hyperresponsiveness. Am J Respir Cell Mol Biol, 45, 642-9.

MATHARU, N. & AHITUV, N. 2015. Minor Loops in Major Folds: Enhancer-Promoter Looping, Chromatin Restructuring, and Their Association with Transcriptional Regulation and Disease. PLoS Genet, 11, e1005640.

MAYER, J. L., KLUMPERS, L., MASLAM, S., DE KLOET, E. R., JOELS, M. & LUCASSEN, P. J. 2006. Brief treatment with the glucocorticoid receptor antagonist mifepristone normalises the corticosterone-induced reduction of adult hippocampal neurogenesis. J Neuroendocrinol, 18, 629-31.

MAZARATI, A. M., SHIN, D., KWON, Y. S., BRAGIN, A., PINEDA, E., TIO, D., TAYLOR, A. N. & SANKAR, R. 2009. Elevated plasma corticosterone level and depressive behavior in experimental temporal lobe epilepsy. Neurobiol Dis, 34, 457-61.

MCCARTHY, D. J., CHEN, Y. & SMYTH, G. K. 2012. Differential expression analysis of multifactor RNA-Seq experiments with respect to biological variation. Nucleic Acids Res, 40, 4288-97.

MCCONNELL, B. B. & YANG, V. W. 2010. Mammalian Krüppel-like factors in health and diseases. Physiol Rev, 90, 1337-81.

MCEWEN, B. S. 2012. Brain on stress: how the social environment gets under the skin. Proc Natl Acad Sci U S A, 109 Suppl 2, 17180-5.

MCEWEN, B. S., WEISS, J. M. & SCHWARTZ, L. S. 1968. Selective retention of corticosterone by limbic structures in rat brain. Nature, 220, 911-2.

MCGAUGH, J. L. 2004. The amygdala modulates the consolidation of memories of emotionally arousing experiences. Annu Rev Neurosci, 27, 1-28.

MCGAUGH, J. L., CAHILL, L. & ROOZENDAAL, B. 1996. Involvement of the amygdala in memory storage: interaction with other brain systems. Proc Natl Acad Sci U S A, 93, 13508-14.

MCGRATH, J. J., FERON, F. P., BURNE, T. H., MACKAY-SIM, A. & EYLES, D. W. 2003. The neurodevelopmental hypothesis of schizophrenia: a review of recent developments. Ann Med, 35, 86-93.

MCKENZIE, A. T., WANG, M., HAUBERG, M. E., FULLARD, J. F., KOZLENKOV, A., KEENAN, A., HURD, Y. L., DRACHEVA, S., CASACCIA, P., ROUSSOS, P. & ZHANG, B. 2018. Brain Cell Type Specific Gene Expression and Co-expression Network Architectures. Sci Rep, 8, 8868.

MCKLVEEN, J. M., MYERS, B., FLAK, J. N., BUNDZIKOVA, J., SOLOMON, M. B., SEROOGY, K. B. & HERMAN, J. P. 2013. Role of prefrontal cortex glucocorticoid receptors in stress and emotion. Biol Psychiatry, 74, 672-9.

MCNEILL, T. H., MASTERS, J. N. & FINCH, C. E. 1991. Effect of chronic adrenalectomy on neuron loss and distribution of sulfated glycoprotein-2 in the dentate gyrus of prepubertal rats. Exp Neurol, 111, 140-4.

MEIJER, O. C., BUURSTEDE, J. C. & SCHAAF, M. J. M. 2019. Corticosteroid Receptors in the Brain: Transcriptional Mechanisms for Specificity and Context-Dependent Effects. Cell Mol Neurobiol, 39, 539-549.

MEIJER, O. C. & DE KLOET, E. R. 1994. Corticosterone suppresses the expression of 5-HT1A receptor mRNA in rat dentate gyrus. Eur J Pharmacol, 266, 255-61.

MEIJER, O. C., KALKHOVEN, E., VAN DER LAAN, S., STEENBERGEN, P. J., HOUTMAN, S. H., DIJKMANS, T. F., PEARCE, D. & DE KLOET, E. R. 2005. Steroid receptor coactivator-1 splice variants differentially affect corticosteroid receptor signaling. Endocrinology, 146, 1438-48.

MEIJER, O. C., STEENBERGEN, P. J. & DE KLOET, E. R. 2000. Differential expression and regional distribution of steroid receptor coactivators SRC-1 and SRC-2 in brain and pituitary. Endocrinology, 141, 2192-9.

MEINEL, S., RUHS, S., SCHUMANN, K., STRATZ, N., TRENKMANN, K., SCHREIER, B., GROSSE, I., KEILWAGEN, J., GEKLE, M. & GROSSMANN, C. 2013. Mineralocorticoid receptor interaction with SP1 generates a new response element for pathophysiologically relevant gene expression. Nucleic Acids Res, 41, 8045-60.

MIFSUD, K. R. & REUL, J. 2018. Mineralocorticoid and glucocorticoid receptor-mediated control of genomic responses to stress in the brain. Stress, 1-14.

MIFSUD, K. R. & REUL, J. M. H. M. 2016. Acute stress enhances heterodimerization and binding of corticosteroid receptors at glucocorticoid target genes in the hippocampus. Proc Natl Acad Sci U S A, 113, 11336-11341.

MIFSUD, K. R., SAUNDERSON, E. A., SPIERS, H., CARTER, S. D., TROLLOPE, A. F., MILL, J. & REUL, J. M. H. M. 2016. Rapid Down-Regulation of Glucocorticoid Gene Expression in the Dentate Gyrus after Acute Stress in vivo: Role of DNA Methylation and microRNA Activity. Neuroendocrinology.

MITCHELL, J. B. & MEANEY, M. J. 1991. Effects of corticosterone on response consolidation and retrieval in the forced swim test. Behav Neurosci, 105, 798-803.

MIZOGUCHI, K., ISHIGE, A., TAKEDA, S., ABURADA, M. & TABIRA, T. 2004. Endogenous glucocorticoids are essential for maintaining prefrontal cortical cognitive function. J Neurosci, 24, 5492-9.

MOALLI, P. A., PILLAY, S., KRETT, N. L. & ROSEN, S. T. 1993. Alternatively spliced glucocorticoid receptor messenger RNAs in glucocorticoid-resistant human multiple myeloma cells. Cancer Res, 53, 3877-9.

MOORE, D. L., BLACKMORE, M. G., HU, Y., KAESTNER, K. H., BIXBY, J. L., LEMMON, V. P. & GOLDBERG, J. L. 2009. KLF family members regulate intrinsic axon regeneration ability. Science, 326, 298-301.

MORIMOTO, M., MORITA, N., OZAWA, H., YOKOYAMA, K. & KAWATA, M. 1996. Distribution of glucocorticoid receptor immunoreactivity and mRNA in the rat brain: an immunohistochemical and in situ hybridization study. Neurosci Res, 26, 235-69.

MORISHIMA, Y., KANELAKIS, K. C., MURPHY, P. J., LOWE, E. R., JENKINS, G. J., OSAWA, Y., SUNAHARA, R. K. & PRATT, W. B. 2003. The hsp90 cochaperone p23 is the limiting component of the

multiprotein hsp90/hsp70-based chaperone system in vivo where it acts to stabilize the client protein: hsp90 complex. J Biol Chem, 278, 48754-63.

MORITA, M., KOBAYASHI, A., YAMASHITA, T., SHIMANUKI, T., NAKAJIMA, O., TAKAHASHI, S., IKEGAMI, S., INOKUCHI, K., YAMASHITA, K., YAMAMOTO, M. & FUJII-KURIYAMA, Y. 2003. Functional analysis of basic transcription element binding protein by gene targeting technology. Mol Cell Biol, 23, 2489-500.

MYCHASIUK, R., MUHAMMAD, A. & KOLB, B. 2016. Chronic stress induces persistent changes in global DNA methylation and gene expression in the medial prefrontal cortex, orbitofrontal cortex, and hippocampus. Neuroscience, 322, 489-99.

NADER, N., CHROUSOS, G. P. & KINO, T. 2009. Circadian rhythm transcription factor CLOCK regulates the transcriptional activity of the glucocorticoid receptor by acetylating its hinge region lysine cluster: potential physiological implications. FASEB J, 23, 1572-83.

NAKKEN, K. O., SOLAAS, M. H., KJELDSEN, M. J., FRIIS, M. L., PELLOCK, J. M. & COREY, L. A. 2005. Which seizure-precipitating factors do patients with epilepsy most frequently report? Epilepsy Behav, 6, 85-9.

NAVA, N., TRECCANI, G., MULLER, H. K., POPOLI, M., WEGENER, G. & ELFVING, B. 2017. The expression of plasticity-related genes in an acute model of stress is modulated by chronic desipramine in a time-dependent manner within medial prefrontal cortex. Eur Neuropsychopharmacol, 27, 19-28.

NELSON, C. E., HERSH, B. M. & CARROLL, S. B. 2004. The regulatory content of intergenic DNA shapes genome architecture. Genome Biol, 5, R25.

NELSON, M. D., SAYKIN, A. J., FLASHMAN, L. A. & RIORDAN, H. J. 1998. Hippocampal volume reduction in schizophrenia as assessed by magnetic resonance imaging: a meta-analytic study. Arch Gen Psychiatry, 55, 433-40.

NEMOTO, T., OHARA-NEMOTO, Y., DENIS, M. & GUSTAFSSON, J. A. 1990. The transformed glucocorticoid receptor has a lower steroid-binding affinity than the nontransformed receptor. Biochemistry, 29, 1880-6.

NICOLAIDES, N. C., CHARMANDARI, E., CHROUSOS, G. P. & KINO, T. 2014. Recent advances in the molecular mechanisms determining tissue sensitivity to glucocorticoids: novel mutations, circadian rhythm and ligand-induced repression of the human glucocorticoid receptor. BMC Endocr Disord, 14, 71.

NISHIHARA, E., YOSHIDA-KOMIYA, H., CHAN, C. S., LIAO, L., DAVIS, R. L., O'MALLEY, B. W. & XU, J. 2003. SRC-1 null mice exhibit moderate motor dysfunction and delayed development of cerebellar Purkinje cells. J Neurosci, 23, 213-22.

NORDEEN, S. K., BONA, B. J., BECK, C. A., EDWARDS, D. P., BORROR, K. C. & DEFRANCO, D. B. 1995. The two faces of a steroid antagonist: when an antagonist isn't. Steroids, 60, 97-104.

OAKLEY, R. H. & CIDLOWSKI, J. A. 2013. The biology of the glucocorticoid receptor: new signaling mechanisms in health and disease. J Allergy Clin Immunol, 132, 1033-44.

OAKLEY, R. H., RAMAMOORTHY, S., FOLEY, J. F., BUSADA, J. T., LU, N. Z. & CIDLOWSKI, J. A. 2018. Glucocorticoid receptor isoform-specific regulation of development, circadian rhythm, and inflammation in mice. FASEB J, 32, 5258-5271.

OHTSUKA, T., SHIMOJO, H., MATSUNAGA, M., WATANABE, N., KOMETANI, K., MINATO, N. & KAGEYAMA, R. 2011. Gene expression profiling of neural stem cells and identification of regulators of neural differentiation during cortical development. Stem Cells, 29, 1817-28.

OITZL, M. S. & DE KLOET, E. R. 1992. Selective corticosteroid antagonists modulate specific aspects of spatial orientation learning. Behav Neurosci, 106, 62-71.

OITZL, M. S., FLUTTERT, M., SUTANTO, W. & DE KLOET, E. R. 1998. Continuous blockade of brain glucocorticoid receptors facilitates spatial learning and memory in rats. Eur J Neurosci, 10, 3759-66.

ONATE, S. A., TSAI, S. Y., TSAI, M. J. & O'MALLEY, B. W. 1995. Sequence and characterization of a coactivator for the steroid hormone receptor superfamily. Science, 270, 1354-7.

OSTER, H., CHALLET, E., OTT, V., ARVAT, E., DE KLOET, E. R., DIJK, D. J., LIGHTMAN, S., VGONTZAS, A. & VAN CAUTER, E. 2017. The Functional and Clinical Significance of the 24-Hour Rhythm of Circulating Glucocorticoids. Endocr Rev, 38, 3-45.

OTTESON, D. C., LIU, Y., LAI, H., WANG, C., GRAY, S., JAIN, M. K. & ZACK, D. J. 2004. Krüppel-like factor 15, a zinc-finger transcriptional regulator, represses the rhodopsin and interphotoreceptor retinoid-binding protein promoters. Invest Ophthalmol Vis Sci, 45, 2522-30.

OU, X. M., CHEN, K. & SHIH, J. C. 2006. Glucocorticoid and androgen activation of monoamine oxidase A is regulated differently by R1 and Sp1. J Biol Chem, 281, 21512-25.

PANGALOS, M. N., SCHECHTER, L. E. & HURKO, O. 2007. Drug development for CNS disorders: strategies for balancing risk and reducing attrition. Nat Rev Drug Discov, 6, 521-32.

PARK, P. J. 2009. ChIP-seq: advantages and challenges of a maturing technology. Nat Rev Genet, 10, 669-80.

PARK, S. W., LEE, C. H., LEE, J. G., LEE, S. J., KIM, N. R., CHOI, S. M. & KIM, Y. H. 2009. Differential effects of ziprasidone and haloperidol on immobilization stress-induced mRNA BDNF expression in the hippocampus and neocortex of rats. J Psychiatr Res, 43, 274-81.

PATTWELL, S. S., BATH, K. G., PEREZ-CASTRO, R., LEE, F. S., CHAO, M. V. & NINAN, I. 2012. The BDNF Val66Met polymorphism impairs synaptic transmission and plasticity in the infralimbic medial prefrontal cortex. J Neurosci, 32, 2410-21.

PAZ, R. D., ANDREASEN, N. C., DAOUD, S. Z., CONLEY, R., ROBERTS, R., BUSTILLO, J. & PERRONE-BIZZOZERO, N. I. 2006. Increased expression of activity-dependent genes in cerebellar glutamatergic neurons of patients with schizophrenia. Am J Psychiatry, 163, 1829-31.

PEARCE, D. & YAMAMOTO, K. R. 1993. Mineralocorticoid and glucocorticoid receptor activities distinguished by nonreceptor factors at a composite response element. Science, 259, 1161-5.

PEARSON, R., FLEETWOOD, J., EATON, S., CROSSLEY, M. & BAO, S. 2008. Krüppel-like transcription factors: a functional family. Int J Biochem Cell Biol, 40, 1996-2001.

PEETERS, P. J., FIERENS, F. L., VAN DEN WYNGAERT, I., GOEHLMANN, H. W., SWAGEMAKERS, S. M., KASS, S. U., LANGLOIS, X., PULLAN, S., STENZEL-POORE, M. P. & STECKLER, T. 2004. Gene expression profiles highlight adaptive brain mechanisms in corticotropin releasing factor overexpressing mice. Brain Res Mol Brain Res, 129, 135-50.

PETTA, I., DEJAGER, L., BALLEGEER, M., LIEVENS, S., TAVERNIER, J., DE BOSSCHER, K. & LIBERT, C. 2016. The Interactome of the Glucocorticoid Receptor and Its Influence on the Actions of Glucocorticoids in Combatting Inflammatory and Infectious Diseases. Microbiol Mol Biol Rev, 80, 495-522.

PFAFFL, M. W. 2001. A new mathematical model for relative quantification in real-time RT-PCR. Nucleic Acids Res, 29, e45.

PILLAI, A. 2008. Decreased expression of Sprouty2 in the dorsolateral prefrontal cortex in schizophrenia and bipolar disorder: a correlation with BDNF expression. PLoS One, 3, e1784.

PIVONELLO, R., SIMEOLI, C., DE MARTINO, M. C., COZZOLINO, A., DE LEO, M., IACUANIELLO, D., PIVONELLO, C., NEGRI, M., PELLECCHIA, M. T., IASEVOLI, F. & COLAO, A. 2015. Neuropsychiatric disorders in Cushing's syndrome. Front Neurosci, 9, 129.

POLMAN, J. A., WELTEN, J. E., BOSCH, D. S., DE JONGE, R. T., BALOG, J., VAN DER MAAREL, S. M., DE KLOET, E. R. & DATSON, N. A. 2012. A genome-wide signature of glucocorticoid receptor binding in neuronal PC12 cells. BMC Neurosci, 13, 118.

POLMAN, J. A. E., DE KLOET, E. R. & DATSON, N. A. 2013. Two Populations of Glucocorticoid Receptor-Binding Sites in the Male Rat Hippocampal Genome. Endocrinology, 154, 1832-1844.

POOLEY, J. R., FLYNN, B. P., GRONTVED, L., BAEK, S., GUERTIN, M. J., KERSHAW, Y. M., BIRNIE, M. T., PELLATT, A., RIVERS, C. A., SCHILTZ, R. L., HAGER, G. L., LIGHTMAN, S. L. & CONWAY-CAMPBELL, B. L. 2017. Genome-Wide Identification of Basic Helix-Loop-Helix and NF-1 Motifs Underlying GR Binding Sites in Male Rat Hippocampus. Endocrinology, 158, 1486-1501.

PORSOLT, R. D., LE PICHON, M. & JALFRE, M. 1977. Depression: a new animal model sensitive to antidepressant treatments. Nature, 266, 730-2.

PRESMAN, D. M., GANGULY, S., SCHILTZ, R. L., JOHNSON, T. A., KARPOVA, T. S. & HAGER, G. L. 2016. DNA binding triggers tetramerization of the glucocorticoid receptor in live cells. Proc Natl Acad Sci U S A, 113, 8236-41.

PRESTON, A. R. & EICHENBAUM, H. 2013. Interplay of hippocampus and prefrontal cortex in memory. Curr Biol, 23, R764-73.

QIAN, X., DROSTE, S. K., GUTIERREZ-MECINAS, M., COLLINS, A., KERSANTE, F., REUL, J. M. H. M. & LINTHORST, A. C. 2011. A rapid release of corticosteroid-binding globulin from the liver restrains the glucocorticoid hormone response to acute stress. Endocrinology, 152, 3738-48.

QIN, S., LIU, M., NIU, W. & ZHANG, C. L. 2011. Dysregulation of Krüppel-like factor 4 during brain development leads to hydrocephalus in mice. Proc Natl Acad Sci U S A, 108, 21117-21.

QIN, S. & ZHANG, C. L. 2012. Role of Krüppel-like factor 4 in neurogenesis and radial neuronal migration in the developing cerebral cortex. Mol Cell Biol, 32, 4297-305.

QIN, W., PAN, J., QIN, Y., LEE, D. N., BAUMAN, W. A. & CARDOZO, C. 2014. Identification of functional glucocorticoid response elements in the mouse FoxO1 promoter. Biochem Biophys Res Commun, 450, 979-83.

QUAEDFLIEG, C. W., VAN DE VEN, V., MEYER, T., SIEP, N., MERCKELBACH, H. & SMEETS, T. 2015. Temporal dynamics of stress-induced alternations of intrinsic amygdala connectivity and neuroendocrine levels. PLoS One, 10, e0124141.

QUINLAN, A. R. 2014. BEDTools: The Swiss-Army Tool for Genome Feature Analysis. Curr Protoc Bioinformatics, 47, 11 12 1-34.

RAADSHEER, F. C., VAN HEERIKHUIZE, J. J., LUCASSEN, P. J., HOOGENDIJK, W. J., TILDERS, F. J. & SWAAB, D. F. 1995. Corticotropin-releasing hormone mRNA levels in the paraventricular nucleus of patients with Alzheimer's disease and depression. Am J Psychiatry, 152, 1372-6.

RAJARAJAN, P., GIL, S. E., BRENNAND, K. J. & AKBARIAN, S. 2016. Spatial genome organization and cognition. Nat Rev Neurosci, 17, 681-691.

RAMAMOORTHY, S. & CIDLOWSKI, J. A. 2013. Ligand-induced repression of the glucocorticoid receptor gene is mediated by an NCoR1 repression complex formed by long-range chromatin interactions with intragenic glucocorticoid response elements. Mol Cell Biol, 33, 1711-22.

RATMAN, D., VANDEN BERGHE, W., DEJAGER, L., LIBERT, C., TAVERNIER, J., BECK, I. M. & DE BOSSCHER, K. 2013. How glucocorticoid receptors modulate the activity of other transcription factors: a scope beyond tethering. Mol Cell Endocrinol, 380, 41-54.

RAWASHDEH, O., JILG, A., JEDLICKA, P., SLAWSKA, J., THOMAS, L., SAADE, A., SCHWARZACHER, S. W. & STEHLE, J. H. 2014. PERIOD1 coordinates hippocampal rhythms and memory processing with daytime. Hippocampus, 24, 712-23.

REDDY, T. E., PAULI, F., SPROUSE, R. O., NEFF, N. F., NEWBERRY, K. M., GARABEDIAN, M. J. & MYERS, R. M. 2009. Genomic determination of the glucocorticoid response reveals unexpected mechanisms of gene regulation. Genome Res, 19, 2163-71.

REUL, J. M. H. M. 2014. Making memories of stressful events: a journey along epigenetic, gene transcription, and signaling pathways. Front Psychiatry, 5, 5.

REUL, J. M. H. M., COLLINS, A., SALIBA, R. S., MIFSUD, K. R., CARTER, S. D., GUTIERREZ-MECINAS, M., QIAN, X. & LINTHORST, A. C. E. 2015. Glucocorticoids, epigenetic control and stress resilience. Neurobiology of Stress, 1, 44-59.

REUL, J. M. H. M. & DE KLOET, E. R. 1985. Two receptor systems for corticosterone in rat brain: microdistribution and differential occupation. Endocrinology, 117, 2505-11.

REUL, J. M. H. M., & DE KLOET, E. R. 1986. Anatomical resolution of two types of corticosterone receptor sites in rat brain with in vitro autoradiography and computerized image analysis. J Steroid Biochem, 24, 269-72.

REUL, J. M. H. M., VAN DEN BOSCH, F. R. & DE KLOET, E. R. 1987. Relative occupation of type-I and type-II corticosteroid receptors in rat brain following stress and dexamethasone treatment: functional implications. J Endocrinol, 115, 459-67.

RIVERS, C., LEVY, A., HANCOCK, J., LIGHTMAN, S. & NORMAN, M. 1999. Insertion of an amino acid in the DNA-binding domain of the glucocorticoid receptor as a result of alternative splicing. J Clin Endocrinol Metab, 84, 4283-6.

ROBINSON, M. D., MCCARTHY, D. J. & SMYTH, G. K. 2010. edgeR: a Bioconductor package for differential expression analysis of digital gene expression data. Bioinformatics, 26, 139-40.

ROCERI, M., HENDRIKS, W., RACAGNI, G., ELLENBROEK, B. A. & RIVA, M. A. 2002. Early maternal deprivation reduces the expression of BDNF and NMDA receptor subunits in rat hippocampus. Mol Psychiatry, 7, 609-16.

ROCHER, C., SPEDDING, M., MUNOZ, C. & JAY, T. M. 2004. Acute stress-induced changes in hippocampal/prefrontal circuits in rats: effects of antidepressants. Cereb Cortex, 14, 224-9.

ROGERSON, F. M., YAO, Y. Z., SMITH, B. J., DIMOPOULOS, N. & FULLER, P. J. 2003. Determinants of spironolactone binding specificity in the mineralocorticoid receptor. J Mol Endocrinol, 31, 573-82.

RONACHER, K., HADLEY, K., AVENANT, C., STUBSRUD, E., SIMONS, S. S., JR., LOUW, A. & HAPGOOD, J. P. 2009. Ligand-selective transactivation and transrepression via the glucocorticoid receptor: role of cofactor interaction. Mol Cell Endocrinol, 299, 219-31.

ROOZENDAAL, B., BOHUS, B. & MCGAUGH, J. L. 1996. Dose-dependent suppression of adrenocortical activity with metyrapone: effects on emotion and memory. Psychoneuroendocrinology, 21, 681-93.

ROOZENDAAL, B., MCEWEN, B. S. & CHATTARJI, S. 2009. Stress, memory and the amygdala. Nat Rev Neurosci, 10, 423-33.

ROOZENDAAL, B. & MCGAUGH, J. L. 1997. Glucocorticoid receptor agonist and antagonist administration into the basolateral but not central amygdala modulates memory storage. Neurobiol Learn Mem, 67, 176-9.

ROOZENDAAL, B., WILLIAMS, C. L. & MCGAUGH, J. L. 1999. Glucocorticoid receptor activation in the rat nucleus of the solitary tract facilitates memory consolidation: involvement of the basolateral amygdala. Eur J Neurosci, 11, 1317-23.

ROSS-INNES, C. S., STARK, R., TESCHENDORFF, A. E., HOLMES, K. A., ALI, H. R., DUNNING, M. J., BROWN, G. D., GOJIS, O., ELLIS, I. O., GREEN, A. R., ALI, S., CHIN, S. F., PALMIERI, C., CALDAS, C. & CARROLL, J. S. 2012. Differential oestrogen receptor binding is associated with clinical outcome in breast cancer. Nature, 481, 389-93.

ROTLLANT, D., ONS, S., CARRASCO, J. & ARMARIO, A. 2002. Evidence that metyrapone can act as a stressor: effect on pituitary-adrenal hormones, plasma glucose and brain c-fos induction. Eur J Neurosci, 16, 693-700.

RUPPRECHT, R., ARRIZA, J. L., SPENGLER, D., REUL, J. M. H. M., EVANS, R. M., HOLSBOER, F. & DAMM, K. 1993. Transactivation and synergistic properties of the mineralocorticoid receptor: relationship to the glucocorticoid receptor. Mol Endocrinol, 7, 597-603.

RUSSO-NEUSTADT, A., HA, T., RAMIREZ, R. & KESSLAK, J. P. 2001. Physical activity-antidepressant treatment combination: impact on brain-derived neurotrophic factor and behavior in an animal model. Behav Brain Res, 120, 87-95.

RYAN, T. J., KOPANITSA, M. V., INDERSMITTEN, T., NITHIANANTHARAJAH, J., AFINOWI, N. O., PETTIT, C., STANFORD, L. E., SPRENGEL, R., SAKSIDA, L. M., BUSSEY, T. J., O'DELL, T. J., GRANT, S. G. & KOMIYAMA, N. H. 2013. Evolution of GluN2A/B cytoplasmic domains diversified vertebrate synaptic plasticity and behavior. Nat Neurosci, 16, 25-32.

SAKIMURA, K., KUTSUWADA, T., ITO, I., MANABE, T., TAKAYAMA, C., KUSHIYA, E., YAGI, T., AIZAWA, S., INOUE, Y., SUGIYAMA, H. & ET AL. 1995. Reduced hippocampal LTP and spatial learning in mice lacking NMDA receptor epsilon 1 subunit. Nature, 373, 151-5.

SALVADOR, E., SHITYAKOV, S. & FORSTER, C. 2014. Glucocorticoids and endothelial cell barrier function. Cell Tissue Res, 355, 597-605.

SANCHEZ, M. M., AGUADO, F., SANCHEZ-TOSCANO, F. & SAPHIER, D. 1998. Neuroendocrine and immunocytochemical demonstrations of decreased hypothalamo-pituitary-adrenal axis responsiveness to restraint stress after long-term social isolation. Endocrinology, 139, 579-87.

SANDELIN, A., ALKEMA, W., ENGSTROM, P., WASSERMAN, W. W. & LENHARD, B. 2004. JASPAR: an open-access database for eukaryotic transcription factor binding profiles. Nucleic Acids Res, 32, D91-4.

SANDI, C., LOSCERTALES, M. & GUAZA, C. 1997. Experience-dependent facilitating effect of corticosterone on spatial memory formation in the water maze. Eur J Neurosci, 9, 637-42.

SANDI, C., WOODSON, J. C., HAYNES, V. F., PARK, C. R., TOUYAROT, K., LOPEZ-FERNANDEZ, M. A., VENERO, C. & DIAMOND, D. M. 2005. Acute stress-induced impairment of spatial memory is associated with decreased expression of neural cell adhesion molecule in the hippocampus and prefrontal cortex. Biol Psychiatry, 57, 856-64.

SANGER, F., NICKLEN, S. & COULSON, A. R. 1977. DNA sequencing with chain-terminating inhibitors. Proc Natl Acad Sci U S A, 74, 5463-7.

SANTHA, P., VESZELKA, S., HOYK, Z., MESZAROS, M., WALTER, F. R., TOTH, A. E., KISS, L., KINCSES, A., OLAH, Z., SEPRENYI, G., RAKHELY, G., DER, A., PAKASKI, M., KALMAN, J., KITTEL, A. & DELI, M. A. 2015. Restraint Stress-Induced Morphological Changes at the Blood-Brain Barrier in Adult Rats. Front Mol Neurosci, 8, 88.

SANTOS, A., GRANELL, E., GOMEZ-ANSON, B., CRESPO, I., PIRES, P., VIVES-GILABERT, Y., VALASSI, E., WEBB, S. M. & RESMINI, E. 2017. Depression and Anxiety Scores Are Associated with Amygdala Volume in Cushing's Syndrome: Preliminary Study. Biomed Res Int, 2017, 2061935.

SAPOLSKY, R. M. & MEANEY, M. J. 1986. Maturation of the adrenocortical stress response: neuroendocrine control mechanisms and the stress hyporesponsive period. Brain Res, 396, 64-76.

SAUNDERSON, E. A., SPIERS, H., MIFSUD, K. R., GUTIERREZ-MECINAS, M., TROLLOPE, A. F., SHAIKH, A., MILL, J. & REUL, J. M. H. M. 2016. Stress-induced gene expression and behavior are controlled by DNA methylation and methyl donor availability in the dentate gyrus. Proc Natl Acad Sci U S A, 113, 4830-5.

SAVORY, J. G., PREFONTAINE, G. G., LAMPRECHT, C., LIAO, M., WALTHER, R. F., LEFEBVRE, Y. A. & HACHE, R. J. 2001. Glucocorticoid receptor homodimers and glucocorticoid-mineralocorticoid receptor heterodimers form in the cytoplasm through alternative dimerization interfaces. Mol Cell Biol, 21, 781-93.

SCAMMELL, J. G., DENNY, W. B., VALENTINE, D. L. & SMITH, D. F. 2001. Overexpression of the FK506-binding immunophilin FKBP51 is the common cause of glucocorticoid resistance in three New World primates. Gen Comp Endocrinol, 124, 152-65.

SCHMIDT, U., BUELL, D. R., IONESCU, I. A., GASSEN, N. C., HOLSBOER, F., COX, M. B., NOVAK, B., HUBER, C., HARTMANN, J., SCHMIDT, M. V., TOUMA, C., REIN, T. & HERRMANN, L. 2015. A role for synapsin in FKBP51 modulation of stress responsiveness: Convergent evidence from animal and human studies. Psychoneuroendocrinology, 52, 43-58.

SCOBIE, K. N., HALL, B. J., WILKE, S. A., KLEMENHAGEN, K. C., FUJII-KURIYAMA, Y., GHOSH, A., HEN, R. & SAHAY, A. 2009. Krüppel-like factor 9 is necessary for late-phase neuronal maturation in the developing dentate gyrus and during adult hippocampal neurogenesis. J Neurosci, 29, 9875-87.

SCOVILLE, W. B. & MILNER, B. 1957. Loss of recent memory after bilateral hippocampal lesions. J Neurol Neurosurg Psychiatry, 20, 11-21.

SEO, M. K., KIM, Y. H., MCINTYRE, R. S., MANSUR, R. B., LEE, Y., CARMONA, N. E., CHOI, A. J., KIM, G. M., LEE, J. G. & PARK, S. W. 2018. Effects of Antipsychotic Drugs on the Epigenetic Modification of Brain-Derived Neurotrophic Factor Gene Expression in the Hippocampi of Chronic Restraint Stress Rats. Neural Plast, 2018, 2682037.

SEVILLA, L. M., LATORRE, V., CARCELLER, E., BOIX, J., VODAK, D., MILLS, I. G. & PEREZ, P. 2015. Glucocorticoid receptor and Klf4 co-regulate anti-inflammatory genes in keratinocytes. Mol Cell Endocrinol, 412, 281-9.

SHAFFER, P. L., JIVAN, A., DOLLINS, D. E., CLAESSENS, F. & GEWIRTH, D. T. 2004. Structural basis of androgen receptor binding to selective androgen response elements. Proc Natl Acad Sci U S A, 101, 4758-63.

SHELINE, Y. I., WANG, P. W., GADO, M. H., CSERNANSKY, J. G. & VANNIER, M. W. 1996. Hippocampal atrophy in recurrent major depression. Proc Natl Acad Sci U S A, 93, 3908-13.

SHEPARD, J. D., BARRON, K. W. & MYERS, D. A. 2000. Corticosterone delivery to the amygdala increases corticotropin-releasing factor mRNA in the central amygdaloid nucleus and anxiety-like behavior. Brain Res, 861, 288-95.

SHEPARD, J. D., BARRON, K. W. & MYERS, D. A. 2003. Stereotaxic localization of corticosterone to the amygdala enhances hypothalamo-pituitary-adrenal responses to behavioral stress. Brain Res, 963, 203-13.

SHEPPARD, K. A., PHELPS, K. M., WILLIAMS, A. J., THANOS, D., GLASS, C. K., ROSENFELD, M. G., GERRITSEN, M. E. & COLLINS, T. 1998. Nuclear integration of glucocorticoid receptor and nuclear factor-kappaB signaling by CREB-binding protein and steroid receptor coactivator-1. J Biol Chem, 273, 29291-4.

SHI, H., SHENG, B., ZHANG, F., WU, C., ZHANG, R., ZHU, J., XU, K., KUANG, Y., JAMESON, S. C., LIN, Z., WANG, Y., CHEN, J., JAIN, M. K. & ATKINS, G. B. 2013. Krüppel-like factor 2 protects against ischemic stroke by regulating endothelial blood brain barrier function. Am J Physiol Heart Circ Physiol, 304, H796-805.

SHI, S., HAYASHI, Y., ESTEBAN, J. A. & MALINOW, R. 2001. Subunit-specific rules governing AMPA receptor trafficking to synapses in hippocampal pyramidal neurons. Cell, 105, 331-43.

SHIMIZU, N., YOSHIKAWA, N., ITO, N., MARUYAMA, T., SUZUKI, Y., TAKEDA, S., NAKAE, J., TAGATA, Y., NISHITANI, S., TAKEHANA, K., SANO, M., FUKUDA, K., SUEMATSU, M., MORIMOTO,

C. & TANAKA, H. 2011. Crosstalk between glucocorticoid receptor and nutritional sensor mTOR in skeletal muscle. Cell Metab, 13, 170-82.

SILLIVAN, S. E., JONES, M. E., JAMIESON, S., RUMBAUGH, G. & MILLER, C. A. 2019. Bioinformatic analysis of long-lasting transcriptional and translational changes in the basolateral amygdala following acute stress. PLoS One, 14, e0209846.

SINCLAIR, D., TSAI, S. Y., WOON, H. G. & WEICKERT, C. S. 2011. Abnormal glucocorticoid receptor mRNA and protein isoform expression in the prefrontal cortex in psychiatric illness. Neuropsychopharmacology, 36, 2698-709.

SLOVITER, R. S., SOLLAS, A. L., DEAN, E. & NEUBORT, S. 1993. Adrenalectomy-induced granule cell degeneration in the rat hippocampal dentate gyrus: characterization of an in vivo model of controlled neuronal death. J Comp Neurol, 330, 324-36.

SLOVITER, R. S., VALIQUETTE, G., ABRAMS, G. M., RONK, E. C., SOLLAS, A. L., PAUL, L. A. & NEUBORT, S. 1989. Selective loss of hippocampal granule cells in the mature rat brain after adrenalectomy. Science, 243, 535-8.

SO, A. Y., CHAIVORAPOL, C., BOLTON, E. C., LI, H. & YAMAMOTO, K. R. 2007. Determinants of cell- and gene-specific transcriptional regulation by the glucocorticoid receptor. PLoS Genet, 3, e94.

SONDER, S. U., MIKKELSEN, M., RIENECK, K., HEDEGAARD, C. J. & BENDTZEN, K. 2006. Effects of spironolactone on human blood mononuclear cells: mineralocorticoid receptor independent effects on gene expression and late apoptosis induction. Br J Pharmacol, 148, 46-53.

SPIGA, F. & LIGHTMAN, S. L. 2009. Dose-dependent effects of corticosterone on nuclear glucocorticoid receptors and their binding to DNA in the brain and pituitary of the rat. Brain Res, 1293, 101-7.

SPIGA, F., WALKER, J. J., TERRY, J. R. & LIGHTMAN, S. L. 2014. HPA axis-rhythms. Compr Physiol, 4, 1273-98.

STARK, R. & BROWN, G. 2011. DiffBind: differential binding analysis of ChIP-Seq peak data.

STARKMAN, M. N., GEBARSKI, S. S., BERENT, S. & SCHTEINGART, D. E. 1992. Hippocampal formation volume, memory dysfunction, and cortisol levels in patients with Cushing's syndrome. Biol Psychiatry, 32, 756-65.

STARKMAN, M. N., GIORDANI, B., GEBARSKI, S. S., BERENT, S., SCHORK, M. A. & SCHTEINGART, D. E. 1999. Decrease in cortisol reverses human hippocampal atrophy following treatment of Cushing's disease. Biol Psychiatry, 46, 1595-602.

STARKMAN, M. N., SCHTEINGART, D. E. & SCHORK, M. A. 1981. Depressed mood and other psychiatric manifestations of Cushing's syndrome: relationship to hormone levels. Psychosom Med, 43, 3-18.

STRAHLE, U., KLOCK, G. & SCHUTZ, G. 1987. A DNA sequence of 15 base pairs is sufficient to mediate both glucocorticoid and progesterone induction of gene expression. Proc Natl Acad Sci U S A, 84, 7871-5.

STRASHIMIROV, D. & BOHUS, B. 1966. Effect of 2-methyl-1,2-bis-3-pyridl-1-propanone (SU-4885) on adrenocortical secretion in normal and hypophysectomized rats. Steroids, 7, 171-80.

SURJIT, M., GANTI, K. P., MUKHERJI, A., YE, T., HUA, G., METZGER, D., LI, M. & CHAMBON, P. 2011. Widespread negative response elements mediate direct repression by agonist-liganded glucocorticoid receptor. Cell, 145, 224-41.

SUSKE, G., BRUFORD, E. & PHILIPSEN, S. 2005. Mammalian SP/KLF transcription factors: bring in the family. Genomics, 85, 551-6.

SUZUKI, A., FUKUSHIMA, H., MUKAWA, T., TOYODA, H., WU, L. J., ZHAO, M. G., XU, H., SHANG, Y., ENDOH, K., IWAMOTO, T., MAMIYA, N., OKANO, E., HASEGAWA, S., MERCALDO, V., ZHANG, Y., MAEDA, R., OHTA, M., JOSSELYN, S. A., ZHUO, M. & KIDA, S. 2011. Upregulation of CREB-mediated transcription enhances both short- and long-term memory. J Neurosci, 31, 8786-802.

SWYGERT, S. G. & PETERSON, C. L. 2014. Chromatin dynamics: interplay between remodeling enzymes and histone modifications. Biochim Biophys Acta, 1839, 728-36.

T HOEN, P. A., ARIYUREK, Y., THYGESEN, H. H., VREUGDENHIL, E., VOSSEN, R. H., DE MENEZES, R. X., BOER, J. M., VAN OMMEN, G. J. & DEN DUNNEN, J. T. 2008. Deep sequencing-based expression analysis shows major advances in robustness, resolution and inter-lab portability over five microarray platforms. Nucleic Acids Res, 36, e141.

TANAKA, M., LI, H., ZHANG, X., SINGH, J., DALGARD, C. L., WILKERSON, M. & ZHANG, Y. 2019. Region- and time-dependent gene regulation in the amygdala and anterior cingulate cortex of a PTSD-like mouse model. Mol Brain, 12, 25.

TANIURA, H., SNG, J. C. G. & YONEDA, Y. 2007. Histone modifications in the brain. Neurochemistry International, 51, 85-91.

TASKER, J. G., DI, S. & MALCHER-LOPES, R. 2005. Rapid central corticosteroid effects: evidence for membrane glucocorticoid receptors in the brain. Integr Comp Biol, 45, 665-71.

TAVERNA, S. D., LI, H., RUTHENBURG, A. J., ALLIS, C. D. & PATEL, D. J. 2007. How chromatin-binding modules interpret histone modifications: lessons from professional pocket pickers. Nat Struct Mol Biol, 14, 1025-40.

TEAM, R. C. 2014. R: A language and environment for statistical computing [Online]. Available: http://www.R-project.org/ [Accessed].

THOMPSON, B. L., ERICKSON, K., SCHULKIN, J. & ROSEN, J. B. 2004. Corticosterone facilitates retention of contextually conditioned fear and increases CRH mRNA expression in the amygdala. Behav Brain Res, 149, 209-15.

TRAPP, T., RUPPRECHT, R., CASTREN, M., REUL, J. M. H. M. & HOLSBOER, F. 1994. Heterodimerization between mineralocorticoid and glucocorticoid receptor: a new principle of glucocorticoid action in the CNS. Neuron, 13, 1457-62.

TREVINO, L. S., BOLT, M. J., GRIMM, S. L., EDWARDS, D. P., MANCINI, M. A. & WEIGEL, N. L. 2016. Differential Regulation of Progesterone Receptor-Mediated Transcription by CDK2 and DNA-PK. Mol Endocrinol, 30, 158-72.

TSAI, K. J., CHEN, S. K., MA, Y. L., HSU, W. L. & LEE, E. H. 2002. Sgk, a primary glucocorticoid-induced gene, facilitates memory consolidation of spatial learning in rats. Proc Natl Acad Sci U S A, 99, 3990-5.

TURNER, J. & CROSSLEY, M. 1999. Mammalian Krüppel-like transcription factors: more than just a pretty finger. Trends Biochem Sci, 24, 236-40.

TURNER, J. D., SCHOTE, A. B., MACEDO, J. A., PELASCINI, L. P. & MULLER, C. P. 2006. Tissue specific glucocorticoid receptor expression, a role for alternative first exon usage? Biochem Pharmacol, 72, 1529-37.

URYU, K., OKUMURA, T., SHIBASAKI, T. & SAKANAKA, M. 1992. Fine structure and possible origins of nerve fibers with corticotropin-releasing factor-like immunoreactivity in the rat central amygdaloid nucleus. Brain Res, 577, 175-9.

VALE, W., SPIESS, J., RIVIER, C. & RIVIER, J. 1981. Characterization of a 41-residue ovine hypothalamic peptide that stimulates secretion of corticotropin and beta-endorphin. Science, 213, 1394-7.

VALLEE, M., MAYO, W., DELLU, F., LE MOAL, M., SIMON, H. & MACCARI, S. 1997. Prenatal stress induces high anxiety and postnatal handling induces low anxiety in adult offspring: correlation with stress-induced corticosterone secretion. J Neurosci, 17, 2626-36.

VAN CAMPEN, J. S., HOMPE, E. L., JANSEN, F. E., VELIS, D. N., OTTE, W. M., VAN DE BERG, F., BRAUN, K. P., VISSER, G. H., SANDER, J. W., JOELS, M. & ZIJLMANS, M. 2016. Cortisol fluctuations relate to interictal epileptiform discharges in stress sensitive epilepsy. Brain, 139, 1673-9.

VAN EEKELEN, J. A., JIANG, W., DE KLOET, E. R. & BOHN, M. C. 1988. Distribution of the mineralocorticoid and the glucocorticoid receptor mRNAs in the rat hippocampus. J Neurosci Res, 21, 88-94.

VAN STEENSEL, B., VAN BINNENDIJK, E. P., HORNSBY, C. D., VAN DER VOORT, H. T., KROZOWSKI, Z. S., DE KLOET, E. R. & VAN DRIEL, R. 1996. Partial colocalization of glucocorticoid and mineralocorticoid receptors in discrete compartments in nuclei of rat hippocampus neurons. J Cell Sci, 109 (Pt 4), 787-92.

VAN WEERT, L., BUURSTEDE, J. C., MAHFOUZ, A., BRAAKHUIS, P. S. M., POLMAN, J. A. E., SIPS, H. C. M., ROOZENDAAL, B., BALOG, J., DE KLOET, E. R., DATSON, N. A. & MEIJER, O. C. 2017.

NeuroD Factors Discriminate Mineralocorticoid From Glucocorticoid Receptor DNA Binding in the Male Rat Brain. Endocrinology, 158, 1511-1522.

VAWTER, M. P., THATCHER, L., USEN, N., HYDE, T. M., KLEINMAN, J. E. & FREED, W. J. 2002. Reduction of synapsin in the hippocampus of patients with bipolar disorder and schizophrenia. Mol Psychiatry, 7, 571-8.

VAZQUEZ, D. M., MORANO, M. I., LOPEZ, J. F., WATSON, S. J. & AKIL, H. 1993. Short-term adrenalectomy increases glucocorticoid and mineralocorticoid receptor mRNA in selective areas of the developing hippocampus. Mol Cell Neurosci, 4, 455-71.

VEKOVISCHEVA, O. Y., AITTA-AHO, T., ECHENKO, O., KANKAANPAA, A., SEPPALA, T., HONKANEN, A., SPRENGEL, R. & KORPI, E. R. 2004. Reduced aggression in AMPA-type glutamate receptor GluR-A subunit-deficient mice. Genes Brain Behav, 3, 253-65.

VELDHUIS, H. D., DE KORTE, C. C. & DE KLOET, E. R. 1985. Glucocorticoids facilitate the retention of acquired immobility during forced swimming. Eur J Pharmacol, 115, 211-7.

WAGNER, C. K. 2006. The many faces of progesterone: a role in adult and developing male brain. Front Neuroendocrinol, 27, 340-59.

WALKER, J. J., SPIGA, F., GUPTA, R., ZHAO, Z., LIGHTMAN, S. L. & TERRY, J. R. 2015. Rapid intra-adrenal feedback regulation of glucocorticoid synthesis. J R Soc Interface, 12, 20140875.

WALL, P. M. & MESSIER, C. 2001. The hippocampal formation--orbitomedial prefrontal cortex circuit in the attentional control of active memory. Behav Brain Res, 127, 99-117.

WALTER, L. M., DEGUISE, M. O., MEIJBOOM, K. E., BETTS, C. A., AHLSKOG, N., VAN WESTERING, T. L. E., HAZELL, G., MCFALL, E., KORDALA, A., HAMMOND, S. M., ABENDROTH, F., MURRAY, L. M., SHORROCK, H. K., PROSDOCIMO, D. A., HALDAR, S. M., JAIN, M. K., GILLINGWATER, T. H., CLAUS, P., KOTHARY, R., WOOD, M. J. A. & BOWERMAN, M. 2018. Interventions Targeting Glucocorticoid-Kruppel-like Factor 15-Branched-Chain Amino Acid Signaling Improve Disease Phenotypes in Spinal Muscular Atrophy Mice. EBioMedicine, 31, 226-242.

WANG, M., HILL, M. N., ZHANG, L., GORZALKA, B. B., HILLARD, C. J. & ALGER, B. E. 2012. Acute restraint stress enhances hippocampal endocannabinoid function via glucocorticoid receptor activation. J Psychopharmacol, 26, 56-70.

WANG, Y., HAN, Y., FAN, E. & ZHANG, K. 2015. Analytical strategies used to identify the readers of histone modifications: A review. Anal Chim Acta, 891, 32-42.

WEBB, E. A., ELLIOTT, L., CARLIN, D., WILSON, M., HALL, K., NETHERTON, J., REED, J., BARRETT, T. G., SALWANI, V., CLAYDEN, J. D., ARLT, W., KRONE, N., PEET, A. C. & WOOD, A. G. 2018. Quantitative Brain MRI in Congenital Adrenal Hyperplasia: In Vivo Assessment of the Cognitive and Structural Impact of Steroid Hormones. J Clin Endocrinol Metab, 103, 1330-1341.

WEI, Q., LU, X. Y., LIU, L., SCHAFER, G., SHIEH, K. R., BURKE, S., ROBINSON, T. E., WATSON, S. J., SEASHOLTZ, A. F. & AKIL, H. 2004. Glucocorticoid receptor overexpression in forebrain: a mouse model of increased emotional lability. Proc Natl Acad Sci U S A, 101, 11851-6.

WESTBERRY, J. M., SADOSKY, P. W., HUBLER, T. R., GROSS, K. L. & SCAMMELL, J. G. 2006. Glucocorticoid resistance in squirrel monkeys results from a combination of a transcriptionally incompetent glucocorticoid receptor and overexpression of the glucocorticoid receptor co-chaperone FKBP51. J Steroid Biochem Mol Biol, 100, 34-41.

WIBLE, C. G. 2013. Hippocampal physiology, structure and function and the neuroscience of schizophrenia: a unified account of declarative memory deficits, working memory deficits and schizophrenic symptoms. Behav Sci (Basel), 3, 298-315.

WILLIAMS, C., MEHRIAN SHAI, R., WU, Y., HSU, Y. H., SITZER, T., SPANN, B., MCCLEARY, C., MO, Y. & MILLER, C. A. 2009. Transcriptome analysis of synaptoneurosomes identifies neuroplasticity genes overexpressed in incipient Alzheimer's disease. PLoS One, 4, e4936.

WILTGEN, B. J., BROWN, R. A., TALTON, L. E. & SILVA, A. J. 2004. New circuits for old memories: the role of the neocortex in consolidation. Neuron, 44, 101-8.

WIMMER, E. A., JACKLE, H., PFEIFLE, C. & COHEN, S. M. 1993. A Drosophila homologue of human Sp1 is a head-specific segmentation gene. Nature, 366, 690-4.

WOLFF, H. D. & HUSTON, P. E. 1959. Schizophrenia associated with Addison's disease. Am J Psychiatry, 116, 365-7.

WONG, J., HYDE, T. M., CASSANO, H. L., DEEP-SOBOSLAY, A., KLEINMAN, J. E. & WEICKERT, C. S. 2010. Promoter specific alterations of brain-derived neurotrophic factor mRNA in schizophrenia. Neuroscience, 169, 1071-84.

WONG, M. L., KLING, M. A., MUNSON, P. J., LISTWAK, S., LICINIO, J., PROLO, P., KARP, B., MCCUTCHEON, I. E., GERACIOTI, T. D., JR., DEBELLIS, M. D., RICE, K. C., GOLDSTEIN, D. S., VELDHUIS, J. D., CHROUSOS, G. P., OLDFIELD, E. H., MCCANN, S. M. & GOLD, P. W. 2000. Pronounced and sustained central hypernoradrenergic function in major depression with melancholic features: relation to hypercortisolism and corticotropin-releasing hormone. Proc Natl Acad Sci U S A, 97, 325-30.

WOJTOWICZ, J. M. & KEE, N. 2006. BrdU assay for neurogenesis in rodents. Nat Protoc, 1, 1399-405.

WRANGE, O., CARLSTEDT-DUKE, J. & GUSTAFSSON, J. A. 1986. Stoichiometric analysis of the specific interaction of the glucocorticoid receptor with DNA. J Biol Chem, 261, 11770-8.

WRANGE, O., ERIKSSON, P. & PERLMANN, T. 1989. The purified activated glucocorticoid receptor is a homodimer. J Biol Chem, 264, 5253-9.

WU, C., LI, F., HAN, G. & LIU, Z. 2013. Abeta(1-42) disrupts the expression and function of KLF2 in Alzheimer's disease mediated by p53. Biochem Biophys Res Commun, 431, 141-5.

XU, G., LI, Y., MA, C., WANG, C., SUN, Z., SHEN, Y., LIU, L., LI, S., ZHANG, X. & CONG, B. 2019. Restraint Stress Induced Hyperpermeability and Damage of the Blood-Brain Barrier in the Amygdala of Adult Rats. Front Mol Neurosci, 12, 32.

YANG, J. & YOUNG, M. J. 2009. The mineralocorticoid receptor and its coregulators. J Mol Endocrinol, 43, 53-64.

YAU, J. L., NOBLE, J. & SECKL, J. R. 1999. Continuous blockade of brain mineralocorticoid receptors impairs spatial learning in rats. Neurosci Lett, 277, 45-8.

YAU, J. L., OLSSON, T., MORRIS, R. G., MEANEY, M. J. & SECKL, J. R. 1995. Glucocorticoids, hippocampal corticosteroid receptor gene expression and antidepressant treatment: relationship with spatial learning in young and aged rats. Neuroscience, 66, 571-81.

YIN, K. J., HAMBLIN, M., FAN, Y., ZHANG, J. & CHEN, Y. E. 2015. Krüppel-like factors in the central nervous system: novel mediators in stroke. Metab Brain Dis, 30, 401-10.

YOKOTA, K., SHIBATA, H., KURIHARA, I., KOBAYASHI, S., SUDA, N., MURAI-TAKEDA, A., SAITO, I., KITAGAWA, H., KATO, S., SARUTA, T. & ITOH, H. 2007. Coactivation of the N-terminal transactivation of mineralocorticoid receptor by Ubc9. J Biol Chem, 282, 1998-2010.

YOSHINAGA, S. K., PETERSON, C. L., HERSKOWITZ, I. & YAMAMOTO, K. R. 1992. Roles of SWI1, SWI2, and SWI3 proteins for transcriptional enhancement by steroid receptors. Science, 258, 1598-604.

YUEN, E. Y., LIU, W., KARATSOREOS, I. N., FENG, J., MCEWEN, B. S. & YAN, Z. 2009. Acute stress enhances glutamatergic transmission in prefrontal cortex and facilitates working memory. Proc Natl Acad Sci U S A, 106, 14075-9.

ZALACHORAS, I., HOUTMAN, R. & MEIJER, O. C. 2013. Understanding stress-effects in the brain via transcriptional signal transduction pathways. Neuroscience, 242, 97-109.

ZENNARO, M. C., KEIGHTLEY, M. C., KOTELEVTSEV, Y., CONWAY, G. S., SOUBRIER, F. & FULLER, P. J. 1995. Human mineralocorticoid receptor genomic structure and identification of expressed isoforms. J Biol Chem, 270, 21016-20.

ZHANG, X. L., POSCHEL, B., FAUL, C., UPRETI, C., STANTON, P. K. & MUNDEL, P. 2013. Essential role for synaptopodin in dendritic spine plasticity of the developing hippocampus. J Neurosci, 33, 12510-8.

ZHANG, Y., LIU, T., MEYER, C. A., EECKHOUTE, J., JOHNSON, D. S., BERNSTEIN, B. E., NUSBAUM, C., MYERS, R. M., BROWN, M., LI, W. & LIU, X. S. 2008. Model-based analysis of ChIP-Seq (MACS). Genome Biol, 9, R137.

ZHE, D., FANG, H. & YUXIU, S. 2008. Expressions of hippocampal mineralocorticoid receptor (MR) and glucocorticoid receptor (GR) in the single-prolonged stress-rats. Acta Histochem Cytochem, 41, 89-95.

ZHOU, M. Y., GOMEZ-SANCHEZ, C. E. & GOMEZ-SANCHEZ, E. P. 2000. An alternatively spliced rat mineralocorticoid receptor mRNA causing truncation of the steroid binding domain. Mol Cell Endocrinol, 159, 125-31.

ZHU, L., ZHONG, M., ZHAO, J., RHEE, H., CAESAR, I., KNIGHT, E. M., VOLPICELLI-DALEY, L., BUSTOS, V., NETZER, W., LIU, L., LUCAST, L., EHRLICH, M. E., ROBAKIS, N. K., GANDY, S. E. & CAI, D. 2013. Reduction of synaptojanin 1 accelerates Abeta clearance and attenuates cognitive deterioration in an Alzheimer mouse model. J Biol Chem, 288, 32050-63.

ZHU, S., TAI, C., MACVICAR, B. A., JIA, W. & CYNADER, M. S. 2009. Glutamatergic stimulation triggers rapid Krüppel-like factor 4 expression in neurons and the overexpression of KLF4 sensitizes neurons to NMDA-induced caspase-3 activity. Brain Res, 1250, 49-62.

ZIV, L., MUTO, A., SCHOONHEIM, P. J., MEIJSING, S. H., STRASSER, D., INGRAHAM, H. A., SCHAAF, M. J., YAMAMOTO, K. R. & BAIER, H. 2013. An affective disorder in zebrafish with mutation of the glucocorticoid receptor. Mol Psychiatry, 18, 681-91.